Technical report on UK supplementary assessment under The Air Quality Directive (2008/50/EC), The Air Quality Framework Directive (96/62/EC) and Fourth Daughter Directive (2004/107/EC) for 2018

Report for The Department for Environment, Food and Rural Affairs, The Welsh Government, The Scottish Government and The Department of the Environment for Northern Ireland

Ricardo Energy & Environment/R/3470

ED 12633 | Issue Number 1 | Date 14/05/2020

Customer:

The Department for Environment, Food and Rural Affairs, The Welsh Government, The Scottish Government and The Department of the Environment for Northern Ireland

Customer reference:

ecm_55496

Confidentiality, copyright & reproduction:

Contact:

Sally Whiting
Ricardo Energy & Environment
Gemini Building, Harwell, Didcot, OX11 0QR,
United Kingdom

t: +44 (0) 1235 75 3186
e: sally.whiting@ricardo.com

Author:

Daniel M Brookes, John R Stedman, Andrew J Kent, Sally L Whiting, Rebecca A Rose, Chris J Williams, Katherine L Pugsley

Approved By:

John Stedman

Date:

14 May 2020

Ricardo Energy & Environment reference:

Ref: ED12633- Issue Number 1

Executive summary

European Union directives on ambient air quality require member states, including the UK, to undertake air quality assessments, and to report the findings of these assessments to the European Commission on an annual basis:

- The Directive on ambient air quality and cleaner air for Europe (2008/50/EC), which is known as the ‘Air Quality Directive’ (AQD)
- The fourth Daughter Directive 2004/107/EC (AQDD4) under the Air Quality Framework Directive (1996/62/EC).

The UK annual air quality assessment for the year 2018 has been undertaken in accordance with the requirements of the AQD and the AQDD4. The assessment takes the form of comparisons of measured and modelled air pollutant concentrations with the limit values, critical levels, target values and long-term objectives set out in the directives. The AQD includes a requirement to deduct the contribution to ambient PM from natural sources. The results were submitted to the European Commission in September 2019 in the form of e-Reporting Data flows (specifically Data flow G on attainment) that each member state must complete and upload onto the Central Data Repository of the European Environment Agency: http://cdr.eionet.europa.eu/gb/eu/aqd/ (CDR, 2019).

The AQD sets limit values for the ambient concentrations to be achieved for:

- sulphur dioxide (SO_2)
- nitrogen dioxide (NO_2)
- particles (PM_{10})
- lead (Pb)
- benzene (C_6H_6)
- carbon monoxide (CO)

The AQD also includes:

- critical levels for the protection of vegetation to be achieved for ambient concentrations of sulphur dioxide (SO_2) and oxides of nitrogen (NO_x)
- a target value, limit values, an exposure concentration obligation and exposure reduction targets for fine particles ($PM_{2.5}$)
- target values and long-term objectives for ozone (O_3)

AQDD4 sets target values for the ambient concentrations to be achieved for:

- Arsenic (As)
- Cadmium (Cd)
- Nickel (Ni)
- Benzo(a)Pyrene (B(a)P)

The UK has been divided into 43 zones for air quality assessment. There are 28 agglomeration zones (large urban areas) and 15 non-agglomeration zones. The status of the zones in relation to the limit values, critical levels, target values and long-term objectives has been assessed.

This report provides a summary of key attainment results from the e-Reporting submission for the AQD and AQDD4 pollutants and technical information on the modelling methods that have been used.

The results of the assessment against limit values are summarised in Table E1. This shows that 36 zones have not achieved full compliance with the annual NO_2 limit value in 2018. Two zones were also non-compliant with the hourly limit value in 2018.

Table E2 summarises the results of the assessment for O_3 in terms of the numbers of zones with exceedances of the target values and long-term objectives. Ozone concentrations typically show considerable variation from year to year as a result of variation in weather conditions.

Table E3 shows that there were no exceedances of the target value, stage 1 limit value, indicative stage 2 limit value (which is not currently in force) or exposure concentration obligation for $PM_{2.5}$.

Table E4 lists no exceedances of old directives in 2018.

The results of the assessment against the target values for AQDD4 pollutants are presented in Table E5. Four zones have not achieved full compliance with the annual Ni target value and three zones have not achieved full compliance with the annual B(a)P target value in 2018. Measured and modelled Ni concentration in the zones with exceedances were higher than in the previous year.

Table E1. Summary results of air quality assessment for 2018: comparison with limit values and critical levels

Pollutant	Averaging time	Number of zones exceeding limit value
SO_2	1-hour	None
SO_2	24-hour	None
SO_2	Annual[1]	None
SO_2	Winter[1]	None
NO_2	1-hour[2]	2 zones measured (Greater London Urban Area, South Wales)
NO_2	Annual	36 zones (9 measured + 27 modelled)
NO_x	Annual[1]	None
PM_{10}	24-hour	None
PM_{10}	Annual	None
Lead	Annual	None
Benzene	Annual	None
CO	8-hour	None

1 - Critical levels rather than LVs applying to vegetation and ecosystem areas only.
2 - No modelling for 1-hour LV

Table E2. Summary results of air quality assessment for 2018 for O_3: comparison with target values and long-term objectives

Pollutant	Averaging time	Number of zones exceeding target value	Number of zones exceeding long term objective
O_3	8-hour	none	43 zones (41 measured + 2 modelled)
O_3	AOT40	none	38 zones (29 measured + 9 modelled)

Table E3. Summary results of air quality assessment for 2018 for $PM_{2.5}$: comparison with target value and limit value and exposure concentration obligation

Pollutant	Averaging time	Number of zones exceeding target value
$PM_{2.5}$	Annual target value (25 µg m^{-3})	None
$PM_{2.5}$	Annual limit value (25 µg m^{-3})	None
$PM_{2.5}$	Annual limit value (Indicative Stage 2, 20 µg m^{-3})[1]	None
$PM_{2.5}$	Exposure concentration obligation (20 µg m^{-3})	Not exceeded

1 – The stage 2 indicative limit value for $PM_{2.5}$ is not currently in force

Table E4. Exceedances of old Directives for 2018

Pollutant	Directive	Averaging time (limit value)	Concentration (µg m^{-3})
NO_2	85/203/EEC	1-hour 98%ile (200 µg m^{-3})	None

Table E5. Summary results of AQDD4 air quality assessment for 2018: comparison with target values

Pollutant	Averaging time	Number of zones exceeding target value
As	Annual	None
Cd	Annual	None
Ni	Annual	4 zones (3 modelled: Sheffield, South Wales, Yorkshire & Humberside, 1 measured: Swansea)
B(a)P	Annual	3 zones (2 modelled: Swansea, South Wales, 1 measured: Yorkshire & Humberside)

Table of contents

1 Introduction

1.1 The EU ambient air quality directives

The European Union directives on ambient air quality were established to assist member states to achieve protection and improvement of the environment. These directives require member states, including the UK, to undertake air quality assessments, and to report the findings of these assessments to the European Commission on an annual basis. Historically this was done according to:

- The Air Quality Framework Directive (1996/62/EC)
- The four Daughter Directives 1999/30/EC, 2000/69/EC, 2002/3/EC and 2004/107/EC.

In June 2008, a new directive came into force: The Council Directive on ambient air quality and cleaner air for Europe (2008/50/EC), which is known as the ‘Air Quality Directive’ (AQD). This directive consolidates the first three Daughter Directives, and was transposed into Regulations in England, Scotland, Wales and Northern Ireland in June 2010. The 4th Daughter Directive (AQDD4), 2004/107/EC, remains in force.

The UK annual air quality assessment for the year 2018 has been undertaken in accordance with the requirements of the AQD and the AQDD4. The assessment comprises comparisons of measured and modelled air pollutant concentrations with the limit values, critical levels, target values and long-term objectives set out in the directives. The results were submitted to the European Commission in September 2019 in the form of e-Reporting Data flows (specifically Data flow G on attainment) that each member state must complete and upload onto the Central Data Repository of the European Environment Agency: http://cdr.eionet.europa.eu/gb/eu/aqd/ (CDR, 2019). The 2018 UK submission on air quality to the European Commission is summarised by the annual Air Pollution in the UK reports (Air Pollution in the UK 2018), which comprise a compliance assessment summary report and a full report, which, in addition, presents air quality modelling data and measurements from the UK national air quality monitoring networks.

The air quality assessment has been reported via the following e-Reporting Data flows required by decision 2011/850/EU:

- B: Zones and agglomerations
- C: Assessment regime
- D: Assessment methods
- E: Primary validated assessment data
- G: Attainment

Information on the supplementary assessment methods (modelling and objective estimations) has been provided in Data flows C and D and model results have been provided in Data flows E and G. Data flow G effectively replaces forms 8, 9 and 19 of the questionnaire previously compiled according to decision 2004/461/EC.

An important change between the Framework and Daughter Directives and the AQD has been a requirement to deduct the contribution to ambient PM from a wider range of natural sources than specified in the Framework and Daughter Directives, prior to the comparison with limit values. This requirement was included for the first time in the assessment of concentrations for 2008 and in accordance with the AQD has also been included in the annual assessments from 2009 to 2018.

The AQD sets limit values (LV) for the ambient concentrations to be achieved for:

- sulphur dioxide (SO_2)
- nitrogen dioxide (NO_2)
- particles (PM_{10})
- lead (Pb)
- benzene (C_6H_6)
- carbon monoxide (CO)

The AQD also includes:

- critical levels (CL) for the protection of vegetation to be achieved for ambient concentrations of sulphur dioxide (SO_2) and oxides of nitrogen (NO_x)

- a target value (TV), limit values, an exposure concentration obligation (ECO) and national exposure reduction targets (NERT) for fine particles ($PM_{2.5}$)
- target values (TVs) and long-term objectives (LTOs) for ozone (O_3)

AQDD4 sets target values to be achieved for:

- arsenic (As)
- cadmium (Cd)
- nickel (Ni)
- polycyclic aromatic hydrocarbons with benzo(a)pyrene (B(a)P) as an indicator species

The number of monitoring sites required for compliance defined within the directives is reduced if other means of assessment, in addition to fixed monitoring sites, are available for inclusion in the annual air quality assessment. Air quality modelling has been carried out to supplement the information available from the UK national air quality monitoring networks.

1.2 This report

This report comprises technical information on the modelling methods that have been used for the assessed year, a summary of key attainment results from the e-Reporting submission for the AQD and AQDD4 pollutants, and key comparisons of findings for measured and modelled air pollutant concentrations with the limit values, critical levels, target values and long-term objectives set out in the directives. The Results of the air quality assessment for 2018 are summarised in Section 2.

Sections 3 to 11 of this report describe the Pollution Climate Mapping (PCM) modelling methods that have been used to calculate concentrations of SO_2, NO_x, NO_2, PM_{10}, $PM_{2.5}$, C_6H_6, O_3, heavy metals (Pb, As, Cd, Ni) and B(a)P for 2018 as part of the assessment of compliance with the limit values, critical levels, target values and long term objectives for each pollutant. This includes:

- A summary of the limit values, critical levels, target values and long-term objectives set out in the directives for each pollutant
- Details of the modelling methods including summaries of inputs, assumptions and schematic flow diagrams of the modelling process
- Source apportionment information
- Information on the verification of the models used and comparisons with data quality objectives

The assessment for CO is described in Section 8. Prior to 2011 a modelling assessment was completed for CO. However, as ambient concentrations throughout the UK have been well below the limit value and assessment thresholds for many years, models are no longer required for CO and the supplementary assessment for 2018 has been based on objective estimation, as it was for 2011-2017.

1.3 Assessment regime and definition of zones

The Framework Directive included a requirement for member states to undertake preliminary assessments of ambient air quality, prior to the implementation of the Daughter Directives under Article 5 of this Directive. The objectives of these assessments were to establish estimates for the overall distribution and levels of pollutants, and to identify additional monitoring required to fulfil obligations within the Framework Directive. The preliminary assessment (Bush, 2000) carried out for 1st Daughter Directive (AQDD1), 1999/30/EC, defined a set of zones to be used for air quality assessment in the UK. The preliminary assessment for the UK for AQDD4 was reported by Bush (2007). The AQD includes a similar requirement for continued assessment under Article 5, the preliminary assessment for the UK fulfilling this requirement was reported by Vincent et al. (2010). The AQD continues the requirement for the establishment of zones and agglomerations under Article 4. Table 1.1 contains details of area, population and urban road length contained in each UK zone and agglomeration. The population data are mid-year estimates for 2017 derived from data provided by the Office for National Statistics for England and Wales, National Records of Scotland and Northern Ireland Statistics and Research Agency. Output area totals have been assigned to 1 km grid squares using residential information from OS address base. The zones and agglomerations map for the UK is presented in

Figure 1-1.

Figure 1-1 - UK zones and agglomerations for 2018

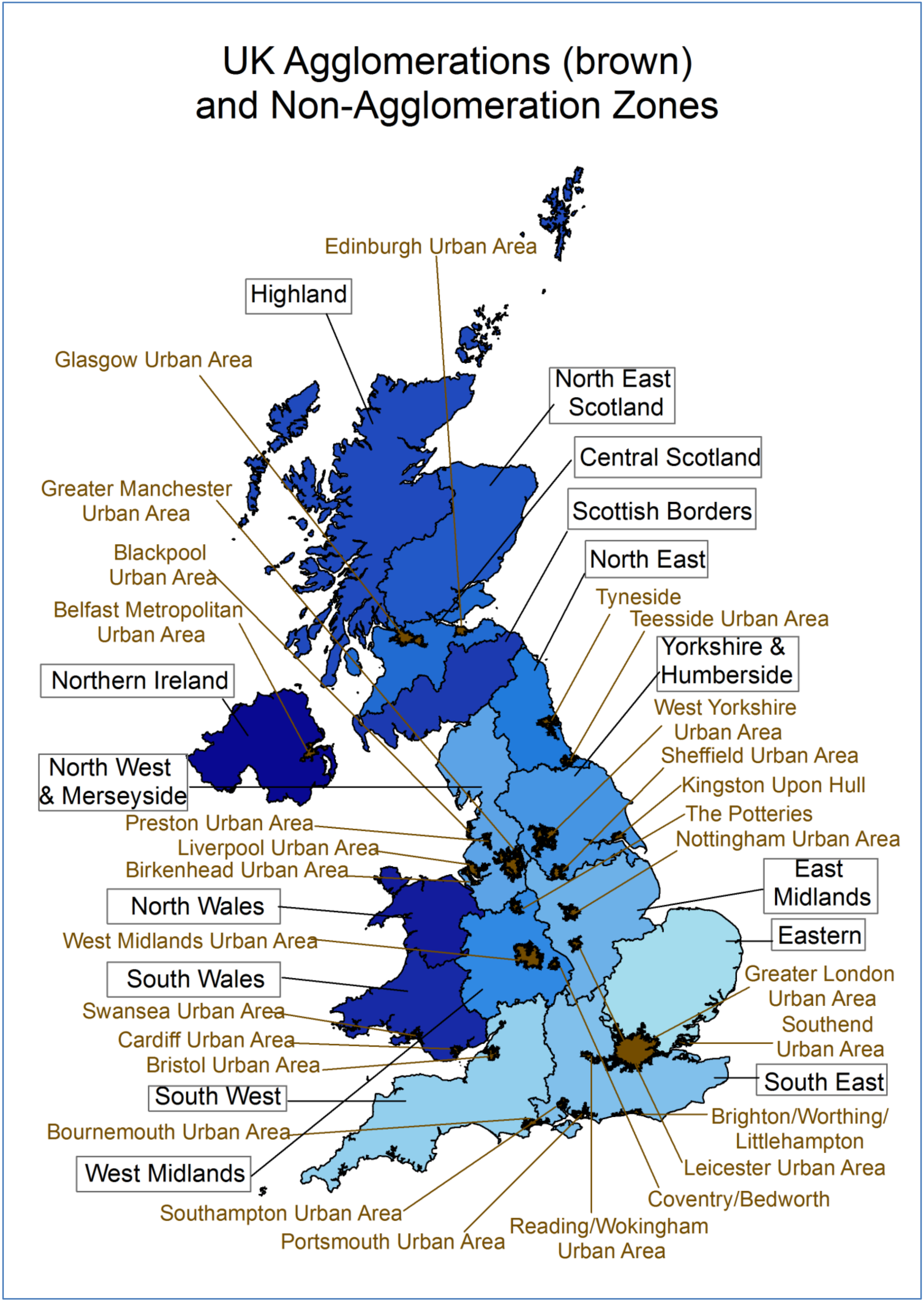

Agglomeration zones (brown)
Non-agglomeration zones (blue)

Table 1.1 - Zones for Air Quality Directive reporting

Zone	Zone code	Ag or non-ag*	Population	Area (km^2)	Number of urban road	Length of urban road links
Greater London Urban Area	UK0001	ag	9611752	1618	1912	592
West Midlands Urban Area	UK0002	ag	2410431	605	396	689
Greater Manchester Urban Area	UK0003	ag	2182858	554	561	436
West Yorkshire Urban Area	UK0004	ag	1364479	352	296	231
Tyneside	UK0005	ag	787438	221	182	222
Liverpool Urban Area	UK0006	ag	774368	198	254	165
Sheffield Urban Area	UK0007	ag	604171	163	109	134
Nottingham Urban Area	UK0008	ag	631551	155	133	135
Bristol Urban Area	UK0009	ag	573456	139	128	84
Brighton/Worthing/Littlehampton	UK0010	ag	439280	94	62	88
Leicester Urban Area	UK0011	ag	455873	101	71	82
Portsmouth Urban Area	UK0012	ag	415784	96	63	81
Teesside Urban Area	UK0013	ag	318620	119	64	140
The Potteries	UK0014	ag	293058	91	119	80
Bournemouth Urban Area	UK0015	ag	394903	121	59	79
Reading/Wokingham Urban Area	UK0016	ag	317663	82	70	45
Coventry/Bedworth	UK0017	ag	348930	76	35	58
Kingston upon Hull	UK0018	ag	280077	85	41	79
Southampton Urban Area	UK0019	ag	316135	79	62	85
Birkenhead Urban Area	UK0020	ag	288808	97	70	55
Southend Urban Area	UK0021	ag	253989	67	31	64
Blackpool Urban Area	UK0022	ag	229694	73	48	42
Preston Urban Area	UK0023	ag	217378	60	37	389
Glasgow Urban Area	UK0024	ag	1135190	367	280	105
Edinburgh Urban Area	UK0025	ag	502072	134	60	69
Cardiff Urban Area	UK0026	ag	342574	86	42	74
Swansea Urban Area	UK0027	ag	214026	83	38	231
Belfast Metropolitan Urban Area	UK0028	ag	555776	216	54	760
Eastern	UK0029	non-	5654414	19491	576	571
South West	UK0030	non-	4614310	24396	428	1189
South East	UK0031	non-	7039726	19115	882	543
East Midlands	UK0032	non-	3685207	15458	413	801
North West & Merseyside	UK0033	non-	3567960	13507	624	523
Yorkshire & Humberside	UK0034	non-	3202803	15019	378	472
West Midlands	UK0035	non-	2805876	12221	372	254
North East	UK0036	non-	1538008	8377	222	365
Central Scotland	UK0037	non-	1980292	9984	233	198
North East Scotland	UK0038	non-	1148282	19024	134	18
Highland	UK0039	non-	395051	43514	10	33
Scottish Borders	UK0040	non-	264463	11400	33	304
South Wales	UK0041	non-	1807147	12645	192	137
North Wales	UK0042	non-	757502	8747	85	270
Northern Ireland	UK0043	non-	1315063	14540	85	592
Total			**66036438**	**253570**	**9944**	**12976**

* ag = agglomeration zone; non-ag = non-agglomeration zone

The status of zones in relation to the limit, target values, critical levels and long-term objectives for the AQD pollutants have been reported to the EU via e-Reporting (CDR, 2019) and a summary of the results of the assessments are included in Section 2. The status has been determined from a combination of monitoring data and model results. A comparison of the results of similar assessments carried out since 2001 (Stedman et al., 2002, 2003, 2005 and 2006; Bush et al., 2006 and 2007; Kent and Stedman, 2007 and 2008; Kent et al., 2007a, 2007b and 2010; Yap et al., 2009; Grice et al., 2009, 2010a and 2010b; Walker et al., 2010 and 2011; Brookes et al., 2011 and 2012, 2013, 2015, 2016, 2017, 2019a and 2019b) has been reported in Air Pollution in the UK 2018.

1.4 Monitoring sites

The monitoring stations operating during 2018 for AQD and AQDD4 reporting have been listed within e-Reporting Data flow C (Assessment Regimes), which can be found on the CDR (CDR, 2019). Not all sites had sufficient data capture during 2018 for data to be reported. The data quality objective (DQO) for AQD/AQDD4 measurements is 90% data capture. The Implementing Provisions on Reporting (IPR) guidance (IPR 2013) states that when checking for compliance the minimum data quality objective can be reduced to take into account the proportion of time taken in a calendar year for planned maintenance and calibration. The IPR states that an estimation of this time is 5%, which makes the data quality objective 85%. For the purposes of compliance reporting all measurements from monitoring sites with at least 85% data capture for the entire year have been included. These have been supplemented with monitoring sites with data capture of 75%-84%. These results have been classified in the assessment as ‘indicative’ for the zones they represent. Monitoring stations with at least 75% data capture have been included in the modelling analysis to ensure that a greater number of operational monitoring sites have been used for model calibration and verification purposes.

The monitoring data for the sites used in the assessment for heavy metals and B(a)P are summarised in Appendix 2.

1.5 Data quality objectives for modelling results and model verification

The AQD sets data quality objectives (DQOs) for modelling uncertainty, within supplementary assessment under the AQD. AQDD4 sets DQOs in terms of uncertainty, which acts as a guide for quality assurance programmes when identifying an acceptable level of uncertainty for assessment methods appropriate for supplementary assessment under the AQDD4. Uncertainty is defined in the AQD as the maximum deviation of the measured and calculated concentration levels for 90% of individual monitoring points over the period considered by the limit value (or target value), without taking into account the timing of events. The uncertainty of modelling should be interpreted as applicable in the region of the appropriate LV or TV. The fixed measurements that have been selected for comparison with the modelling results should be representative of the scale covered by the model. Final guidance clarifying the recommended methods for assessing model performance with respect to the DQOs has yet to be agreed. The comparisons with monitoring data presented in this report have therefore included data from all sites including those with measured values not in the vicinity of the LVs or TVs and a highly detailed assessment of the spatial representativity of the sites has not been carried out.

Under the AQD, DQOs have been set at 50% for hourly averages, daily averages and 8-hour averages of SO_2, NO_2, NO_x, CO and O_3. DQOs have been set at 30% for annual averages of SO_2, NO_2 and NO_x. For PM_{10}, $PM_{2.5}$ and Pb the DQO for annual averages is 50%. DQOs have not been defined for daily averages of PM_{10}. Under the AQDD4 DQOs have been set at 60% for annual averages of As, Cd, Ni and B(a)P.

The models used to calculate the maps of NO_x, NO_2, PM_{10}, $PM_{2.5}$, C_6H_6, O_3, and B(a)P presented in this report have been calibrated using data from the national monitoring network sites. Data from these sites alone does not allow an independent assessment of the validity of the mapped estimates in relation to the DQOs for modelling. Measurement data from sites not included in the calibration are described as ‘verification sites’ in this report and are used in addition to the national monitoring network sites to make this assessment, except for C_6H_6 and B(a)P where no independent data are available. Data from sites quality assured by Ricardo under contract and not part of the national network, including Local Authority sites with data available from the Air Quality England website, Scottish Air Quality Archive monitoring sites, Welsh Air Quality Network monitoring sites, Northern Ireland Automatic Urban Network sites, and Heathrow Airwatch sites, have therefore been used for the verification of the modelled estimates. The description ‘Verification Sites’ is used to describe the independent monitoring sites included in the verification analysis. Monitoring data has also been obtained for the London Air Quality Network (LAQN) and other local authority monitoring networks for which data are provided by Kings College London (ERG). The ‘Verification Sites’ used for the 2018 assessment are listed in Appendix 1.

The model used to calculate maps of SO_2 presented in this report is not calibrated because modelled values provide a reasonably good fit to measured concentrations and to avoid the risk of overfitting for the high percentile metrics. Modelled results have therefore been compared to and verified using a combination of national network monitoring data along with the ‘Verification Sites’ listed in Appendix 1. The models used to calculate maps of air pollution from heavy metals (Pb, As, Cd, Ni) presented in this report are also not calibrated. Results have been compared to and verified using national network monitoring data for those sites that are listed Appendix 2 in order to ensure that the model assumptions and parameter values selected provide good agreement with measurements. Sites with data capture of at least 75% have been included in the verification analysis. Model verification results are listed in the sections on each pollutant.

1.6 Air quality modelling

Full details of the modelling methods implemented are given in Sections 3 to 11 including summaries of inputs, assumptions and schematic flow diagrams of the modelling process. A brief introduction is presented here.

1.6.1 Background concentration maps

Maps showing background concentrations for NO_X, SO_2 and C_6H_6 have been calculated at a 1 km x 1 km resolution for the relevant metrics set out in the AQD. These maps have been calculated by summing contributions from the following sources:

- Large point sources[1] – modelled using the air dispersion model ADMS and emissions estimates from the UK National Atmospheric Emissions Inventory 2017 (NAEI 2017).
- Small point sources – modelled using the small points model and emissions estimates from the NAEI 2017.
- EU Emissions Trading Scheme[2] (ETS) point sources – those above the large point source modelling threshold or with emission release characteristics are modelled as large point sources those below the modelling threshold are modelled using the small points model and emissions estimates from the NAEI 2017.
- Distant sources – characterised by the rural background concentration.
- Area sources[3] related to domestic combustion – modelled using a time varying dispersion kernel and emissions estimates from the NAEI 2017.
- Area sources related to combustion in industry – modelled using the small points model and emissions estimates from the NAEI 2017.
- Area sources related to road traffic – modelled using a dispersion kernel using time varying emissions and emissions estimates from the NAEI 2017.
- Other area sources – modelled using a dispersion kernel and annual emissions estimates from the NAEI 2017.
- Fugitive point source emissions – modelled using fugitive source kernel model and an estimate of the fugitive component of emissions derived from the NAEI 2017 (C_6H_6 only).

1 km x 1 km background concentration maps for B(a)P have been calculated using a similar approach except that a regional background has not been included and area sources related to industrial combustion and ETS point sources not meeting the large point source modelling criteria have been modelled using an area source dispersion kernel.

For PM_{10} and $PM_{2.5}$ a similar approach has been used to generate 1 km x 1 km background concentration maps. For these pollutants, the following additional contributions have also been included:

---

[1] Point source emissions are defined as emissions of a known amount from a known location (e.g. a power station).
[2] Emissions Trading Scheme point emissions estimates for Air Quality pollutants based on reported carbon emissions
[3] Area source emissions are defined as ‘diffuse emissions’ from many unspecified locations (e.g. emissions from domestic heating, or from shipping).

- Secondary inorganic aerosol – derived by interpolation and scaling of measurements of SO_4, NO_3 and NH_4 at rural sites.
- Secondary organic aerosol – semi-volatile organic compounds formed by the oxidation of non-methane volatile organic compounds. Estimates derived from results from the NAME model
- Regional primary particles – from results from the TRACK model and emissions estimates from the NAEI 2017 and EMEP.
- Regional calcium rich dusts from re-suspension of soils – modelled using a dispersion kernel and information on land use.
- Regional iron rich dusts from re-suspension – assumed to be a constant value, estimated measurements made in the vicinity of Birmingham.
- Iron rich dusts from re-suspension due to vehicle activity – modelled using a dispersion kernel and vehicle activity data for heavy duty vehicles.
- Sea salt – derived by interpolation and scaling of measurements of chloride at rural sites.
- Residual – assumed to be a constant value.

A similar approach has also been used for Pb, As, Cd and Ni to generate 1 km x 1 km background concentration maps. For these pollutants, the following additional contributions have also been included:

- Regional concentrations – derived from estimates of primary PM from regional sources calculated using the TRACK model and emissions estimates from the NAEI 2017 and EMEP.
- Re-suspension from bare soils – derived from estimates of re-suspension of PM modelled using a dispersion kernel and information on land use.
- Re-suspension as a result of vehicle movements – derived from estimates of re-suspension of PM modelled using a dispersion kernel and vehicle activity data for heavy duty vehicles.

1.6.2 Roadside concentration maps

Maps showing modelled roadside concentrations of NO_X, PM_{10}, $PM_{2.5}$ and C_6H_6 have been calculated for 9351 urban major road census points (A-roads and motorways) across the UK. Some of the lengths of road associated with each census point cross zone boundaries and thus a total of 9944 road links have been included in the analysis. The road lengths have been split between zones for assessment where a road has length in more than one zone. These roadside concentrations have been calculated by adding a ‘roadside increment’ concentration component (derived from the road link emission) to the modelled background concentration for each road. This roadside increment concentration has been calculated using the PCM Roads Kernel Model (PCM-RKM). The PCM-RKM, based upon dispersion kernels generated by the ADMS-Roads dispersion model, represents a more process-based approach than the previous empirical method (e.g. Brookes et al., 2015). It provides a more robust assessment, whilst retaining the link with measurement data by using AURN measurement data to calibrate this component of the model. Full details of the PCM-RKM are provided in Appendix 7.

1.6.3 NO_2 maps

Background and roadside NO_2 concentration maps have been calculated by applying a calibrated version of the updated oxidant-partitioning model. This model describes the complex inter-relationships between NO, NO_2 and O_3 as a set of chemically coupled species (Jenkin, 2004; Murrells et al., 2008; Jenkin, 2012).

1.6.4 Key input data

Emissions inventory data used in this modelling is taken from the NAEI 2017 (Richmond et al., 2019). Emission estimates for area and point sources (taking into account plant closure) have been scaled forward from 2017 to 2018. Work carried out to calculate emissions from aircraft and shipping within the PCM model is described in Appendix 5. Dispersion modelling has been done using ADMS 5.2 using meteorological data from Waddington for 2018. UK national network monitoring data has been used to calibrate the background and roadside models, as discussed above in Section 1.5. Further details on inputs and assumptions are provided in Sections 3 to 11.

1.6.5 Ozone maps

Maps of the O_3 metrics specified in the AQD have been calculated using a different modelling approach to the approach used for other pollutants in this report. This is because of the complex chemistry involved in the production and destruction of O_3. An empirical method based on a combination of interpolation of O_3 measurements at rural sites and model results for NO_x is used to model O_3 concentrations. This is described in Section 9.

1.7 Air quality in Gibraltar in 2018

Air quality monitoring and assessments are also undertaken in Gibraltar and the results of the assessment are submitted to the Commission each year via a separate e-Reporting Data flows to those compiled for the UK (CDR, 2019). Further information on air quality monitoring in Gibraltar can be found at http://www.gibraltarairquality.gi.

2 Results of the air quality assessment for 2018

The results of the air quality assessments for AQD pollutants SO_2, NO_2 and NO_X, PM_{10}, $PM_{2.5}$, Pb, C_6H_6, CO and O_3 have been listed in Table 2.1 to Table 2.5. Results of the air quality assessments for AQDD4 pollutants As, Cd, Ni and B(a)P are summarised in Table 2.6. These tables summarise information from e-Reporting Data flow G (Attainment) submitted to the CDR (CDR, 2019) relating to compliance with the respective LV, TV or LTO. The tables have been completed as follows:

- Where all measurements were within the relevant LVs in 2018, the table shows this as “OK”.
- Where compliance was determined by supplementary assessment (modelling), this is shown as “OK (m)”. In general, where the status of a location was determined by supplementary assessment, this is indicated by (m) as done here for compliance.
- Where locations were identified as exceeding a LV, this is identified with “>LV”.

A similar approach has been used to summarise results in relation to critical levels (CLs), TVs and LTOs. Zones that complied with the relevant CLs, LVs, TVs or LTOs are shaded blue, while those in exceedance are shaded red. For O_3, exceedances of the LTO but not the TV are shaded purple. “n/a” means that an assessment is not relevant for a zone, such as for the vegetation critical level in agglomeration zones.

Measurements are regarded as the primary basis for the compliance status if both measurements and supplementary assessment estimates show that a threshold has been exceeded. Where locations have been identified as exceeding by modelling this indicates that modelled concentrations were higher than measured concentrations or that measurements were not available (or not required for that zone as determined by a 5-yearly assessment of concentrations relative to lower and upper assessment thresholds in the AQD) and modelled values were therefore used. Modelled concentrations may be higher than measured concentrations because the modelling studies provide estimates of concentrations over the entire zone. It is possible that the locations of the monitoring sites do not correspond to the location of the highest concentration in the zone, for example, there may be no roadside monitoring sites in a zone. Compliance can be determined by modelling where measurements are not available for a zone.

CO concentrations were not modelled for 2018 therefore in zones where measurements were not available compliance has been determined through objective estimation. These are represented as ‘(m)’ in the tables below as objective estimation is treated as a modelling approach in e-Reporting. The objective estimation process is explained further in Section 8.

Table 2.2 shows that 36 zones have not achieved full compliance with the annual NO_2 limit value in 2018. Two zones were also non-compliant with the hourly limit value in 2018. The 1-hour limit value of 200 $\mu g\ m^{-3}$ as a 98th percentile specified in Directive 85/203/EEC was not exceeded in 2018.

Table 2.3 shows that all zones were compliant with both the daily mean limit value and annual mean limit value for PM_{10} before subtraction of natural sources (required by the AQD under Article 20). The exposure concentration obligation for the average of annual mean $PM_{2.5}$ concentrations measured in urban areas of 20 $\mu g\ m^{-3}$ was also met (see Section 6.6).

Table 2.4 shows that all zones were compliant with the limit values for lead, CO and benzene.

Table 2.5 shows that the TV for health was met and the LTO for health for O_3 was exceeded in all zones. The TV for vegetation was met and the LTO for vegetation for O_3 was exceeded in all zones, except for five zones, where both were met.

Table 2.6 shows that three zones have not achieved full compliance with the annual B(a)P target value and four zones have not achieved full compliance with the annual Ni target value in 2018.

Table 2.1 - List of zones and agglomerations in relation to limit value and critical level exceedances for SO_2 in 2018

Zone	Zone code	SO_2 LV for health (1hr mean)	SO_2 LV for health (24hr mean)	SO_2 CL for vegetation (annual mean)	SO_2 CL for vegetation (winter mean)
Greater London Urban Area	UK0001	OK	OK	n/a	n/a
West Midlands Urban Area	UK0002	OK (m)	OK (m)	n/a	n/a
Greater Manchester Urban Area	UK0003	OK	OK	n/a	n/a
West Yorkshire Urban Area	UK0004	OK	OK	n/a	n/a
Tyneside	UK0005	OK (m)	OK (m)	n/a	n/a
Liverpool Urban Area	UK0006	OK	OK	n/a	n/a
Sheffield Urban Area	UK0007	OK (m)	OK (m)	n/a	n/a
Nottingham Urban Area	UK0008	OK	OK	n/a	n/a
Bristol Urban Area	UK0009	OK (m)	OK (m)	n/a	n/a
Brighton/Worthing/Littlehampton	UK0010	OK (m)	OK (m)	n/a	n/a
Leicester Urban Area	UK0011	OK (m)	OK (m)	n/a	n/a
Portsmouth Urban Area	UK0012	OK (m)	OK (m)	n/a	n/a
Teesside Urban Area	UK0013	OK	OK	n/a	n/a
The Potteries	UK0014	OK (m)	OK (m)	n/a	n/a
Bournemouth Urban Area	UK0015	OK (m)	OK (m)	n/a	n/a
Reading/Wokingham Urban Area	UK0016	OK (m)	OK (m)	n/a	n/a
Coventry/Bedworth	UK0017	OK (m)	OK (m)	n/a	n/a
Kingston upon Hull	UK0018	OK	OK	n/a	n/a
Southampton Urban Area	UK0019	OK	OK	n/a	n/a
Birkenhead Urban Area	UK0020	OK (m)	OK (m)	n/a	n/a
Southend Urban Area	UK0021	OK (m)	OK (m)	n/a	n/a
Blackpool Urban Area	UK0022	OK (m)	OK (m)	n/a	n/a
Preston Urban Area	UK0023	OK (m)	OK (m)	n/a	n/a
Glasgow Urban Area	UK0024	OK (m)	OK (m)	n/a	n/a
Edinburgh Urban Area	UK0025	OK	OK	n/a	n/a
Cardiff Urban Area	UK0026	OK (m)	OK (m)	n/a	n/a
Swansea Urban Area	UK0027	OK	OK	n/a	n/a
Belfast Urban Area	UK0028	OK	OK	n/a	n/a
Eastern	UK0029	OK	OK	OK	OK
South West	UK0030	OK (m)	OK (m)	OK (m)	OK (m)
South East	UK0031	OK	OK	OK	OK
East Midlands	UK0032	OK	OK	OK	OK
North West & Merseyside	UK0033	OK (m)	OK (m)	OK (m)	OK (m)
Yorkshire & Humberside	UK0034	OK	OK	OK (m)	OK (m)
West Midlands	UK0035	OK (m)	OK (m)	OK (m)	OK (m)
North East	UK0036	OK (m)	OK (m)	OK (m)	OK (m)
Central Scotland	UK0037	OK	OK	OK (m)	OK (m)
North East Scotland	UK0038	OK (m)	OK (m)	OK (m)	OK (m)
Highland	UK0039	OK (m)	OK (m)	OK (m)	OK (m)
Scottish Borders	UK0040	OK (m)	OK (m)	OK (m)	OK (m)
South Wales	UK0041	OK	OK	OK	OK (m)
North Wales	UK0042	OK (m)	OK (m)	OK (m)	OK (m)
Northern Ireland	UK0043	OK	OK	OK (m)	OK (m)

Table 2.2 - List of zones and agglomerations in relation to limit value and critical level exceedances for NO_2 and NO_X in 2018 (* zones for which time extensions applied until 2015)

Zone	Zone code	NO_2 LV for health (1-hr mean)	NO_2 LV for health (annual mean)	NO_x CL for vegetation (annual mean)
Greater London Urban Area	UK0001	> LV	> LV	n/a
West Midlands Urban Area	UK0002	OK	> LV (m)	n/a
Greater Manchester Urban Area	UK0003	OK	> LV (m)	n/a
West Yorkshire Urban Area	UK0004	OK	> LV	n/a
Tyneside	UK0005	OK	> LV (m)	n/a
Liverpool Urban Area	UK0006	OK	> LV (m)	n/a
Sheffield Urban Area	UK0007	OK	> LV (m)	n/a
Nottingham Urban Area*	UK0008	OK	> LV (m)	n/a
Bristol Urban Area	UK0009	OK	> LV	n/a
Brighton/Worthing/Littlehampton	UK0010	OK	OK	n/a
Leicester Urban Area*	UK0011	OK	> LV (m)	n/a
Portsmouth Urban Area*	UK0012	OK	> LV (m)	n/a
Teesside Urban Area	UK0013	OK	> LV (m)	n/a
The Potteries	UK0014	OK	> LV	n/a
Bournemouth Urban Area	UK0015	OK	> LV (m)	n/a
Reading/Wokingham Urban Area	UK0016	OK	> LV (m)	n/a
Coventry/Bedworth	UK0017	OK	> LV (m)	n/a
Kingston upon Hull	UK0018	OK	> LV (m)	n/a
Southampton Urban Area	UK0019	OK	> LV (m)	n/a
Birkenhead Urban Area*	UK0020	OK	OK	n/a
Southend Urban Area*	UK0021	OK	> LV (m)	n/a
Blackpool Urban Area	UK0022	OK	OK	n/a
Preston Urban Area	UK0023	OK	OK	n/a
Glasgow Urban Area	UK0024	OK	> LV	n/a
Edinburgh Urban Area*	UK0025	OK	> LV	n/a
Cardiff Urban Area*	UK0026	OK (m)	> LV (m)	n/a
Swansea Urban Area	UK0027	OK	> LV (m)	n/a
Belfast Urban Area	UK0028	OK	> LV	n/a
Eastern	UK0029	OK	> LV	OK
South West	UK0030	OK	> LV (m)	OK
South East	UK0031	OK	> LV (m)	OK
East Midlands	UK0032	OK	> LV (m)	OK
North West & Merseyside	UK0033	OK	> LV (m)	OK (m)
Yorkshire & Humberside	UK0034	OK	> LV (m)	OK
West Midlands	UK0035	OK	> LV (m)	OK (m)
North East	UK0036	OK	> LV (m)	OK (m)
Central Scotland*	UK0037	OK	> LV (m)	OK (m)
North East Scotland	UK0038	OK	> LV (m)	OK (m)
Highland	UK0039	OK	OK	OK (m)
Scottish Borders	UK0040	OK	OK	OK
South Wales	UK0041	> LV	> LV	OK
North Wales*	UK0042	OK	> LV (m)	OK
Northern Ireland	UK0043	OK	OK	OK (m)

Table 2.3 - List of zones and agglomerations in relation to limit value exceedances for PM_{10}, limit value and target value exceedances for $PM_{2.5}$ in 2018 (after subtraction of contribution from natural sources where applicable)

Zone	Zone code	PM_{10} LV for health (24-hr mean)	PM_{10} LV for health (annual mean)	$PM_{2.5}$ LV for health (annual mean) Stage 1	$PM_{2.5}$ LV for health (annual mean) Stage 2*
Greater London Urban Area	UK0001	OK	OK	OK	OK
West Midlands Urban Area	UK0002	OK	OK	OK	OK
Greater Manchester Urban Area	UK0003	OK	OK	OK	OK
West Yorkshire Urban Area	UK0004	OK	OK	OK	OK
Tyneside	UK0005	OK	OK	OK	OK
Liverpool Urban Area	UK0006	OK	OK	OK	OK
Sheffield Urban Area	UK0007	OK	OK	OK	OK
Nottingham Urban Area	UK0008	OK	OK	OK	OK
Bristol Urban Area	UK0009	OK	OK	OK	OK
Brighton/Worthing/Littlehampton	UK0010	OK (m)	OK (m)	OK	OK
Leicester Urban Area	UK0011	OK	OK	OK	OK
Portsmouth Urban Area	UK0012	OK	OK	OK (m)	OK (m)
Teesside Urban Area	UK0013	OK	OK	OK	OK
The Potteries	UK0014	OK	OK	OK	OK
Bournemouth Urban Area	UK0015	OK (m)	OK (m)	OK	OK
Reading/Wokingham Urban Area	UK0016	OK	OK	OK	OK
Coventry/Bedworth	UK0017	OK	OK	OK	OK
Kingston upon Hull	UK0018	OK	OK	OK	OK
Southampton Urban Area	UK0019	OK (m)	OK (m)	OK	OK
Birkenhead Urban Area	UK0020	OK (m)	OK (m)	OK	OK
Southend Urban Area	UK0021	OK (m)	OK (m)	OK (m)	OK (m)
Blackpool Urban Area	UK0022	OK (m)	OK (m)	OK	OK
Preston Urban Area	UK0023	OK (m)	OK (m)	OK	OK
Glasgow Urban Area	UK0024	OK	OK	OK	OK
Edinburgh Urban Area	UK0025	OK	OK	OK	OK
Cardiff Urban Area	UK0026	OK	OK	OK	OK
Swansea Urban Area	UK0027	OK	OK	OK	OK
Belfast Urban Area	UK0028	OK	OK	OK	OK
Eastern	UK0029	OK	OK	OK	OK
South West	UK0030	OK	OK	OK	OK
South East	UK0031	OK	OK	OK	OK
East Midlands	UK0032	OK	OK	OK	OK
North West & Merseyside	UK0033	OK	OK	OK	OK
Yorkshire & Humberside	UK0034	OK	OK	OK	OK
West Midlands	UK0035	OK	OK	OK	OK
North East	UK0036	OK	OK	OK	OK
Central Scotland	UK0037	OK	OK	OK	OK
North East Scotland	UK0038	OK	OK	OK	OK
Highland	UK0039	OK (m)	OK (m)	OK (m)	OK (m)
Scottish Borders	UK0040	OK (m)	OK (m)	OK (m)	OK (m)
South Wales	UK0041	OK	OK	OK	OK
North Wales	UK0042	OK (m)	OK (m)	OK (m)	OK (m)
Northern Ireland	UK0043	OK	OK	OK	OK

* The stage 2 indicative limit value for $PM_{2.5}$ is not currently in force.

Table 2.4 - List of zones and agglomerations in relation to limit value exceedances for lead, benzene and CO in 2018

Zone	Zone code	Lead LV for health (annual mean)	Benzene LV for health (annual mean)	CO LV for health (8-hr mean)
Greater London Urban Area	UK0001	OK	OK	OK
West Midlands Urban Area	UK0002	OK (m)	OK	OK (m)
Greater Manchester Urban Area	UK0003	OK (m)	OK	OK (m)
West Yorkshire Urban Area	UK0004	OK (m)	OK	OK
Tyneside	UK0005	OK (m)	OK	OK (m)
Liverpool Urban Area	UK0006	OK (m)	OK	OK (m)
Sheffield Urban Area	UK0007	OK	OK	OK (m)
Nottingham Urban Area	UK0008	OK (m)	OK	OK (m)
Bristol Urban Area	UK0009	OK (m)	OK (m)	OK (m)
Brighton/Worthing/Littlehampton	UK0010	OK (m)	OK (m)	OK (m)
Leicester Urban Area	UK0011	OK (m)	OK (m)	OK (m)
Portsmouth Urban Area	UK0012	OK (m)	OK (m)	OK (m)
Teesside Urban Area	UK0013	OK (m)	OK	OK (m)
The Potteries	UK0014	OK (m)	OK	OK (m)
Bournemouth Urban Area	UK0015	OK (m)	OK (m)	OK (m)
Reading/Wokingham Urban Area	UK0016	OK (m)	OK (m)	OK (m)
Coventry/Bedworth	UK0017	OK (m)	OK (m)	OK (m)
Kingston upon Hull	UK0018	OK (m)	OK (m)	OK (m)
Southampton Urban Area	UK0019	OK (m)	OK	OK (m)
Birkenhead Urban Area	UK0020	OK (m)	OK (m)	OK (m)
Southend Urban Area	UK0021	OK (m)	OK (m)	OK (m)
Blackpool Urban Area	UK0022	OK (m)	OK (m)	OK (m)
Preston Urban Area	UK0023	OK (m)	OK (m)	OK (m)
Glasgow Urban Area	UK0024	OK (m)	OK	OK (m)
Edinburgh Urban Area	UK0025	OK (m)	OK (m)	OK
Cardiff Urban Area	UK0026	OK (m)	OK (m)	OK
Swansea Urban Area	UK0027	OK	OK (m)	OK
Belfast Urban Area	UK0028	OK	OK	OK
Eastern	UK0029	OK	OK	OK (m)
South West	UK0030	OK	OK	OK (m)
South East	UK0031	OK	OK	OK (m)
East Midlands	UK0032	OK	OK (m)	OK (m)
North West & Merseyside	UK0033	OK	OK	OK (m)
Yorkshire & Humberside	UK0034	OK	OK	OK (m)
West Midlands	UK0035	OK	OK	OK (m)
North East	UK0036	OK (m)	OK	OK (m)
Central Scotland	UK0037	OK	OK	OK (m)
North East Scotland	UK0038	OK (m)	OK (m)	OK (m)
Highland	UK0039	OK (m)	OK (m)	OK (m)
Scottish Borders	UK0040	OK	OK (m)	OK (m)
South Wales	UK0041	OK	OK (m)	OK (m)
North Wales	UK0042	OK (m)	OK (m)	OK (m)
Northern Ireland	UK0043	OK (m)	OK (m)	OK (m)

Table 2.5 - List of zones and agglomerations in relation to target value and long-term objective exceedances for ozone in 2018 (*Met TV, > LTO means that the target value was achieved but the long-term objective was not)

Zone	Zone code	O_3 TV and LTO for health (8-hr mean)	O_3 TV and LTO for vegetation (AOT40)
Greater London Urban Area	UK0001	Met TV, > LTO	Met TV, > LTO
West Midlands Urban Area	UK0002	Met TV, > LTO	Met TV, > LTO
Greater Manchester Urban Area	UK0003	Met TV, > LTO	Met TV, > LTO
West Yorkshire Urban Area	UK0004	Met TV, > LTO	Met TV, > LTO (m)
Tyneside	UK0005	Met TV, > LTO	Met TV, > LTO (m)
Liverpool Urban Area	UK0006	Met TV, > LTO	Met TV, > LTO (m)
Sheffield Urban Area	UK0007	Met TV, > LTO	Met TV, > LTO
Nottingham Urban Area	UK0008	Met TV, > LTO	Met TV, > LTO (m)
Bristol Urban Area	UK0009	Met TV, > LTO	Met TV, > LTO
Brighton/Worthing/Littlehampton	UK0010	Met TV, > LTO	Met TV, > LTO
Leicester Urban Area	UK0011	Met TV, > LTO	Met TV, > LTO
Portsmouth Urban Area	UK0012	Met TV, > LTO	Met TV, > LTO (m)
Teesside Urban Area	UK0013	Met TV, > LTO	Met TV, > LTO (m)
The Potteries	UK0014	Met TV, > LTO	Met TV, > LTO
Bournemouth Urban Area	UK0015	Met TV, > LTO	Met TV, > LTO
Reading/Wokingham Urban Area	UK0016	Met TV, > LTO	Met TV, > LTO
Coventry/Bedworth	UK0017	Met TV, > LTO	Met TV, > LTO
Kingston upon Hull	UK0018	Met TV, > LTO	Met TV, > LTO (m)
Southampton Urban Area	UK0019	Met TV, > LTO	Met TV, > LTO
Birkenhead Urban Area	UK0020	Met TV, > LTO	Met TV, > LTO
Southend Urban Area	UK0021	Met TV, > LTO	Met TV, > LTO
Blackpool Urban Area	UK0022	Met TV, > LTO	Met TV, > LTO
Preston Urban Area	UK0023	Met TV, > LTO	Met TV, > LTO
Glasgow Urban Area	UK0024	Met TV, > LTO	OK
Edinburgh Urban Area	UK0025	Met TV, > LTO	OK
Cardiff Urban Area	UK0026	Met TV, > LTO	Met TV, > LTO
Swansea Urban Area	UK0027	Met TV, > LTO	Met TV, > LTO (m)
Belfast Urban Area	UK0028	Met TV, > LTO (m)	OK
Eastern	UK0029	Met TV, > LTO	Met TV, > LTO
South West	UK0030	Met TV, > LTO	Met TV, > LTO
South East	UK0031	Met TV, > LTO	Met TV, > LTO
East Midlands	UK0032	Met TV, > LTO	Met TV, > LTO
North West & Merseyside	UK0033	Met TV, > LTO	Met TV, > LTO
Yorkshire & Humberside	UK0034	Met TV, > LTO	Met TV, > LTO
West Midlands	UK0035	Met TV, > LTO	Met TV, > LTO
North East	UK0036	Met TV, > LTO	Met TV, > LTO (m)
Central Scotland	UK0037	Met TV, > LTO	OK
North East Scotland	UK0038	Met TV, > LTO (m)	OK
Highland	UK0039	Met TV, > LTO	Met TV, > LTO
Scottish Borders	UK0040	Met TV, > LTO	Met TV, > LTO
South Wales	UK0041	Met TV, > LTO	Met TV, > LTO
North Wales	UK0042	Met TV, > LTO	Met TV, > LTO
Northern Ireland	UK0043	Met TV, > LTO	Met TV, > LTO

Table 2.6 - List of zones and agglomerations where levels exceed or do not exceed target values for arsenic, cadmium, nickel and benzo(a)pyrene in 2018

Zone	Zone code	As TV	Cd TV	Ni TV	B(a)P TV
Greater London Urban Area	UK0001	OK	OK	OK	OK
West Midlands Urban Area	UK0002	OK (m)	OK (m)	OK (m)	OK (m)
Greater Manchester Urban Area	UK0003	OK (m)	OK (m)	OK (m)	OK
West Yorkshire Urban Area	UK0004	OK (m)	OK (m)	OK (m)	OK
Tyneside	UK0005	OK (m)	OK (m)	OK (m)	OK
Liverpool Urban Area	UK0006	OK (m)	OK (m)	OK (m)	OK
Sheffield Urban Area	UK0007	OK	OK	> TV (m)	OK
Nottingham Urban Area	UK0008	OK (m)	OK (m)	OK (m)	OK
Bristol Urban Area	UK0009	OK (m)	OK (m)	OK (m)	OK (m)
Brighton/Worthing/Littlehampton	UK0010	OK (m)	OK (m)	OK (m)	OK (m)
Leicester Urban Area	UK0011	OK (m)	OK (m)	OK (m)	OK (m)
Portsmouth Urban Area	UK0012	OK (m)	OK (m)	OK (m)	OK (m)
Teesside Urban Area	UK0013	OK (m)	OK (m)	OK (m)	OK
The Potteries	UK0014	OK (m)	OK (m)	OK (m)	OK (m)
Bournemouth Urban Area	UK0015	OK (m)	OK (m)	OK (m)	OK (m)
Reading/Wokingham Urban Area	UK0016	OK (m)	OK (m)	OK (m)	OK (m)
Coventry/Bedworth	UK0017	OK (m)	OK (m)	OK (m)	OK (m)
Kingston upon Hull	UK0018	OK (m)	OK (m)	OK (m)	OK (m)
Southampton Urban Area	UK0019	OK (m)	OK (m)	OK (m)	OK (m)
Birkenhead Urban Area	UK0020	OK (m)	OK (m)	OK (m)	OK (m)
Southend Urban Area	UK0021	OK (m)	OK (m)	OK (m)	OK (m)
Blackpool Urban Area	UK0022	OK (m)	OK (m)	OK (m)	OK (m)
Preston Urban Area	UK0023	OK (m)	OK (m)	OK (m)	OK (m)
Glasgow Urban Area	UK0024	OK (m)	OK (m)	OK (m)	OK
Edinburgh Urban Area	UK0025	OK (m)	OK (m)	OK (m)	OK
Cardiff Urban Area	UK0026	OK (m)	OK (m)	OK (m)	OK
Swansea Urban Area	UK0027	OK	OK	> TV	> TV (m)
Belfast Urban Area	UK0028	OK	OK	OK	OK
Eastern	UK0029	OK	OK	OK	OK
South West	UK0030	OK	OK	OK	OK
South East	UK0031	OK	OK	OK	OK
East Midlands	UK0032	OK	OK	OK	OK
North West & Merseyside	UK0033	OK	OK	OK	OK
Yorkshire & Humberside	UK0034	OK	OK	> TV (m)	> TV
West Midlands	UK0035	OK	OK	OK	OK (m)
North East	UK0036	OK (m)	OK (m)	OK (m)	OK
Central Scotland	UK0037	OK	OK	OK	OK
North East Scotland	UK0038	OK (m)	OK (m)	OK (m)	OK (m)
Highland	UK0039	OK (m)	OK (m)	OK (m)	OK
Scottish Borders	UK0040	OK	OK	OK	OK (m)
South Wales	UK0041	OK	OK	> TV (m)	> TV (m)
North Wales	UK0042	OK (m)	OK (m)	OK (m)	OK (m)
Northern Ireland	UK0043	OK (m)	OK (m)	OK (m)	OK

3 NO_2/NO_X

3.1 Introduction

3.1.1 Limit values

Two limit values for ambient NO_2 concentrations are set out in the Air Quality Directive (AQD). These have been specified for the protection of human health and came into force from 01/01/2010. These limit values are:

- An annual mean concentration of 40 µg m^{-3}.
- An hourly concentration of 200 µg m^{-3}, with 18 permitted exceedances each year.

A critical level for NO_X for the protection of vegetation has also been specified in the Directive:

- An annual mean concentration 30 µg m^{-3} (NO_x as NO_2).

Because this critical level is designed to protect vegetation, it only applies in vegetation areas as defined in the Directive. This critical level has been in force since 2001.

Results of the assessment in terms of comparisons of the modelled concentrations with the annual mean limit value for NO_2 and critical level for NO_X have been reported in e-Reporting Data flow G (CDR, 2019).

3.1.2 Annual mean modelling

Annual mean concentrations of NO_X and NO_2 have been modelled for the UK for 2018 at background and roadside locations. Figure 3-1 and Figure 3-2 present maps of annual mean NO_2 concentrations for these locations in 2018. These maps have been used for comparison with the annual mean NO_2 limit value described above. To calculate NO_2 annual mean maps, NO_X annual mean concentration maps at background and roadside locations were first calculated.

The modelling methods for annual mean NO_X and NO_2 have been developed over several years (Stedman and Bush, 2000, Stedman et al., 2001a, Stedman et al., 2001b, Stedman et al., 2002, 2003, 2005 and 2006, Kent et al., 2007a and 2007b, Grice et al., 2009, 2010a and 2010b, Brookes et al., 2011, 2012, 2013, 2015, 2016, 2017, 2019a and 2019b).

Figure 3-1 - Annual mean background NO_2 concentration, 2018 ($\mu g\ m^{-3}$)

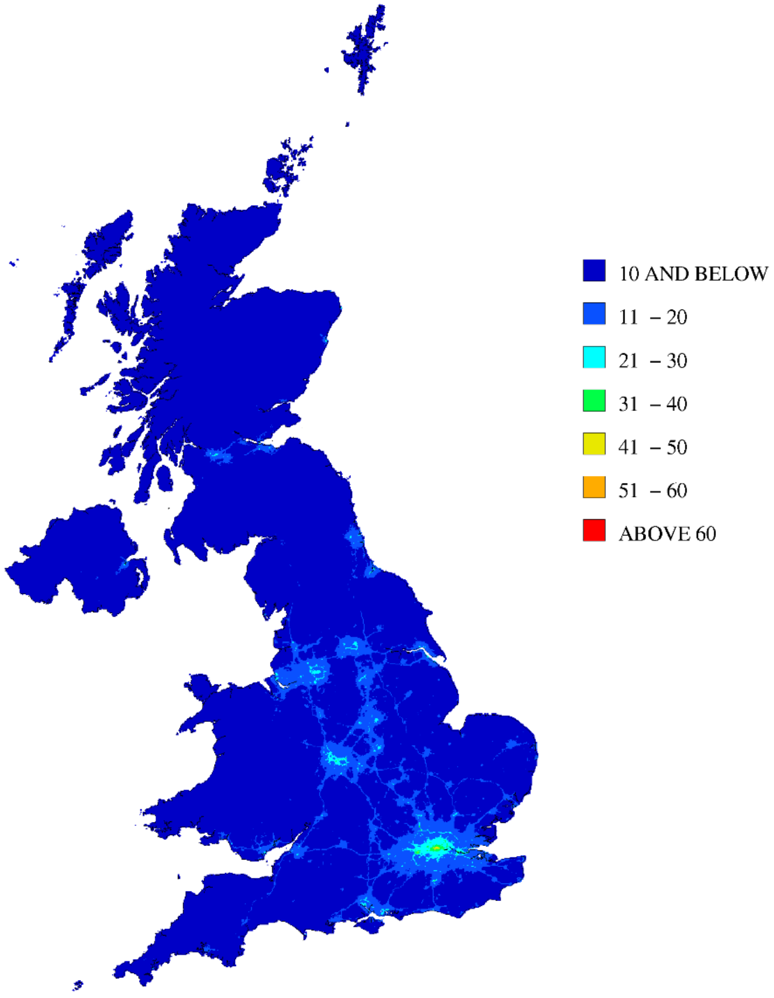

Figure 3-2 - Urban major roads, annual mean roadside NO_2 concentration, 2018 ($\mu g\ m^{-3}$)

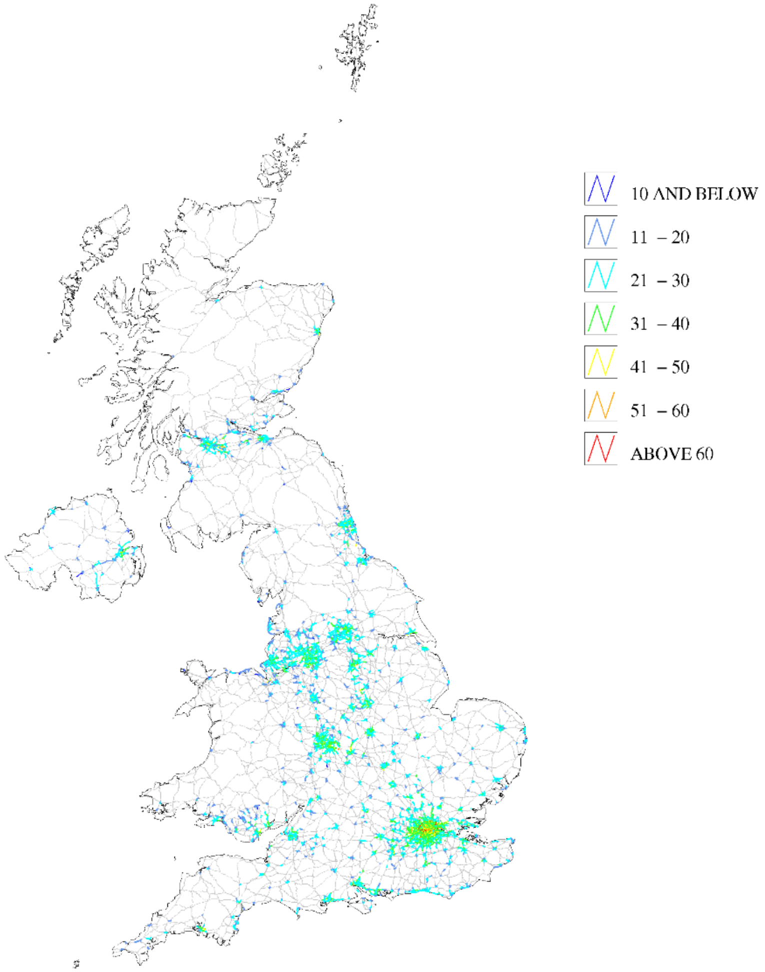

Figure 3-3 - Annual mean map of NO_X concentrations for comparison with the NO_X vegetation critical level, 2018 ($\mu g\ m^{-3}$, as NO_2)

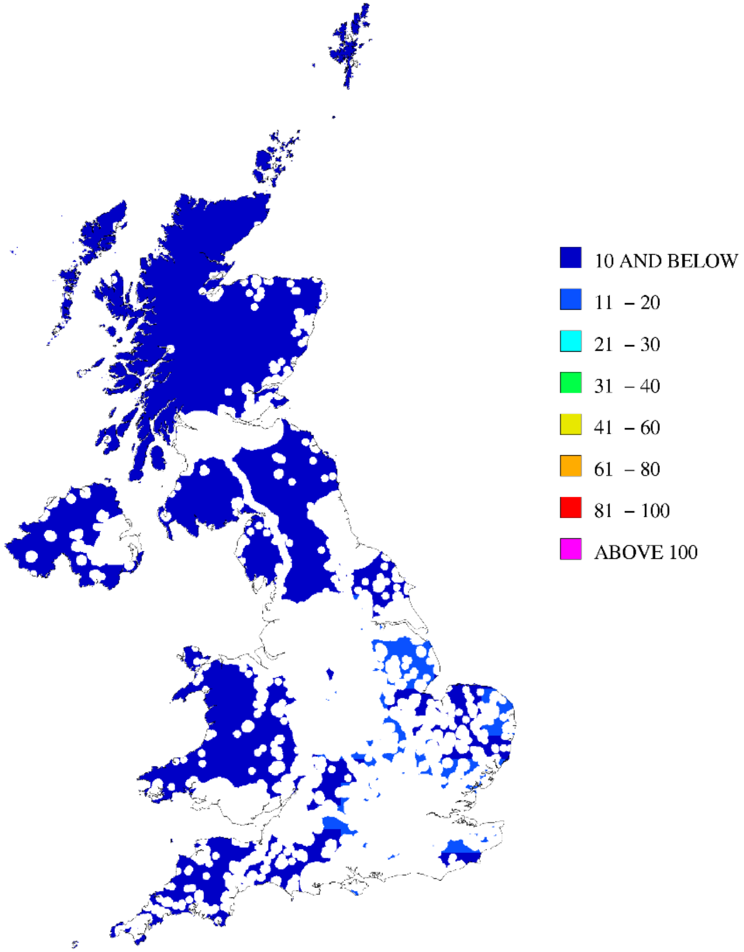

Figure 3-4 - Plot of annual mean against 99.8th percentile hourly NO_2 concentrations in 2018

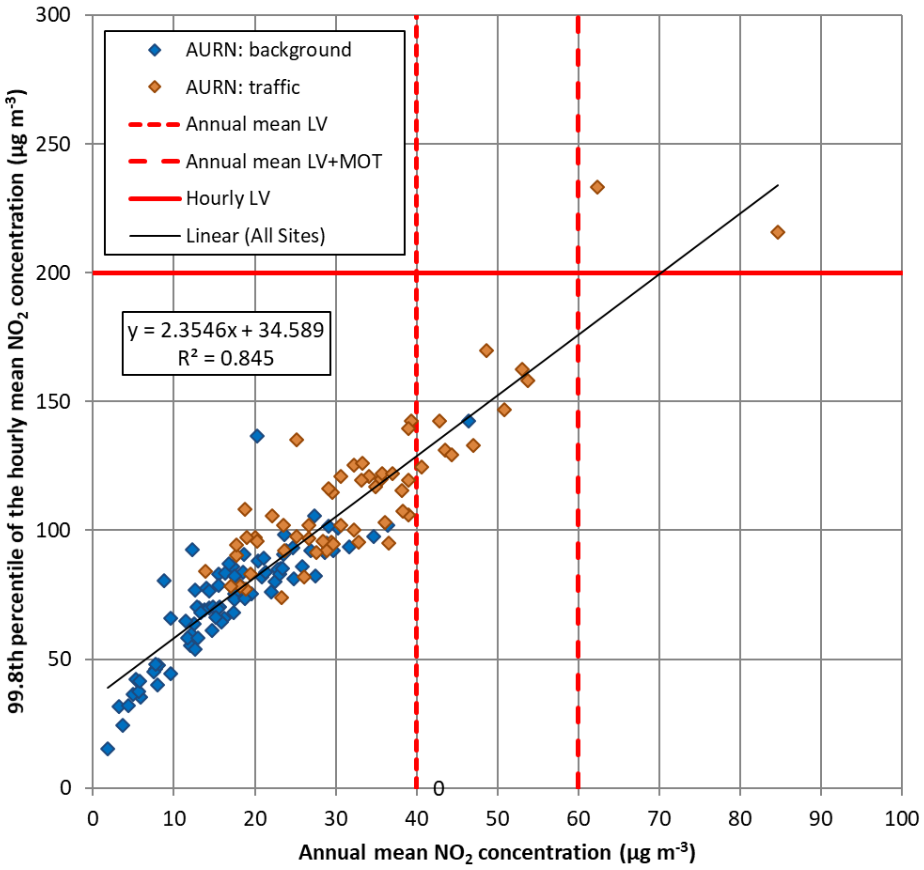

3.1.3 Overview of the PCM model for NO_x and NO_2

Figure 3-5 shows a simplified flow diagram of the PCM model for NO_x and NO_2. A summary of the PCM model method, input and assumptions for NO_x and NO_2 is presented in Table 3.1.

Figure 3-5 - Flow diagram for PCM NO_x and NO_2 model

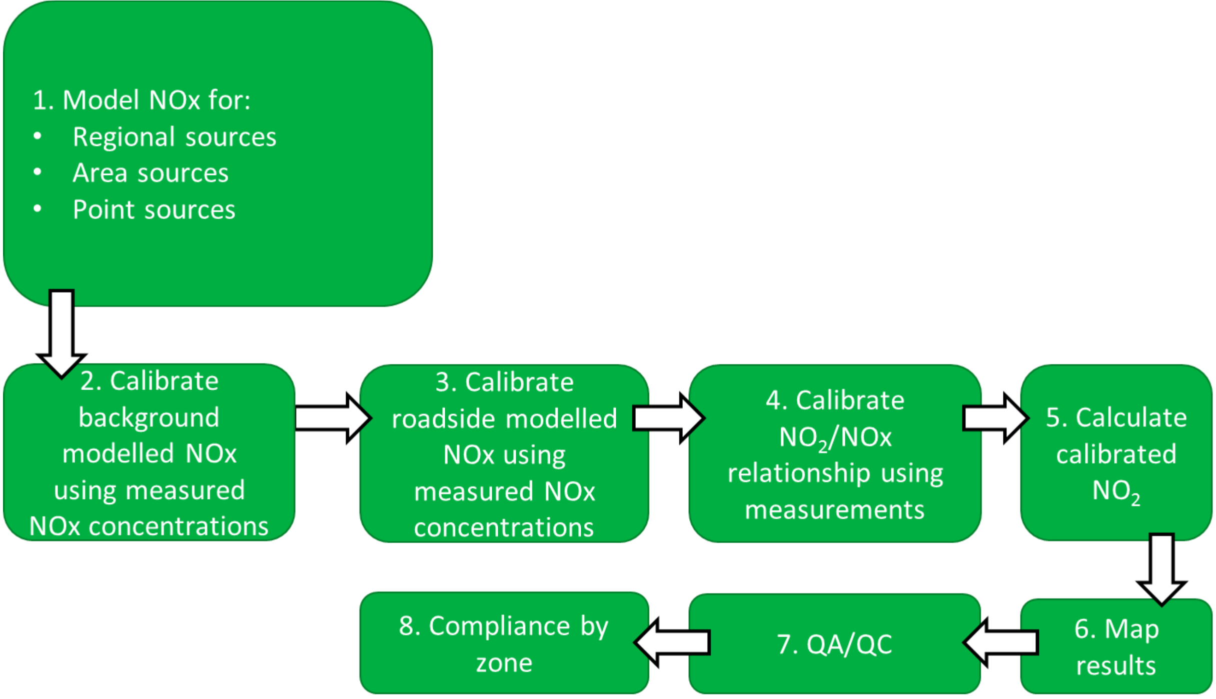

Table 3.1 - PCM model method, input and assumptions summary for NO_x and NO_2

Heading	Component	Details
General	Pollutant	NO_x and NO_2
	Year	2018
	Locations modelled	Background and traffic locations
	Metric	Annual mean
Input data	Emission inventory	NAEI 2017
	Energy projections	Energy Projections 2017
	Road traffic counts	2017
	Road transport activity projections	DfT (2018) traffic (re-based to 2017 NAEI), DfT (2019) car sales projections, TfL traffic (2019) and fleet (2018) projections for London
	Road transport emission factors	COPERT 5
	Measurement data	2018
	Meteorological data	Hourly data from Waddington 2018
Model components	Regional	Interpolated from Rural NOx measurements adjusted for local contribution
	Large point sources	389 sources modelled using ADMS 5.2
	Small point sources	PCM small points model
	ETS point sources	PCM small points model
	Large ETS point sources	80 sources modelled using ADMS 5.2
	Area sources	PCM dispersion kernels generated using ADMS 5.2. Time varying emissions for road transport and domestic sources. PCM small points model for industrial combustion emissions.

Heading	Component	Details
	Roadside increment	PCM Roads Kernel Model using ADMS-Roads 4.1
Calibration	Model calibrated?	Yes
	Number of background stations in calibration	81
	Number of traffic stations in calibration	46
Pollutant specific	Method used to calculate NO_2 from NO_x	Oxidant partitioning model, calibrated for 2018
	Source of f-NO_2 assumptions	NAEI January 2019

3.1.4 Outline of the annual mean model for NO_X

The 1 km x 1 km annual mean background NO_X concentration map has been calculated by summing the contributions from:

- Large point sources
- Small point sources
- Distant sources (characterised by the rural background concentration)
- Local area sources
- Point sources with emissions estimates for air quality pollutants based on reported carbon emissions (ETS points)

The area source model has been calibrated using data from the national automatic monitoring networks (AURN) for 2018. At locations close to busy roads an additional roadside contribution has been added to account for contributions to total NO_X from road traffic sources. The contributions from each of these components are described in Section 3.3.

3.1.5 Outline of the annual mean model for NO_2

NO_2 concentrations have been calculated from the modelled NO_X concentrations derived using the approach outlined above using a calibrated version of the updated oxidant-partitioning model described in Section 3.4. This model describes the complex inter-relationships between NO, NO_2 and ozone as a set of chemically coupled species (Jenkin, 2004; Murrells et al., 2008; Jenkin, 2012). This approach provides additional insights into the factors controlling ambient levels of NO_2 (and O_3), and how they may vary with NO_X concentration.

3.1.6 Annual mean NO_X concentration in vegetation areas

The background NO_X map has also been used to generate a map of annual mean NO_X concentrations in vegetation areas for comparison with the NO_X critical level described above; this map is shown in Figure 3-3. This map has been calculated by removing non-vegetation areas from the background NO_X map and calculating the zonal mean of the 1 km x 1 km grid squares for a 30 km x 30 km grid so that it complies with the criteria set out in the AQD. Mean concentrations on a 30 km x 30 km grid have been used to prevent the influence of any urban area appearing unrealistically large on adjacent vegetation areas. Thus, the modelled concentrations in vegetation areas should be representative of approximately 1000 km^2 as specified in the AQD for monitoring sites used to assess concentrations for the vegetation critical level.

3.1.7 Assessment for the 1-hour limit value

Hourly concentrations for comparison with the 1-hour limit value have not been modelled due to the considerable uncertainties involved in modelling at such a fine temporal scale.

The annual mean limit value is expected to be more stringent than the 1-hour limit value in the majority of situations (AQEG, 2004). This is illustrated in Figure 3-4 which is a scatter plot of annual mean NO_2 in 2018 against the 99.8th percentile of hourly mean concentration (equivalent to 18 exceedances in the same year). This plot shows that more sites exceed the annual mean limit value of 40 µg m^{-3} than the 200 µg m^{-3} hourly limit value.

3.1.8 Chapter structure

This chapter describes modelling work carried out for 2018 to assess compliance with the NO_X critical level and annual mean NO_2 limit value. Emission estimates for NO_X are described in Section 3.2.

Section 3.3 describes the NO_X modelling methods. Details of the methods used to estimate ambient NO_2 from NO_X are presented in Section 3.4. Verification of and source apportionment for the modelling results are presented in Section 3.5.

3.2 NO_X emissions

The NO_X modelling is underpinned by the UK National Atmospheric Emissions Inventory 2017 (NAEI 2017) NO_X emissions estimates (Richmond et al., 2019). Emissions projections have been provided by the NAEI (Passant, 2019) based on BEIS EEP 2018 energy and emissions projections (BEIS, 2018). Figure 3-6 shows the UK total NO_X emissions for 2017 and emissions projections for 2020, 2025 and 2030 split by SNAP code, with the coding described in Table 3.2. Values for intermediate years have been interpolated in this figure. The figure shows that NO_X emissions in 2018 are dominated by three main sources:

- SNAP 7: road transport (exhaust emissions)
- Combustion point sources (SNAP codes 1, 2 and 3)
- SNAP 8: other transport & mobile machinery (ships)

NO_X emissions are predicted to decrease by just over a third between 2017 and 2030, with a decline in road transport exhaust emissions and combustion point sources over this period.

Figure 3-6 - Total UK NO_X emissions for 2017 and emissions projections up to 2030 by SNAP code from NAEI 2017

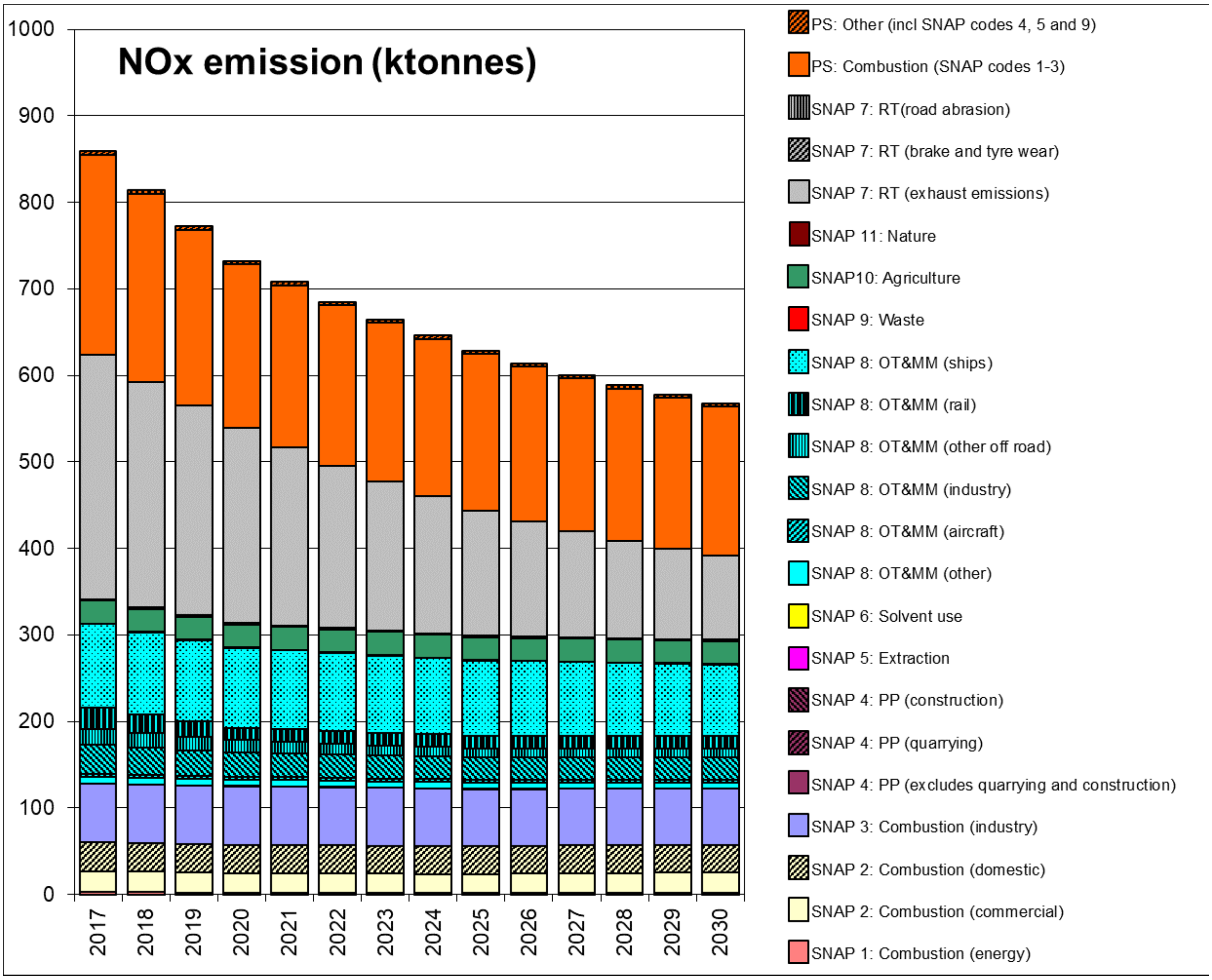

Table 3.2 - Description of SNAP sector coding

Short code	Description
SNAP 1: Combustion (energy)	SNAP 1: Combustion in energy production & transformation
SNAP 2: Combustion (commercial)	SNAP 2: Combustion in Commercial, Institutional & residential & agriculture (excludes domestic)
SNAP 2: Combustion (domestic)	SNAP 2: Combustion in Commercial, Institutional & residential & agriculture (domestic only)
SNAP 3: Combustion (industry)	SNAP 3: Combustion in industry
SNAP 4: PP (excludes quarrying and construction)	SNAP 4: Production processes (excludes quarrying and construction)
SNAP 4: PP (quarrying)	SNAP 4: Production processes (quarrying)
SNAP 4: PP (construction)	SNAP 4: Production processes (construction)
SNAP 5: Extraction	SNAP 5: Extraction & distribution of fossil fuels
SNAP 6: Solvent use	SNAP 6: Solvent use
SNAP 8: OT&MM (other)	SNAP 8: Other Transport & mobile machinery (other)
SNAP 8: OT&MM (aircraft)	SNAP 8: Other Transport & mobile machinery (aircraft)
SNAP 8: OT&MM (industry)	SNAP 8: Other Transport & mobile machinery (industry off road mobile machinery)
SNAP 8: OT&MM (other off road)	SNAP 8: Other Transport & mobile machinery (other off road mobile machinery)
SNAP 8: OT&MM (rail)	SNAP 8: Other Transport & mobile machinery (rail)
SNAP 8: OT&MM (ships)	SNAP 8: Other Transport & mobile machinery (ships)
SNAP 9: Waste	SNAP 9: Waste treatment and disposal
SNAP10: Agriculture	SNAP10: Agriculture forestry & land use change
SNAP 11: Nature	SNAP 11: Nature
SNAP 7: RT (exhaust emissions)	SNAP 7: Road transport (exhaust emissions)
SNAP 7: RT (brake and tyre wear)	SNAP 7: Road transport (brake and tyre wear)
SNAP 7: RT (road abrasion)	SNAP 7: Road transport (road abrasion)
PS: Combustion (SNAP codes 1-3) *	Combustion point sources (SNAP codes 1-3)
PS: Other (incl. SNAP codes 4, 5 and 9) *	Other point sources (including SNAP codes 4, 5 and 9)

* PS stands for Point Sources. Emissions that are mapped by the NAEI as area sources are summarised using the split in the rows above, and those that are mapped as point sources are summarised using the split in the last 2 rows of Table 3.2.

3.3 NO_X modelling

3.3.1 NO_X contributions from large point sources

Point sources in the NAEI 2017 have been classified as large if they fulfil either of the following criteria:

- Annual NO_X emissions in the NAEI 2017 are greater than 500 tonnes for any given plant
- Stack parameters are already available for any given plant in the PCM stack parameters database (described in more detail below)

Contributions to ground level annual mean NO_X concentrations from large point sources in the NAEI 2017 were estimated by modelling each source explicitly using the atmospheric dispersion model ADMS 5.2 and sequential meteorological data for 2018 from Waddington. A total of 389 large point sources were modelled. Surface roughness was assumed to be 0.1 m at both the dispersion and meteorological sites. Concentrations were calculated for a 99 km x 99 km square composed of a regularly spaced 1 km x 1 km resolution receptor grid. Each receptor grid was centred on the point source. For each large point source information was retrieved from the PCM stack parameters database. This database has been developed over a period of time under the Modelling of Ambient Air Quality (MAAQ) contract and its predecessors. The database is updated annually as required. Data sources for this database include a survey of Part A authorisation notices held by the Environment Agency and previously collated datasets on emission release parameters from large SO_2 point sources (Abbott and Vincent, 1999). Parameters used in the modelling from the stack parameters database include:

- Stack height
- Stack diameter
- Discharge velocity
- Discharge temperature

Where release parameters were unavailable, engineering assumptions have been applied based on information available for similar plant.

The NAEI emissions for large point sources are for the year 2017; however, the year 2018 has been modelled for the assessment. The modelled concentrations for 2018 have been scaled to 2018 using projection factors calculated from NAEI source sector specific emissions total for point sources for 2017 and NAEI emissions projections for 2018 (Passant, 2019). Closure of plant or activities are taken into account when deriving the source sector projection factors by subtracting the base year emissions associated with plant closure from the relevant source sector total for point sources for the NAEI base year. Any point sources in the NAEI base year that closed before the start or early in the current assessment year are removed from the modelling, based on recommendations from the NAEI team (Passant pers. comm. 2018a).

3.3.2 NO_X contributions from small point sources

Contributions from NO_X point sources in the NAEI 2017 that were not classified as large point sources (see Section 3.3.1) were modelled using the small point source model described in Appendix 3. In line with the method applied for the large point sources the NAEI 2017 emissions for small point sources have been scaled to 2018 using the same source sector specific projection factors applied to the large point sources.

3.3.3 NO_X contributions from ETS point sources

The NAEI 2017 includes point source emissions estimates derived from carbon emissions data reported under the EU-Emissions Trading Scheme (ETS), most recently described in Tsagatakis et al. (2019). These point sources are referred to as ETS points in this report. These derived air quality pollutant emissions are particularly uncertain and therefore in previous assessments (e.g. Brookes et al., 2017) emissions were capped at reporting thresholds and treated as small point sources. For the 2016 assessment (Brookes et al., 2019a) the NAEI recommended treating the ETS points that have emissions greater than the large points modelling threshold as large points and not to apply a cap (Passant pers. comm. 2017). The 2018 assessment continues this approach. Thus, based on the criteria for the treatment of large point sources described above (Section 3.3.1), 80 ETS point sources were modelled as an additional set of large point sources (using the approach described in Section 3.3.1). ETS points that were not classified as large point sources were modelled using the small points approach (described in Appendix 3). In line with the method applied for the large point sources, the NAEI 2017 emissions for ETS point sources have been scaled to 2018 using the same source sector specific projection factors applied to the large point sources.

3.3.4 NO_X contribution from rural background concentrations

Rural annual mean background NO_X concentrations have been estimated using:

- NO_X measurements at 12 selected rural AURN sites.
- NO_X estimated from NO_2 measurements at 18 rural NO_2 diffusion tube sites from the UK Eutrophying and Acidifying Atmospheric Pollutants Network.

Figure 3-7 shows the locations of these monitoring sites and the interpolated rural map.

Rural NO_X was estimated from rural NO_2 at diffusion tube sites by dividing by 0.7835. This factor, which is a typical NO_X/NO_2 ratio measured at rural automatic monitoring sites (Stedman et al., 2003), does not vary significantly between years or across the country. Measurements have then been corrected to remove the contribution from point source and local area sources to avoid double counting these contributions later in the modelling process.

The correction procedure is as follows:

Corrected rural background (µg m^{-3}) = Uncorrected rural background (µg m^{-3}) – (A + B + C),

where: *A* is an estimate of the contribution from area source components, derived using the area source contributions from the 2017 modelling (scaled using the ratio of 2017 and 2018 emissions),

B is the sum of contributions from large point sources based on 2017 modelling,

C is the sum of contributions from small and ETS point sources based on 2017 modelling.

The correction is applied based on 2017 model results for local area and point sources because calibrated model results for these sources for 2018 are calculated later in the modelling process and rely on a calibration that requires the subtraction of the corrected rural contribution. Automatic sites, where available have been used in preference to diffusion tubes as these are considered to be more accurate. An interpolation of corrected rural measurement data by Inverse distance weighted (IDW) interpolation has been used to map regional background concentrations throughout the UK.

Figure 3-7 - Rural background NO$_X$ concentrations map with monitoring sites used in the interpolation (annual mean NO$_X$ concentrations for 2018 (µg m^{-3}, as NO$_2$) are shown below the site name)

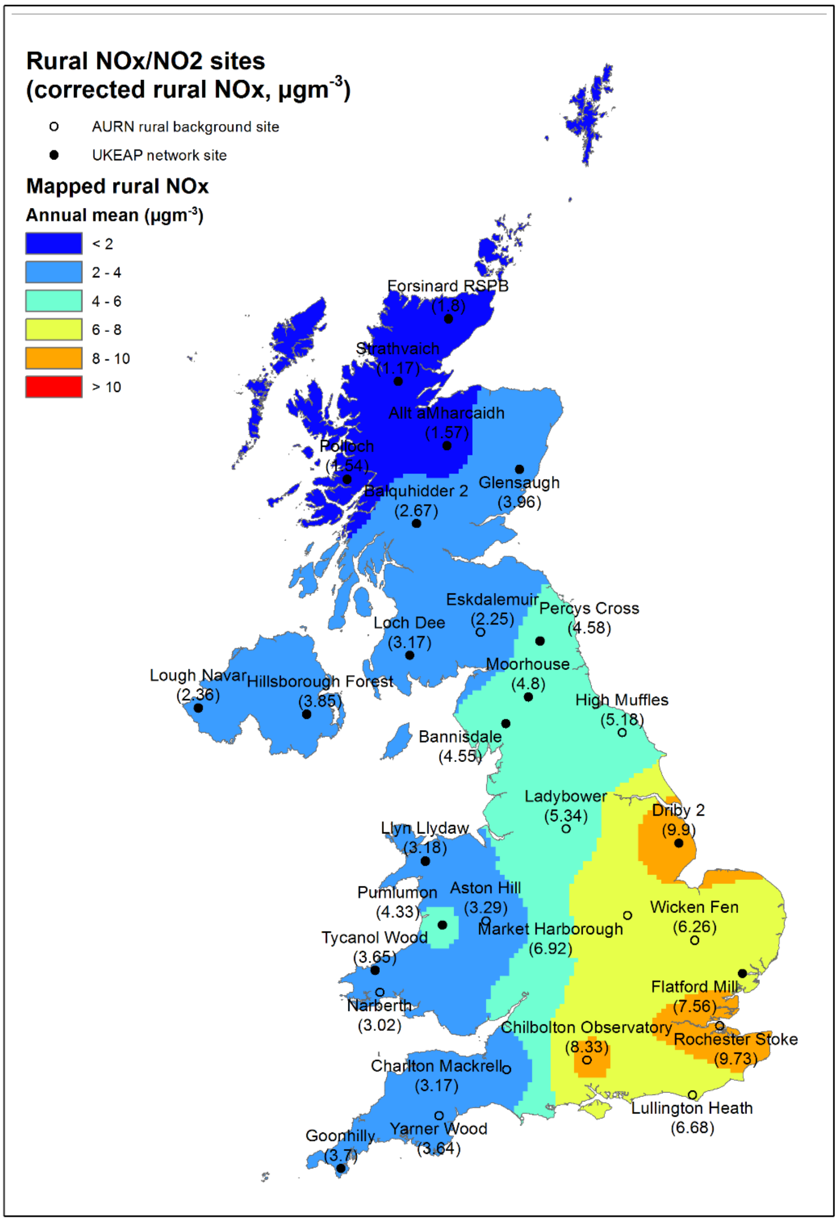

3.3.5 NO_X contributions from local area sources

In the NAEI 2017, NO_X area source emissions maps have been calculated for each source code-activity code combination using distribution grids that have been generated using appropriate surrogate statistics. These NO_X emissions grids are then added together to give SNAP code sector NO_X area source emission grids. The full method is described in Tsagatakis et al. (2019). To calculate NO_X area source emission grids for 2018 emissions projections from the NAEI (Passant, 2019) for each source code-activity code combination have been used to scale 2017 emissions forwards to 2018. The emissions projections are based on BEIS EEP 2018 energy and emissions projections (BEIS, 2018). The 2017 area source NO_X emissions have been mapped using updated distribution grids produced for the NAEI 2017 (Tsagatakis et al. 2019).

The 2018 area source emissions maps have then been used to calculate uncalibrated area source concentration maps for each SNAP code sector. With the exception of SNAP sector 3 (combustion in industry), this has been done by applying an ADMS 5.2 derived dispersion kernel to the emission maps to calculate the contribution to ambient concentrations on a 1 km x 1 km receptor grid, from the area source emissions within a 33 km x 33 km square surrounding each receptor. Hourly sequential meteorological data from Waddington in 2018 have been used to construct the dispersion kernels. Appendix 4 describes these kernels in more detail and explains how they have been calculated.

Since 2011 a dispersion kernel approach including a time varying emission profile based on degree days has been applied to the SNAP 2 domestic area sources sector to weight these emissions more realistically by time of day and meteorological conditions. The approach to derive the time varying emissions profile is described in Appendix 4. A degree day scaling factor has also been applied to all of SNAP 2 to project changes in combustion activity related to inter-year variation in meteorology. This scaling factor was derived from the ratio of the annual average degree days for 2018 to the annual average degree days for 2017. A degree day is a unit used to determine the heating requirements of buildings, representing a fall of one degree below a specified average outdoor temperature.

A development introduced for the 2011 assessment was a revision to the methodology for treating the SNAP 3 (combustion in industry) area source component (i.e. the component of the UK SNAP 3 national total not accounted for by regulated processes). Since 2011 the small points model (described in Appendix 3) has been applied to derive concentrations resulting from SNAP 3 area source emissions. By using the small points method for this sector, a more realistic release height, buoyancy and momentum of discharge is used based on the magnitude of the emission for small industrial chimneys.

Figure 3-8 shows the calibration of the area source model. The modelled concentrations from all point sources, SNAP 3 area sources and corrected rural NO_X concentrations have been subtracted from the measured annual mean NO_X concentration at background sites. This concentration is compared with the modelled area source contribution (excluding SNAP 3) to annual mean NO_X concentrations to calculate the calibration coefficients used in the area source modelling.

As part of the calibration process emission caps have been applied to certain sectors; this is because the use of surrogate statistics for mapping area source emissions sometimes results in unrealistically large concentrations in some grid squares for a given sector. The emission caps applied are given in Table 3.3.

The modelled area source contributions for each sector except SNAP 3 were multiplied by the coefficient to calculate the calibrated area source contribution for each grid square in the country. The point source contributions, SNAP 3 area source component and regional rural concentrations were then added, resulting in a map of background annual mean NO_X concentrations.

Figure 3-8 - Calibration of area source NO_X model, 2018 ($\mu g\ m^{-3}$, as NO_2)

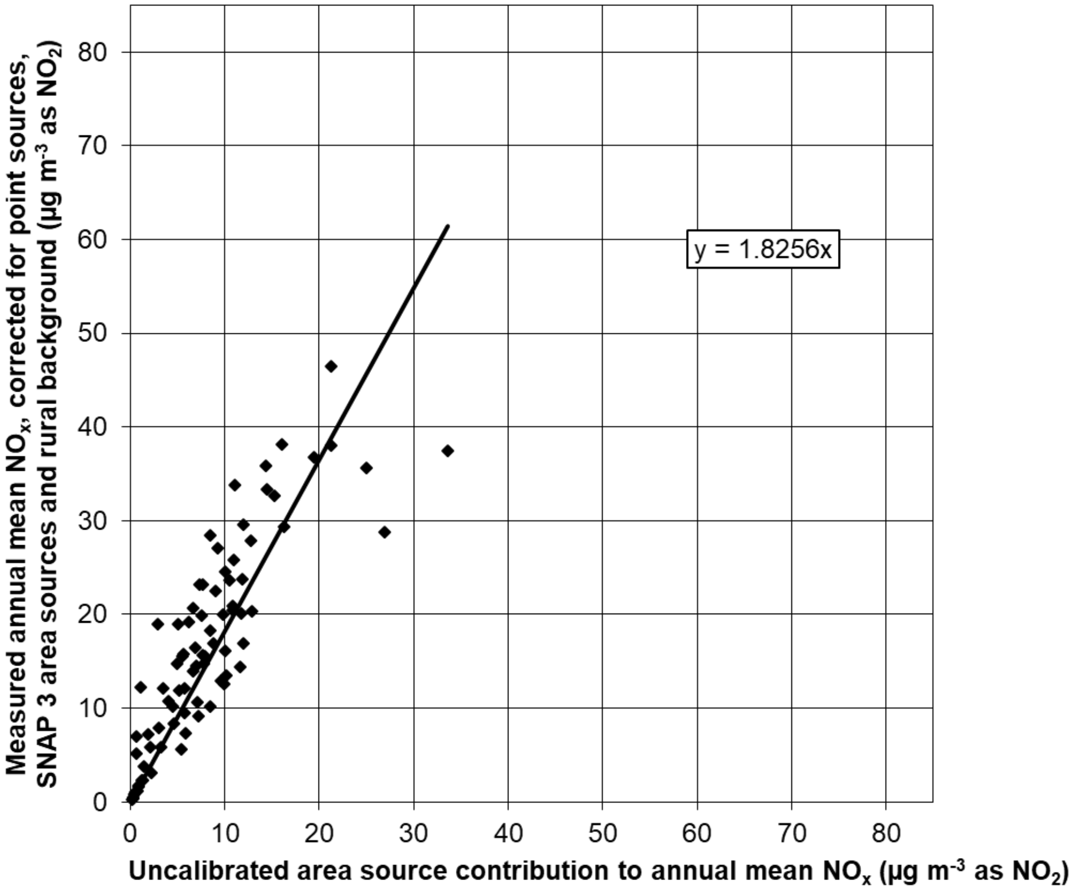

Table 3.3 - Emission caps applied to NO_X sector grids

SNAP code	Description	Cap applied (t/a/km^2)
SNAP 1 (Upstream oil and gas production, combustion at gas separation plant OPG)	Combustion in energy production & transformation	30
SNAP 8 (shipping only)	Other Transport & Mobile Machinery	100

3.3.6 NO_X Roadside concentrations

The modelled annual mean concentration of NO_X at a roadside location is made up of two parts: the background concentration (as described above) and a roadside increment:

roadside NO_X concentration = background NO_X concentration + NO_X roadside increment.

The NAEI has provided estimates of NO_X emissions for major road links in the UK for 2017 (Richmond et al., 2019) and these have been adjusted to provide estimates of emissions in 2018. The emissions estimates for NO_X from road transport sources include the following assumptions:

- Department for Transport (DfT) 2018 traffic forecasts (re-based to traffic used in the 2017 NAEI), DfT (2019) car sales projections including the uptake of low carbon passenger cars and LGVs with electric and hybrid electric propulsion systems, and Transport for London (2019) traffic and fleet (2018) projections for London
- NO_X emission factors from COPERT 5

The PCM Roads Kernel Model (PCM-RKM) described in Appendix 7 has been used to calculate the roadside increment. The PCM-RKM is based upon dispersion kernels generated by the ADMS-Roads dispersion model (v4.1) and represents a more process-based approach than the previous empirical method. It provides a more robust assessment, whilst retaining the link with measurement data provided using AURN measurement data to calibrate this component of the model.

Figure 3-9 shows the calibration of this model at roadside monitoring sites. In this figure, the measured roadside increment at the roadside monitoring sites is calculated as the measured concentration minus the background NO_X component, which is determined from the background NO_X concentration map described in Section 3.3.5 above. The modelled NO_X roadside increment is calculated directly using the road link emissions alone. The total modelled roadside NO_X concentration is then given from the equation above by adding the calibrated background NO_X modelled concentration to the calibrated NO_X roadside increment modelled concentration. The average distance from the kerb for the roadside and kerbside monitoring sites used to calibrate the roadside increment model is approximately 4 m. The calculated roadside concentrations are therefore representative of this distance from the kerb. Roadside concentrations for urban major road links (A-roads and motorways) only are reported to the EU and included in this report.

Figure 3-9 - Calibration of NO_X PCM RKM model, 2018 (µg m^{-3}, as NO_2)

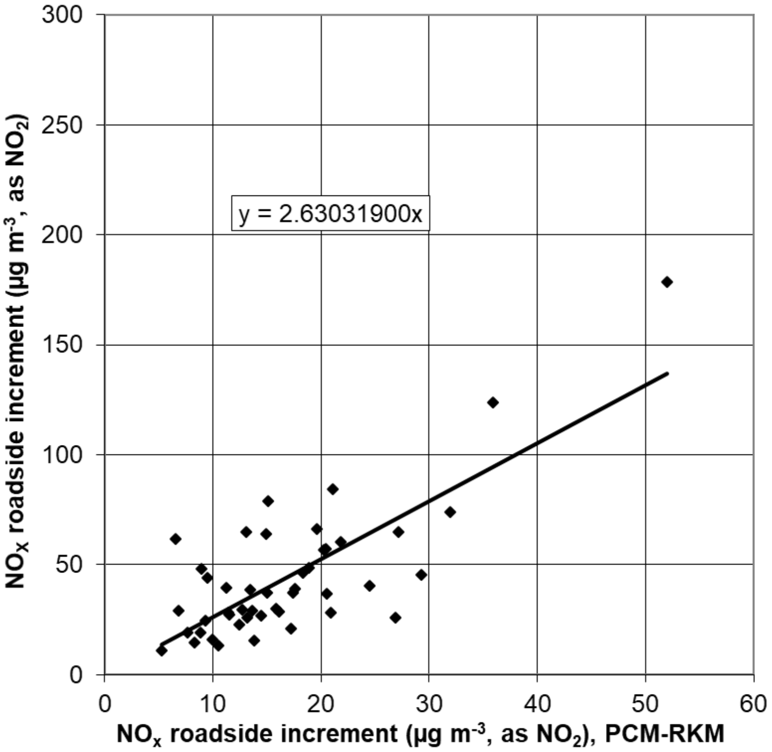

3.4 NO_2 Modelling

3.4.1 Introduction

Maps of estimated annual mean NO_2 concentrations (Figure 3-1 and Figure 3-2) have been calculated from the modelled NO_X concentrations using a calibrated version of the updated oxidant-partitioning model (Jenkin, 2004; Murrells et al., 2008; Jenkin, 2012). This model uses representative equations to account for the chemical coupling of O_3, NO and NO_2 within the atmosphere. A key advantage of this approach for modelling NO_2 concentrations is that emission scenarios can be directly addressed by varying regional oxidant levels and/or primary NO_2 emissions.

3.4.2 The updated oxidant-partitioning model

The oxidant-partitioning model, developed by Jenkin (2004), enables NO_2 concentrations to be calculated using the following equations:

$$[NO_2] = [OX].f(NO_x) \qquad (i)$$
$$[OX] = f\text{-}NO_2.[NO_x] + [OX]_B \qquad (ii)$$

Where [OX] is the total oxidant (the sum of NO_2 and O_3), f-NO_2 is the primary NO_2 emission fraction (defined as the proportion of NO_X emitted directly as NO_2), $[OX]_B$ is the regional oxidant and f(NO_X) is a function, the value of which is determined by the concentration of NO_X. NO_X, NO_2, O_3 and OX are all expressed as ppb in these equations: 1 ppb of O_3 = 2 µg m^{-3}; 1 ppb of NO_2 = 1.91 µg m^{-3}. By convention when NO_X is expressed in µg m^{-3} it is expressed as "µg m^{-3} as NO_2" therefore 1 ppb of NO_X = 1.91 µg m^{-3} of NO_X as NO_2.

In Jenkin (2004), $[NO_2]/[OX]$ (i.e. $f(NO_X)$) was calculated using two equations, one of which represented background locations and the other roadside locations. Updated equations for $[NO_2]/[OX]$ were subsequently developed in Murrells et al. (2008). More recently, Jenkin (2012) found that short term variability in NO_x concentrations is a major cause of the scatter in the relationship between $[NO_2]/[OX]$ and $[NO_x]$. The ratio of the upper to the lower quartile of hourly concentrations has been found to be a good indicator of this variability. The ratio increases with decreasing NO_x concentrations at roadside and background sites. This dependence has been used to interpolate between equations based on a constant NO_x quartile ratio. This led to two equations for calculating $[NO_2]/[OX]$, one of which represents background locations and the other roadside locations. These are the equations that are currently used in the modelling. These are an improvement over the equations presented in Murrells et al. (2008) because the background equation requires less adjustment in the background adjustment calibration and the roadside equation enables linear calibration adjustment for roadside.

Jenkin (2012) presented two equations for calculating $[NO_2]/[OX]$ as a function of $[NO_X]$ (i.e. $f(NO_X)$). These are:

- One background relationship, which has been derived using data from background sites.
- One roadside relationship, which has been derived using data from roadside sites.

The two relationships are presented in Table 3.4 below.

Table 3.4 - The two relationships in the updated oxidant-partitioning model (Jenkin, 2012)

PCM Category	Relationship (where y = $[NO_2]/[OX]$ and x = $[NO_x]$, in ppb)
Background	y = -2.5124E-13x^6 + 1.5805E-10x^5 – 4.1429E-08x^4 + 5.8239E-06x^3 – 4.8076E-04x^2 + 2.5916E-02x
Roadside	y = -2.0901E-13x^6 + 1.5001E-10x^5 – 4.2894E-08x^4 + 6.2659E-06x^3 – 5.0720E-04x^2 + 2.5322E-02x

The following sections describe the method for calculating an average regional oxidant value for the UK (Section 3.4.3), local oxidant calculations for background and roadside locations (Section 3.4.4), calculating $[NO_2]/[OX]$ in the PCM model and how the updated oxidant-partitioning model has been applied in the UK to background and roadside locations (Section 3.4.5).

3.4.3 UK regional oxidant

A fixed regional oxidant value for the whole of the UK has been used. The regional oxidant value for 2018 was calculated to be 32.8 ppb. This value was derived from an analysis of annual mean data for O_3, NO_2 and total nitrogen oxides (NO_X) at 60 AURN sites. These sites were selected using the criterion that the annual mean $[NO_X]$ in 2018 was less than or equal to 25 ppb, so that the contribution to [OX] derived from primary NO_2 was comparatively small. A constant f-NO_2 value of 0.093 was used to correct for the contribution from local oxidant.

3.4.4 Local oxidant calculations

Local oxidant is calculated in the updated oxidant-partitioning model as:

$$\text{Local oxidant} = f\text{-}NO_2.[NO_X]. \qquad (iv)$$

Where $f\text{-}NO_2$ is the fraction of NO_x emissions emitted as primary NO_2 (by volume). Therefore, to calculate local oxidant levels, the $f\text{-}NO_2$ levels from different local sources need to be understood. In general, it is possible to make a distinction between $f\text{-}NO_2$ from road traffic sources and $f\text{-}NO_2$ from non-road traffic sources. $f\text{-}NO_2$ from road traffic sources is thought to have risen during the early 2000s, although this trend displays considerable variation with location (AQEG, 2007; Carslaw et al., 2011). By comparison, $f\text{-}NO_2$ from non-traffic sources has remained relatively constant with time.

3.4.4.1 $f\text{-}NO_2$ for road traffic sources on individual road links

Figure 3-10 shows fleet average $f\text{-}NO_2$ projections by vehicle type for London and the rest of the UK from the NAEI.

$f\text{-}NO_2$ for all petrol vehicles is very low (less than 5%). $f\text{-}NO_2$ for diesel cars and LGVs is much greater and is expected to decline somewhat in the future. $f\text{-}NO_2$ for HGVs and buses is lower and is also expected to decline. $f\text{-}NO_2$ projections for London show the impact of specific measured applied to London buses and the London low emission zone (LEZ) and ultra-low emission zone (ULEZ).

Figure 3-10 - Fleet average *f-NO$_2$* projections by vehicle type for a) London and b) rest of the UK from NAEI

a) London

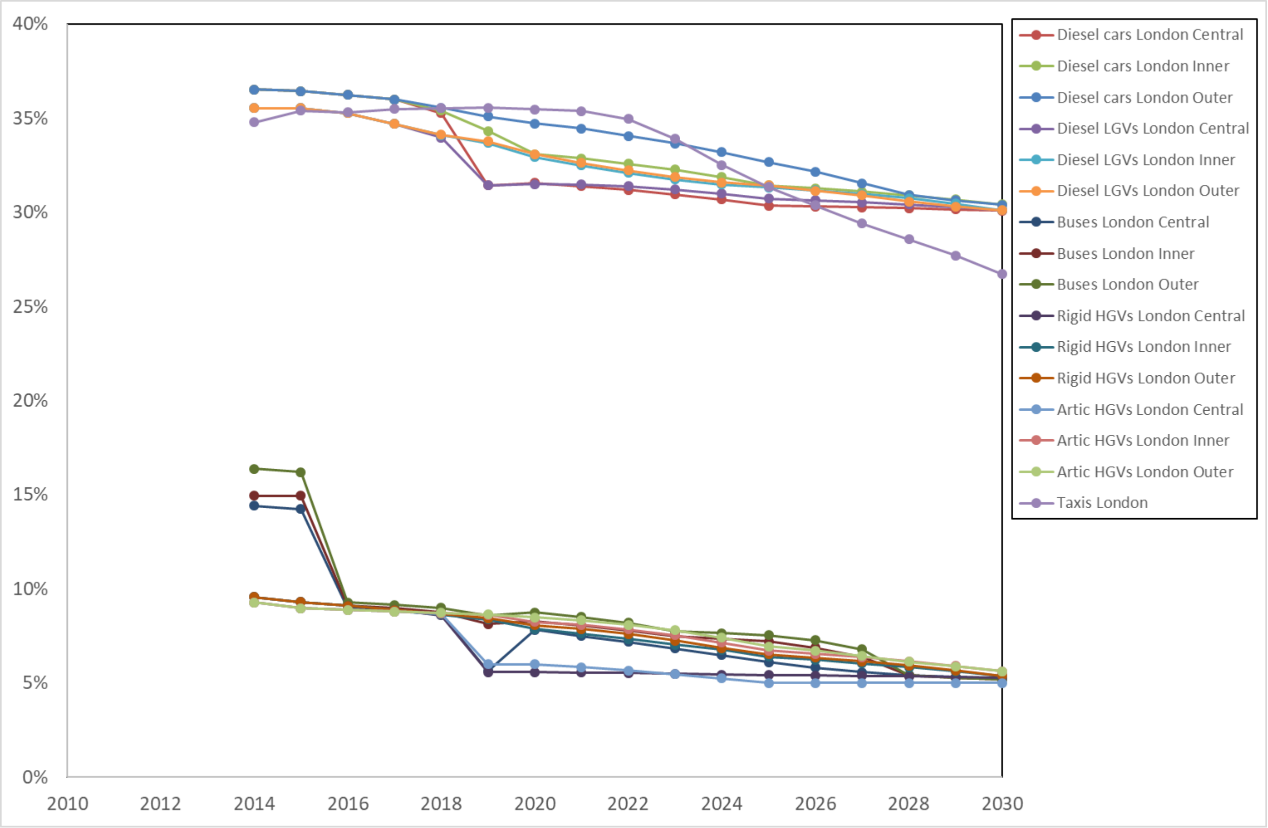

b) Rest of the UK

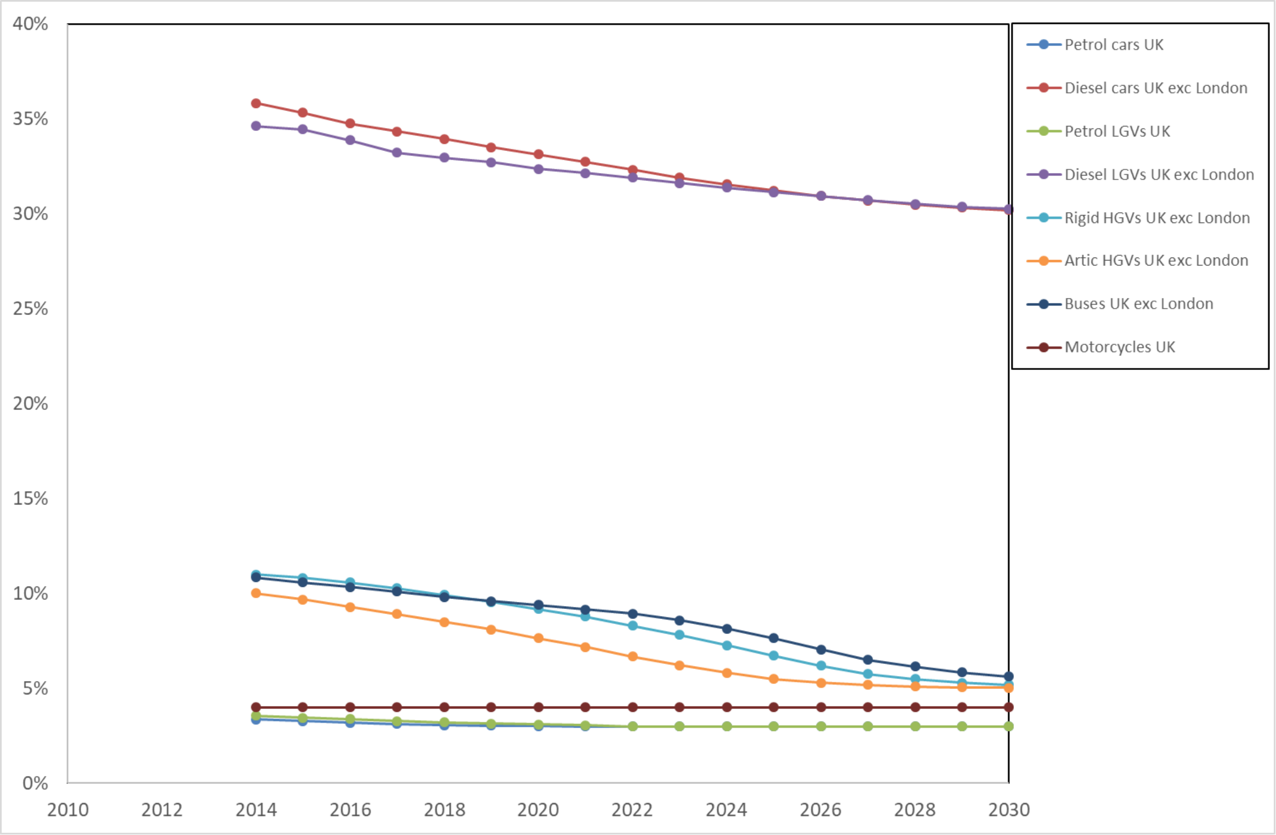

3.4.4.2 *f-NO_2* for background sources

Table 3.5 shows the *f-NO_2* values used for background sources in 2018. The non-road *f-NO_2* values used for background calculations in Table 3.5 have been taken directly from Jenkin (2004), as there is little evidence that this has changed significantly over the past few years. The road traffic *f-NO_2* values for background calculations have been calculated using the average of the major road link *f-NO_2* values for each area type.

Table 3.5 - Local oxidant coefficients (*f-NO_2*) for background concentrations in 2018

DfT Area type[1]	Region	Non-road *f-NO_2* for background calculations	Road *f-NO_2* for background calculations
1	Central London	0.140	0.228
2	Inner London	0.128	0.243
3	Outer London	0.093	0.265
4	Inner Conurbations	0.093	0.260
5	Outer Conurbations	0.093	0.272
6	Urban (population > 250,000)	0.093	0.275
7	Urban (population > 100,000)	0.093	0.275
8	Urban (population > 25,000)	0.093	0.275
9	Urban (population > 10,000)	0.093	0.277
10	Rural	0.093	0.283

[1] Locations in Northern Ireland have been assigned area types according to how built up the local environment is because the DfT area types map does not cover Northern Ireland. A map of the distribution of DfT area types is included in Appendix 4.

3.4.4.3 Local oxidant calculations

A map of local oxidant for the background NO_2 calculations was generated by splitting the background annual mean NO_X map into its two constituent components:

- NO_X from background non-road traffic emissions (includes rural background component)
- NO_X from background road-traffic emissions

These components were multiplied by the relevant *f-NO_2* value from Table 3.5 and then added together to give a total local oxidant. Figure 3-11 shows the UK background local oxidant map for 2018.

Local oxidant on individual road links was calculated by splitting the total annual mean NO_X for the road link into its three constituent components:

- NO_X from background non-road traffic emissions (includes rural background component)
- NO_X from background road-traffic emissions
- Roadside increment NO_X concentrations from emissions on the specific road link under consideration

The background components were then multiplied by the relevant *f-NO_2* value from Table 3.5 and the roadside increment NO_X was multiplied by the specific *f-NO_2* calculated for that road link. These local oxidant values were then added together to give a total local oxidant for the road.

Figure 3-11 - Background local oxidant map for 2018 (ppb)

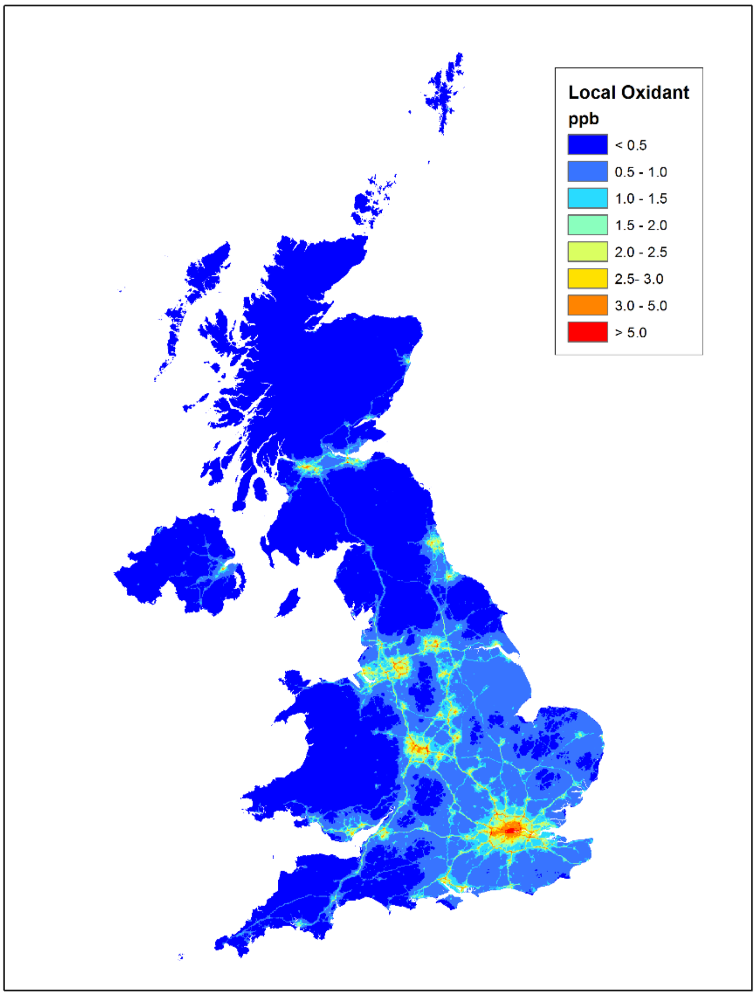

3.4.5 Calculating $[NO_2]/[OX]$ in the PCM model

As described in Section 3.4.2, two relationships for calculating $[NO_2]/[OX]$ have been derived in Jenkin (2012). The ratio of $[NO_2]/[OX]$ has been considered separately for background and roadside locations in this analysis as there are separate relationships for these locations. Background and roadside sites tend to behave differently because of differences in the 'age' of the NO_X at these locations.

3.4.5.1 Background

For background locations, the background relationship has been calibrated using data from AURN background sites for 2018. The calibration plot for background sites is shown in Figure 3-12. Figure 3-13 a and b show verification plots of measured NO_2 against modelled NO_2 calculated from measured NO_X using the uncalibrated background relationship and calibrated background relationship respectively. The agreement is better for the calibrated model. The background oxidant partitioning curves are only valid for annual mean NO_X concentrations up to 267.4 µg m^{-3} (as advised by Jenkin (2012)) hence NO_X concentrations above this value have been set to 267.4 µg m^{-3}.

Figure 3-12 - Background NO_2 calibration curve (NB verification sites are shown for reference here, but were not used in calculating the calibration), 2018

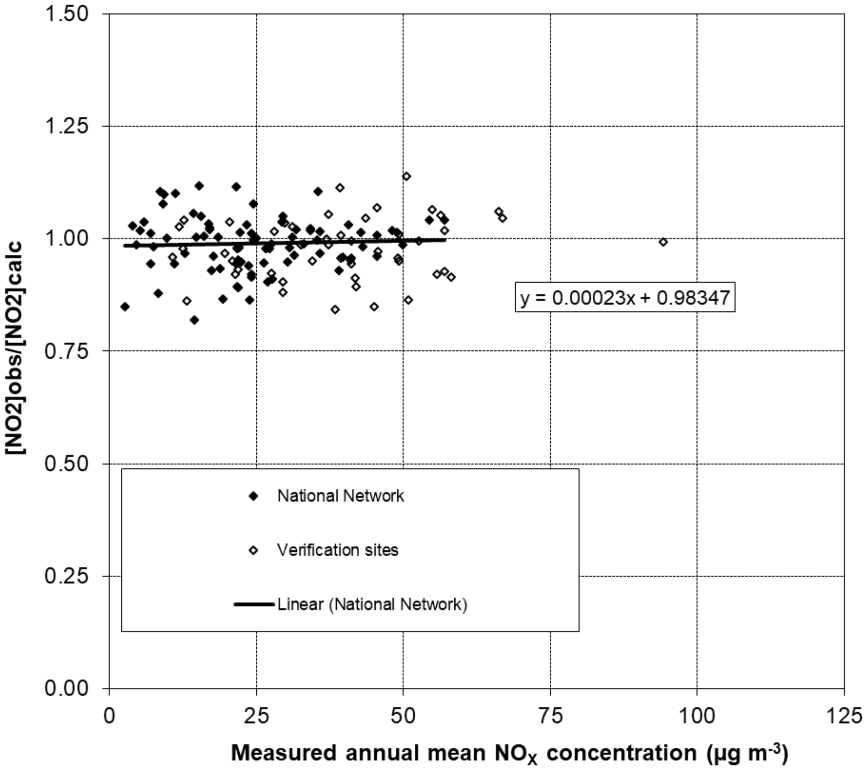

Figure 3-13 - Verification of background relationship at background locations in 2018

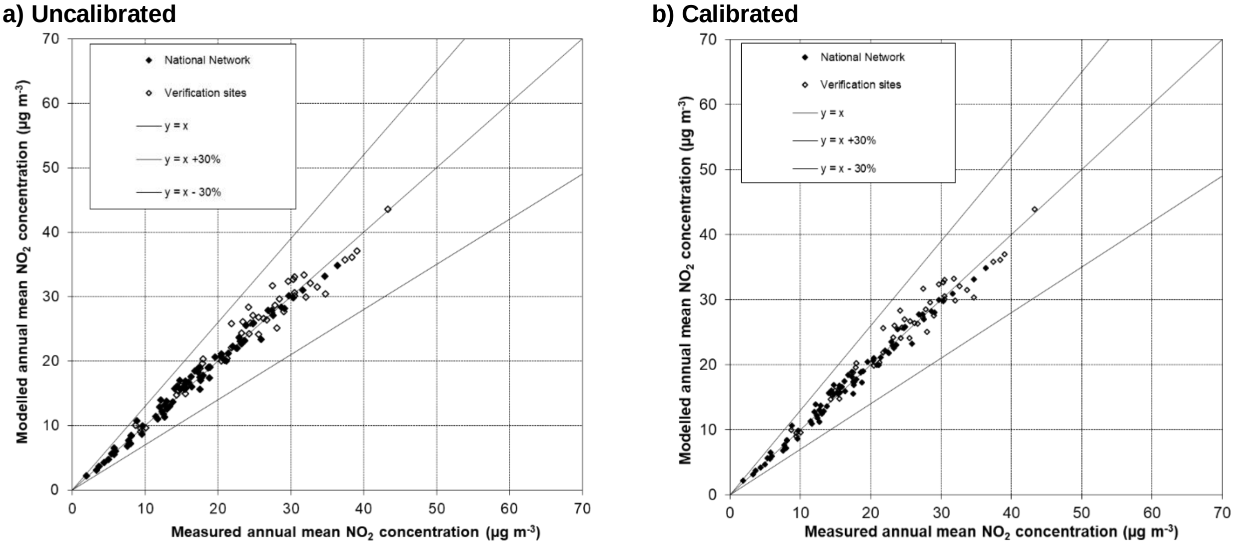

3.4.5.2 Roadside

For roadside locations, the roadside relationship has been selected and an additional calibration has been applied using data from AURN roadside sites for 2018. The model has been calibrated by plotting the ratio of measured NO_2 to modelled NO_2 as a function of NO_X for each AURN roadside sites for 2018 and then fitting a straight line through these points. Figure 3-14 shows this ratio for each site and the straight line that was fitted though the data. The verification sites are also shown on this plot for reference although they were not used to calibrate the model.

Figure 3-14 - Roadside NO_2 calibration curve (NB verification sites are shown for reference here, but were not used in calculating the calibration factors), 2018

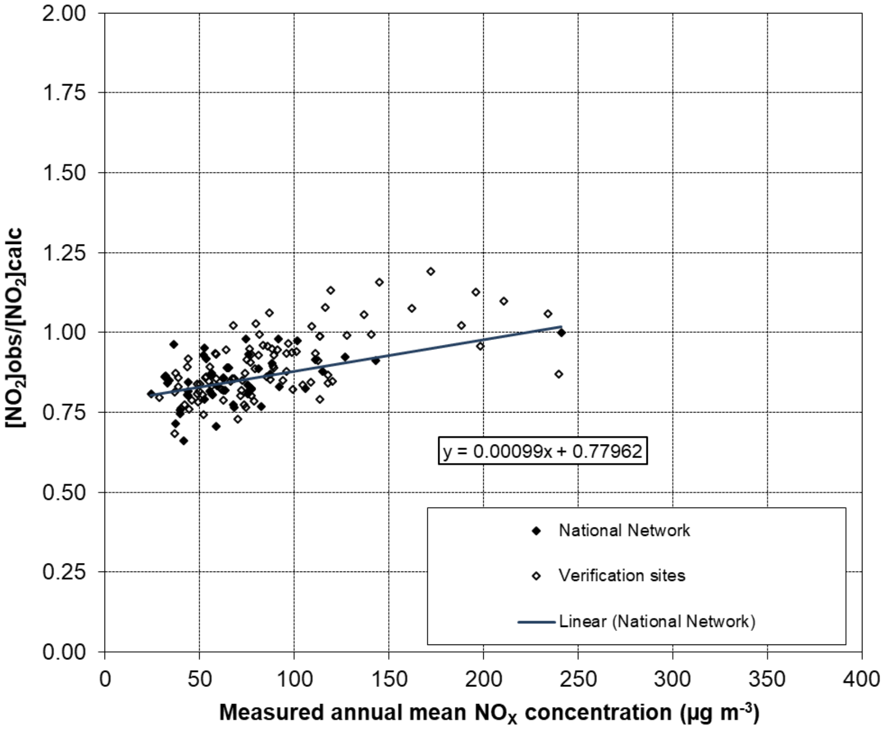

Figure 3-15a shows a verification plot of measured NO_2 against modelled NO_2 calculated from measured NO_X using the uncalibrated roadside relationship. Figure 3-15b shows the same information but using the calibrated roadside relationship. It is clear that the calibrated model provides a better fit to the monitoring data in the vicinity of the limit value of 40 µg m^{-3}. The roadside oxidant partitioning curves are only valid for annual mean NO_X concentrations up to 382 µg m^{-3} (as advised by Jenkin (2012)) hence NO_X concentrations above this value have been set to 382 µg m^{-3}.

Figure 3-15 - Verification of roadside relationship at roadside locations in 2018

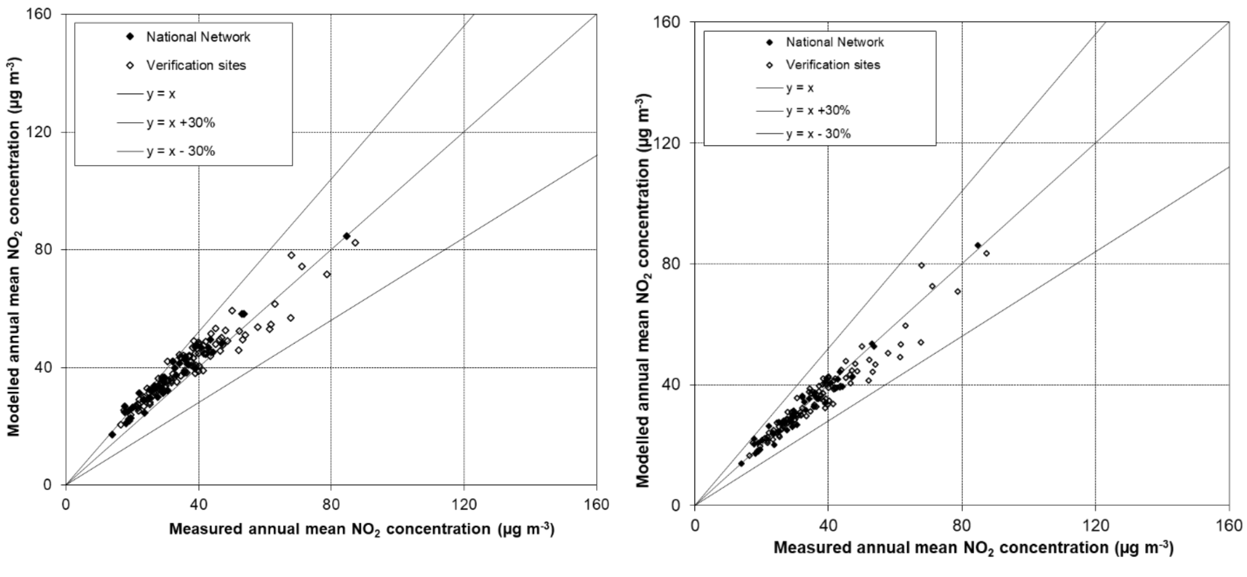

a) Uncalibrated **b) Calibrated**

3.5 Results

3.5.1 Source apportionment

Figure 3-16 and Figure 3-17 show the modelled NO_X source apportionment at AURN background and roadside sites respectively for 2018. This shows that while road transport is the dominant source at most locations, both background and roadside, contributions from other sectors such as domestic, commercial, off road mobile machinery and industry are also significant at many sites. Contributions from aircraft and shipping are evident at some sites. No source apportionment is given for NO_2 because this is not a physically meaningful concept because of the non-linear relationship between NO_X and NO_2.

Figure 3-16 - Annual mean NO_X source apportionment at background AURN monitoring sites in 2018 (area type of each site is shown in parenthesis after its name – see Table 3.5)

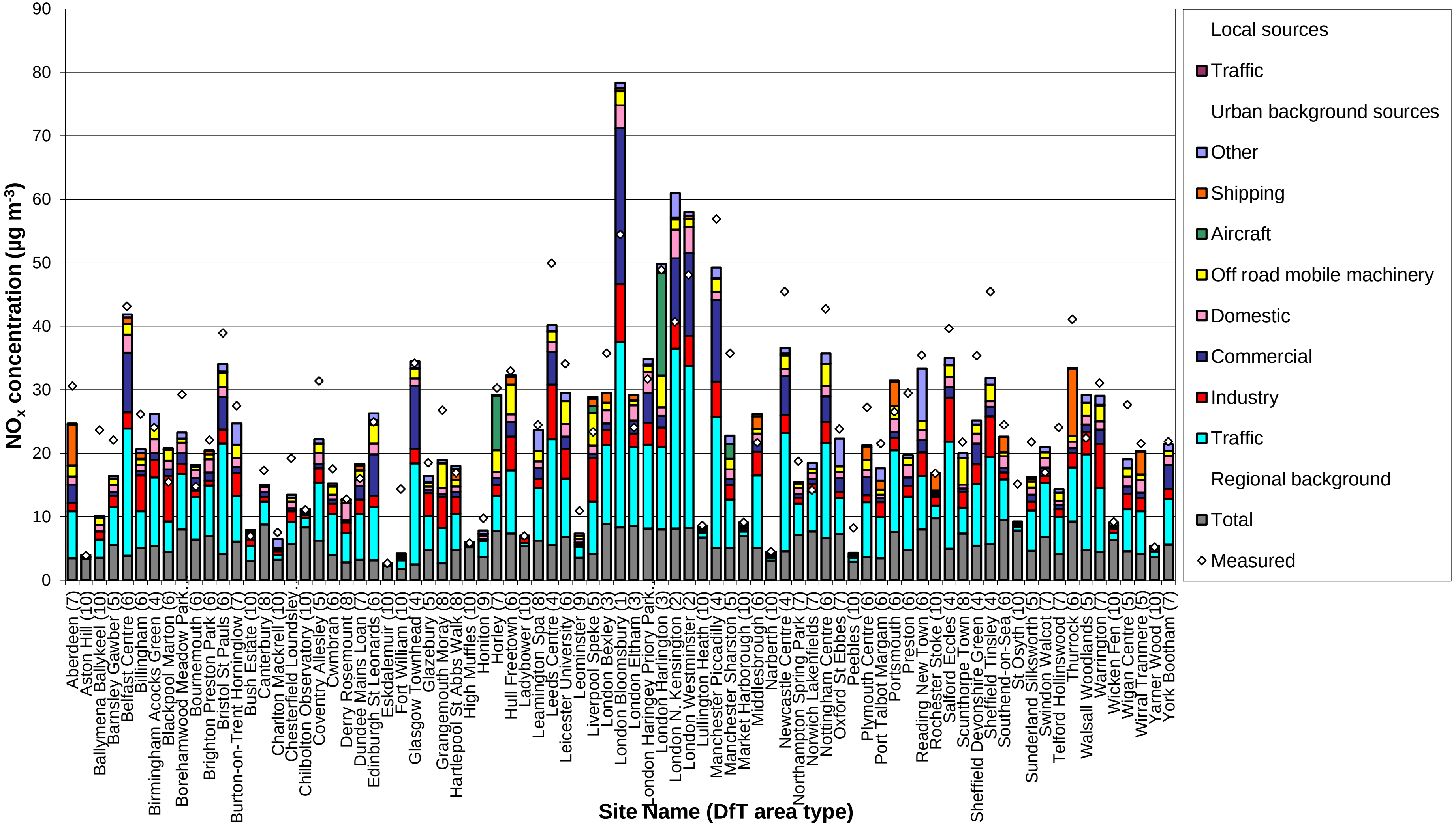

Figure 3-17 - Annual mean NO_X source apportionment at roadside AURN monitoring sites in 2018 (area type of each site is shown in parenthesis after its name – see Table 3.5)

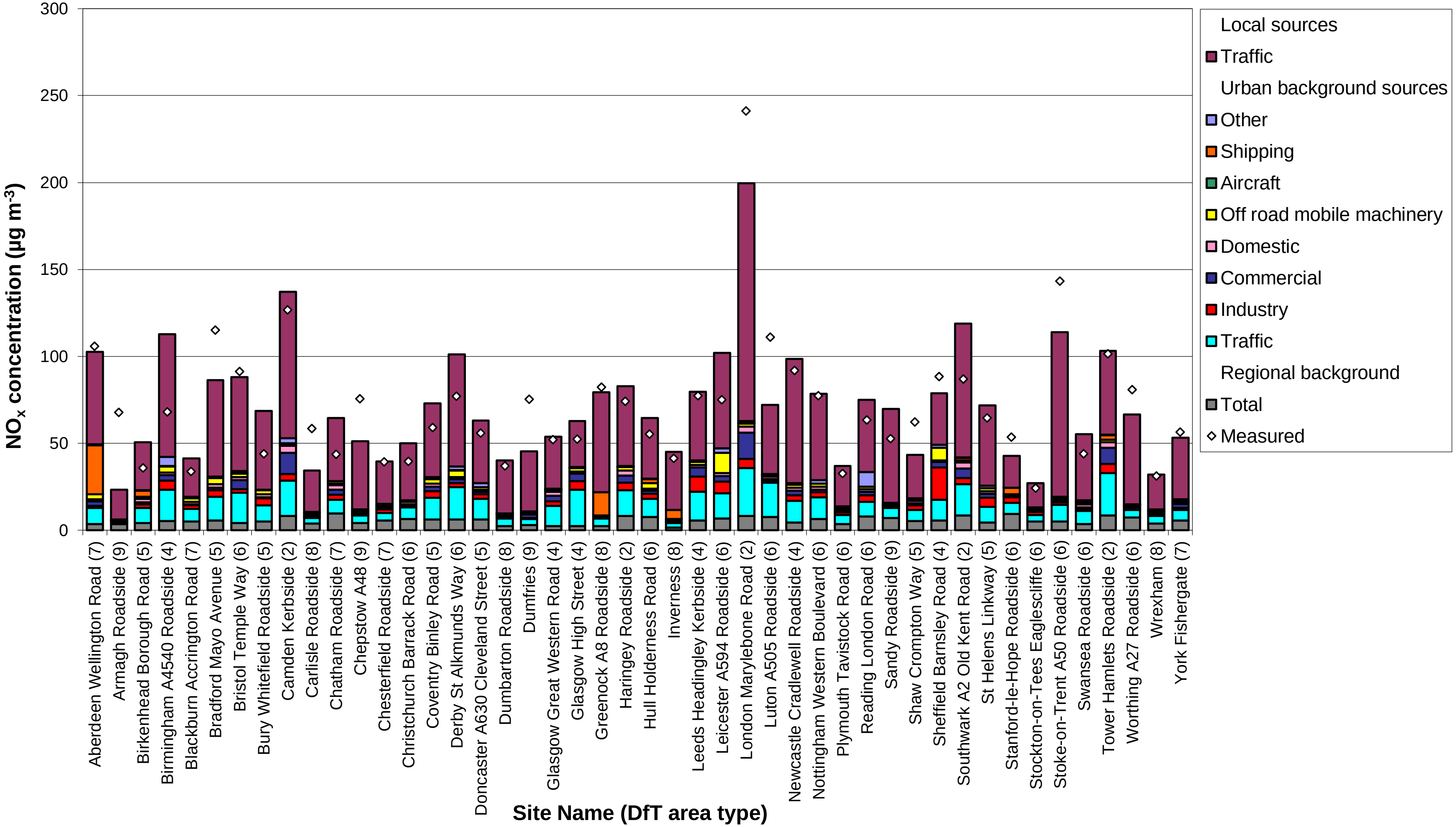

3.5.2 Verification of mapped values

Figure 3-18 and Figure 3-19 show comparisons of modelled and measured annual mean NO_X and NO_2 concentration in 2018 at background monitoring site locations. Figure 3-20 and Figure 3-21 show similar comparisons for roadside sites. Both the national network sites used to calibrate the models and the verification sites are shown. Lines representing y = x – 30 % and y = x + 30% are also shown (this is the AQD data quality objective for modelled annual mean NO_2 and NO_X concentrations – see Section 1.5). There is no requirement under the AQD to report modelled annual mean NO_X concentrations for comparison with limit values for the protection of human health (the NO_X limit value for the protection of vegetation only applies in vegetation areas). However, comparisons of modelled and measured NO_X concentrations and of the modelled NO_X concentrations with the data quality objectives are presented here alongside the comparisons for NO_2. This provides an additional check on the reliability of the modelled estimates of NO_2 because the non-linear relationships between NO_X and NO_2 tend to cause modelled NO_2 concentrations to be relatively insensitive to differences between measured and modelled values of NO_X.

Summary statistics for the comparison between modelled and measured NO_X and NO_2 concentrations are listed in Table 3.6 and Table 3.7. The percentages of monitoring sites for which the modelled annual mean concentrations fall outside the data quality objectives is generally greater for NO_X than for NO_2, for the reasons discussed above.

Figure 3-18 - Verification of background annual mean NO_X model 2018

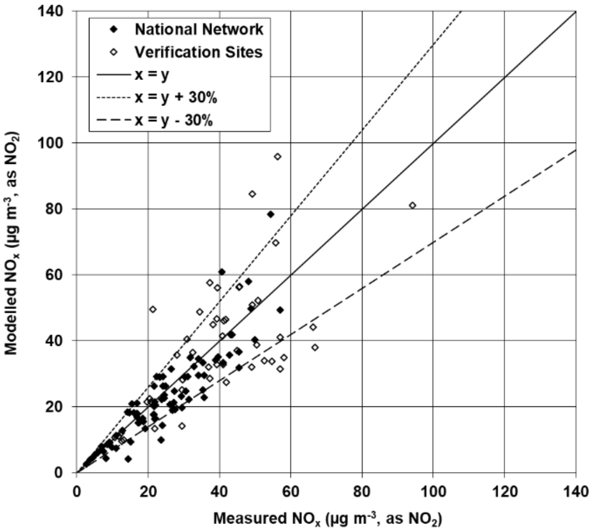

Figure 3-19 - Verification of background annual mean NO_2 model 2018

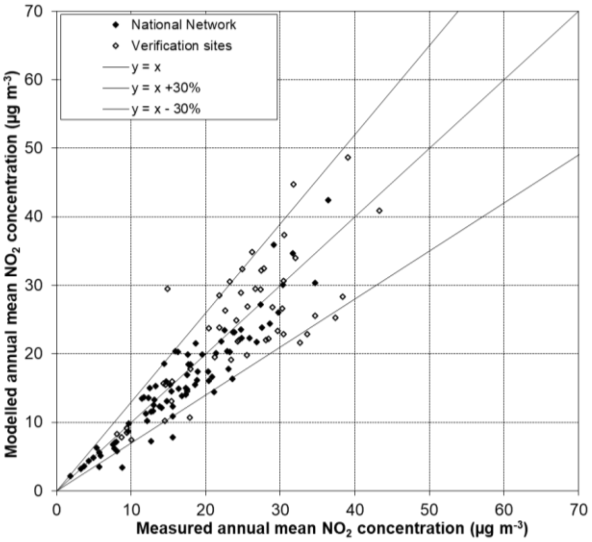

Figure 3-20 - Verification of roadside annual mean NO_X model 2018

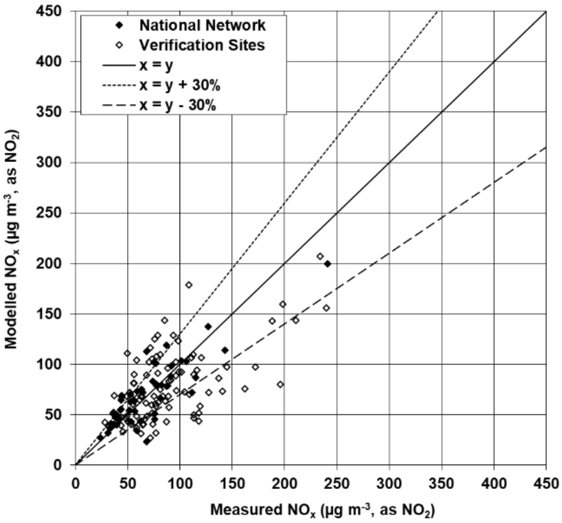

Figure 3-21 - Verification of roadside annual mean NO_2 model 2018

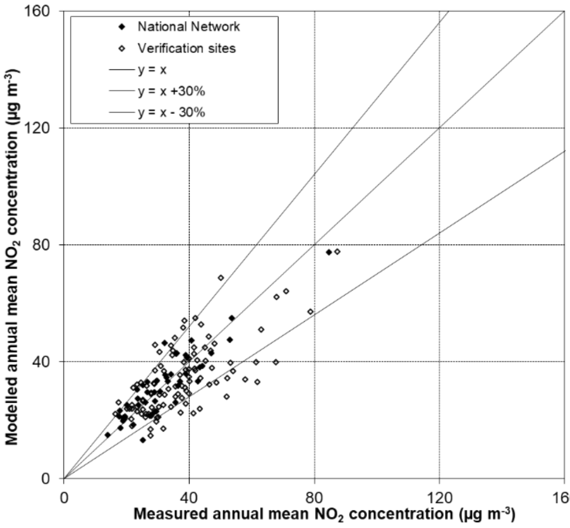

Table 3.6 - Summary statistics for comparison between modelled and measured NO_X and NO_2 concentrations at background sites (µg m^{-3}, as NO_2)

		Mean of measurements (µg m^{-3}, as NO_2)	Mean of model estimates (µg m^{-3}, as NO_2)	R^2	% outside data quality objectives	Number of sites in assessment
NO_X	National Network	24.5	22.7	0.73	17.3	81
	Verification Sites	39.0	37.9	0.46	34.0	50
NO_2	National Network	16.7	15.6	0.88	8.6	81
	Verification Sites	24.2	23.9	0.60	20.0	50

Table 3.7 - Summary statistics for comparison between modelled and measured NO_X and NO_2 concentrations at roadside sites (µg m^{-3}, as NO_2)

		Mean of measurements (µg m^{-3}, as NO_2)	Mean of model estimates (µg m^{-3}, as NO_2)	R^2	% outside data quality objectives	Number of sites in assessment
NO_X	National Network	71.1	71.3	0.73	30.4	46
	Verification Sites	85.6	75.8	0.39	48.0	102
NO_2	National Network	32.0	32.2	0.81	8.7	46
	Verification Sites	37.1	33.8	0.50	30.4	102

4 SO_2

4.1 Introduction

4.1.1 Limit values

Two limit values for ambient SO_2 concentrations are set out in the AQD for the protection of human health. These limit values have been in force since 1st January 2005 and are specified as follows:

- An hourly concentration of 350 µg m^{-3}, with 24 permitted exceedances each year
- A 24-hour mean concentration of 125 µg m^{-3}, with 3 permitted exceedances each year.

A critical level for SO_2 for the protection of vegetation has also been specified in the AQD:

- An annual mean and winter mean concentration of 20 µg m^{-3}.

The critical level is designed to protect vegetation, so it only applies in vegetation areas as defined in the Directive. The critical level has been in force since 2001.

4.1.2 Annual mean and winter mean modelling

A map of annual mean SO_2 concentrations for 2018 in vegetation areas has been calculated for comparison with the annual mean critical level described above; this map is shown in Figure 4-2. This map has been calculated by removing non-vegetation areas from the background SO_2 annual mean map and calculating the zonal mean of the 1 km x 1 km grid squares for a 30 km x 30 km grid so that it complies with the criteria set out in the AQD. Mean concentrations on a 30 km x 30 km grid have been used to prevent the influence of any urban area appearing unrealistically large on adjacent vegetation areas. Thus, the modelled concentrations in vegetation areas should be representative of approximately 1000 km^2 as specified in the AQD for monitoring sites used to assess concentrations for the vegetation critical level.

A map of winter mean SO_2 concentrations for the period October 2017 to March 2018 has also been calculated for comparison with the winter mean critical level and is shown in Figure 4-3. This map was calculated by multiplying the annual mean map for 2018 by the ratio between the average concentration measured at rural SO_2 monitoring sites during the 2017-2018 winter period and the annual concentration for 2018.

4.1.3 Modelling for comparison with the hourly and 24-hour limit values

Maps of the 99.73 percentile of the hourly mean and the 99.18 percentile of the 24-hour mean SO_2 concentrations have been calculated for 2018. They are shown in Figure 4-4 and Figure 4-5 respectively. These percentile concentrations correspond to the number of allowed exceedances of the 1-hour and 24-hour limit values for SO_2 described above.

4.1.4 Overview of the PCM model for SO_2

Figure 4-1 shows a simplified flow diagram of the PCM model for SO_2. A summary of the PCM model method, input and assumptions for SO_2 is presented in Table 4.1.

Figure 4-1 - Flow diagram for PCM SO_2 model

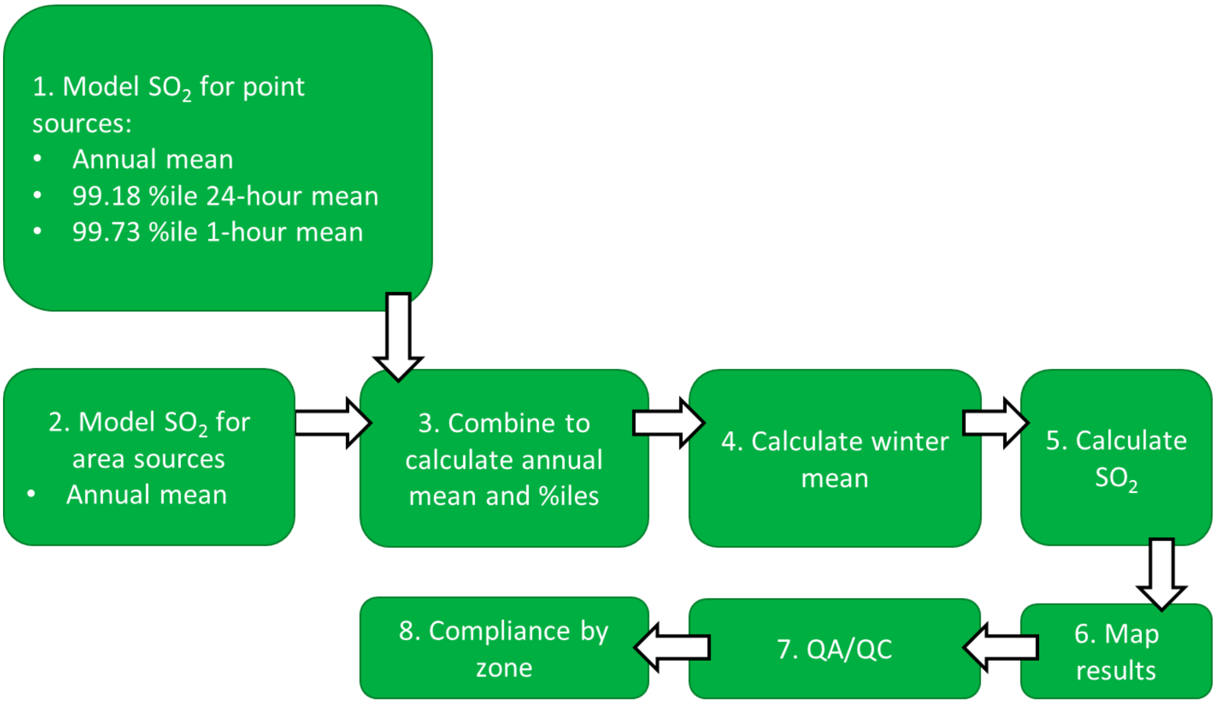

Table 4.1 - PCM model method, input and assumptions summary for SO_2

Heading	Component	Details
General	Pollutant	SO_2
	Year	2018
	Locations modelled	Background
	Metric	Annual mean Winter Mean (2017-2018) 99.18 percentile daily mean 99.73 percentile hourly mean
Input data	Emission inventory	NAEI 2017
	Energy projections	Energy Projections 2017
	Road traffic counts	2017
	Road transport activity projections	DfT (2018) traffic (re-based to 2017 NAEI), DfT (2019) car sales projections, TfL traffic (2019) and fleet (2018) projections for London
	Road transport emission factors	COPERT 5
	Measurement data	2018
	Meteorological data	Hourly data from Waddington 2018
Model components	Regional	Constant derived from Abbott & Vincent (2006)
	Large point sources	441 sources modelled using ADMS 5.2
	Small point sources	PCM small points model
	ETS point sources	PCM small points model
	Large ETS point sources	140 sources modelled using ADMS 5.2
	Area sources	PCM dispersion kernels generated using ADMS 5.2. Time varying emissions for road transport and domestic sources. PCM small points model for industrial combustion emissions.
	Roadside increment	n/a

Heading	Component	Details
Calibration	Model calibrated?	No
	Number of background stations in calibration	n/a
	Number of traffic stations in calibration	n/a
Pollutant specific	Annual mean	Modelled directly
	Winter mean	Calculated from annual mean using scaling factor derived from ambient measurements at rural monitoring stations
	99.18 percentile daily mean	Maximum of values calculated by scaling and combining annual mean components or scaling and combining annual and percentile components
	99.73 percentile hourly mean	Maximum of values calculated by scaling and combining annual mean components or scaling and combining annual and percentile components

4.1.5 Outline of annual mean and winter mean modelling

The 1 km x 1 km annual mean background SO_2 concentration map has been calculated by summing the contributions from:

- Large point sources
- Small point sources
- Point sources with emissions estimates for air quality pollutants based on reported carbon emissions (ETS points)
- Local area sources
- Distant sources

The contributions from each of the above components were modelled as described in Section 4.3.1.

4.1.6 Outline of modelling for comparison with the hourly and 24-hour limit values

The 1 km x 1 km percentile SO_2 concentration maps have been calculated by combining the contributions from the same list of sources as for the annual mean modelling. Details of the method can be found in Section 4.3.2.

4.1.7 Chapter structure

This chapter describes modelling work carried out for 2018 to assess compliance with the SO_2 limit values and critical levels described above. Emission estimates for SO_2 are described in Section 4.2. Section 4.3.1 describes the SO_2 modelling methods for the annual and winter means. Section 4.3.2 describes the SO_2 modelling methods for the percentile metrics (for comparison with the hourly and 24-hour limit values). Model verification and source apportionment information are presented in Section 4.4.

Figure 4-2 - Annual mean SO_2 concentration, 2018 (µg m^{-3}) in vegetation areas

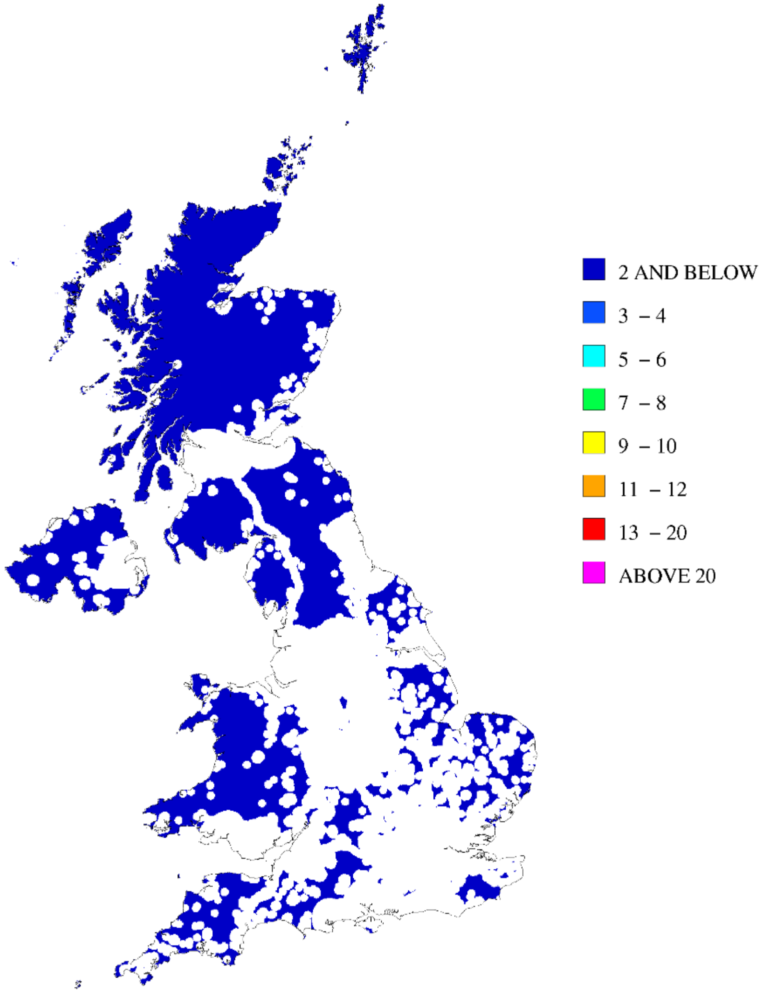

Figure 4-3 - Winter mean SO_2 concentration, 2017-2018 (µg m^{-3}) in vegetation areas

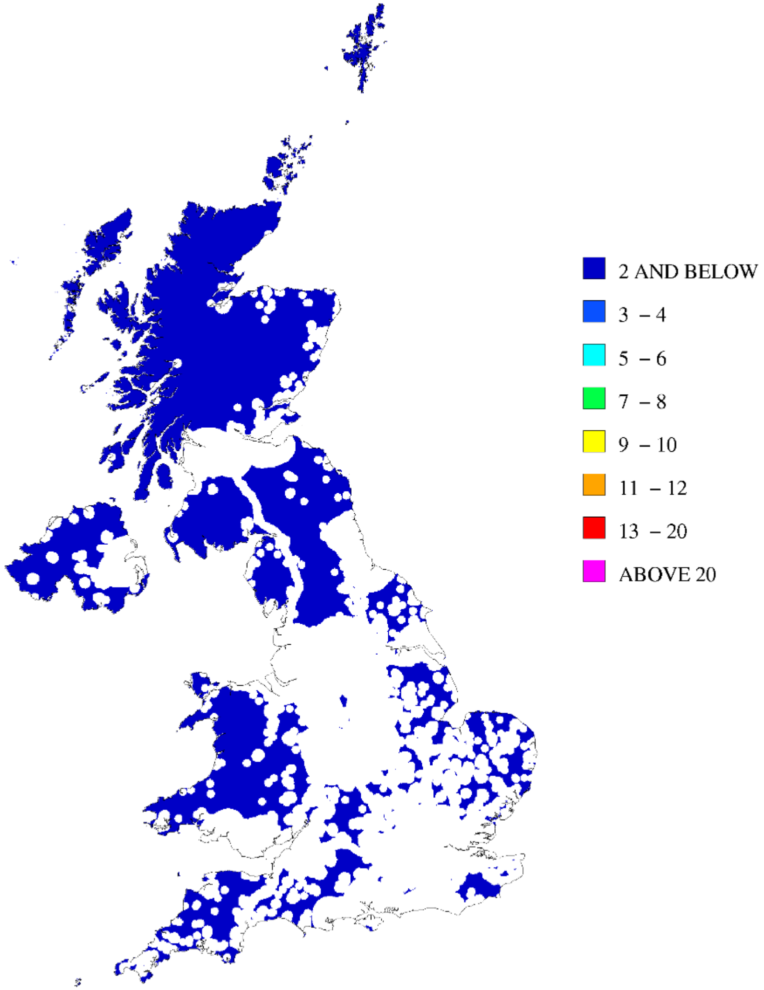

Figure 4-4 - 99.73 percentile of 1-hour mean SO_2 concentration, 2018 (µg m^{-3})

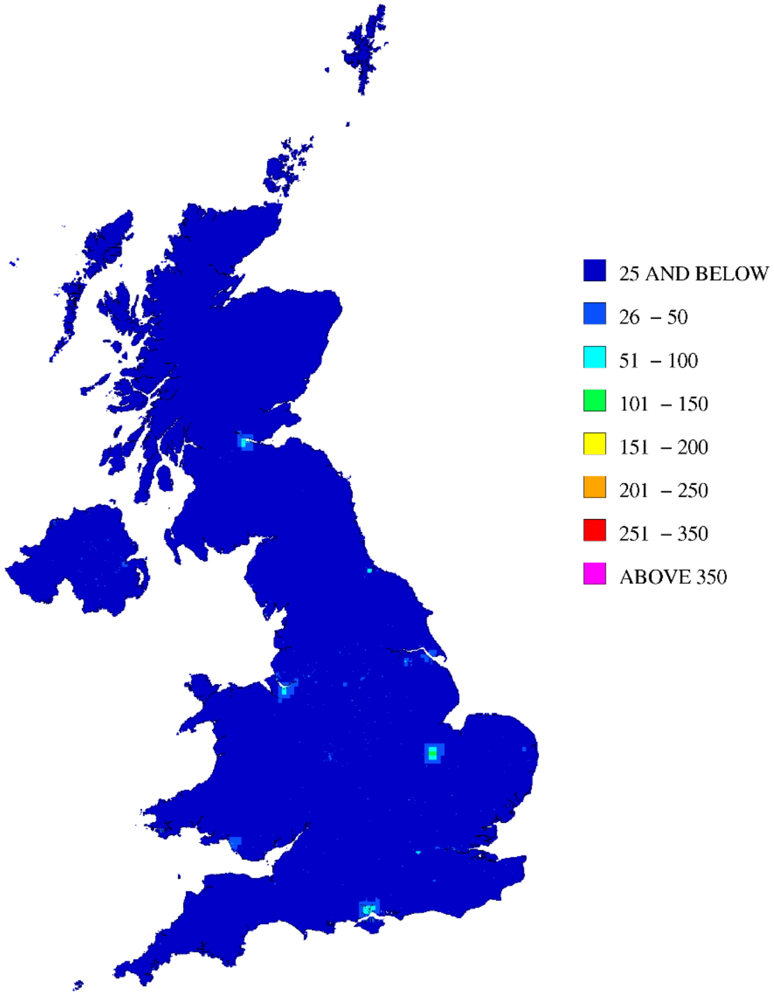

Figure 4-5 - 99.18 percentile of 24-hour mean SO_2 concentration, 2018 (µg m^{-3})

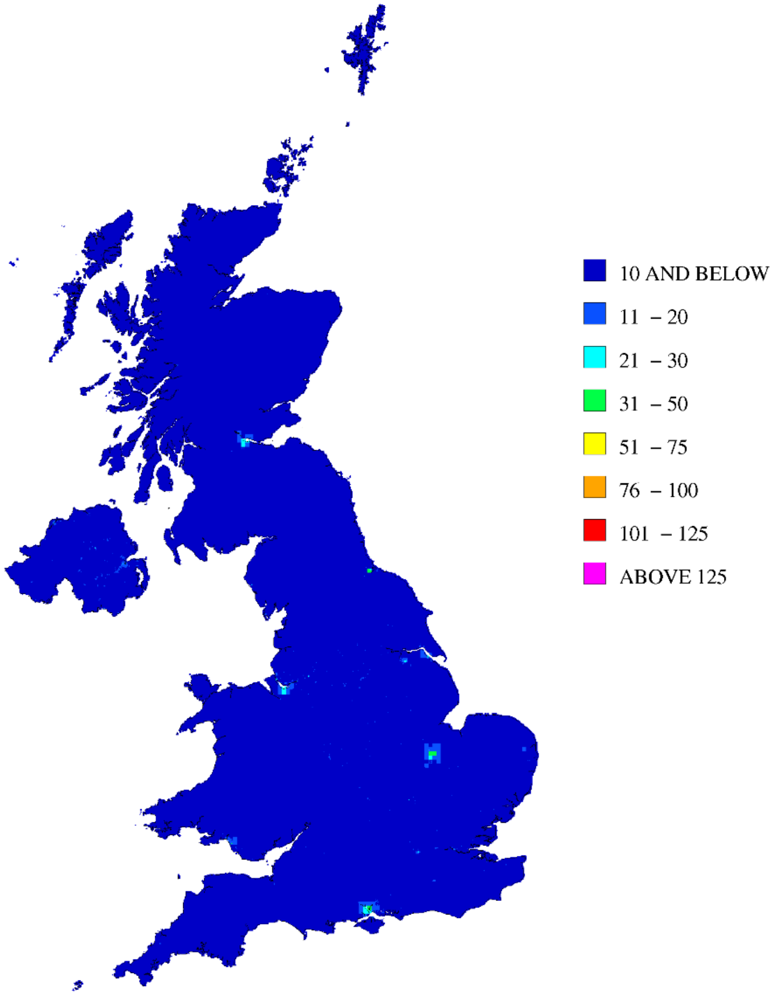

4.2 SO_2 emissions

Estimates of the emissions of SO_2 from the UK National Atmospheric Emissions Inventory 2017 (NAEI 2017) have been used in this study (Richmond et al., 2019). Emissions projections have been provided by the NAEI (Passant, 2019) based on BEIS EEP 2018 energy and emissions projections (BEIS, 2018). Figure 4-6 shows the UK total SO_2 emissions for 2017 and emissions projections for 2020, 2025 and 2030 split by SNAP code, with the coding described in Table 3.2. Values for intermediate years have been interpolated in this figure.

The emissions are dominated by point source emissions from combustion in energy production and transformation. The predicted trend in total emissions is for a decrease in SO_2 emissions from 2017 onwards, dominated by a reduction in emissions from combustion point sources. Emissions from combustion (industry), combustion (domestic) and shipping are also expected to decline.

Figure 4-6 - Total UK SO_2 emissions for 2017 and emissions projections up to 2030 by SNAP code from NAEI 2017

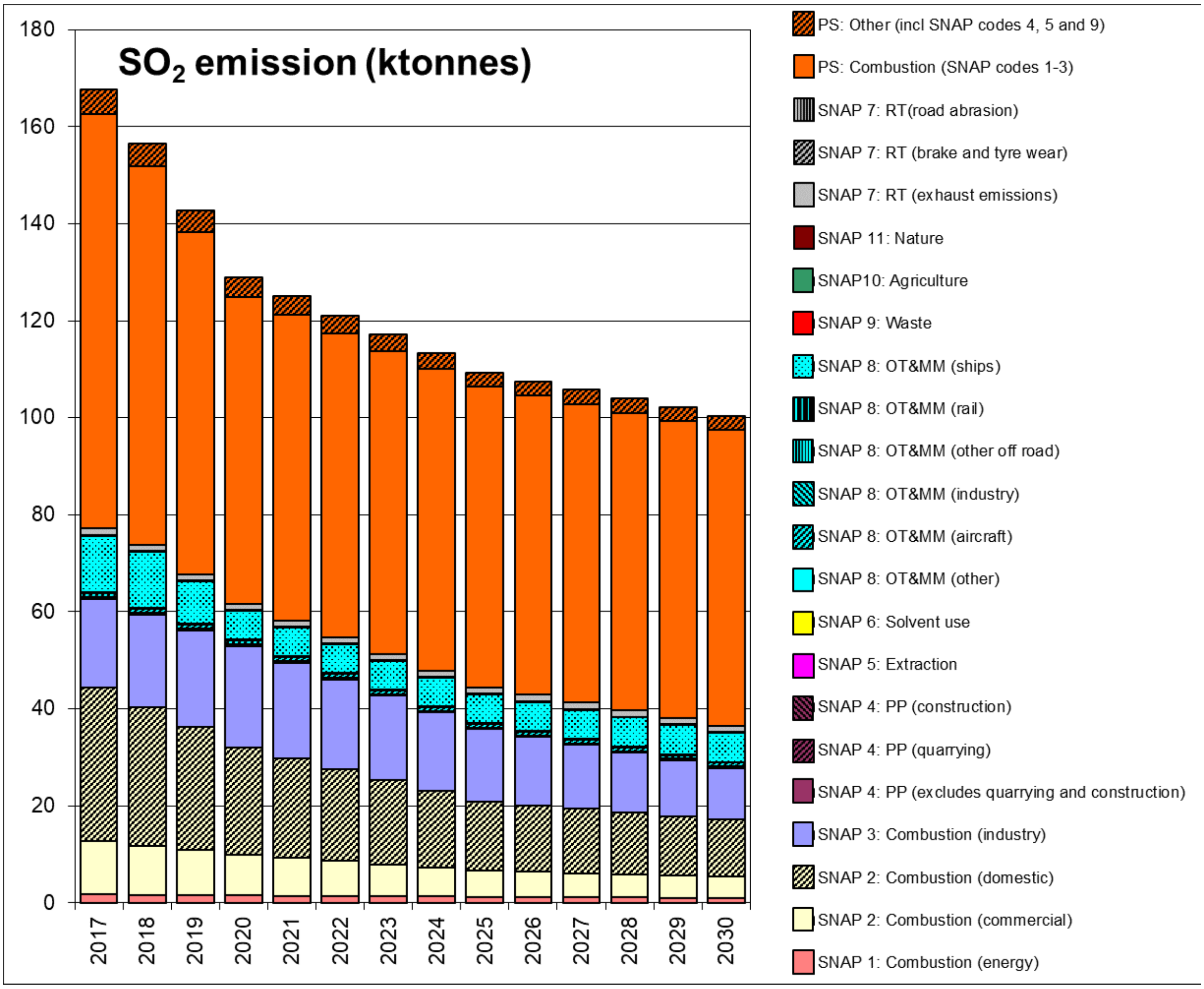

4.3 SO_2 modelling

The modelling methods for SO_2 were developed by Abbott and Vincent (1999, 2006). Emissions from point and area sources have been modelled separately and the results combined to produce the concentration maps.

4.3.1 Annual mean and winter mean modelling

4.3.1.1 SO_2 contributions from large and small point sources

Point sources in the NAEI 2017 have been classified as large if they fulfil either of the following criteria:

- Annual SO_2 emissions in the NAEI 2017 are greater than 500 tonnes for any given plant
- Stack parameters are already available for any given plant in the PCM stack parameters database (described in Section 3.3.1)

The contribution to ambient concentrations from large point sources were predicted using the dispersion model ADMS 5.2. Surface roughness was assumed to be 0.1 m at both dispersion and meteorological sites.

Prior to 2016 the large points modelling for SO_2 used hourly emissions profiles for the power stations with the largest releases provided by the Environment Agency (England and Wales) or Scottish Power (Scotland). However, from 2016 onwards these data are not available because of changes to permit requirements under the Industrial Emissions Directive (IED, 2010). Previously (e.g. Brookes et al., 2017) power station with large SO_2 releases for which hourly emissions profiles were not available, were modelled using time varying emissions profiles typical of electricity generation in summer and winter derived from the National Grid Seven Year Statement for 2011 (NETS 2011 SYS). Given the lack of reported emissions profiles, these typical profiles have been applied to treat the time variation in emissions for power stations in the 2018 assessment modelling for SO_2. These temporal profiles have been applied in combination with the NAEI 2017 emission estimates for these sources projected to 2018 using factors derived from NAEI source sector total emissions for point sources for 2017 and NAEI emissions projections for 2018 (Passant, 2019).

Concentrations resulting from emissions from other large SO_2 point sources were modelled using the projected NAEI emissions without time varying emissions. Closure of plant or activities are taken into account when deriving the source sector projection factors by subtracting the base year emissions associated with plant closure from the relevant source sector total for point sources for the NAEI base year. A total of 441 large point sources were modelled using emission release characteristics from the PCM stack parameters database.

Concentrations resulting from the projected emissions from small point sources were modelled using the small point source model described in Appendix 3. In line with the method applied for the large point sources the NAEI 2017 emissions for small point sources have been scaled to 2018 using the same source sector specific projection factors applied to the large point sources. Any point sources in the NAEI base year which closed before the start or early in the current assessment year are removed from the modelling, based on recommendations from the NAEI team (Passant pers. comm. 2018a).

The NAEI 2017 includes point source emissions estimates derived from carbon emissions data reported under the EU-Emissions Trading Scheme (ETS), most recently described in Tsagatakis et al. (2019). These point sources are referred to as ETS points in this report. These derived air quality pollutant emissions are particularly uncertain and therefore in previous assessments (e.g. Brookes et al., 2017) emissions were capped at reporting thresholds and treated as small point sources. For the 2016 and 2017 assessment (Brookes et al., 2019a, 2019b) the NAEI recommended treating the ETS points that have emissions greater than the large points modelling threshold as large points and not to apply a cap (Passant pers. comm. 2017). The 2018 assessment continues this approach. Thus, based on the criteria for the treatment of large point sources described above, 140 ETS point sources were modelled as an additional set of large point sources (using the approach described above). ETS points that were not classified as large point sources were modelled using the SO_2 small points approach described above.

For the large point sources (including large ETS points), concentrations were predicted for 5 km x 5 km resolution receptor grids within a set of receptor areas (known as tiles), which together cover the UK. The size of the receptor areas was typically 100 km x 100 km, extending out to 150 km where appropriate. All sources within the receptor area and extending out 100 km from the tile border were assumed to influence concentrations within the receptor area. Concentrations have been modelled using sequential meteorological data for 2018 from Waddington in Lincolnshire. This site has been chosen as the most representative of meteorology in the vicinity of the largest point sources in the UK. This approach ensures that the combined impact of several sources on ambient high percentile concentrations is estimated correctly. While not essential for the estimation of the annual mean, this method enables both the annual mean and high percentiles to be calculated from the same set of dispersion model calculations.

4.3.1.2 SO_2 contributions from local area sources

The 2018 area source SO_2 emissions maps have been calculated from the NAEI 2017 emissions maps following the method described in Section 3.3.5. Except for SNAP sector 3 (combustion in industry), the contribution to ambient SO_2 concentrations from area sources was calculated using a dispersion kernel approach. Concentrations are predicted for a 1 km x 1 km receptor grid, from the area source emissions within a 33 km x 33 km square surrounding each receptor. Dispersion kernels were calculated using ADMS 5.2 and hourly sequential meteorological data for 2018 from Waddington. Modelling of the area sources is described in more detail in Appendix 4.

Revised methods introduced in the 2012 compliance assessment (Brookes et al., 2013) for modelling the contributions to SO_2 from SNAP 2 (domestic and non-domestic combustion) and SNAP 3 (combustion in industry) area sources were used and have been described in Section 3.3.5.

The use of surrogate statistics for mapping area source emissions sometimes results in unrealistically large concentrations in some grid squares for a given sector. Emission caps have therefore been applied to certain sectors. The emission caps applied are given in Table 4.2.

Table 4.2 - Emissions caps applied to SO_2 sector grids

SNAP code	Description	Cap applied (t/a/km^2)
SNAP 8 (Shipping only)	Other Transport & Mobile Machinery	35

4.3.1.3 Deriving annual and winter mean concentration maps

The point source and area source contributions are summed without calibration, along with an estimate (0.19 µg m^{-3}) of the contribution from the long-range transport of SO_2 sources from continental European sources to derive the annual mean concentration. The long-range transport contribution was derived by a linear least-squares fit between the measured and modelled concentrations (Abbott and Vincent, 2006). The model is not calibrated for SO_2 because modelled values provide a reasonably good fit to measured concentrations and to avoid the risk of overfitting for the high percentile metrics.

The map of winter mean SO_2 concentrations was derived from the annual mean map by multiplying with a factor of 0.9144, which is the ratio between the average concentration measured at rural SO_2 monitoring sites during the 2017-2018 winter periods and annual concentration for 2018.

Measured concentrations from UK Acid Gases and Aerosols Monitoring Network (AGANet) sites, selected rural and urban background sites in the national automatic monitoring networks were compared with the modelled results. A list of the additional sites used in model verification is included in Appendix 1. The comparison plot for 2018 is shown in Figure 4-7.

Figure 4-7 - Comparison plot for 2018 annual mean SO_2 concentration

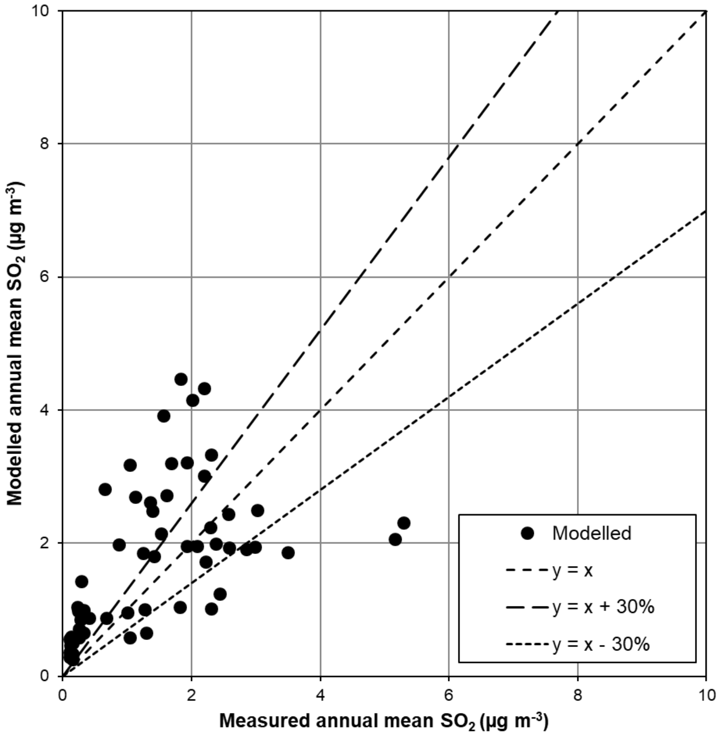

4.3.2 Modelling percentile concentrations for comparison with the 1-hour and 24-hour limit values

The methodology to produce the percentile maps is based on research on combining concentrations arising from area and industrial sources undertaken for the Environment Agency (Abbott and Vincent, 2006). This methodology aims to derive an estimate of the percentile concentrations at locations distant from the industrial sources. A weighted regression analysis was carried out by Abbott and Vincent, assuming that the variance of the residuals was proportional to the modelled concentration.

The regression model was of the form:

$$c_{measured} = \max\begin{bmatrix} Ac_{modelled\_industrial,\%ile} + 2(c_{modelled\_area} + c_{long\_range})_{annual} \\ 2Ac_{modelled\_industrial,annual} + k(c_{modelled\_area} + c_{long\_range})_{annual} \end{bmatrix}$$

The constant *A* was obtained from the regression analysis. The background multiplier factor, *k*, was derived from monitoring data. The factor “2”, used to scale the $(c_{modelled\_area} + c_{long\_range})_{annual}$ and $c_{modelled\_industrial,annual}$ components, has been shown to be a robust factor that allows short-term average concentrations to be estimated from modelled annual mean concentrations arising from non-industrial or industrial sources (Abbott et al., 2005). Table 4.3 presents the *A* and *k* factors used in the derivation of the maps.

Table 4.3 - Factors for percentile models

Metric	Constant (*A*)	Background multiplier factor (*k*)	c_{long_range}
99.73 percentile of 1-hour values	1.09	10.1	0.19
99.18 percentile of 24-hour values	1.23	3.3	0.19

The justification for treating industrial point sources and area emissions separately is because peaks in high percentile modelled contributions from point sources may not coincide with peaks in high percentile background concentrations – a problem that is more pronounced in emissions from large industrial point sources because the meteorological conditions that give rise to high concentrations from tall stacks can be very different from those that produce high concentrations from emissions at low level. Figure 4-8 and Figure 4-9 provide an intermediate quality check at selected rural and urban background sites which form part of the national network.

Figure 4-8 - Comparison plot for 2018 99.73 percentile of 1-hour mean SO_2 concentrations

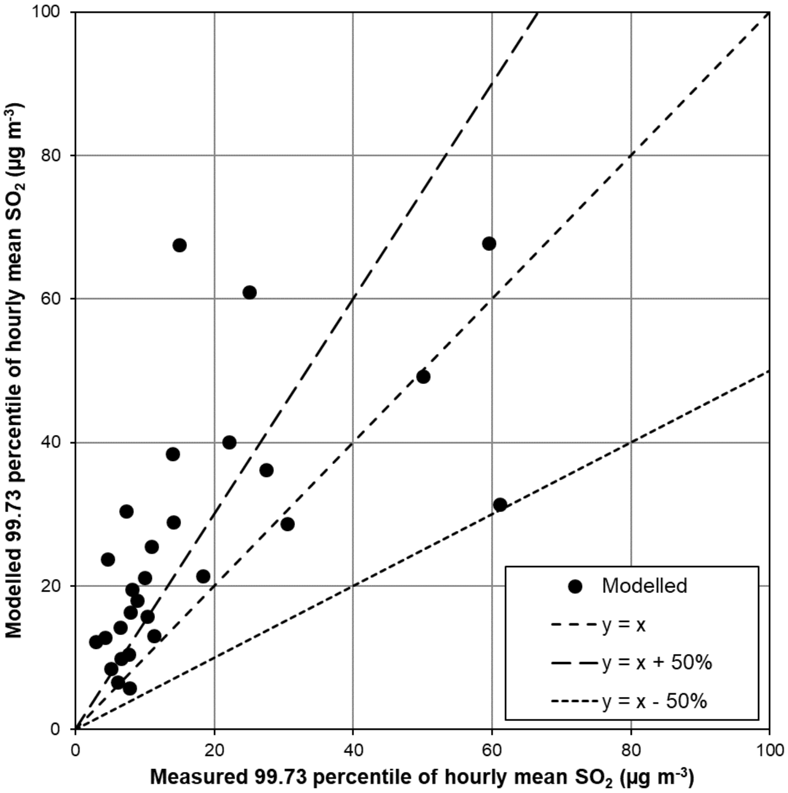

Figure 4-9 - Comparison plot for 2018 99.18 percentile of 24-hour mean SO_2 concentrations

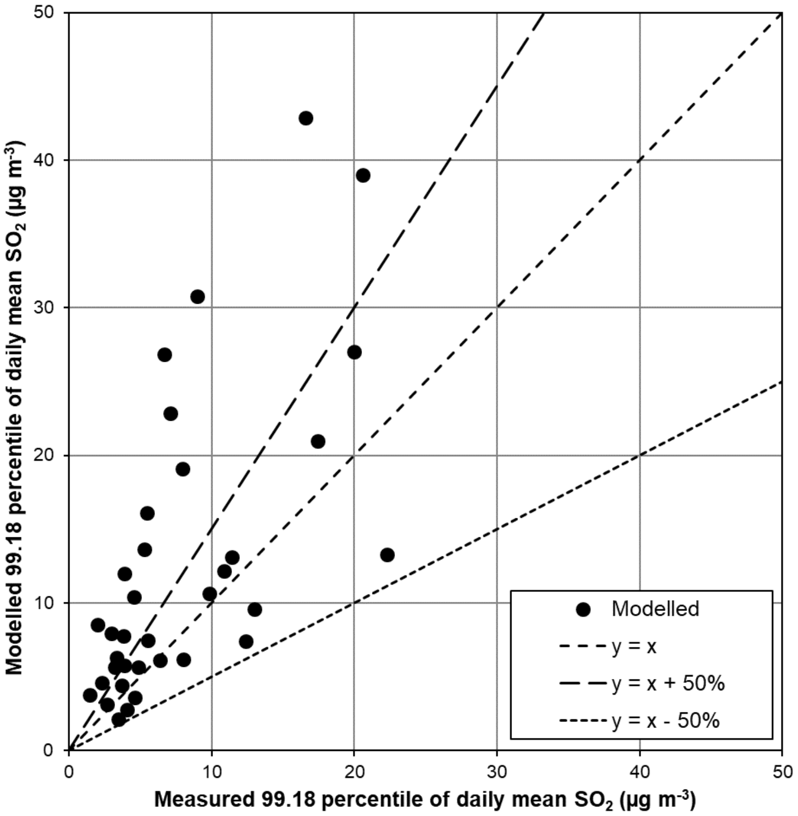

An alternative method was used to derive the high percentile concentrations in Northern Ireland. This was required because area sources, predominately emissions from domestic solid and liquid fuel use, make a more significant contribution to observed high percentile concentrations in Northern Ireland than in the rest of the United Kingdom. Additionally, the smaller number of point sources in Northern Ireland means that these sources make a much smaller contribution to the observed high percentile concentrations.

Maps of high percentile concentrations in Northern Ireland have been calculated from the mapped annual mean SO_2 concentrations using a linear least-squares fit between measured annual mean and measured high percentile concentrations in Northern Ireland over a ten-year period from 2008 to 2018 at AURN National Network and Ricardo Calibration Club monitoring sites. Ten years of data have been used to enable the calculation of robust estimates. Figure 4-10 and Figure 4-11 show the relationship between the annual mean and the 99.73 percentile of 1-hour mean values and the 99.18 percentile of 24-hour mean values at the sampling sites in Northern Ireland.

The equations used to derive the high percentile maps are:

Predicted 99.73%ile in Northern Ireland = 8.7406 × Modelled Annual Mean + 0.9748 µg m^{-3}, and

Predicted 99.18%ile in Northern Ireland = 4.2889 × Modelled Annual Mean + 0 µg m^{-3}.

Figure 4-10 - Relationship between mean concentration and 99.73 percentile of 1-hour concentrations at sampling sites in Northern Ireland, 2008-2018

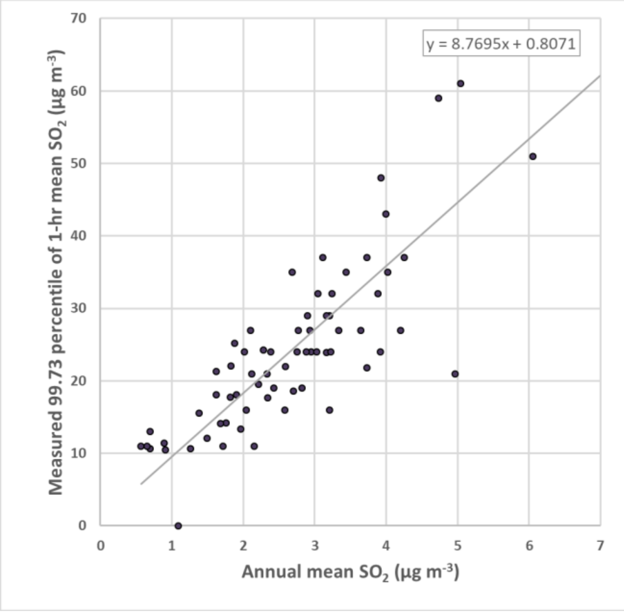

Figure 4-11 - Relationship between mean concentration and 99.18 percentile of 24-hour concentrations at sampling sites in Northern Ireland, 2008-2018

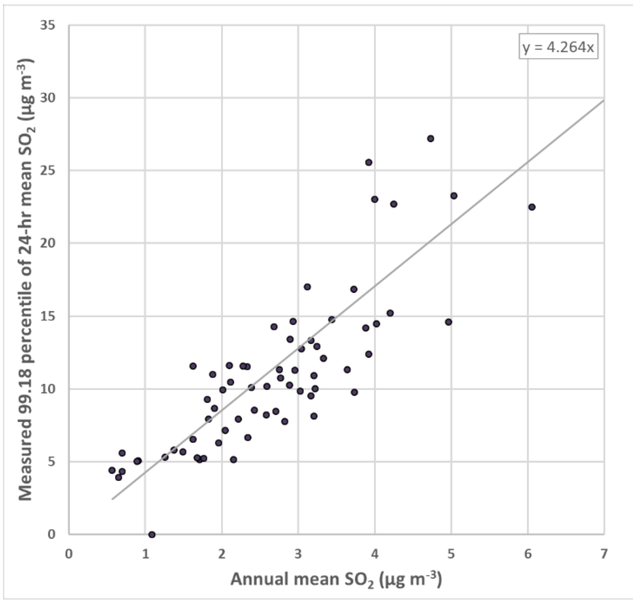

4.4 Results

4.4.1 Verification of mapped values

Figure 4-12, Figure 4-13 and Figure 4-14 show comparisons of modelled and measured annual mean, 99.73 percentile of 1-hour mean and 99.18 percentile of 24-hour mean SO_2 concentrations in 2018 at monitoring site locations in the UK. Both the national network sites and the verification sites are shown. Lines representing y = x – 30 % and y = x + 30% or y = x – 50 % and y = x + 50% are also shown (the AQD data quality objective for modelled annual mean and percentile SO_2 concentrations respectively – see Section 1.5). The 'National Network Sites' include AURN sites and (for annual means only) Acid Gases and Aerosols Monitoring Network (AGANet) sites. 'Verification sites' include ad-hoc monitoring sites and Ricardo Calibration Club monitoring sites. A complete list of the AURN sites used is presented in Data flow C of the e-Reporting submission (CDR, 2019). Details of other verification sites are presented in Table A1.2 of Appendix 1 which also includes sites maintained by Hanson Building Products Ltd.

Figure 4-12 - Verification of annual mean SO_2 model, 2018

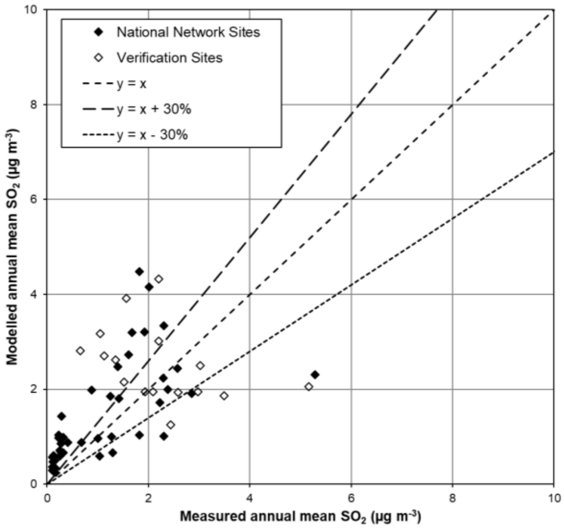

Figure 4-13 - Verification of 99.73 percentile of 1-hour mean SO_2 model, 2018

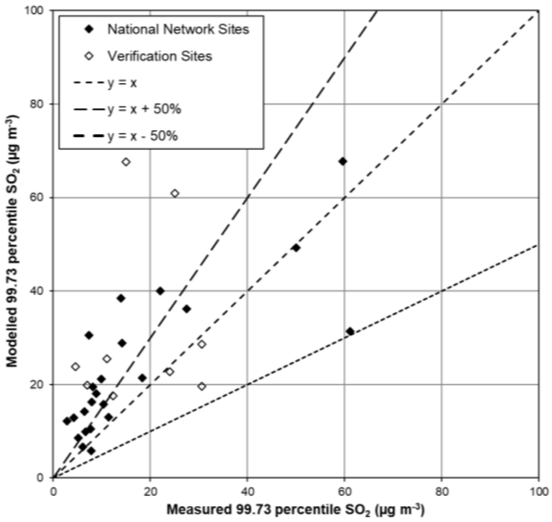

Figure 4-14 -Verification of 99.18 percentile of 24-hour mean SO_2 model, 2018

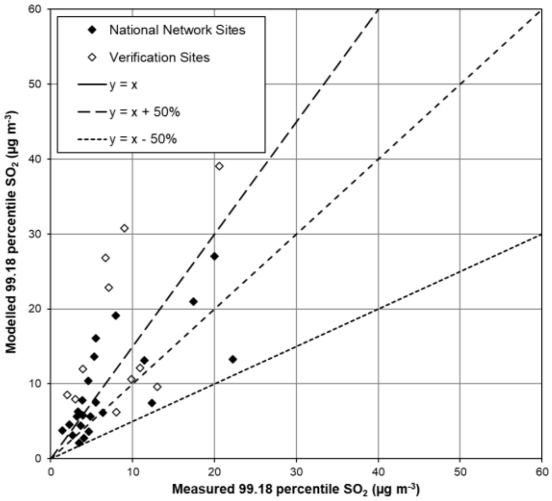

Summary statistics comparing modelled and measured SO_2 concentrations for annual mean, 99.73 percentile of hourly values and 99.18 percentile are listed in Table 4.4, Table 4.5 and Table 4.6, respectively.

For the National Network (comprising sites belonging to the combined the AURN and AGANet networks) the measured annual average concentration over all these sites (1.2 µg m^{-3}) compared reasonably with the modelled concentrations predicted at the same sites (1.7 µg m^{-3}). However, only about 20% of the sites fell within the DQO. Reasons for poor performance are likely to be very local emission sources not adequately represented in the emission inventory. Note that the 1 km x 1 km grid annual mean map is not compared directly with the annual mean limit value; the zonal mean of the 1 km x 1 km grid squares in vegetation areas has been calculated for a 30 km x 30 km grid, as discussed above.

For the 99.73 percentile of 1-hour mean concentrations and the 99.18 percentile of 24-hour mean concentrations there is again reasonable agreement between measured and modelled means at the AURN sites and quality check sites (AURN and AGANet sites). Due to the more generous data quality objectives for the short-term percentile concentrations, fewer sites, as expected, will fall outside the DQO limits.

Table 4.4 - Summary statistics for comparison between modelled and measured annual mean concentrations of SO_2 at background sites

	Mean of measurements (µg m^{-3})	Mean of model estimates (µg m^{-3})	R^2	% of sites outside DQO of ±30%	Number of sites in assessment
National Network[a]	1.15	1.47	0.40	80.5%	41
Verification Sites	2.21	2.51	0.146	75%	16

a includes measurement data from sites in Defra's AURN and AGANet

Table 4.5 - Summary statistics for comparison between modelled and measured 99.73 percentile of 1-hour mean concentrations of SO_2 at background sites

	Mean of measurements (µg m^{-3})	Mean of model estimates (µg m^{-3})	R^2	% of sites outside DQO of ±50%	Number of sites in assessment
National Network[b]	16.41	22.96	0.63	56.5%	23
Verification Sites	33.03	50.21	0.26	61.5%	13

b includes measurement data from sites in Defra's AURN only

Table 4.6 - Summary statistics for comparison between modelled and measured 99.18 percentile of 24-hour mean concentrations of SO_2 at background sites

	Mean of measurements (µg m^{-3})	Mean of model estimates (µg m^{-3})	R^2	% of sites outside DQO of ±50%	Number of sites in assessment
National Network[c]	6.96	9.13	0.54	39.14%	23
Verification Sites	13.23	19.69	0.14	69.2%	13

c includes measurement data from sites in Defra's AURN only

4.4.2 Source apportionment

Figure 4-15 shows the source apportionment for modelled annual mean concentrations of SO_2 at AURN monitoring sites for 2018. Measured annual mean concentrations at each site are shown for reference. The figure shows that annual mean SO_2 concentrations at most sites are dominated by contributions from industrial emissions treated as either point sources or area sources. Some sites also have significant contributions from shipping, commercial and domestic sources of emissions.

Figure 4-15 - Annual mean SO_2 source apportionment at AURN monitoring sites in 2018 (the area type of each site is shown in parenthesis after its name – see Table 3.5)

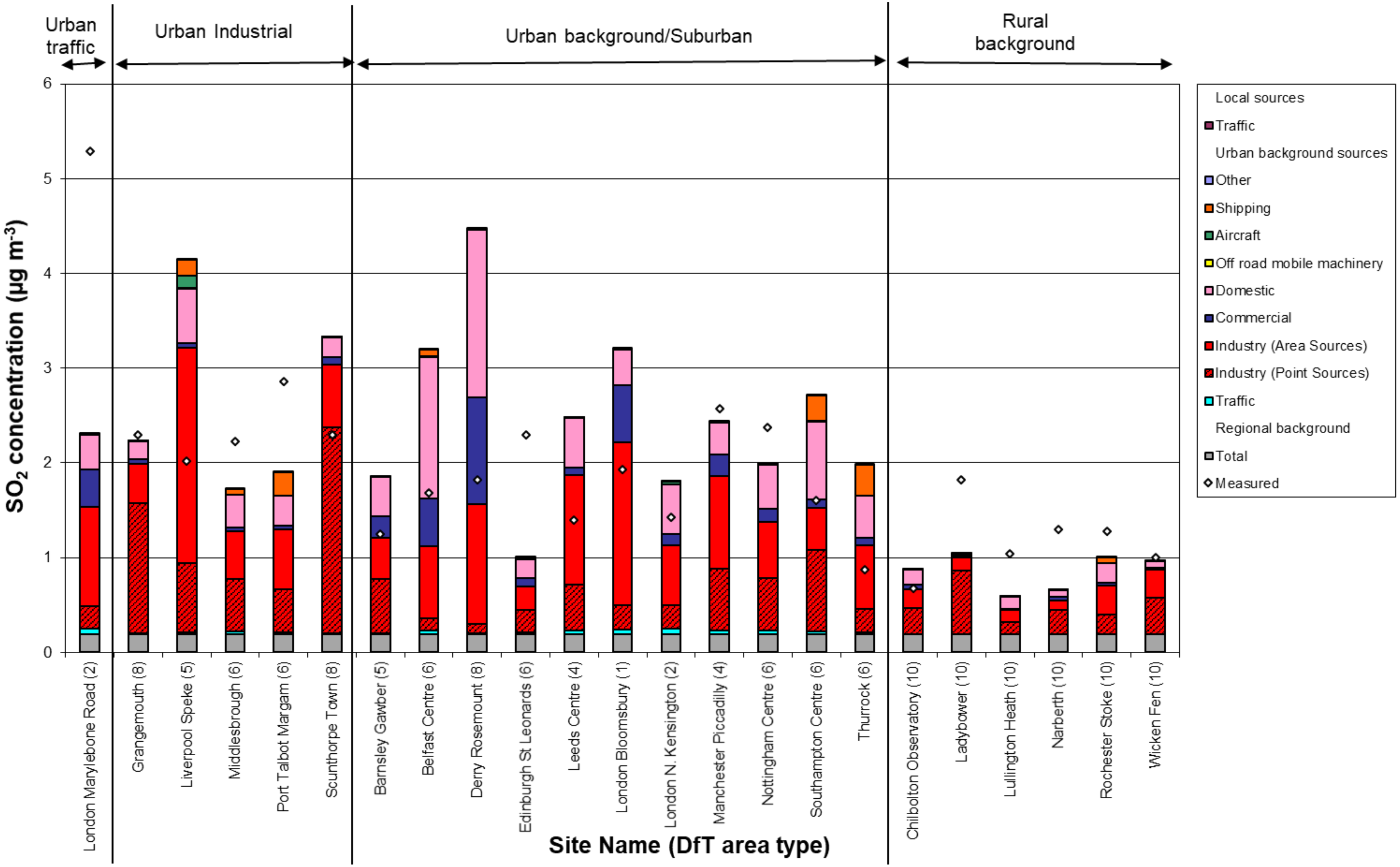

5 PM_{10}

5.1 Introduction

5.1.1 Limit values

Two limit values for ambient PM_{10} concentrations are set out in the AQD. These have been specified for the protection of human health and came into force from 01/01/2005. These limit values are:

- An annual mean concentration of 40 µg m^{-3}.
- A 24-hour mean concentration of 50 µg m^{-3}, with 35 permitted exceedances each year

Results of the assessment in terms of comparisons of the modelled concentrations with the annual mean and 24-hour mean limit values for PM_{10} have been reported in e-Reporting Data flow G (CDR, 2019).

5.1.2 Annual mean model

Maps of annual mean PM_{10} in 2018 at background and roadside locations are shown in Figure 5-1 and Figure 5-2. These maps have been calibrated using PM_{10} measurements within the national network for which co-located $PM_{2.5}$ measurements are also available. The models for PM_{10} and $PM_{2.5}$ are designed to be fully consistent. Each component is either derived from emission estimates for PM_{10} or $PM_{2.5}$ or the contributions to the fine and coarse particle size fractions are estimated separately. This enables us to carry out an additional sense check that the calibration parameters for the two pollutants are reasonably consistent. Measurements from national network sites without collocated $PM_{2.5}$ instruments have been used as an additional verification dataset (and similarly $PM_{2.5}$ sites without PM_{10} have been used as an additional verification dataset for $PM_{2.5}$). Measurements from gravimetric instruments within the national network and from non-national network sites have also been used to verify the mapped estimates. Appropriate scaling factors have been applied prior to comparison where required.

A detailed description of the Pollution Climate Mapping (PCM) models for PM in 2004 has been provided by Stedman et al. (2007). The methods used to derive the maps for 2018 are largely the same as was adopted for the 2017 maps described in Brookes et al. (2019b).

Figure 5-1 - Annual mean background PM_{10} concentration, 2018 (µg m^{-3}, gravimetric)

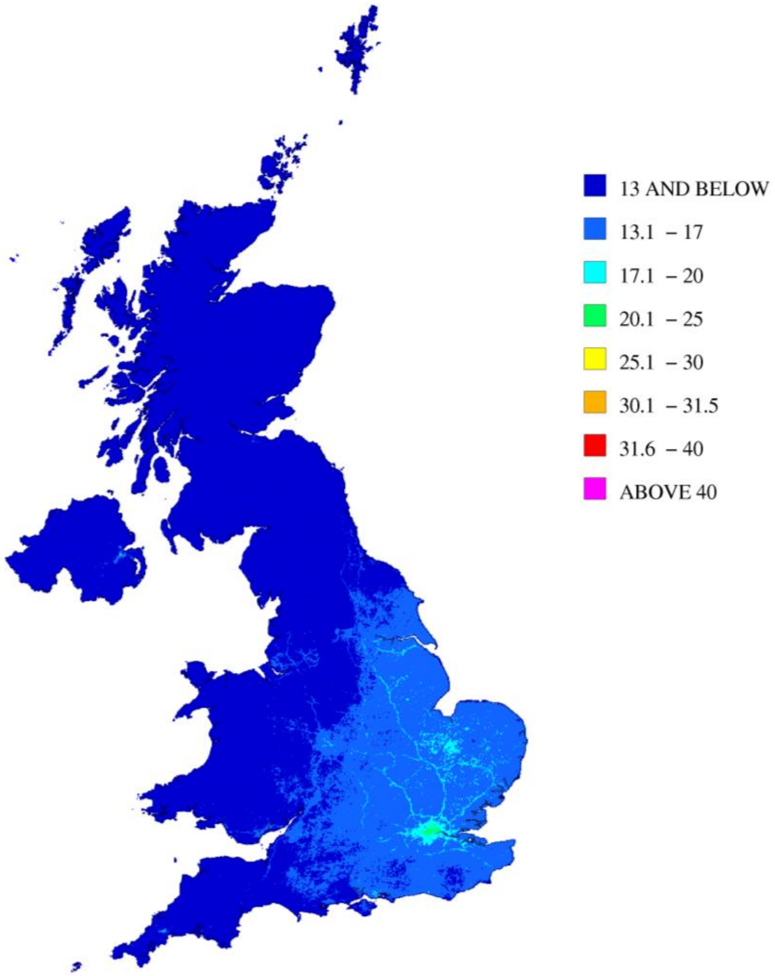

Figure 5-2 - Urban major roads, annual mean roadside PM_{10} concentration, 2018 (µg m^{-3}, gravimetric)

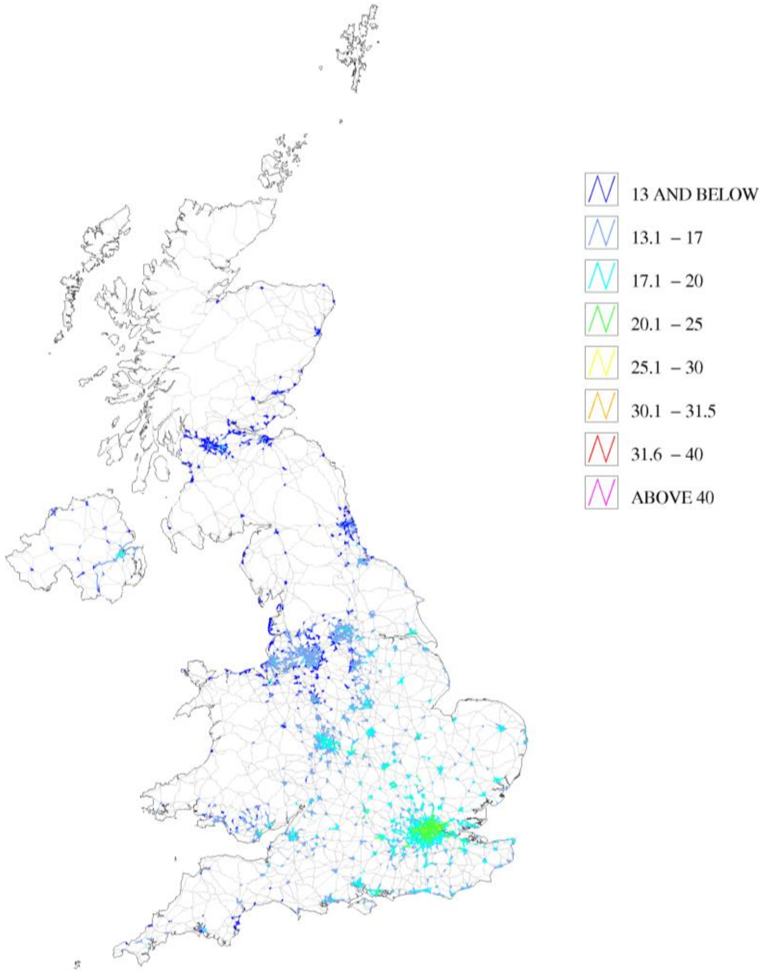

5.1.3 Overview of the PCM model for PM_{10}

Figure 5-3 shows a simplified flow diagram of the PCM model for PM_{10}. A summary of the PCM model method, input and assumptions for PM_{10} is presented in Table 5.1.

Figure 5-3 - Flow diagram for PCM PM_{10} model

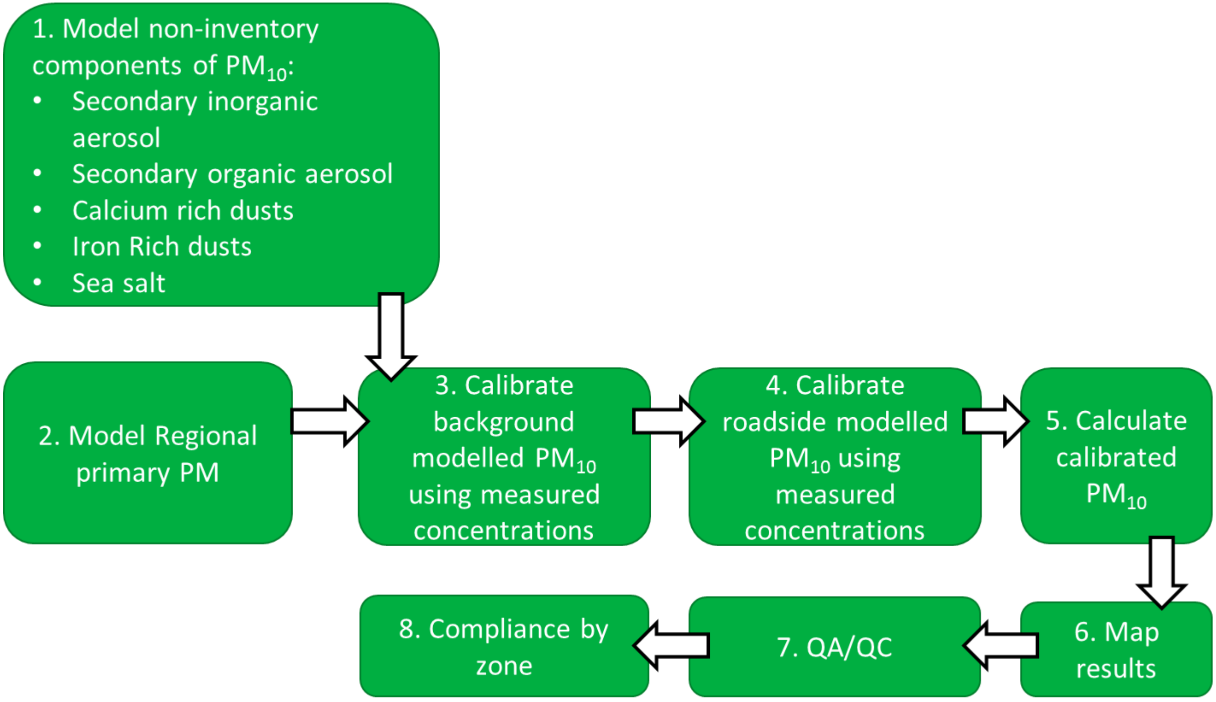

Table 5.1 – PCM model method, input and assumptions summary for PM_{10}

Heading	Component	Details
General	Pollutant	PM_{10}
	Year	2018
	Locations modelled	Background and traffic locations
	Metric	Annual mean
Input data	Emission inventory	NAEI 2017
	Energy projections	Energy Projections 2017
	Road traffic counts	2017
	Road transport activity projections	DfT (2018) traffic (re-based to 2017 NAEI), DfT (2019) car sales projections, TfL traffic (2019) and fleet (2018) projections for London
	Road transport emission factors	COPERT 5
	Measurement data	2018
	Meteorological data	Hourly data from Waddington 2018
Model components	Regional	See details under “pollutant specific” heading
	Large point sources	287 sources modelled using ADMS 5.2
	Small point sources	PCM small points model
	ETS point sources	PCM small points model
	Large ETS point sources	137 sources modelled using ADMS 5.2
	Area sources	PCM dispersion kernels generated using ADMS 5.2. Time varying emissions for road transport and domestic sources. PCM small points model for industrial combustion emissions.

Heading	Component	Details
	Roadside increment	PCM Roads Kernel Model using ADMS-Roads 4.1
Calibration	Model calibrated?	Yes
	Number of background stations in calibration	28 (stations with both PM_{10} and $PM_{2.5}$)
	Number of traffic stations in calibration	14 (stations with both PM_{10} and $PM_{2.5}$)
Pollutant specific	Secondary inorganic aerosol	Interpolated from SO_4, NO_3 and NH_4 measurements at a network of 27 rural stations, scaling factors applied for size fraction, bound water and counterions
	Secondary organic aerosol	Results from the NAME model for 2008
	Regional primary particles	Calculated using the TRACK receptor oriented, Lagrangian statistical model
	Regional calcium rich dusts from re-suspension of soils	Modelled using information on land cover (bare soil, root and cereal crops) and dispersion kernel incorporating emissions and dispersion processes
	Regional iron rich dusts from re-suspension	Assigned a constant value of 1 µg m^{-3}
	Iron rich dusts from re-suspension due to vehicle activity	Modelled using information on vehicle movements on major roads (HDV) and dispersion kernel incorporating emissions and dispersion processes
	Sea Salt	Interpolated measurements of Cl, scaling factor applied for sea water composition
	Residual	A value assigned based on best fit to PM_{10} and $PM_{2.5}$ measurements: zero, no residual required for 2018

5.1.4 Outline of the annual mean model

The maps of annual mean background PM_{10} concentrations have been calculated by summing contributions from different sources:

- Secondary inorganic aerosol (sulphate, nitrate and ammonium, formed in the atmosphere by chemical reactions from gaseous species (SO_2, NO_x and NH_3)
- Secondary organic aerosol (non-volatile organic molecules formed in the atmosphere from volatile organic compounds by chemical oxidation reactions)
- Large point sources of primary particles
- Small point sources of primary particles
- Point sources with emissions estimates for air quality pollutants based on reported carbon emissions (ETS points)
- Regional primary particles
- Area sources related to domestic combustion
- Area sources related to combustion in industry
- Area sources related to road traffic
- Other area sources
- Regional calcium rich dusts from re-suspension of soils
- Regional iron rich dusts from re-suspension
- Iron rich dusts from re-suspension due to vehicle activity
- Sea salt
- Residual (zero for 2018)

The concentrations of many of these components have been estimated separately for the fine and coarse fraction. This enables a consistent method to be adopted for estimation of PM_{10} (the sum of the fine and coarse fractions) and $PM_{2.5}$ (fine fractions only). These component pieces are aggregated to a single 1 km x 1 km background PM_{10} grid. An additional roadside increment is added for roadside locations.

The results from the annual mean model can be directly compared with the annual mean limit value in order to carry out the air quality assessment.

5.1.5 Compliance assessment for the 24-hour limit value

24-hour mean concentrations have not been explicitly modelled for comparison with the 24-hour limit value. An annual mean concentration of 31.5 µg m^{-3}, gravimetric has been taken to be equivalent to 35 days with 24-hour mean concentrations greater than 50 µg m^{-3} gravimetric (the 24-hour limit value) for 2018. A modelled annual mean concentration of greater than this value has been taken to indicate a modelled exceedance of the 24-hour mean limit value. This approach was initially proposed by Stedman et al. (2001a) who recommended a value of 31.5 µg m^{-3} based on an analysis of monitoring data for the period 1992 to 1999. An analysis of monitoring data (Brookes et al., 2011) showed that the value of 31.5 µg m^{-3} was still valid up to and including 2010. An analysis of monitoring data for 2018 shown in Figure 5-4 showed that this value is appropriate and precautionary for 2018.

Figure 5-4 - The relationship between the 90th percentile of 24-hour mean PM_{10} concentration and annual mean concentration (µg m^{-3}) for 2018

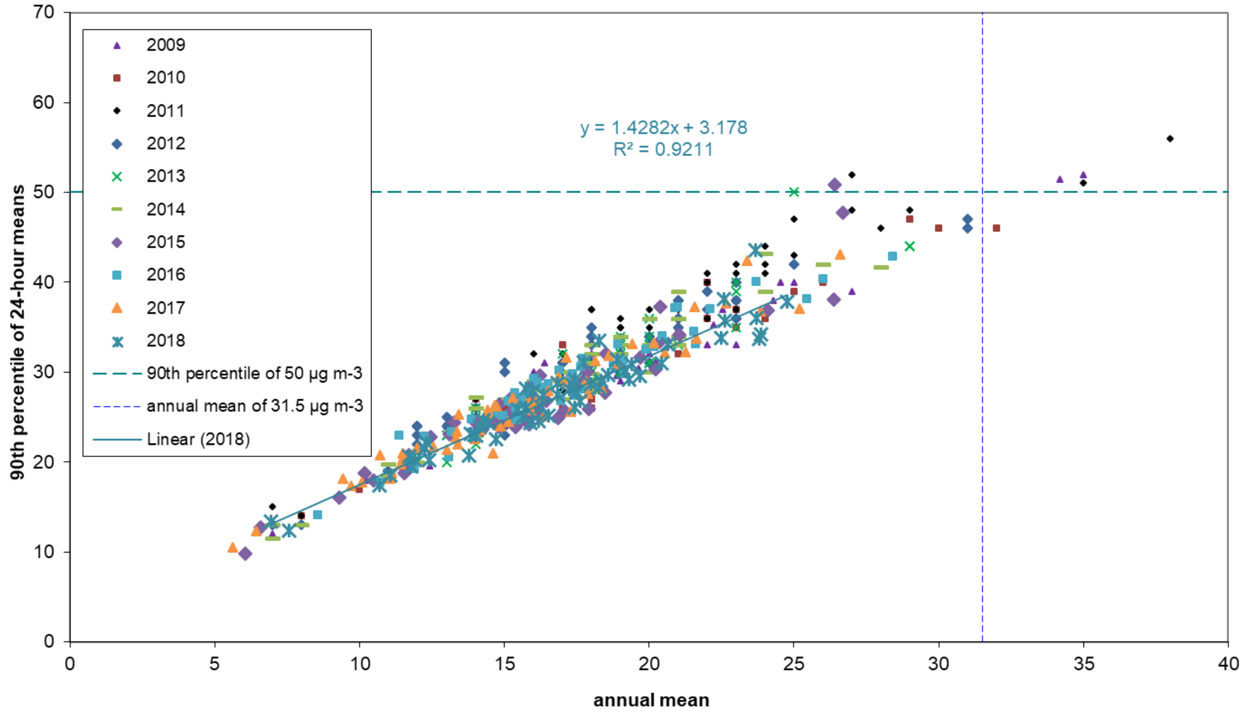

5.1.6 Chapter structure

This chapter describes modelling work carried out for 2018 to assess compliance with the PM_{10} limit values described above. Emission estimates for primary PM are described in Section 5.2, Section 5.3 describes the PM_{10} modelling methods, the modelling results are presented in Section 5.4.The methods used to subtract the contribution from natural sources (sea salt) and the results of this subtraction are presented in Section 5.5.

5.2 PM_{10} emissions

Estimates of the emissions of primary PM from the UK National Atmospheric Emission Inventory 2017 (NAEI 2017) have been used in this study (Richmond et al., 2019). Emissions projections have been provided by the NAEI (Passant, 2019) based on BEIS EEP 2018 energy and emissions projections (BEIS, 2018).

Figure 5-5 shows UK total PM_{10} emissions for 2017 and emissions projections for 2020, 2025 and 2030 split by SNAP code, with the coding described in Table 3.2. Values for intermediate years have been interpolated in this figure. Figure 5-5 shows that PM_{10} emissions in 2017 include contributions from a wide range of different source sectors. Some of the sectors with the largest contribution to the total in 2017 include domestic combustion, road traffic (exhaust, road abrasion and brake and tyre wear), agriculture, construction and combustion point sources.

Maps of emissions from area sources for 2018 were derived from the 2017 inventory maps using specific scaling factors derived for each combination of source and activity (typically fuel type), as described for NO_X (Section 3.3.5). The emissions from point sources were scaled in a similar way, see Section 3.3.1. The methods used to calculate ambient concentrations from the estimates of primary PM emissions are described below for point, area, road link and regional sources.

Figure 5-5 - Total UK PM_{10} emissions for 2017 and emissions projections up to 2030 by SNAP code from NAEI 2017

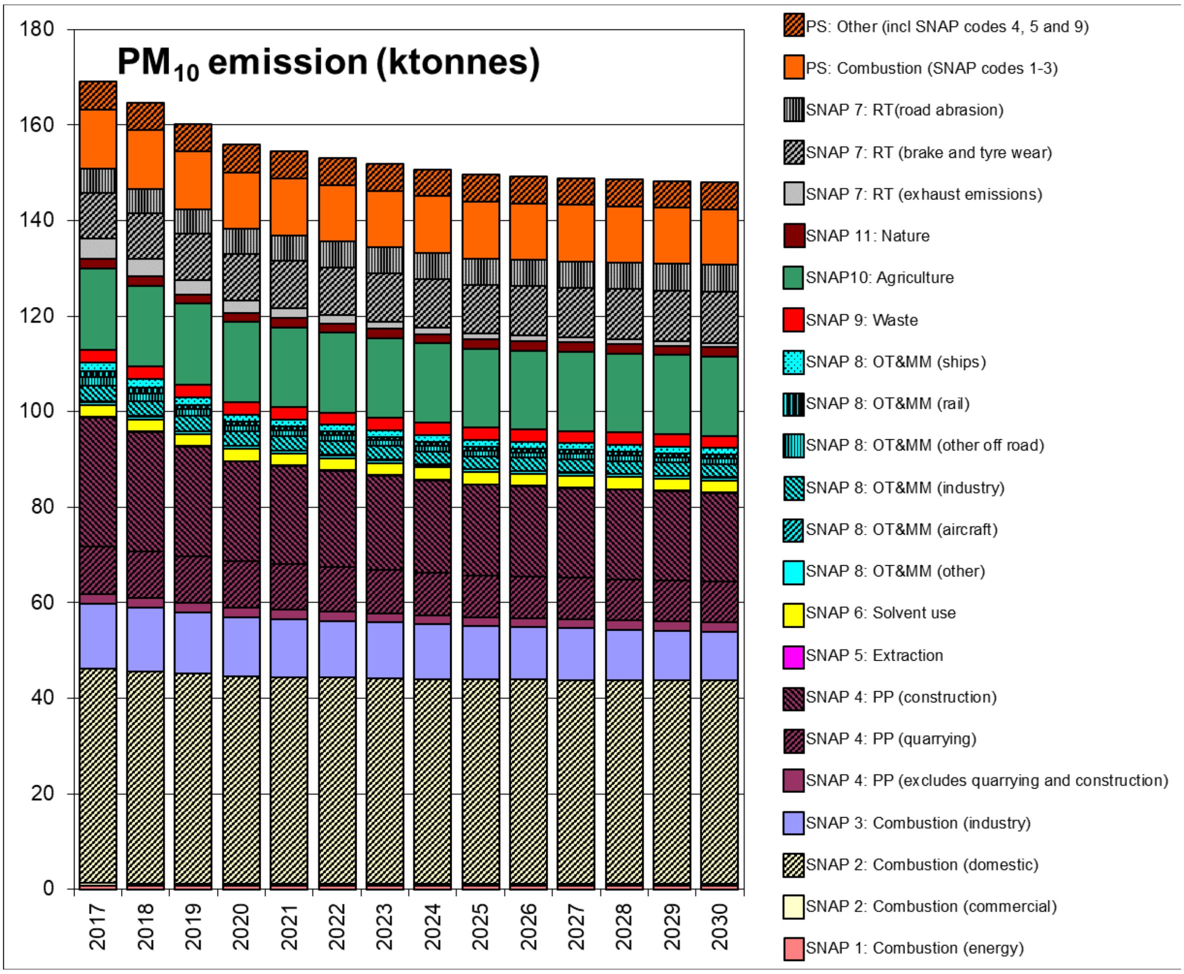

5.3 PM_{10} modelling

5.3.1 Contributions from secondary inorganic aerosol

Maps of secondary inorganic aerosol (SIA) concentrations across the UK have been calculated from rural measurements of sulphate, nitrate and ammonium concentrations by interpolation, followed by the application of scaling factors derived from mass closure modelling. Monthly measurements are available for 27 rural monitoring sites within the UKEAP AGANet and NAMN networks for 2018 (some sites were excluded due to low data capture). The measurement method used within the AGANet was changed at the beginning of 2016. This revised method typically results in higher measured concentrations of sulphate and nitrate (Tang et al., 2015). Concentration surfaces on a 5 km x 5 km grid were calculated from the measurement data using inverse distance weighting (IDW).

These secondary components were then split into fine and coarse fractions and non-volatile and volatile components using coefficients derived with reference to the detailed PM sampling carried out during the PUMA campaign at the University of Birmingham urban background monitoring site in June and July 1999 (Harrison et al., 2006 and summarised by Kent et al., 2007a). Fine PM is used to describe $PM_{2.5}$ and coarse PM is used to describe $PM_{2.5\text{-}10}$ in this report.

The non-volatile secondary PM has been assumed to be sampled by a TEOM instrument, a gravimetric instrument should sample the sum of the non-volatile and volatile components. These secondary components were also scaled according to ‘bound water’ associated with the mass of water embedded within the particles (AQEG, 2005). Particle bound water is associated with the hygroscopic anions (Harrison et al., 2006). This has been assumed to contribute to the fine and coarse components gravimetric but not the TEOM. Therefore, a particle bound water scaling factor of 1.279 has been applied to the SIA components for the gravimetric maps to account for the additional mass of water associated with the particulate matter (see Table 5.2). The scaling factors for bound water and counter ions (non-volatile) have not been used in this study but would be appropriate for mapping TEOM concentrations. The factor for coarse mode nitrate is higher as this includes the mass of the counter-ion (sodium or calcium).

The split between coarse and fine nitrate was revised for the 2006 modelling assessment with reference to measurement data from the TRAMAQ (Abdalmogith et al., 2006) and Birmingham (Harrison and Yin, 2006) studies. The revised method has also been used in this assessment. The split between fine and coarse PM is simple to interpret for most PM constituents but is more complex for nitrate PM because there are two modes. The fine nitrate mode consists of ammonium nitrate, which is volatile, and is all in the fine $PM_{2.5}$ fraction. The coarse mode consists of sodium nitrate, which is split half and half between fine $PM_{2.5}$ and coarse $PM_{2.5\text{-}10}$ fractions (Abdalmogith et al., 2006). Measurement data from the Birmingham study (Harrison and Yin, 2006) shows that the fine $PM_{2.5}$ nitrate to coarse $PM_{2.5\text{-}10}$ ratio was 3.5:1. Thus the fine mode nitrate to coarse mode nitrate ratio was 1.25:1. The factors for nitrate in Table 5.2 have been derived from a combination of this factor of 1.25 and the half and half split of the coarse mode nitrate into the fine $PM_{2.5}$ and coarse $PM_{2.5\text{-}10}$ fractions.

Table 5.2 - Scaling factors for size fraction, bound water and counter ion mass for secondary inorganic and organic aerosol

Pollutant	Size fraction	Scaling factor for size fraction	Scaling factor for bound water and counter-ion mass	Scaling factor for bound water and counter-ion mass (non-volatile)
SO_4	Fine	0.94	1.279	1.00
	Coarse	0.06	1.279	1.00
NO_3	Fine mode	0.556	1.279	0.00
	Coarse mode fine	0.222	1.60	1.32
	Coarse mode coarse	0.222	1.60	1.32
NH_4	Fine	0.97	1.279	0.86
	Coarse	0.03	1.279	1.00
SOA	Fine	1.00	1.0	0.00
	Coarse	0.0	1.0	0.00

5.3.2 Contributions from secondary organic aerosol

Estimates of annual mean secondary organic aerosol (SOA) concentrations in 2008 from the NAME Model on a 20 km x 20 km grid across the UK have been provided by Redington and Derwent (2013). SOA concentrations are assumed to have remained at 2008 levels in 2018 and this is reasonable because the majority (about 80% as a population-weighted mean) of the SOA is from biogenic sources. NAME is a Lagrangian dispersion model that simulates the dispersion, chemistry and deposition processes occurring in the atmosphere, utilising three dimensional meteorological fields from the Met Office Unified Model (Redington et al. 2009). The chemistry scheme includes the formation of anthropogenic and biogenic SOA, details of the scheme can be found in Redington and Derwent (2013). The SOA component has been assumed to fall within the $PM_{2.5}$ fraction.

5.3.3 Contributions from large and small point sources

Contributions to ground level annual mean primary PM concentrations from large point sources (those with annual emission greater than 200 tonnes, or for which emission release characteristics are known) in the NAEI 2017 have been estimated by modelling each source explicitly using the atmospheric dispersion model ADMS 5.2. Hourly sequential meteorological data for 2018 from Waddington was applied. Surface roughness was assumed to be 0.1 m at the dispersion site and 0.1 m at the meteorological site. Concentrations were calculated for a 99 km x 99 km square composed of a regularly spaced 1 km x 1 km resolution receptor grid. Each receptor grid was centred on the point source. A total of 287 point sources were modelled using emission release characteristics from the PCM stack parameters database (described in Section 3.3.1). The NAEI emissions for point sources for 2017 were scaled in order to provide values for 2018 as described in Section 3.3.1.

Contributions from PM point sources with less than 200 tonnes per annum release and for which emission characteristics were not known were modelled using the ‘small points’ model originally described by Stedman et al. (2005) and summarised in Appendix 3. This model consists of separate ‘in-square’ and ‘out-of-square’ components, in which concentrations are estimated using dispersion kernels, which have been calculated by using ADMS to model the dispersion of unit emissions from a central source to a grid of receptors at a spatial resolution of 1 km x 1 km squares. In line with the method applied for the large point sources the NAEI 2017 emissions for small point sources of PM have been scaled to 2018 using the same source sector specific projection factors applied to the large point sources.

The NAEI 2017 includes point source emissions estimates derived from carbon emissions data reported under the EU-Emissions Trading Scheme (ETS), most recently described in Tsagatakis et al. (2019). These point sources are referred to as ETS points in this report. These derived air quality pollutant emissions are particularly uncertain and therefore in previous assessments (e.g. Brookes et al., 2017) emissions were capped at reporting thresholds and treated as small point sources. For the 2016 assessment (Brookes et al., 2019a) the NAEI recommended treating the ETS points that have emissions greater than the large points modelling threshold as large points and not to apply a cap (Passant pers. comm. 2017). The 2018 assessment continues this approach. Thus, based on the criteria for the treatment of large point sources described above, 137 ETS point sources were modelled as an additional set of large point sources (using the approach described above). ETS points that were not classified as large point sources were modelled using the PM_{10} small points approach described above.

5.3.4 Contributions from distant sources of primary particles

Contributions from long-range transport of primary particles on a 20 km x 20 km grid have been estimated using the TRACK receptor oriented, Lagrangian statistical model (Lee et al., 2000). Emissions of primary PM_{10} were taken from the NAEI for UK sources and from EMEP (WebDab data, http://www.ceip.at/) for sources in the rest of Europe. Primary PM_{10} was modelled as an inert tracer. All sources within 10 km of the receptor point were excluded from the TRACK model to allow the area source model and the point source model to be nested within this long-range transport model without duplicating source contributions.

5.3.5 Iron and calcium rich dusts

5.3.5.1 Introduction

The NAEI does not explicitly include estimates of the emissions of iron or calcium rich dusts. Various process-based or more empirically based methods have therefore been applied to estimate the contribution of these dusts to ambient PM_{10} concentrations across the UK for sources not included in the NAEI.

The contributions have been split into three categories:

- Regional calcium rich dusts from re-suspension of soils
- Regional iron rich dusts from re-suspension
- Iron rich dusts from re-suspension due to vehicle activity

A method for estimating the mass of iron (Fe) and calcium (Ca) rich dusts was included in the modelling method for PM_{10} for the first time in 2006. The PCM models were revised for 2008 to incorporate a more process-based modelling approach for regional calcium rich dusts from re-suspension of soils and iron rich dusts from re-suspension due to vehicle activity. The revised models developed from those proposed by Abbott (2008) were also used for this 2018 assessment. The method for regional iron rich dusts remains largely unchanged and is based on a more empirical approach.

The starting point for the assessment of iron and calcium rich dusts is the measurements of a range of PM components including Fe and Ca reported by Harrison and Yin (2006) for three monitoring sites in the Birmingham area. Measurements were made and urban background site (BCCS) from May 2004 to May 2005, an urban roadside site (BROS) from May 2005 to November 2005 and at a rural site about 20 km from the city (CPSS) from November 2005 to May 2006. Measurements were not made at the different sites simultaneously, but the measurement periods were sufficiently long that they can be used to provide reasonable estimates of the urban and roadside increments of various PM components. The measurement data for Fe and Ca are summarised in Table 5.3.

Table 5.3 - Measured concentration of iron and calcium and derived estimates of iron and calcium rich dusts (μg m^{-3})

	CPSS (rural)	BCCS (urban)	Conversion factor	rural x factor	Urban increment x factor
Fe fine	0.06	0.10	9.0	0.54	0.36
Fe coarse	0.14	0.24	9.0	1.26	0.89
Ca fine	0.03	0.09	4.3	0.13	0.26
Ca coarse	0.12	0.30	4.3	0.52	0.77

Table 5.3 also includes the conversion factors suggested by Harrison et al., (2006) for use within their pragmatic mass closure model. This factor converts the mass of elemental Fe to iron related dusts and the mass of elemental Ca to calcium related dusts. The urban increment in the table has been calculated by subtracting the data for CPSS from that for the urban BCCS site. It is clear that there is an urban increment for both fine and coarse iron and calcium rich dusts. Measurement data for the BROS roadside site indicates that there is a roadside increment on top of the urban increment for Fe but not for Ca. Thus, it is reasonable to assume that the urban increment for iron rich dusts is associated with emissions generated by road traffic but that the urban increment for calcium rich dusts is associated with urban emissions that are not related to traffic activity.

5.3.5.2 Regional calcium rich dusts

The regional concentration of Ca rich dusts was assumed to be a constant value across the UK in the 2006 and 2007 assessments (Kent et al., 2007b; Grice et al., 2009). Abbott (2008) developed a method to estimate the ambient concentration of Ca rich PM_{10} dusts resulting from the re-suspension of soils in rural areas. The starting points for this method are the proportion of bare soil, root crops and cereal crops in 1 km x 1 km grid squares across the UK within the Land Cover Map 2000 (2009). The concentration of Ca rich dusts cannot be calculated using the standard approach of using an estimate of the annual emissions and an air dispersion model. This is because the rate of re-suspension and the atmospheric dispersion of these emissions are both dependant on the meteorological conditions.

The emission rate will be higher when the wind is stronger, but the dispersion of these emissions will also be more efficient under these conditions.

The method presented by Abbott (2008) makes use of combined emission and dispersion kernels for cereal and root crop fields and for bare soils. Concentrations were calculated for each hour of the year based on hourly sequential meteorological data from twelve sites throughout the UK for 1999. This year was selected because the data were readily available.

The method of Abbott (2008) has been adapted for use within the PCM models by using an inverse distance weighted average of the results from the different kernels for each receptor location. This revised method avoids the discontinuities caused by the use of a simpler nearest meteorological site to the receptor method used in the original work.

Figure 5-6a shows the results for regional Ca rich dusts. The highest concentrations are predicted to be in eastern areas where bare soils, root and arable crops are more common and there is less rainfall. A maximum value for this component has been set as 5 µg m^{-3} within the map. This value has been chosen as an estimate of the maximum likely concentration for a grid square average based on a comparison of this map with available PM_{10} measurements in the locations with the highest predicted contributions.

5.3.5.3 Urban calcium rich dusts

Prior to 2016 an empirical method was used to estimate the urban increment for Ca rich dusts Brookes et al. (2017). The NAEI for 2017 that has been used for the 2018 air quality assessment modelling includes a revised method for estimating emissions of PM from construction, first introduced in the NAEI for 2016, that results in an increase in the estimate of emissions from this source. The emissions estimates for this source have been multiplied by a factor of 0.75 in order to achieve mass closure and provide a consistent calibration of the models for PM_{10} and $PM_{2.5}$. This revision means that urban calcium rich dusts are now accounted for within the dispersion modelling and a separate empirically modelled contribution from re-suspension of soils due to urban activity is no longer required.

5.3.5.4 Regional iron rich dusts

A constant value for the regional contribution to Fe rich dusts of 1 µg m^{-3} has been applied across the UK. This residual value has been chosen to provide the best fit to the measurements from the Birmingham study (Harrison and Yin, 2006) and available urban background particulate Fe measurements once the estimated contribution from re-suspension due to vehicle movements has been taken into account. Figure 5-6b shows this constant contribution across the UK.

5.3.5.5 Iron rich dusts from re-suspension associated with vehicle movements

The assessments for 2006 and 2007 used an empirical method for the Fe rich dusts associated with re-suspension from vehicle movements based on the use of vehicle km statistics for 1 km x 1 km squares (Grice et al., 2009). Abbott (2008) developed a more process-based approach to estimating this contribution, which takes vehicle km statistics for heavy-duty vehicles (heavy good vehicles and buses) as its starting point. The re-suspension contribution associated with light duty vehicles is expected to be minor compared with that from heavy duty vehicles. These estimates are likely to be subject to greater uncertainty than the estimates for re-suspension from soils because there is little information on the availability of material on road surfaces to be re-suspended.

Abbott (2008) calculated two sets of combined emission and dispersion kernels for each of the 12 meteorological stations for 1999: one to represent rural conditions and one to represent urban conditions. The estimated re-suspension rate was considerably higher for rural conditions due to the higher speeds assumed. These two sets of kernels were then used to calculate the contribution to PM_{10} concentrations according to the proportion of urban and rural land cover in each 1 km x 1 km grid square. A detailed examination of the results from this assessment has shown that the concentrations in urban areas were largely driven by the small proportion of rural land cover in these urban areas. The urban kernels have therefore been chosen to apply to all roads within the PCM model.

Figure 5-6c shows the results for Fe rich dusts from vehicle movements. The highest concentrations are associated with the roads with the highest flows of heavy-duty vehicles. A maximum value for this component has been set as 2.5 µg m^{-3} within the map. This value has been chosen as an estimate of the maximum likely concentration for a grid square average based on a comparison of this map with available PM_{10} measurements in the locations with the highest predicted contributions.

An indication that the method is providing reasonable estimates the total of Fe rich dusts is provided by Figure 5-7, which shows a comparison of modelled annual mean Fe (the sum of regional and vehicle related Fe) with ambient Fe measurements at non-industrial and non-roadside sites for 2018 from the national metals monitoring network. The modelled estimates are clearly of the correct magnitude and provide a reasonable description of the rural to urban gradients.

Figure 5-6

a) Contribution to PM_{10} from regional Ca rich dusts associated with re-suspension from soils (µg m^{-3})

b) Contribution to PM_{10} from regional Fe rich dusts (µg m^{-3})

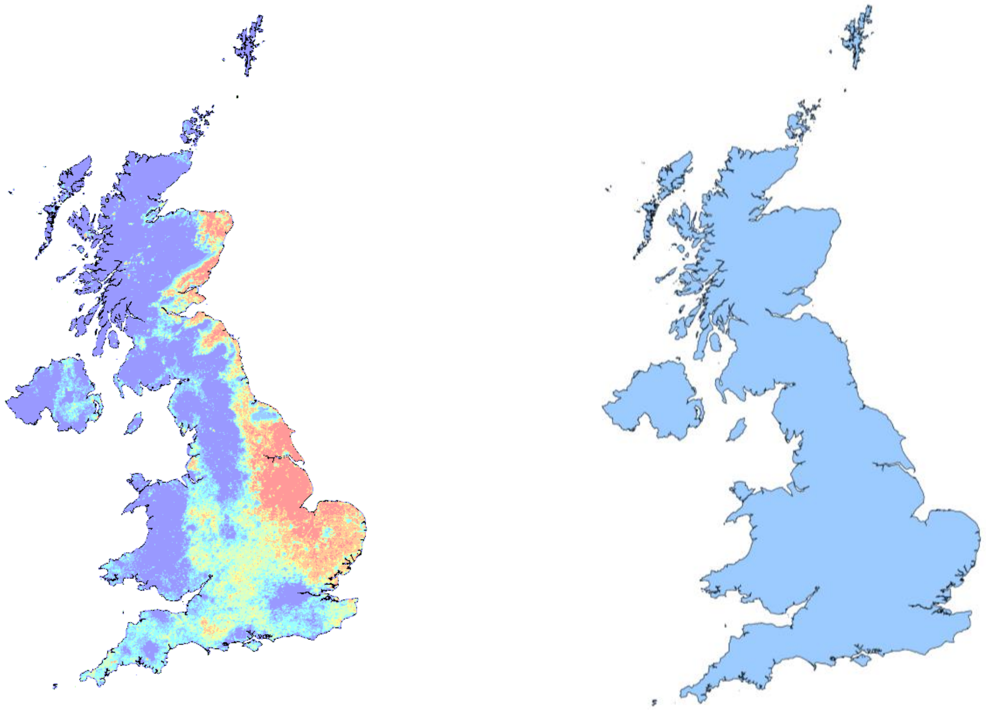

c) Contribution to PM_{10} from Fe rich dusts associated with vehicle movements (µg m^{-3})

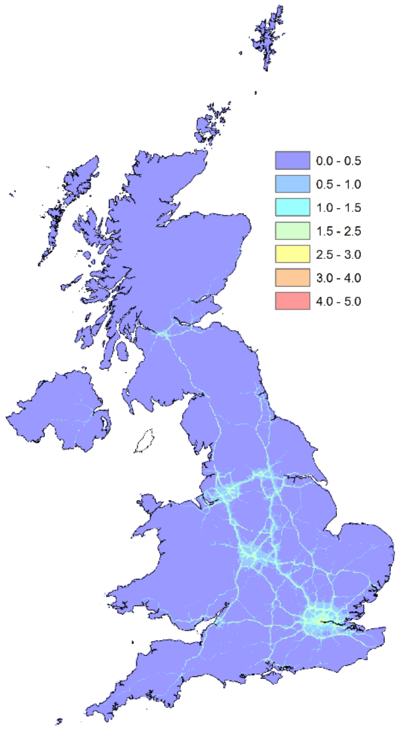

Figure 5-7 - Comparison of modelled and measured annual mean elemental Fe concentrations 2018 (µg m^{-3})

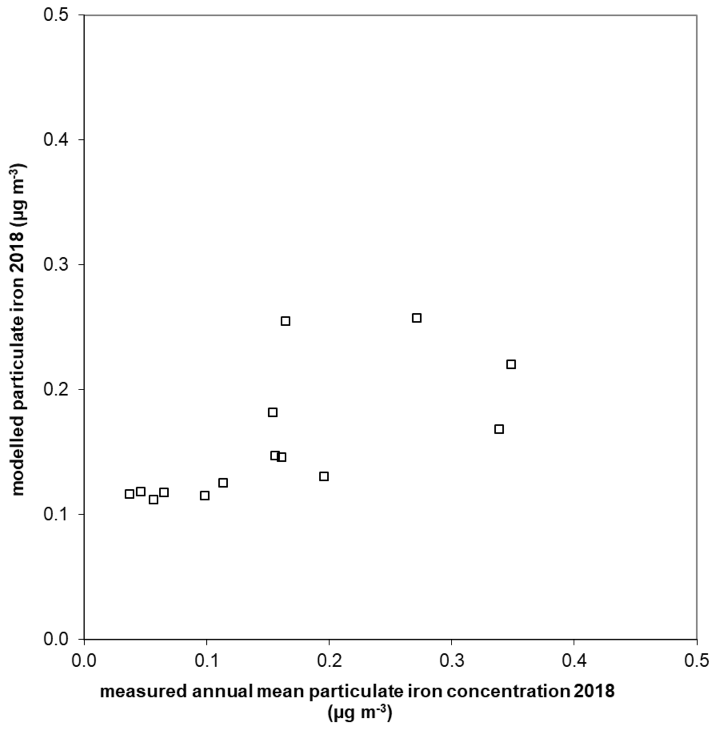

5.3.5.6 Application to the mapping of heavy metal concentrations

Abbott (2008) also suggested a method for estimating the contributions to the ambient concentrations of heavy metals from soil and vehicle related re-suspension processes. Section 10.3 on the modelling of heavy metal concentrations describe how the maps of PM mass from rural re-suspension of soils and re-suspension associated with vehicle movements have been used to estimate the contributions to the ambient concentration of heavy metals using a combination of information on the heavy metal content of soils and enhancement factors.

5.3.6 Sea salt

The contribution to ambient PM from sea salt has been derived directly from measurements of particulate chloride from sites within the UKEAP AGANet for 2018. Data from a network of 27 rural sites were interpolated using inverse distance weighting onto a 5 km x 5 km grid. A scaling factor of 1.648 was applied to convert elemental chloride mass to sodium chloride mass. 73% of the sea salt mass was assumed to be in the coarse fraction and 27% in the fine fraction. This split was derived from measurement data presented by APEG (1999) and Harrison and Yin (2006).

The use of chloride is potentially subject to both positive and negative artefacts. Sea salt is not the only source of particulate chloride in the atmosphere. HCl is emitted from coal burning but reductions in coal use and flue gas abatement are likely to have reduced atmospheric HCl and ammonium chloride concentrations considerably. There will also be loss of chloride from marine aerosol due to reactions with nitric acid. The resulting sodium nitrate PM has been considered to be of anthropogenic origin and the contribution to PM mass from this sodium nitrate is explicitly included in the modelled concentrations presented. If sodium were used as the marker for sea salt rather than chloride, then this sodium nitrate would tend to be included in the natural component.

In addition to selecting chloride as the marker for sea salt, the analysis was simplified by assuming that the sea salt consists of sodium chloride only. Thus, the measured chloride concentration has been scaled by a factor of 1.648. An alternative approach would be to scale by 1.809 to take account of the full composition of sea salt. The composition of sea salt is dominated by chloride and sodium. Other components contributing more than 1% by mass are sulphate, magnesium, calcium and potassium. Sulphate is already explicitly included in the modelled concentrations and a sea salt correction has not been applied to the measured concentrations used in the PCM model. Adding a further sea salt sulphate component would lead to double counting. The other components (magnesium, calcium and potassium) have, in effect, been treated as sodium by the use of a scaling factor of 1.648. The ratio of (chloride + sodium) to chloride in sea salt is 1.552, while the ratio of (chloride + sodium + magnesium + calcium + potassium) to chloride is 1.658. Thus, the simplification of sea salt as pure sodium chloride has not had a large impact on the total mass assumed apart from the contribution from sea salt sulphate, which, as a simplification, has been included with the rest of the sulphate as anthropogenic.

5.3.7 Contributions from area sources

Figure 5-8 shows the calibration of the area source model. The modelling method makes use of an ADMS derived dispersion kernel to calculate the contribution to ambient concentrations at a central receptor location from area source emissions within a 33 km x 33 km square surrounding each receptor. Hourly sequential meteorological data from Waddington in 2018 was used to construct the dispersion kernels, as described in Appendix 4. A total of 28 background monitoring sites within the national network had sufficient data capture for PM_{10} and $PM_{2.5}$ in 2018 to be used to calibrate the model. Only sites with valid data for PM_{10} and $PM_{2.5}$ have been used to calibrate the PM_{10} and $PM_{2.5}$ models, as described in Section 5.1.

Revised methods introduced in the 2011 assessment (Brookes et al., 2012) for modelling the contributions to PM_{10} from SNAP 2 (domestic and non-domestic combustion) and SNAP 3 (combustion in industry) area sources were used and have been described in Section 3.3.5.

The methods used to estimate the spatial distribution of emissions from domestic wood combustion were revised for the NAEI 2015 to incorporate new information from a survey of domestic wood use (BEIS, 2016). The revised spatial distribution places a larger proportion of these emissions in large urban areas than in previous assessments.

The NAEI for 2017 that has been used for the 2018 air quality assessment modelling includes a revised method for estimating emissions of PM from construction (first introduced in the NAEI for 2016) that has resulted in an increase in the estimate of emissions from this source. The emissions estimates for this source have been multiplied by a factor of 0.75 in order to achieve mass closure and provide a consistent calibration of the models for PM_{10} and $PM_{2.5}$. This revision means that urban calcium rich dusts are now accounted for within the dispersion modelling and a separate empirically modelled contribution from re-suspension of soils due to urban activity is no longer required.

As part of the calibration process emission caps have been applied to certain sectors; this is because the use of surrogate statistics for mapping area source emissions sometimes results in unrealistically large concentrations in some grid squares for a given sector. The emission caps applied are given in Table 5.4.

With the exception of area sources associated with SNAP sector 3 (combustion in industry), the area source model has been calibrated using ambient PM monitoring data from the UK national networks. The modelled large point and small point source, SIA, SOA, iron and calcium rich dust, long range transport primary PM, sea salt and the residual concentrations have been subtracted from the measured annual mean PM concentration at background sites and compared with the modelled area source contribution to annual mean PM concentration. A residual concentration of zero was found to provide the best fit to the monitoring data for both PM_{10} and $PM_{2.5}$ in 2018.

The modelled area source contribution (excluding SNAP 3) was multiplied by the relevant empirical coefficient to calculate the calibrated area source contribution for each grid square in the country. The area source contribution was then added to the contributions from SNAP 3 area sources, secondary organic and inorganic particles, from small and large point sources, from regional primary particles, from sea salt, from calcium and iron rich dusts and the residual, resulting in a map of background annual mean gravimetric PM_{10} concentrations.

Figure 5-8 - Calibration of PM_{10} area source model 2018 ($\mu g\ m^{-3}$, gravimetric)

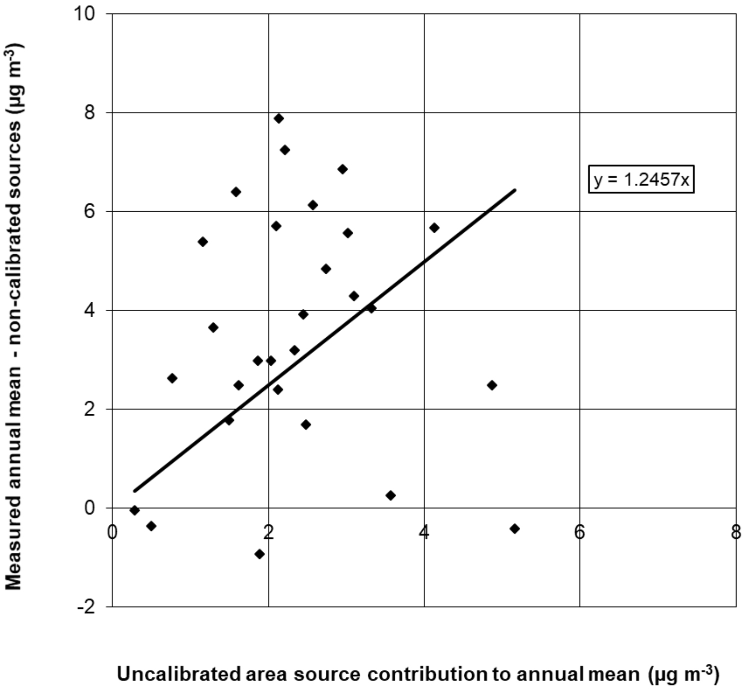

Table 5.4 - Emission caps applied to PM_{10} sector grids

SNAP code	Description	Cap applied (t/a/km^2)
SNAP 6 (Solvent use)	Industrial coatings - metal and plastic Metal and plastic coatings	6
SNAP 8 (Other Transport & mobile machinery)	Industrial off-road mobile machinery_Gas oil	3
SNAP 8 (Other Transport & mobile machinery)	Industrial off-road mobile machinery Gas oil	3
SNAP 4 (Production process)	Stockpiles	15

5.3.8 Roadside concentrations

The modelled annual mean concentration of PM_{10} at a roadside location is made up of two parts: the background concentration (as described above) and a roadside increment:

roadside PM_{10} concentration = background PM_{10} concentration + PM_{10} roadside increment.

The NAEI has provided estimates of PM_{10} emissions for major road links in the UK for 2017 (Richmond et al., 2019) and these have been adjusted to provide estimates of emissions in 2018. The roadside increment model for PM_{10} has been calibrated using data from monitoring sites with valid data for both PM_{10} and $PM_{2.5}$ in 2018. The PCM Roads Kernel Model (PCM-RKM) described in Appendix 7 has been used to calculate the roadside increment. The PCM-RKM is based upon dispersion kernels generated by the ADMS-Roads dispersion model (v4.1) and represents a more process-based approach than the previous empirical method. It provides a more robust assessment, whilst retaining the link with measurement data provided using AURN measurement data to calibrate this component of the model. Figure 5-9 shows the calibration of this model at roadside monitoring sites. Roadside concentrations for urban major road links (A-roads and motorways) only are reported to the EU and included in this report.

Figure 5-9 - Calibration of PM_{10} PCM-RKM model 2018 (µg m^{-3}, gravimetric)

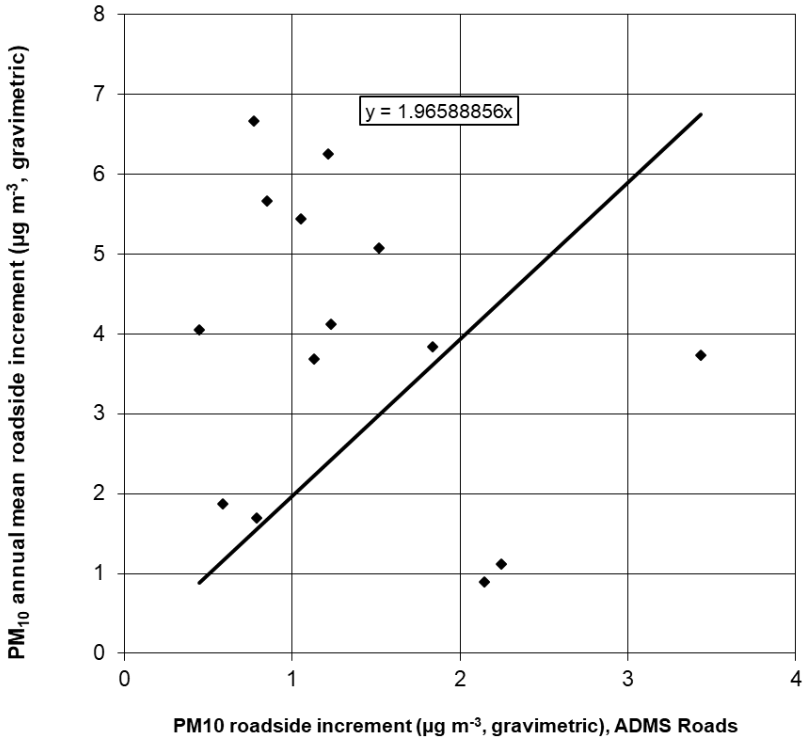

5.4 Results

5.4.1 Verification of mapped values

Figure 5-10 and Figure 5-11 show comparisons of modelled and measured annual mean PM_{10} concentration in 2018 at background and roadside monitoring site locations. Lines representing y = x – 50 % and y = x + 50% are also shown because 50% is the AQD data quality objective for modelled annual mean PM_{10} concentrations – see Section 1.5. Summary statistics for the comparison between modelled and measured PM_{10} concentrations are presented in Table 5.5 and Table 5.6.

There are a number of different categories of monitoring sites within these tables and graphs. This is because there are some sites in the national network at which only PM_{10} or $PM_{2.5}$ are measured, but not both. TEOM PM_{10} data adjusted using the VCM model (http://www.volatile-correction-model.info/), are available for some verification sites.

The agreement between the measurement data and the modelled values is generally good.

Figure 5-10 - Verification of background annual mean PM_{10} model 2018

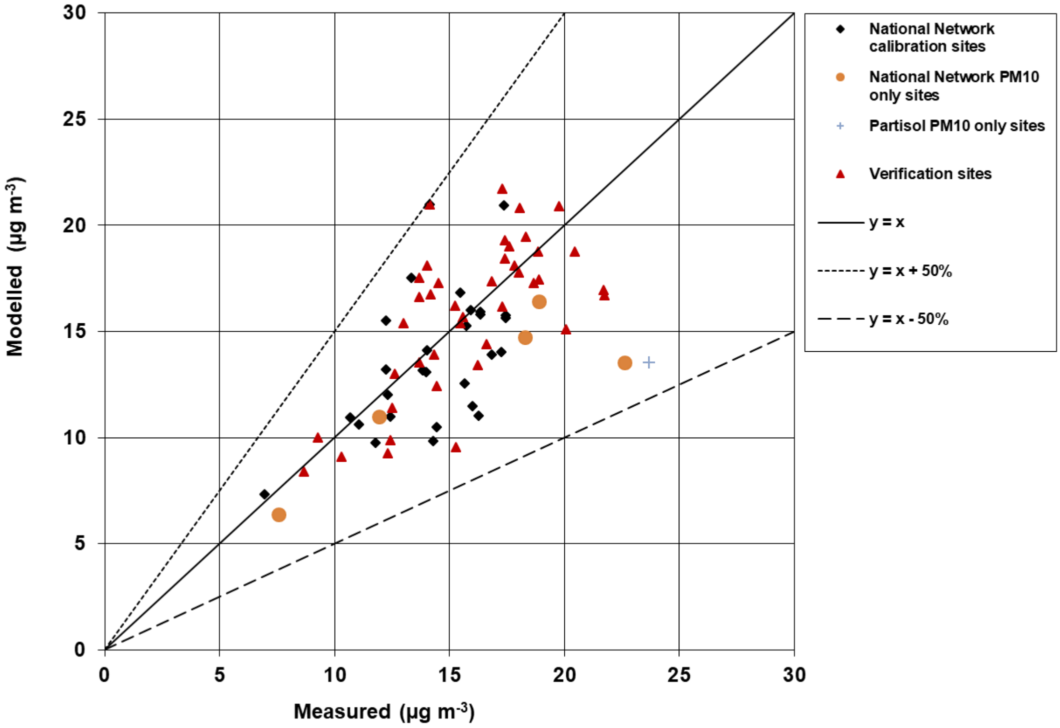

Figure 5-11 - Verification of roadside annual mean PM_{10} model 2018

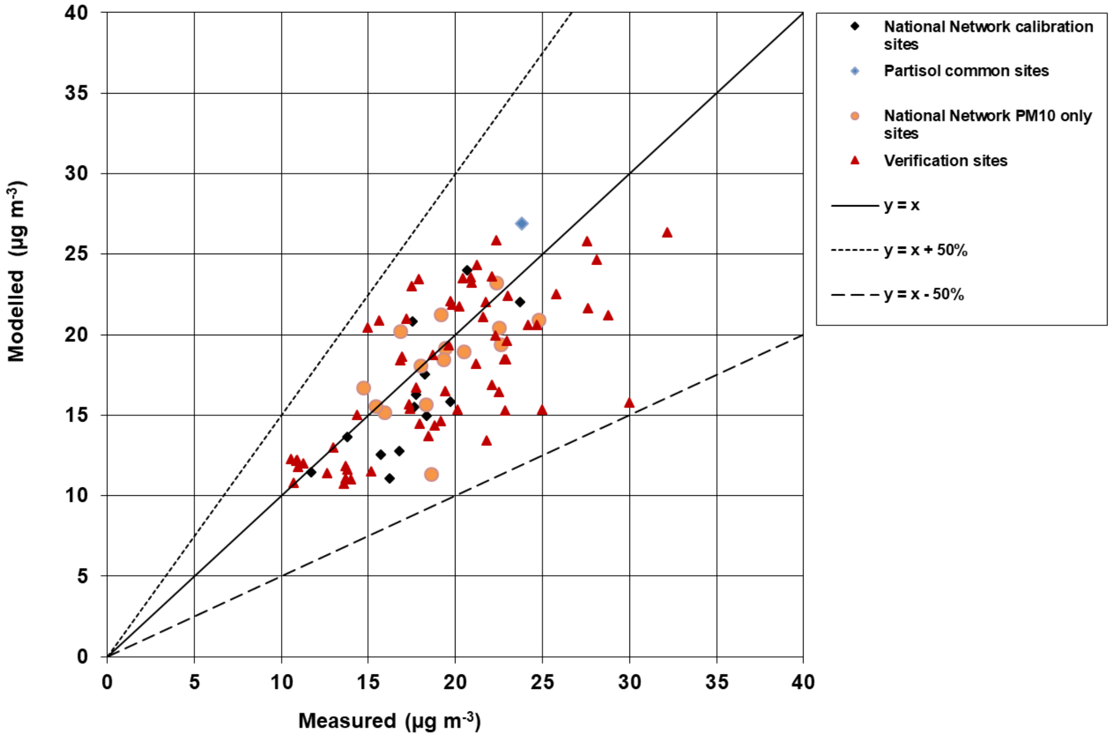

Table 5.5 - Summary statistics for comparison between gravimetric modelled and measured concentrations of PM_{10} at background sites

	Mean of measurements ($\mu g\ m^{-3}$, grav)	Mean of model estimates ($\mu g\ m^{-3}$, grav)	R^2	% outside data quality objectives	Number of sites
National network Calibration	14.4	13.7	0.31	0	28
National network Partisol*	-	-	-	-	-
National network PM10 only sites	15.9	12.4	0.74	0	5
National network Partisol PM10 only sites	23.7	13.5	-	0	1
Verification sites	15.8	15.8	0.46	0	41

* There were no sites in this category in 2018

Table 5.6 - Summary statistics for comparison between gravimetric modelled and measured concentrations of PM_{10} at roadside sites

	Mean of measurements ($\mu g\ m^{-3}$, grav)	Mean of model estimates ($\mu g\ m^{-3}$, grav)	R^2	% outside data quality objectives	Number of sites
National network Calibration	18.0	16.8	0.69	0	14
National network Partisol	23.8	26.9	-	0	1
National network PM10 only sites	19.2	18.3	0.35	0	15
National network Partisol PM10 only sites*	-	-	-	-	-
Verification sites	19.4	17.9	0.46	0	64

* There were no sites in this category in 2018

5.4.2 PM_{10} source apportionment at monitoring sites

Figure 5-12 and Figure 5-13 show the modelled annual mean PM_{10} source apportionment for 2018 at national network background and roadside monitoring sites respectively. The measured concentration at each site is also shown for reference.

At background locations, the contributions from non-emissions inventory sources (i.e. regional background sources and urban dusts), which are shown in grey on the figures, dominate with a particularly large contribution from secondary inorganic aerosols. The smaller contribution from urban background emissions sources, shown in colour on the figures, is dominated in most locations by domestic, traffic (exhaust emissions, brake and tyre wear and road abrasion) and industry.

At roadside locations the source apportionment follows a very similar pattern to background locations, except that there is an extra local road traffic component composed of local exhaust emissions and local brake and tyre wear and local road abrasion emissions. Depending on the magnitude of the local traffic emissions, local traffic emissions can contribute up to about 7 $\mu g\ m^{-3}$ of PM_{10} at the roadside monitoring sites.

Figure 5-12 - Annual mean PM_{10} source apportionment at background national network monitoring sites in 2018

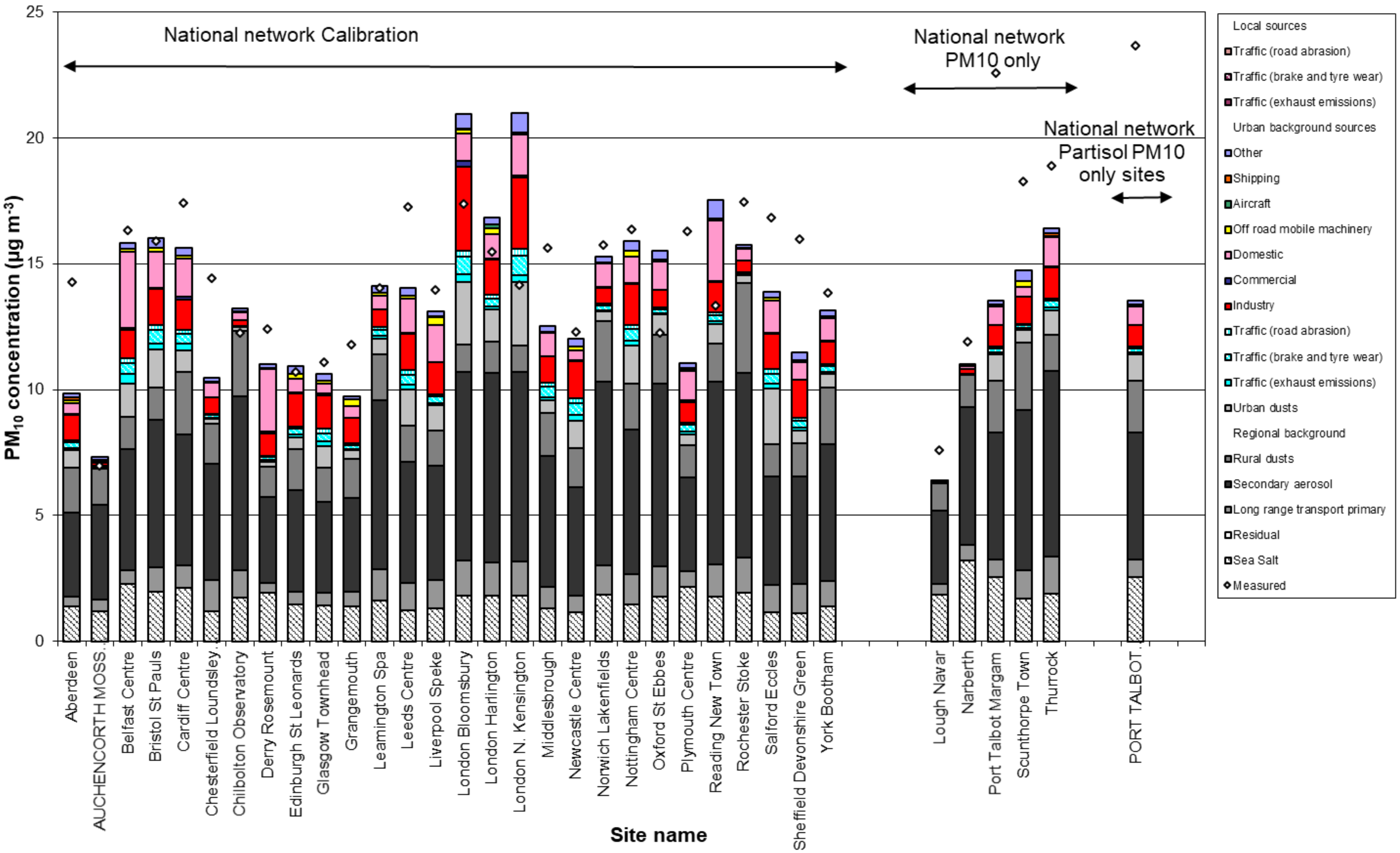

Figure 5-13 - Annual mean PM_{10} source apportionment at national network roadside monitoring sites in 2018

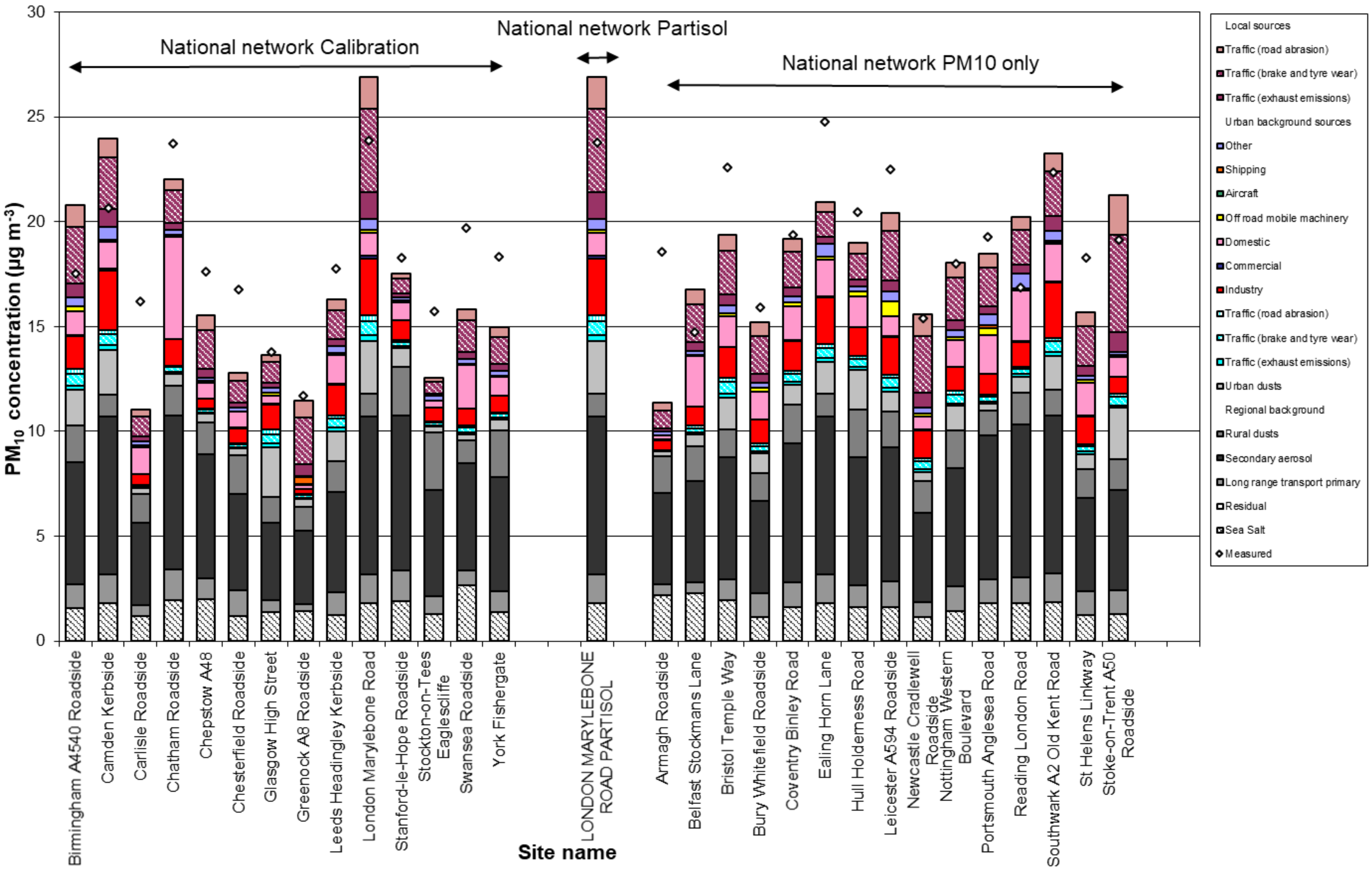

5.5 Subtraction of sea salt component

5.5.1 Introduction

The AQD (Article 20) requires member states to attribute exceedances of limit values due to natural sources when reporting the results of air quality assessments. The definition of natural sources in this directive includes sea spray. An assessment of concentrations with the contribution from natural sources subtracted is provided in e-reporting Data flow G (CDR, 2019) for locations with measured or modelled exceedances of the limit values. 2018 is the eleventh year for which the contribution from natural sources has been subtracted. Where exceedances are attributed to natural sources, subtraction is a requirement of the Directive.

5.5.2 Map of annual mean sea salt PM_{10}

The method used to estimate the sea salt contribution to annual mean PM_{10} concentrations across the UK has been described in Section 5.3.6. The map of annual mean sea salt PM_{10} can be used to subtract this contribution directly from measured or modelled annual mean concentrations. The uncertainties associated with estimating the sea salt contribution to annual mean PM_{10} from measurements of particulate chloride have been discussed in Section 5.3.6. It is recognised that the interpolated map of sea salt concentrations will not capture the steep gradients in sea salt concentration very close to the coast. Thus, the analysis presented may underestimate the sea salt contribution to exceedances in coastal areas.

5.5.3 Method for the 24-hour limit value

A method has also been developed to estimate the contribution from sea salt to exceedances of the 24-hour limit value for PM_{10} of no more than 35 days with concentration greater than 50 µg m^{-3}. This method has been described in detail by Defra (2009). This method makes use of the relationship between the number of days with concentrations greater than 50 µg m^{-3} and annual mean concentrations described by Stedman et al. (2001a). There is some scatter around the best-fit line of the relationship shown in Figure 5-4. Using the best-fit line relationship within the annual method for subtracting sea salt has been considered appropriate since this should give the best central estimate of the sea salt contribution.

An estimate of the number of days with a PM_{10} concentration greater than 50 µg m^{-3} associated with the contribution to annual mean concentration from sea salt has been calculated by applying the relationship of Stedman et al. (2001a) in the vicinity of the limit value. This has been done by calculating the difference between the number of days corresponding to 31.5 µg m^{-3} minus half the sea salt concentration and the number of days corresponding to 31.5 µg m^{-3} plus half the sea salt concentration.

Daily chloride measurements are available for two sites in the south east of the UK. These measurements can be used to calculate a daily sea salt subtraction for PM_{10} monitoring data. This method is not applicable to model results and will be less reliable for sites not in the south east of the UK. For these reasons the method based on annual mean sea salt concentrations has been used across the UK as described above. Defra (2009) have provided a comparison of the annual and daily methods for the years 2005, 2006 and 2007 which shows that the agreement between the methods is reasonably good.

5.5.4 Results

There were no reported exceedances of the 24-hour or annual mean limit values for PM_{10} in 2018.

6 $PM_{2.5}$

6.1 Introduction

6.1.1 Limit and Target values

The Air Quality Directive (AQD) includes a target value (TV) for annual mean $PM_{2.5}$ which came into force from 01/01/2010. This target value is:

- An annual mean concentration of 25 µg m^{-3}.

Two limit values have also been set for ambient $PM_{2.5}$ concentrations in the AQD. These limit values are:

- Stage 1 limit value – An annual mean concentration of 25 µg m^{-3}.
- Stage 2 indicative limit value – An annual mean concentration of 20 µg m^{-3}

The Stage 1 limit value came into force on 01/01/2015, the Stage 2 indicative limit value is due to come into force 01/01/2020. There were no measured or modelled exceedances of the annual mean target value, Stage 1 or Stage 2 limit value for $PM_{2.5}$ in 2018.

An exposure reduction target and an exposure concentration obligation have also been set for $PM_{2.5}$.

Results of the assessment in terms of comparisons of the modelled concentrations with the annual mean limit and target values for $PM_{2.5}$ have been reported in e-Reporting Data flow G (CDR, 2019).

6.1.2 Annual mean model

Maps of annual mean $PM_{2.5}$ in 2018 at background and roadside locations are shown in Figure 6-1 and Figure 6-2.

Full details of the models used to calculate concentrations of PM_{10} and $PM_{2.5}$ are provided in Chapter 5. The maps have been calibrated using measurements within the national network for which co-located PM_{10} measurements are also available for 2018. The models for PM_{10} and $PM_{2.5}$ are designed to be fully consistent, with each component either derived from emission estimates for PM_{10} or $PM_{2.5}$, or the contributions to the fine and coarse particle size fractions are estimated separately. This enables us to carry out an additional sense check that the calibration parameters for the two pollutants are reasonably consistent. Measurements from national network sites without collocated PM_{10} instruments have been used as an additional verification dataset.

The concentrations of many of the modelled components have been estimated separately for the fine and coarse fraction. This enables a consistent method to be adopted for estimation of PM_{10} (the sum of the fine and coarse fractions) and $PM_{2.5}$ (fine fractions only). The mass fractions of each component assigned to $PM_{2.5}$ are listed in Section 6.3.1. The component pieces are then aggregated to a single 1 km x 1 km background $PM_{2.5}$ grid. An additional roadside increment is added for roadside locations.

The results from the annual mean model can be directly compared with the annual mean target and limit values in order to carry out the air quality assessment.

Figure 6-1 - Annual mean background $PM_{2.5}$ concentration, 2018 ($\mu g\ m^{-3}$, gravimetric)

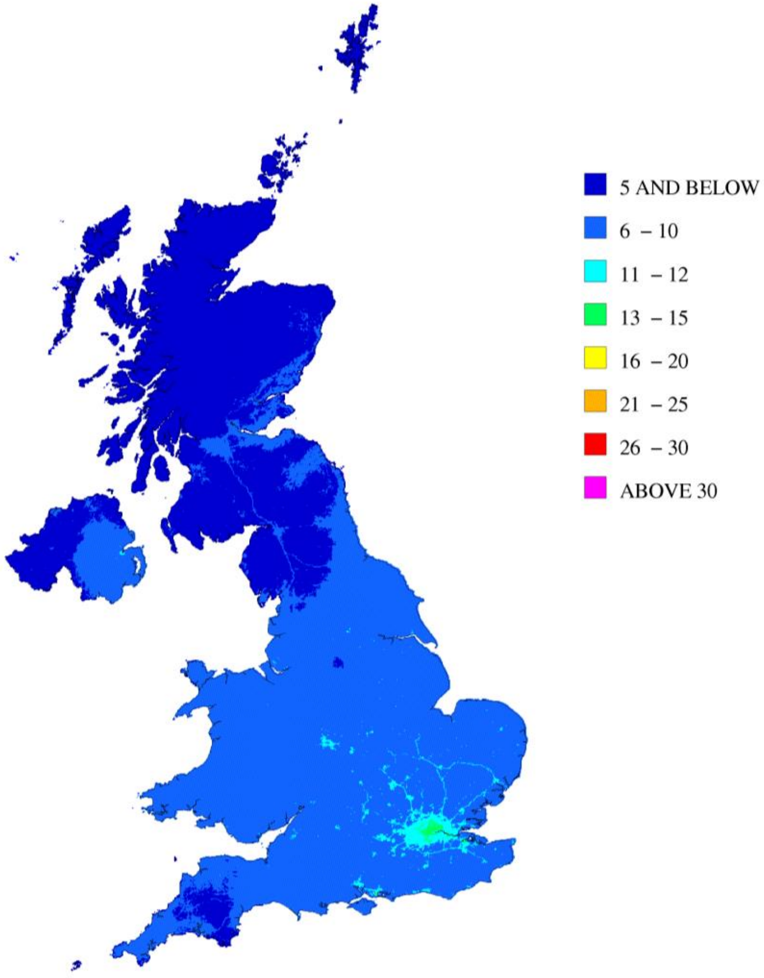

Figure 6-2 - Urban major roads, annual mean roadside $PM_{2.5}$ concentration, 2018 ($\mu g\ m^{-3}$, gravimetric)

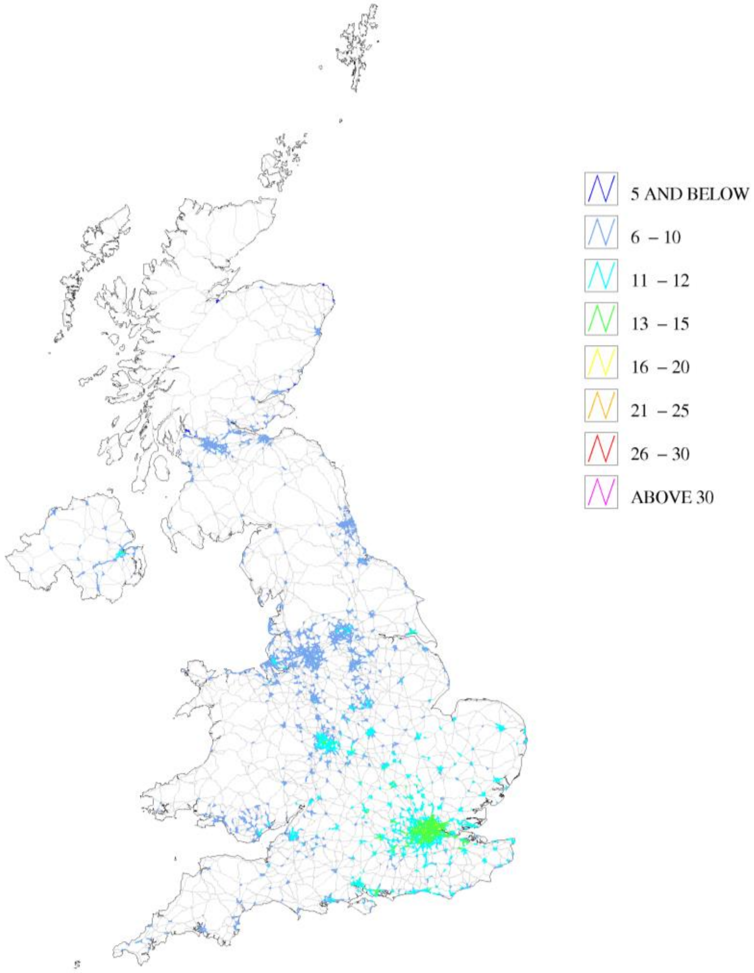

6.1.3 Overview of the PCM model for $PM_{2.5}$

Figure 6-3 shows a simplified flow diagram of the PCM model for $PM_{2.5}$. A summary of the PCM model method, input and assumptions for $PM_{2.5}$ is presented in Table 6.1.

Figure 6-3 - Flow diagram for PCM $PM_{2.5}$ model

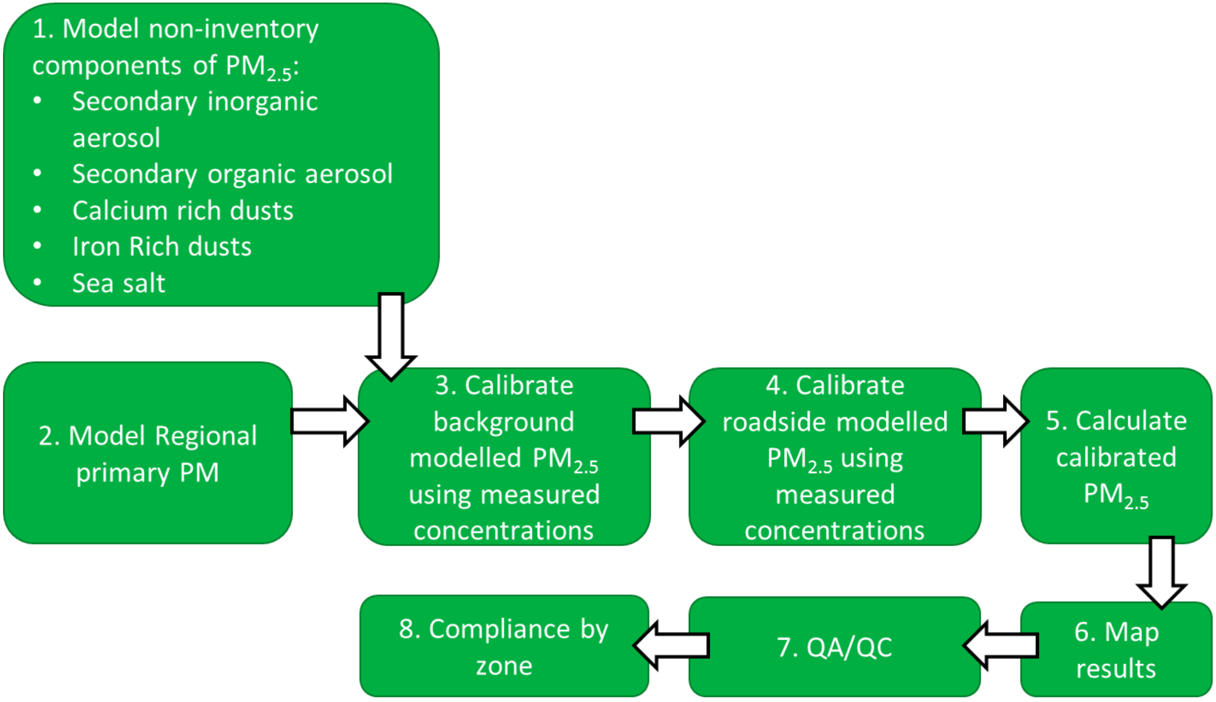

1. Model non-inventory components of $PM_{2.5}$:
   - Secondary inorganic aerosol
   - Secondary organic aerosol
   - Calcium rich dusts
   - Iron Rich dusts
   - Sea salt

2. Model Regional primary PM

3. Calibrate background modelled $PM_{2.5}$ using measured concentrations

4. Calibrate roadside modelled $PM_{2.5}$ using measured concentrations

5. Calculate calibrated $PM_{2.5}$

6. Map results

7. QA/QC

8. Compliance by zone

Table 6.1 - PCM model method, input and assumptions summary for $PM_{2.5}$

Heading	Component	Details
General	Pollutant	$PM_{2.5}$
	Year	2018
	Locations modelled	Background and traffic locations
	Metric	Annual mean
Input data	Emission inventory	NAEI 2017
	Energy projections	Energy Projections 2017
	Road traffic counts	2017
	Road transport activity projections	DfT (2018) traffic (re-based to 2017 NAEI), DfT (2019) car sales projections, TfL traffic (2019) and fleet (2018) projections for London
	Road transport emission factors	COPERT 5
	Measurement data	2018
	Meteorological data	Hourly data from Waddington 2018
Model components	Regional	See details under “pollutant specific” heading
	Large point sources	287 sources modelled using ADMS 5.2
	Small point sources	PCM small points model
	ETS point sources	PCM small points model
	Large ETS point sources	137 sources modelled using ADMS 5.2
	Area sources	PCM dispersion kernels generated using ADMS 5.2. Time varying emissions for road transport and domestic sources. PCM small points model for industrial combustion emissions.

Heading	Component	Details
	Roadside increment	PCM Roads Kernel Model using ADMS-Roads 4.1
Calibration	Model calibrated?	Yes
	Number of background stations in calibration	28 (stations with both PM_{10} and $PM_{2.5}$)
	Number of traffic stations in calibration	14 (stations with both PM_{10} and $PM_{2.5}$)
Pollutant specific	Secondary inorganic aerosol	Interpolated from SO_4, NO_3 and NH_4 measurements at 26 rural stations, scaling factors applied for size fraction, bound water and counterions
	Secondary organic aerosol	Results from the NAME model for 2008
	Regional primary particles	Calculated using the TRACK receptor oriented, Lagrangian statistical model
	Regional calcium rich dusts from re-suspension of soils	Modelled using information on land cover (bare soil, root and cereal crops) and dispersion kernel incorporating emissions and dispersion processes
	Regional iron rich dusts from re-suspension	Assigned a constant value of 0.5 µg m^{-3}
	Iron rich dusts from re-suspension due to vehicle activity	Modelled using information on vehicle movements on major roads (HDV) and dispersion kernel incorporating emissions and dispersion processes
	Sea Salt	Interpolated measurements of Cl, scaling factor applied for sea water composition
	Residual	A value assigned based on best fit to PM_{10} and $PM_{2.5}$ measurements: zero, no residual required

6.1.4 Chapter Structure

This chapter describes modelling work carried out for 2018 to assess compliance with the $PM_{2.5}$ limit and target values described above. Emission estimates for primary PM are described in Section 6.2, Section 6.3 describes the $PM_{2.5}$ modelling methods. The modelling results in terms of verification and source apportionment are presented in Section 6.4. The methods used to subtract the contribution from natural sources (sea salt) and the results of this subtraction are presented in Section 6.5. The method used to calculate the average exposure indicator (AEI) for annual mean $PM_{2.5}$ and an assessment of compliance with the exposure concentration obligation is presented in Section 6.6.

6.2 $PM_{2.5}$ emissions

Estimates of the emissions of primary PM from the UK National Atmospheric Emission Inventory 2017 (NAEI 2017) have been used in this study (Richmond et al., 2019). Emissions projections have been provided by the NAEI (Passant, 2019) based on BEIS EEP 2018 energy and emissions projections (BEIS, 2018).

Figure 6-4 shows UK total $PM_{2.5}$ emissions for 2017 and emissions projections for 2020, 2025 and 2030 split by SNAP code, with the coding described in Table 3.2. Values for intermediate years have been interpolated in this figure. Figure 6-4 shows that $PM_{2.5}$ emissions in 2017 include contributions from a wide range of different source sectors. Some of the sectors with the largest contribution to the total in 2017 include domestic combustion, road traffic (exhaust, road abrasion and brake and tyre wear), combustion point sources and combustion in industry.

Maps of emissions from area sources for 2018 were derived from the 2017 inventory maps using specific scaling factors derived for each combination of source activity (typically fuel type), as described for NO_X (Section 3.3.5). The emissions from point sources were scaled in a similar way, see

Section 3.3.1. The methods used to calculate ambient concentrations from the estimates of primary PM emissions are described below for point, area, road link and regional sources.

Figure 6-4 - Total UK $PM_{2.5}$ emissions for 2017 and emissions projections up to 2030 by SNAP code from NAEI 2017

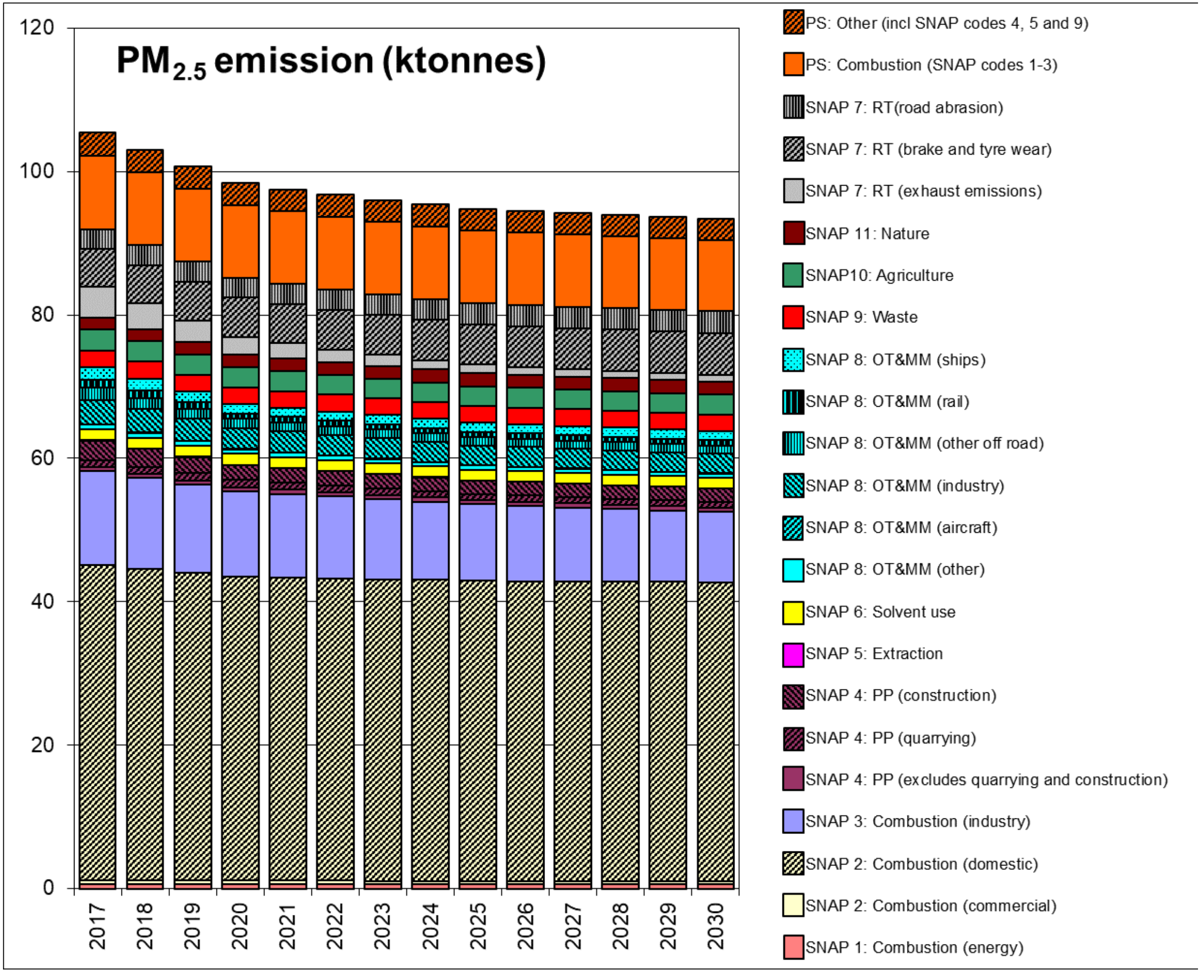

6.3 $PM_{2.5}$ modelling

6.3.1 $PM_{2.5}$ mass fractions

The proportions of the PM mass for each component assigned to the $PM_{2.5}$ fraction within the PCM models are listed in Table 6.2. The proportions for secondary inorganic aerosols have been derived as described in Section 5.3.1. The proportions for local point and area sources are based on the NAEI emission inventories for $PM_{2.5}$ and PM_{10} (Richmond et al., 2019). The NAEI $PM_{2.5}$ emission inventory has been derived from the PM_{10} emission inventory by the application of estimates of the mass fraction represented by $PM_{2.5}$ for different sources and fuels. Overall the UK total mass emissions for $PM_{2.5}$ for 2017 were about 63% of the value for PM_{10}. The proportions for calcium and iron rich dusts have been derived with reference to the monitoring data presented in Section 5.3.5 and to provide good fit to the available co-located $PM_{2.5}$ and PM_{10} measurements. The proportions for calcium and iron rich dusts were updated for 2017 and again for 2018 in order to account for the revised method for measurement of SIA (Tang et al., 2015) and revised spatial distribution of emissions from domestic wood combustion and to provide a consistent calibration for PM_{10} and $PM_{2.5}$. The proportion for sea salt has been derived as described in Section 5.3.6.The proportion for secondary organic aerosol, has been set at 1.0 for $PM_{2.5}$ so as to provide best fit to the available measurements.

Table 6.2 - The proportion of PM mass assigned to the $PM_{2.5}$ and $PM_{2.5-10}$ size fractions

Component	Fine fraction ($PM_{2.5}$)	Coarse fraction ($PM_{2.5-10}$)
SO_4	0.94	0.06
NO_3	0.556 (fine mode), 0.222 (coarse mode)	- (fine mode), 0.222 (coarse mode)
NH_4	0.97	0.03
SOA	1.00	-
Large point sources of primary particles	$PM_{2.5}$ emission inventory*	PM_{10} emission inventory
Small point sources of primary particles	$PM_{2.5}$ emission inventory*	PM_{10} emission inventory
Regional primary particles	$PM_{2.5}$ emission inventory*	PM_{10} emission inventory
Area sources of primary particles	$PM_{2.5}$ emission inventory*	PM_{10} emission inventory
Rural calcium rich dusts from re-suspension of soils	0.25	0.75
Regional iron rich dusts from re-suspension	0.50	0.50
Iron rich dusts from re-suspension due to vehicle activity	0.50	0.50
Sea salt	0.27	0.73
Residual	n/a	n/a

* The NAEI $PM_{2.5}$ emission inventory has been derived from the PM_{10} emission inventory by the application of estimates of the mass fraction represented by $PM_{2.5}$ for different sources and fuels.

6.3.2 Contributions from large and small point sources

The contributions from large and small point sources have been calculated in the same way as for the PM_{10} model described in Section 5.3.3.

6.3.3 Contributions from area sources

Figure 6-5 shows the calibration of the area source model for $PM_{2.5}$. The calibration coefficient for $PM_{2.5}$ is quite similar to the calibration coefficient for PM_{10}. The small difference is considered to be well within the uncertainty of the PM_{10} and $PM_{2.5}$ measurements and the $PM_{2.5}$ mass fractions within the emission inventory. A reasonably good agreement between the calibration coefficients for area sources is one of the criteria for the choice of mass fraction parameters for $PM_{2.5}$ within the PCM model.

As part of the calibration process emission caps have been applied to certain sectors; this is because the use of surrogate statistics for mapping area source emissions sometimes results in unrealistically large concentrations in some grid squares for a given sector. The emission caps applied are given in Table 6.3.

Figure 6-5 - Calibration of PM$_{2.5}$ area source model 2018 (µg m^{-3}, gravimetric)

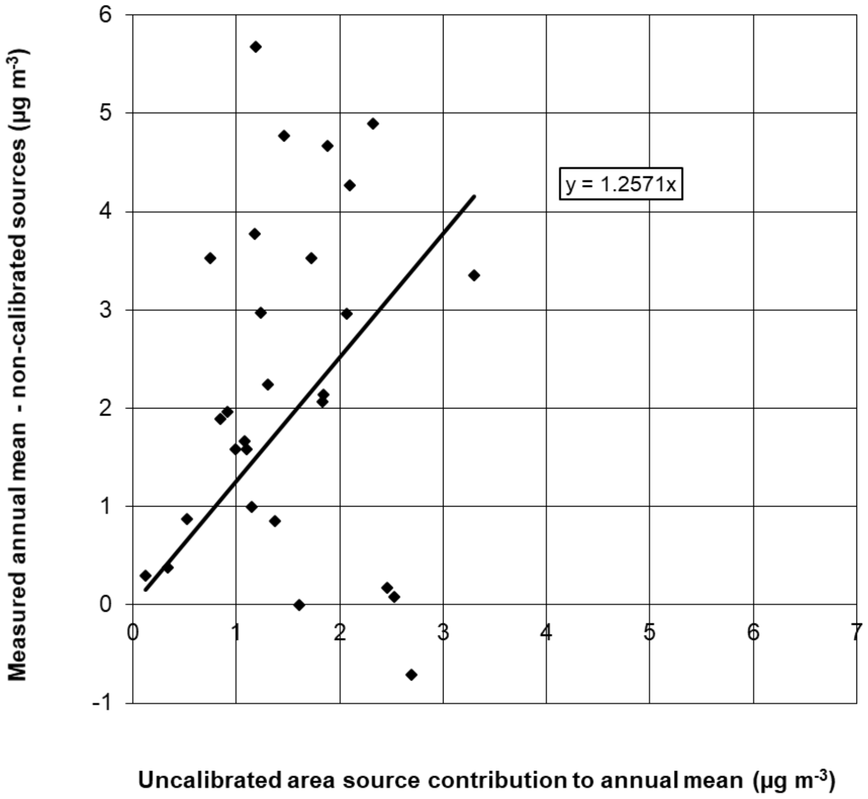

Table 6.3 - Emission caps applied to PM$_{2.5}$ sector grids

SNAP code	Description	Cap applied (t/a/km^2)
SNAP 8 (Other Transport & mobile machinery)	Industrial off-road mobile machinery, Gas oil	2.3
SNAP 8 (Other Transport & mobile machinery)	Shipping	5
SNAP 4 (Production process)	Stockpiles	9

6.3.4 Roadside concentrations

Figure 6-6 shows the calibration of the roadside increment model for annual mean $PM_{2.5}$ concentrations.

Figure 6-6 - Calibration of $PM_{2.5}$ roadside increment model 2018 (µg m^{-3}, gravimetric)

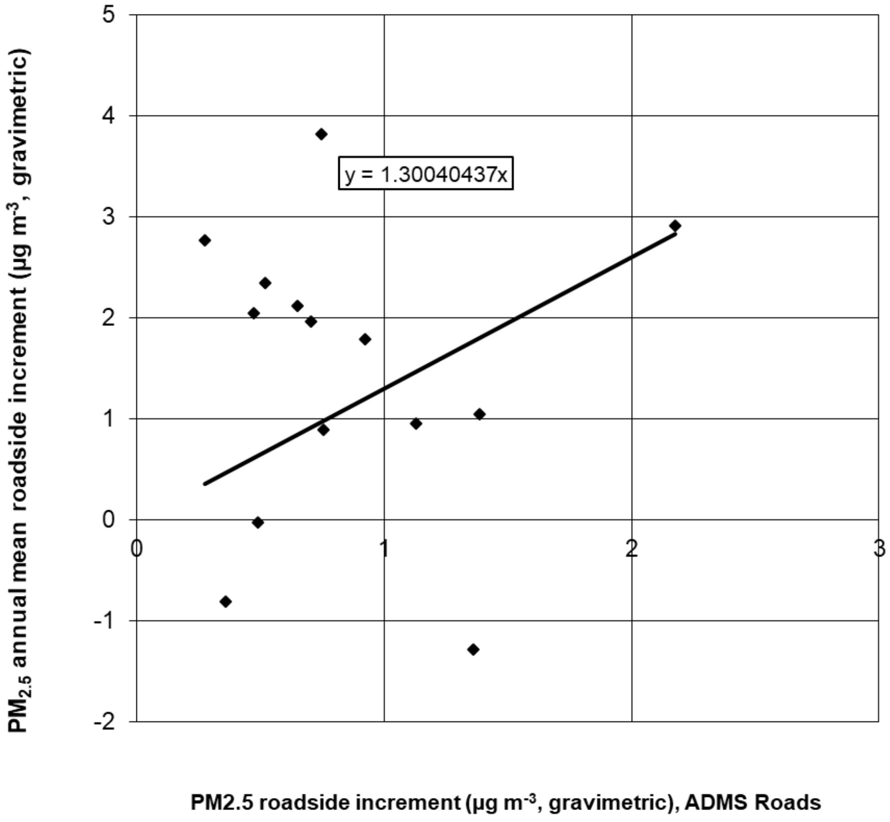

6.4 Results

6.4.1 Verification of mapped concentrations

Figure 6-7 and Figure 6-8 show comparisons of modelled and measured annual mean $PM_{2.5}$ concentrations in 2018 at background and roadside monitoring site locations. Lines representing y = x – 50 % and y = x + 50% are also shown because 50% is the AQD data quality objective for modelled annual mean $PM_{2.5}$ concentrations – see Section 1.5.

Summary statistics for the comparison between modelled and measured $PM_{2.5}$ concentrations are presented in Table 6.4 and Table 6.5.

There are several different categories of monitoring sites within these tables and graphs. This is because there are some sites in the national network at which only PM_{10} or $PM_{2.5}$, but not both are measured.

The agreement between the measurement data and the modelled values is generally good.

Figure 6-7 - Verification of background annual mean $PM_{2.5}$ model 2018

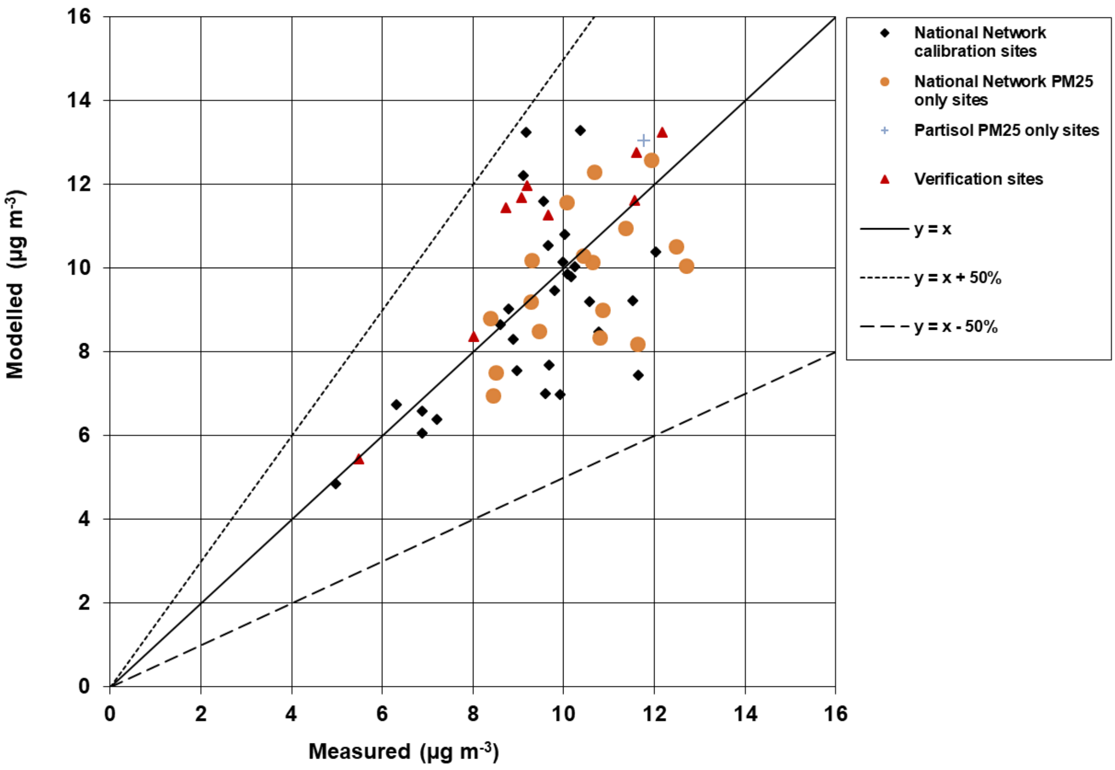

Figure 6-8 - Verification of roadside annual mean $PM_{2.5}$ model 2018

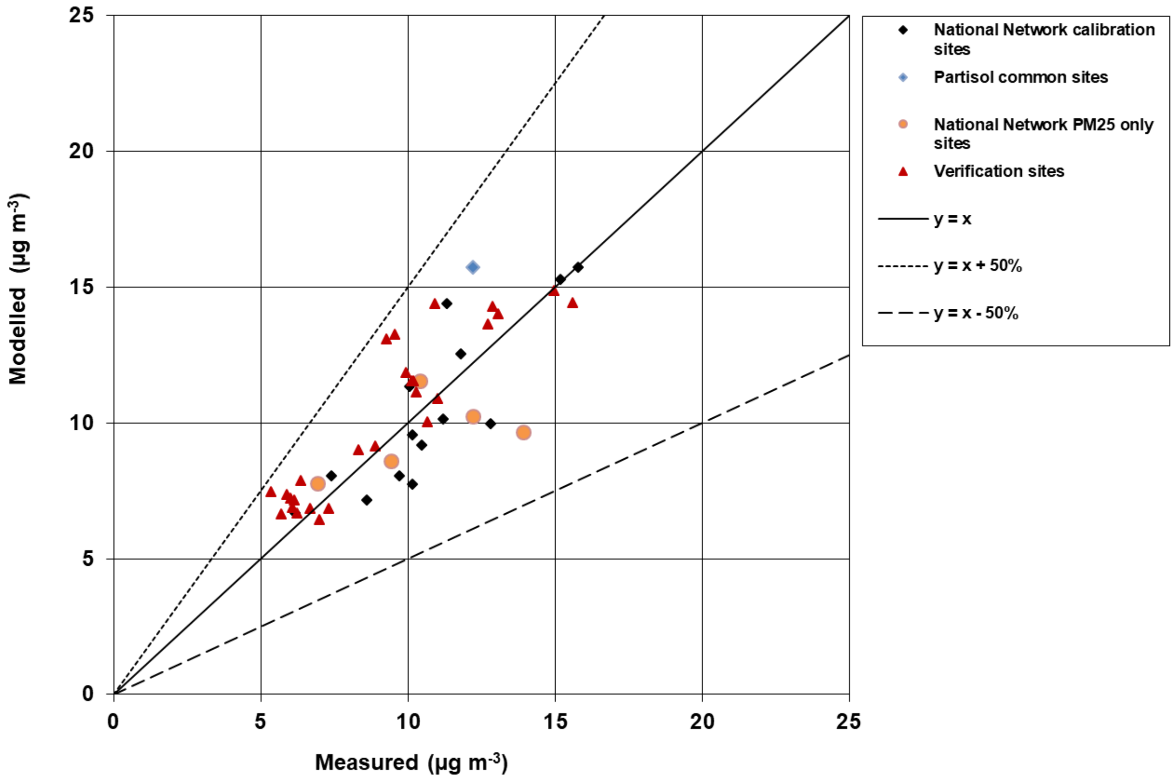

Table 6.4 - Summary statistics for comparison between gravimetric modelled and measured concentrations of $PM_{2.5}$ at background sites

	Mean of measurements ($\mu g\ m^{-3}$, grav)	Mean of model estimates ($\mu g\ m^{-3}$, grav)	R^2	% outside data quality objectives	Number of sites
National network (Calibration)	9.3	9.0	0.30	0	28
National network Partisol*	-	-	-	-	-
National network PM25 only sites	10.4	9.7	0.27	0	17
National network Partisol PM25 only sites	11.8	13.0	-	0	1
Verification sites	9.5	10.9	0.78	0	9

* There were no sites in this category in 2018

Table 6.5 - Summary statistics for comparison between gravimetric modelled and measured concentrations of $PM_{2.5}$ at roadside sites

	Mean of measurements ($\mu g\ m^{-3}$, grav)	Mean of model estimates ($\mu g\ m^{-3}$, grav)	R^2	% outside data quality objectives	Number of sites
National network (Calibration)	10.8	10.4	0.73	0	14
National network Partisol	12.2	15.7	-	0	1
National network PM25 only sites	10.6	9.6	0.32	0	5
National network Partisol PM25 only sites*	-	-	-	-	-
Verification sites	9.1	10.2	0.83	0	27

* There were no sites in this category in 2018

6.4.2 $PM_{2.5}$ source apportionment at monitoring sites

Figure 6-9 and Figure 6-10 show the modelled annual mean $PM_{2.5}$ source apportionment for 2018 at national network background and roadside monitoring sites respectively. The measured concentration at each site is also shown for reference.

At background locations, the contributions from non-emissions inventory sources (i.e. regional background sources and urban dusts), which are shown in grey on the figures, dominate with a particularly large contribution from secondary inorganic aerosols. The smaller contribution from urban background emissions sources, shown in colour on the figures, are dominated in most locations by domestic, traffic and industry.

At roadside locations the source apportionments follow a very similar pattern to background locations, except that there is an extra local road traffic component composed of local exhaust emissions, local brake and tyre wear emissions and local road abrasion emissions.

Overall regional secondary PM make a proportionally larger contribution to the total mass for $PM_{2.5}$ than for PM_{10}.

Figure 6-9 - Annual mean $PM_{2.5}$ source apportionment at background national network monitoring sites 2018

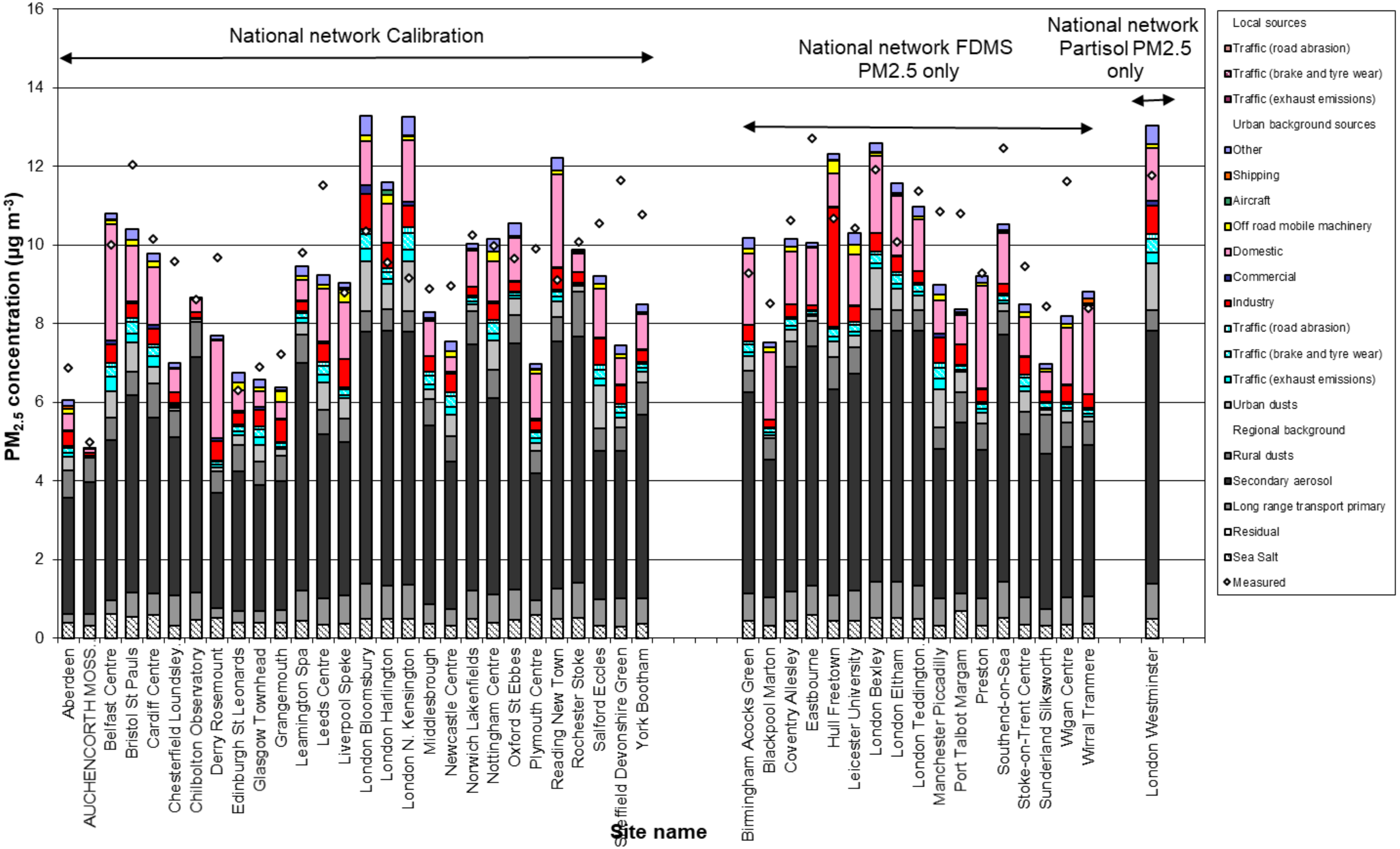

Figure 6-10 - Annual mean $PM_{2.5}$ source apportionment at roadside national network monitoring sites 2018

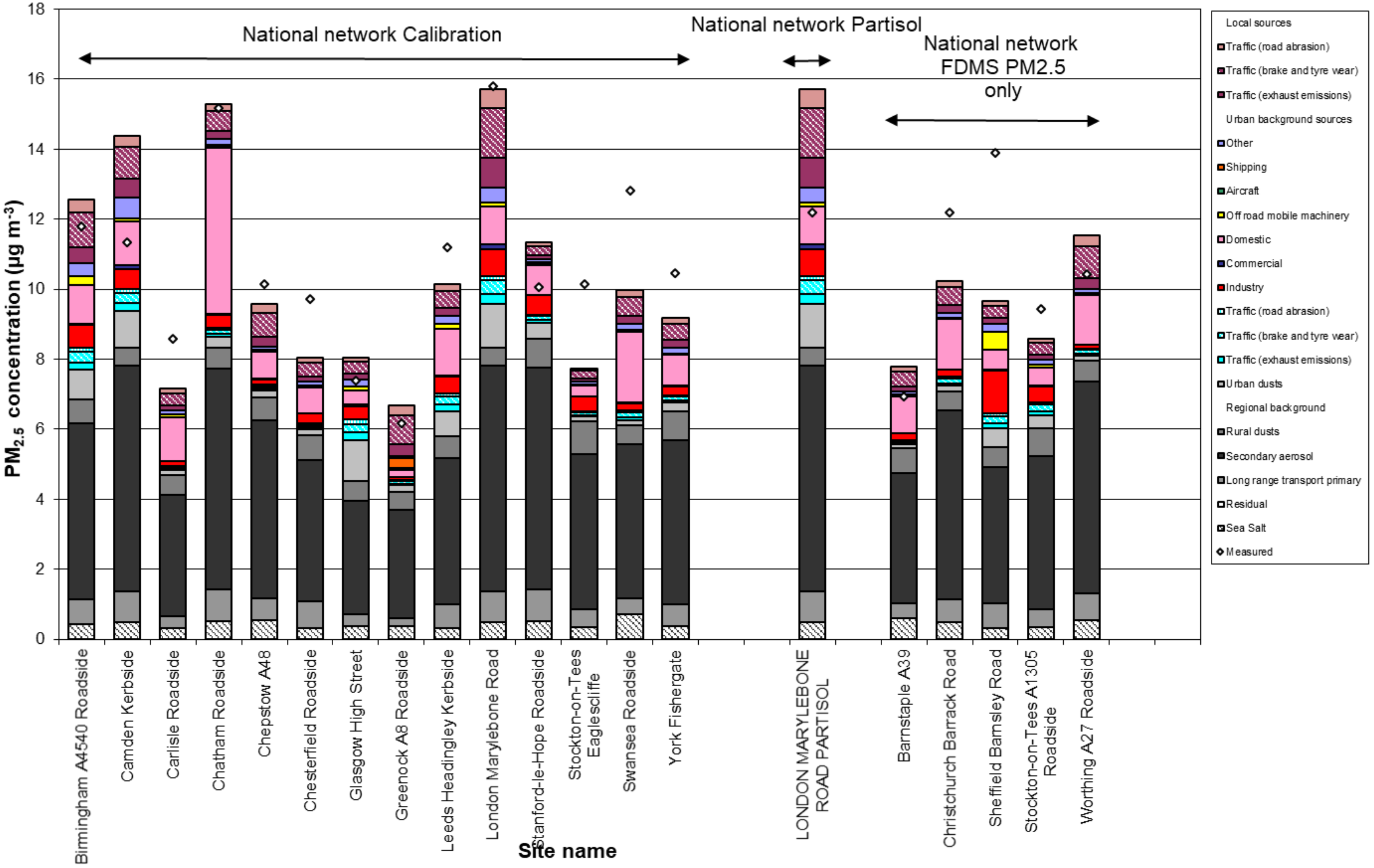

6.5 Subtraction of sea salt component

6.5.1 Introduction

The AQD (Article 20) requires member states to attribute exceedances of limit values due to natural sources when reporting the results of air quality assessments. The definition of natural sources in this directive includes sea spray. An assessment of concentrations with the contribution from natural sources subtracted is provided in e-reporting Data flow G (CDR, 2019) for locations with measured or modelled exceedances of the limit values. 2018 is the sixth year for which the contribution from natural sources has been subtracted for $PM_{2.5}$ for formal reporting within the framework of e-Reporting. Where exceedances are attributed to natural sources, subtraction is a requirement of the Directive.

6.5.2 Map of annual mean sea salt $PM_{2.5}$

The method used to estimate the sea salt contribution to annual mean $PM_{2.5}$ concentrations across the UK has been described in Section 5.3.6. The map of annual mean sea salt $PM_{2.5}$ can be used to subtract this contribution directly from measured or modelled annual mean concentrations. The uncertainties associated with estimating the sea salt contribution to annual mean $PM_{2.5}$ from measurements of particulate chloride have been discussed in Section 5.3.6. It is recognised that the interpolated map of sea salt concentrations will not capture the steep gradients in sea salt concentration very close to the coast. Thus, the analysis presented may underestimate the sea salt contribution to exceedances in coastal areas.

6.5.3 Results

There were no measured or modelled exceedances of the annual mean target value, Stage 1 or Stage 2 limit value for $PM_{2.5}$ in 2018. Therefore, there was no requirement to subtract the natural contribution.

6.6 Average Exposure Indicator

An exposure reduction target (ERT) and an exposure concentration obligation (ECO) for $PM_{2.5}$ have been set within the AQD. Both environmental objectives are based on the value calculated for the average exposure indicator (AEI). The AEI is calculated as the three-year average of annual mean measurements at urban background and suburban background monitoring sites (listed in Appendix 6) across a member state.

The AEI for the reference year 2018 has been calculated from measurements made during the years 2016, 2017 and 2018. The method used to calculate the AEI for the 2018 reference year is the same as was used for the previous assessments (Brookes et al., 2012, 2013, 2015, 2016, 2017, 2019a and 2019b). An assessment of compliance with the ECO is also presented in this section.

The AEI for the UK has been calculated using the method set out in guidance received for comment from the Commission on 3rd August 2012. This guidance was entitled “Procedures for Determining a National Average Exposure Indicator, for Assessment of a National Exposure Reduction Target, Requirements for Quality Assurance/Quality Control, and Requirements for the Estimation of their Measurement Uncertainties”. The guidance sets out recommended processes but recognises that Member States may adopt other procedures, and it confirms the order of the calculation method for this three-year average. An average is calculated across all of the sites for each year and the three-year average is then calculated from the values calculated for each year. The guidance also proposes a method for weighting the averages for each year according to the data capture achieved.

A total of 43 urban background and suburban background sites were included in the calculation for the 2018 assessment. The calculation is based on the following excerpt from the AQUILA guidance.

$$AEI(p) = \frac{\sum_{i=1}^{n}(\overline{x}_i d_i)}{\sum_{i=1}^{n}(d_i)}$$

$$\overline{x}_i = \frac{\sum_{j=1}^{k}(x_{ij})}{k}$$

Where: d_i is the data capture at the i^{th} station, for all stations where $d_i \geq 75\%$, $\overline{x_i}$ is the annual mean concentration in the year p at station i with the total of n stations, X_{ij} is the daily or hourly average concentration measured at station i during every valid sampling day or hour j, and k is the number of valid sampling days or hours during the year at that site.

$$AEI = \frac{\sum_p AEI(p)}{3}$$

One Site that only had a single valid year of data has been included in the calculation in order to provide a more representative calculation of average exposure. It is expected that there will be forced changes in site selection and equipment types between 2010 and 2020 which will impact on the uncertainty of the calculation.

The years 2016, 2017 and 2018 were used for the calculation, with means of 9.9, 9.7 and 10.0 µg m^{-3} respectively.

The mean of these three values (rounded to integer) is 10 µg m^{-3}. This is the AEI for the reference year of 2018. This value is compliant with the ECO of 20 µg m^{-3} to be achieved by 2015 set within the AQD.

The baseline AEI (based upon the years 2009, 2010, 2011) determined the National Exposure Reduction Target (NERT), to be achieved by 2020. With a value of 13 µg m^{-3} as the baseline AEI, the AQD requires the UK to reduce the AEI by 15% from this value of 13 µg m^{-3} in the three-year average for the reference year 2020.

7 Benzene

7.1 Introduction

7.1.1 Limit values

A single limit value for ambient benzene concentrations is set out in the AQD. This limit value has been specified for the protection of human health and came into force on 01/01/2010. The limit value is an annual mean concentration of 5 µg m^{-3}.

Modelled and measured benzene concentrations for 2018 were below the limit value for all zones.

7.1.2 Annual mean model

Maps of annual mean benzene concentrations at background and roadside locations in 2018 are presented in Figure 7-2 and Figure 7-3 respectively.

Benzene concentrations have been calculated using a similar approach to that adopted for NO_X although a different approach has been adopted for the modelling of fugitive and process emissions from point sources.

7.1.3 Overview of the PCM model for benzene

Figure 7-1 shows a simplified flow diagram of the PCM model for benzene. A summary of the PCM model method, input and assumptions for benzene is presented in Table 7.1.

Figure 7-1 – Flow diagram for PCM benzene model

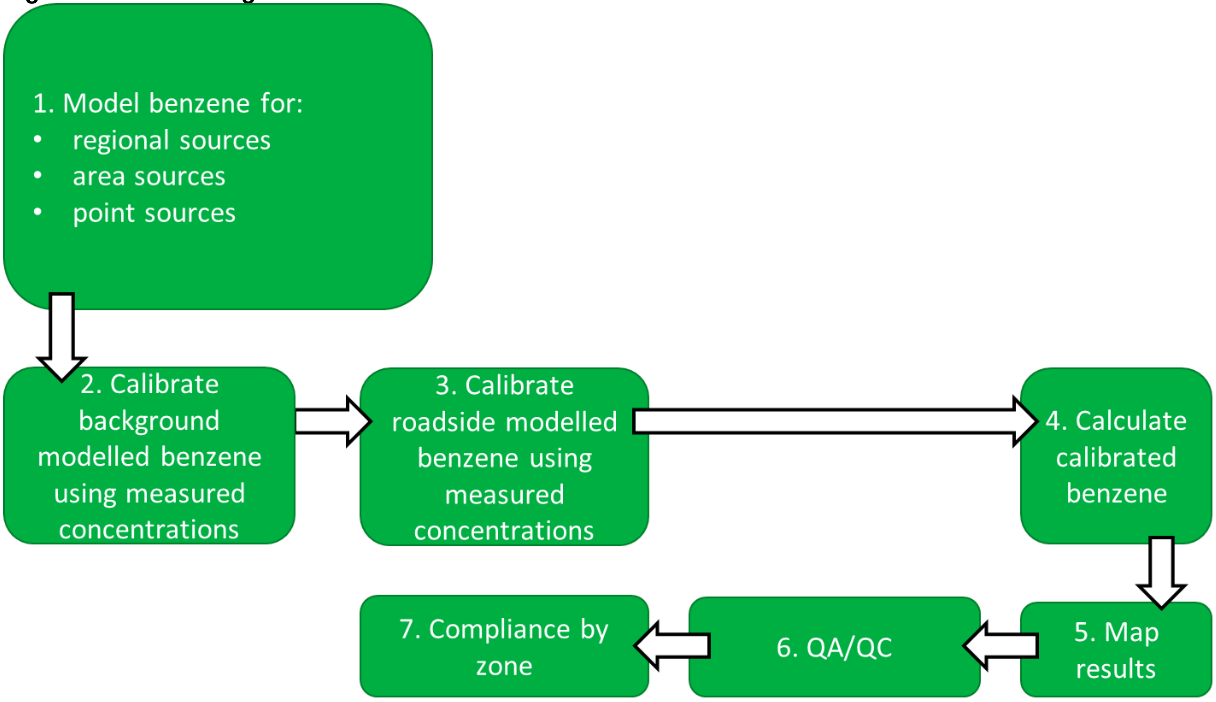

Table 7.1 – PCM model method, input and assumptions summary for benzene

Heading	Component	Details
General	Pollutant	Benzene
	Year	2018
	Locations modelled	Background and traffic locations
	Metric	Annual mean
Input data	Emission inventory	NAEI 2017
	Energy projections	Energy Projections 2017
	Road traffic counts	2017

Heading	Component	Details
	Road transport activity projections	DfT (2018) traffic (re-based to 2017 NAEI), DfT (2019) car sales projections, TfL traffic (2019) and fleet (2018) projections for London
	Road transport emission factors	COPERT 5
	Measurement data	2018
	Meteorological data	Hourly data from Waddington 2018
Model components	Regional	Interpolated from rural NOx measurements adjusted for local contribution, scaled using measured benzene and NOx at Chilbolton
	Combustion point sources	11 sources modelled using ADMS 5.2
	Fugitive and process point sources	PCM fugitive and process points model for benzene
	ETS point sources	PCM fugitive and process points model for benzene
	Large ETS point sources	32 sources modelled using ADMS 5.2
	Area sources	PCM dispersion kernels generated using ADMS 5.2. Time varying emissions for road transport and domestic sources. PCM small points model for industrial combustion emissions.
	Roadside increment	PCM Roads Kernel Model using ADMS-Roads 4.1
Calibration	Model calibrated?	Yes
	Number of background stations in calibration	16
	Number of traffic stations in calibration	10
Pollutant specific	n/a	n/a

7.1.4 Outline of the annual mean model for benzene

The map of annual mean background benzene concentrations includes contributions from:

- Distant sources (characterised by an estimate of rural background concentration)
- Combustion point sources
- Fugitive and process point sources
- Point sources with emissions estimates for air quality pollutants based on reported carbon emissions (ETS points)
- Local area sources

The area source model has been calibrated using measurements from the national monitoring networks. At locations close to urban roads an additional roadside contribution was added to account for contributions to total benzene from road traffic sources.

7.1.5 Chapter structure

This chapter describes modelling work carried out for 2018 to assess compliance with the benzene annual mean limit value described above. Emission estimates for benzene are described in Section 7.2, Section 7.3 describes the benzene modelling methods, and the modelling results in terms of verification and source apportionment are presented in Section 7.4.

Figure 7-2 - Annual mean background benzene concentration, 2018 (µg m^{-3})

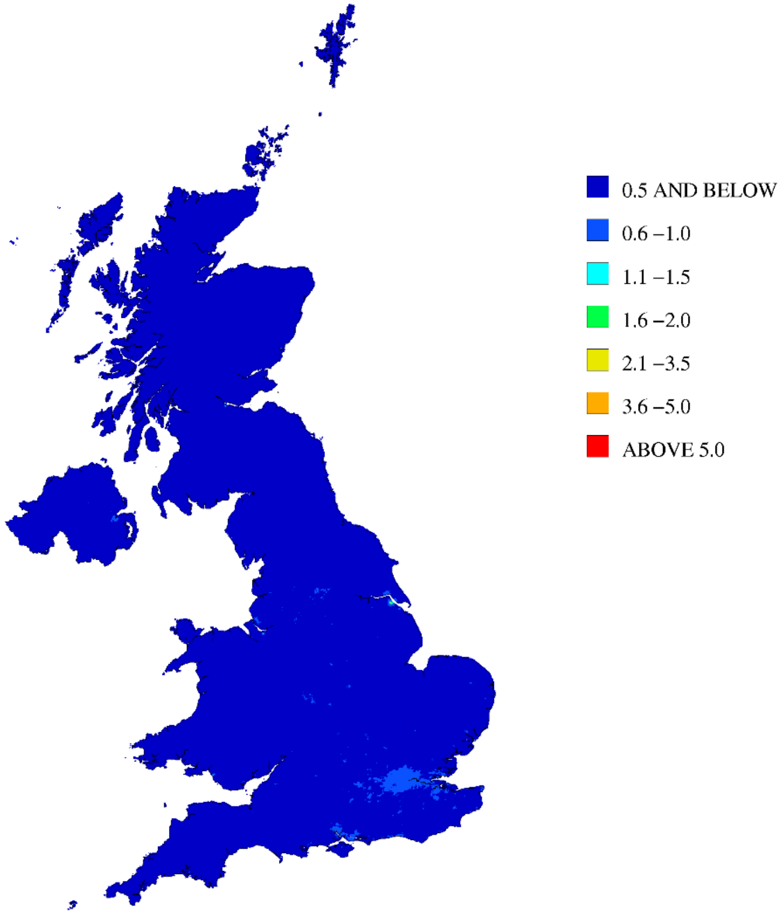

Figure 7-3 - Urban major roads, annual mean roadside benzene concentration, 2018 (µg m^{-3})

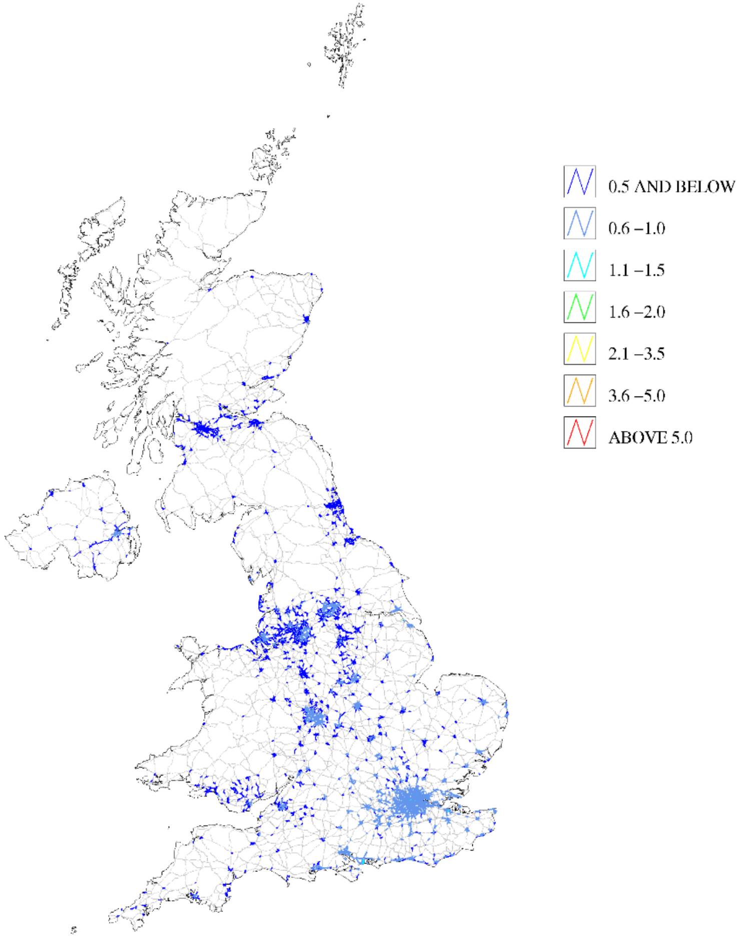

7.2 Benzene emissions

Estimates of the emissions of benzene from the UK National Atmospheric Emission Inventory 2017 (NAEI 2017) have been used in this study (Richmond et al., 2019). Emissions projections have been provided by the NAEI (Passant, 2019) based on BEIS EEP 2018 energy and emissions projections (BEIS, 2018). Figure 7-4 shows the UK total benzene emissions for 2017 and emissions projections for 2020, 2025 and 2030 split by SNAP code, with the coding described in Table 3.2. Values for intermediate years have been interpolated in this figure. The emissions include contributions from a variety of source sectors. The largest contributor is domestic combustion which is projected to show a small increase to 2020 and then remain relatively flat into the future. Decreases in emissions are largely related to road transport exhaust emissions and extraction. Increases in emissions are largely related to point source combustion processes and domestic combustion.

Figure 7-4 - Total UK benzene emissions for 2017 and emissions projections up to 2030 by SNAP code from NAEI 2017.

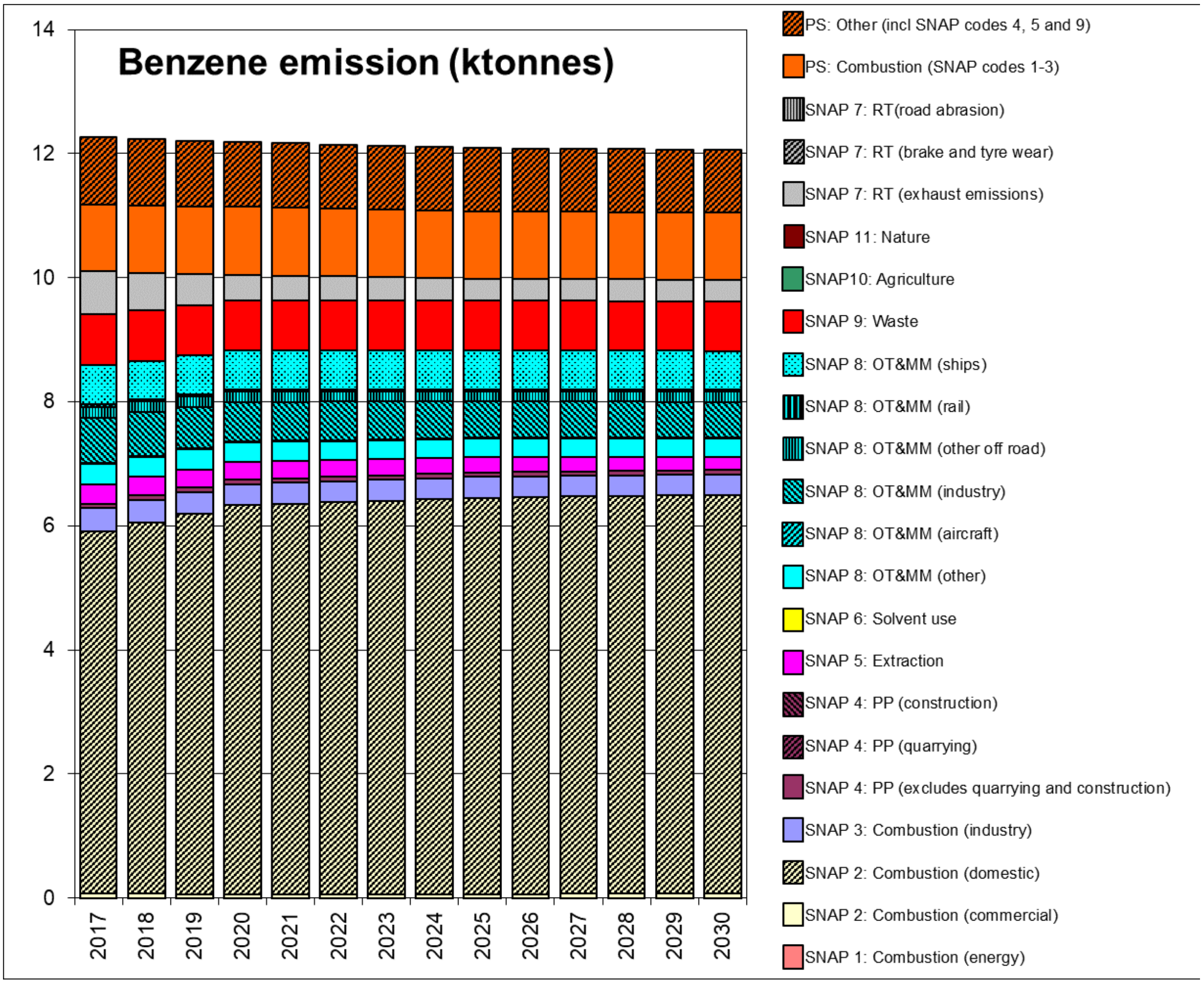

7.3 Benzene modelling

7.3.1 Contributions from large point sources

Following a similar methodology as for NO_x, benzene point sources in the NAEI 2017 have been classified as large if they fulfil any of the following criteria:

- Annual benzene emissions in the NAEI 2017 are greater than 5 tonnes for any given plant
- Stack parameters are already available for any given plant in the PCM stack parameters database (described in more detail in Section 3.3.1)
- Emissions are not associated with fugitive releases

Contributions to ground level annual mean benzene concentrations from large point sources in the NAEI 2017 were estimated by modelling each source explicitly using the atmospheric dispersion model ADMS 5.2 and sequential meteorological data for 2018 from Waddington. A total of 11 point sources were modelled as large point sources. Surface roughness was assumed to be 0.1 m at both the dispersion site and meteorological site. Concentrations were calculated for a 99 km x 99 km square composed of a regularly spaced 1 km x 1 km resolution receptor grid. Each receptor grid was centred on the point source. For each large point source information was retrieved from the PCM stack parameters database.

The NAEI emissions for combustion point sources are for the year 2017; however, the year 2018 has been modelled for the assessment. The NAEI emissions for point sources for 2017 were therefore scaled to provide values for 2018 as described in Section 3.3.1.

The NAEI 2017 includes point source emissions estimates derived from carbon emissions data reported under the EU-Emissions Trading Scheme (ETS), most recently described in Tsagatakis et al. (2019). These point sources are referred to as ETS points in this report. These derived air quality pollutant emissions are particularly uncertain and therefore in previous assessments (e.g. Brookes et al., 2017) emissions were capped at reporting thresholds and treated as small point sources. For the 2016 and 2017 assessments (Brookes et al., 2019a, 2019b) the NAEI recommended treating the ETS points that have emissions greater than the large points modelling threshold as large points and not to apply a cap (Passant pers. comm. 2017). The 2018 assessment continues this approach. Thus, based on the criteria for the treatment of large point sources described above, 32 ETS point sources were modelled as an additional set of large point sources (using the approach described above). ETS points that were not classified as large point sources were modelled using the benzene fugitive and small points approach described next.

7.3.2 Contributions from fugitive and small point sources

The contributions to ambient concentrations from fugitive and small point sources were modelled using a small points model similar to that described in Appendix 3, adapted specifically for fugitive and small point sources of benzene. In line with the method applied for the large point sources the NAEI 2017 emissions for fugitive and small point sources have been scaled to 2018 using the same source sector specific projection factors applied to the large point sources.

The emissions from these sources are not generally as well characterised in terms of exact location and release parameters as emissions from large combustion related sources. Separate models are used for the concentration in the 1 km x 1 km grid square that includes the source (the ‘in-square’ concentration) and the concentration in surrounding grid squares (the ‘out-square’ concentration). The ‘out-square’ concentration has been estimated using a dispersion kernel similar to the one used for area sources of benzene. The ‘in square’ concentration has been estimated by assuming a volume source of dimensions 200 m x 200 m x 30 m in the centre of the square with the concentration estimated as the average across receptors excluding those inside the central 800 m x 800 m of the 1000 m x 1000 m grid square. These parameters have been chosen to provide the best fit to the range and maximum of available monitoring data in the vicinity of refineries (Grice et al., 2009).

7.3.3 Contributions from rural background concentrations

Regional rural benzene concentrations were estimated from the map of rural NO_x concentration described in Section 3.3.4. The rural NO_x map was scaled using the ratio of measured annual mean benzene and NO_X concentrations at the rural Chilbolton monitoring site in 2018, a value of 0.041 for 2018.

7.3.4 Contributions from area sources

The 2018 area source benzene emissions maps have been calculated from the NAEI 2017 emissions maps following the method applied for NO_X, described in Section 3.3.5. An ADMS derived dispersion kernel has been used to calculate the contribution to ambient concentrations at a central receptor location from the area source emissions (excluding SNAP 3) within a 33 km x 33 km square surrounding each receptor. Hourly sequential meteorological data from Waddington in 2018 has been used to construct the dispersion kernels, as described in Appendix 4.

Revised methods introduced in the 2011 assessment (Brookes et al., 2012) for modelling the contributions to benzene from SNAP 2 (domestic and non-domestic combustion) and SNAP 3 (combustion in industry) area sources were used and have been described in Section 3.3.5.

The calibration coefficient for the area source model is derived by linear regression of a corrected measured annual mean background benzene concentration versus the modelled uncalibrated area source contribution. The measurements were derived from three sites within the national automatic hydrocarbon network and 13 non-automatic hydrocarbon sites. The corrected background concentration is derived by subtraction of the modelled contributions from SNAP 3 area sources, point sources and estimated rural benzene from the measured annual mean concentration at automatic and non-automatic pumped tube background monitoring sites. Figure 7-5 shows the calibration of the area source model.

The modelled area source contribution (excluding SNAP 3) was multiplied by the background calibration coefficient to calculate the calibrated area source contribution for each grid square in the country. The SNAP 3 area source contribution, point source contributions and regional rural concentration were then added, resulting in a map of total background annual mean benzene concentrations.

Figure 7-5 - Calibration of area source benzene model, 2018 (µg m^{-3})

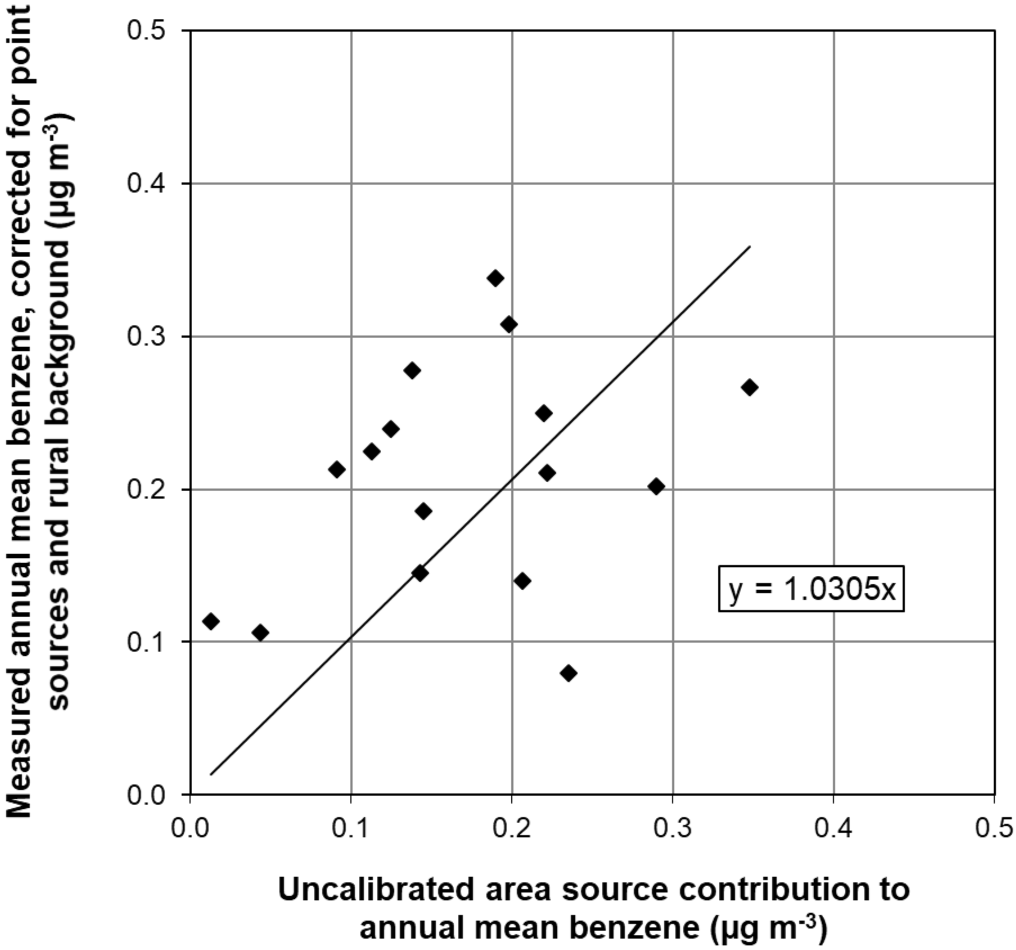

7.3.5 Roadside concentrations

Roadside annual mean concentrations of benzene for 2018 have been modelled using a similar method to the NO_X modelling described in Section 3.3.6. The NAEI provides estimates of benzene emissions for major road links in the UK for 2017 (Richmond et al., 2019) and these have been adjusted to provide estimates of emissions in 2018. The projections for benzene road transport emissions include the inputs and assumptions summarised in Table 7.1.

The PCM Roads Kernel Model (PCM-RKM) described in Appendix 7 has been used to calculate the roadside increment. The PCM-RKM is based upon dispersion kernels generated by the ADMS-Roads dispersion model (v4.1) and represents a more process-based approach than the previous empirical method. It provides a more robust assessment, whilst retaining the link with measurement data provided using measurement data to calibrate this component of the model. Figure 7-6 shows the calibration of this model at roadside monitoring sites. Roadside concentrations for urban major road links (A-roads and motorways) only are reported to the EU and included in this report.

Measurements from one site within the national automatic hydrocarbon network and 9 non-automatic hydrocarbon sites were used to calibrate the roadside model.

Figure 7-6 - Calibration of benzene roadside increment model, 2018 (µg m^{-3})

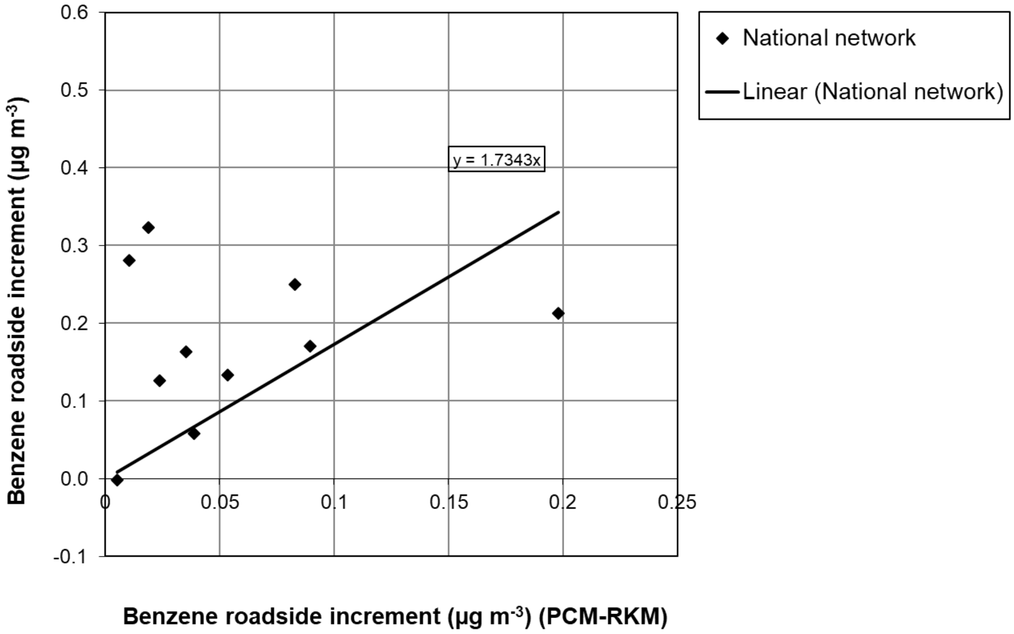

7.4 Results

7.4.1 Verification of mapped values

Figure 7-7 and Figure 7-8 show comparisons of the modelled and measured annual mean benzene concentrations for background and roadside locations. Lines showing y = x – 50% and y = x + 50% are included in these charts (the data quality objective for modelled benzene concentrations specified by the AQD – see Section 1.5).

Three monitoring sites that were not included in the calibration are included in Figure 7-7. Summary statistics for the comparison between modelled and measured benzene concentrations are listed in Table 7.2 and Table 7.3.

Figure 7-7 - Verification of background annual mean benzene model 2018

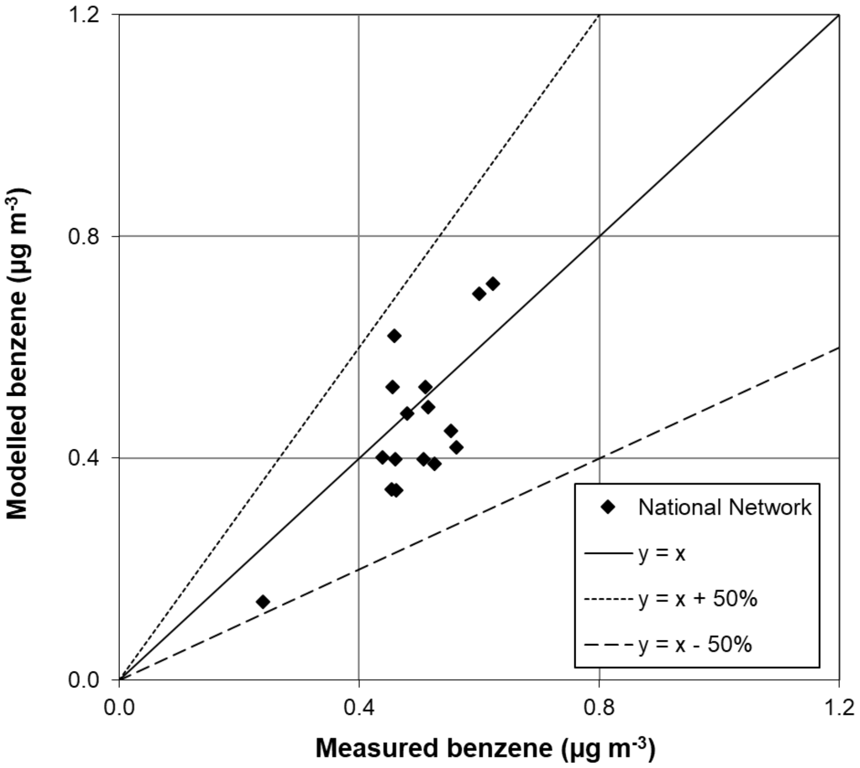

Figure 7-8 - Verification of roadside annual mean benzene model 2018

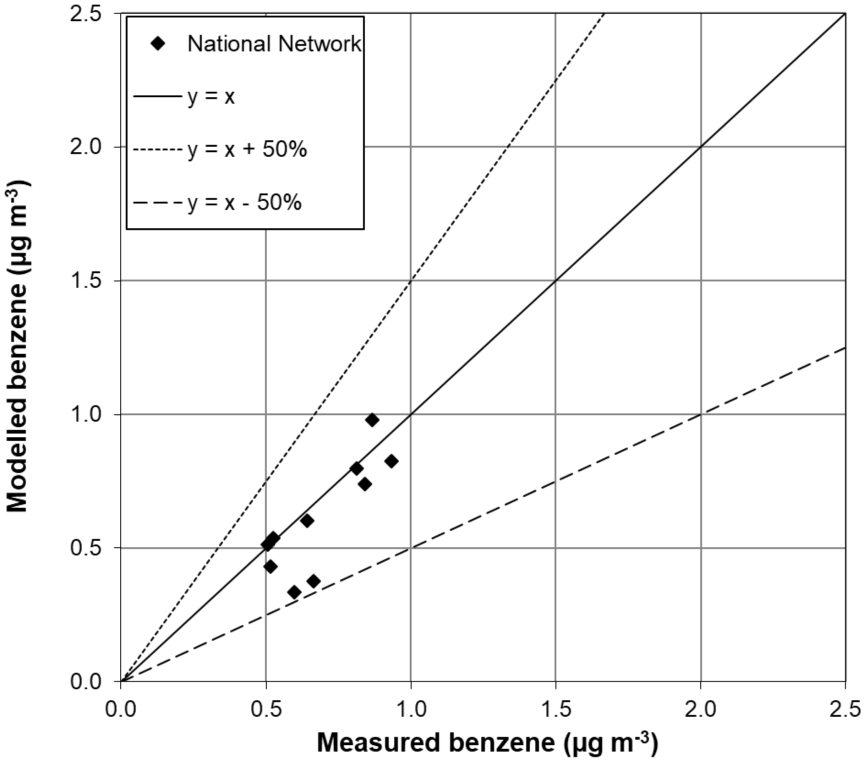

Table 7.2 - Summary statistics for comparison between modelled and measured benzene concentrations at background sites (µg m^{-3})

	Mean of measurements (µg m^{-3})	Mean of modelled (µg m^{-3})	R^2	%outside data quality objectives	Number of sites
National Network Sites	0.49	0.46	0.57	0	16

Table 7.3 - Summary statistics for comparison between modelled and measured benzene concentrations at roadside sites (µg m^{-3})

	Mean of measurements (µg m^{-3})	Mean of modelled (µg m^{-3})	R^2	%outside data quality objectives	Number of sites
National Network Sites	0.69	0.61	0.41	0	10

7.4.2 Benzene source apportionment at monitoring sites

Figure 7-9 and Figure 7-10 show the modelled annual mean benzene source apportionment for 2018 at background and roadside monitoring sites, respectively. The measured concentration at each site is also shown for reference. The regional background is an important component in the source apportionment for the majority of background monitoring sites. Contributions from domestic and industry sources are also important for many sites classified as urban and suburban background. The roadside source apportionment in Figure 7-10 shows that local traffic sources contribute up to 0.4 µg m^{-3} of benzene at these roadside sites.

Figure 7-9 - Annual mean benzene source apportionment at background monitoring sites in 2018 (the area type of each site is shown in parenthesis after its name)

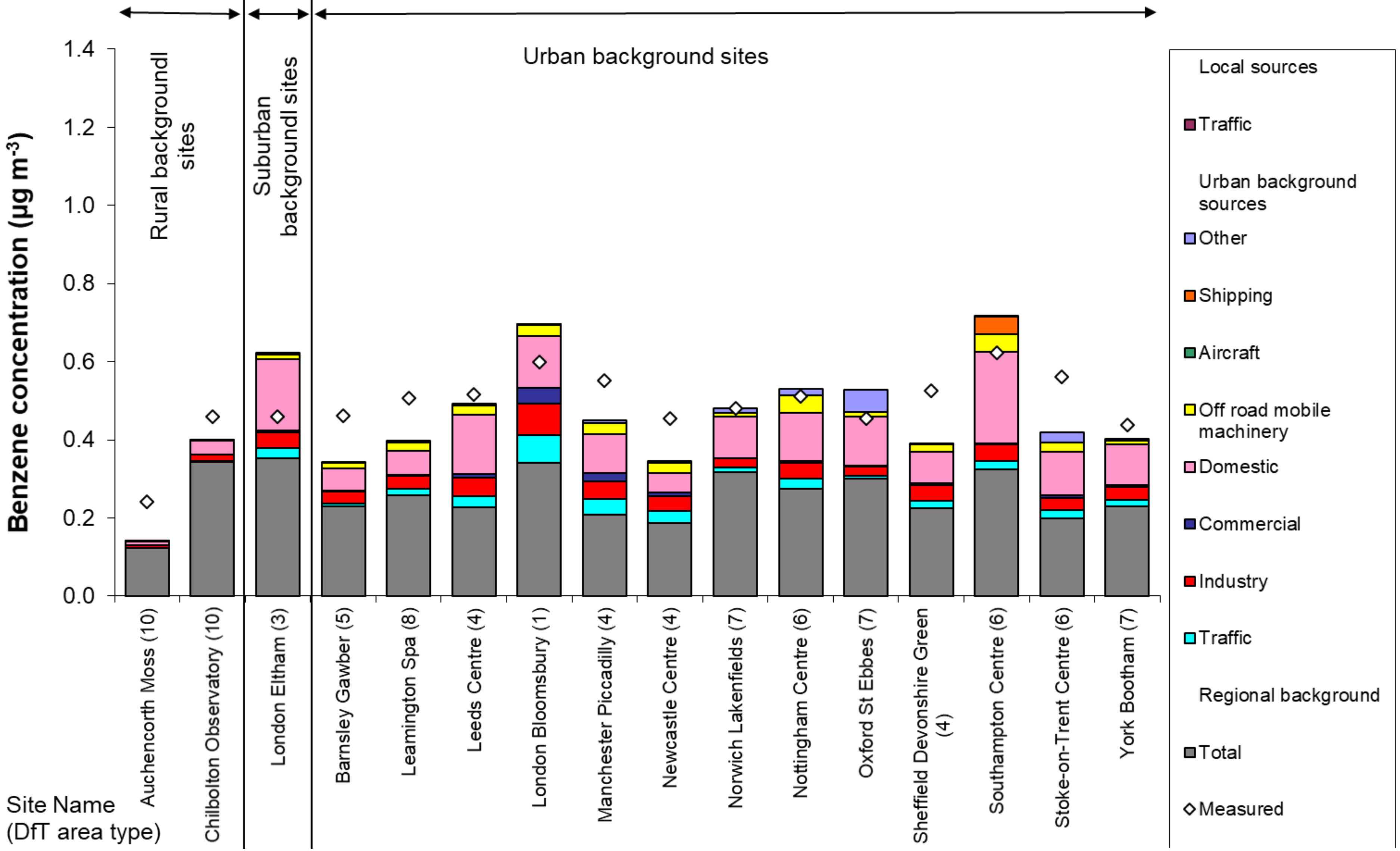

Figure 7-10 - Annual mean benzene source apportionment at roadside monitoring sites in 2018 (the area type of each site is shown in parenthesis after its name)

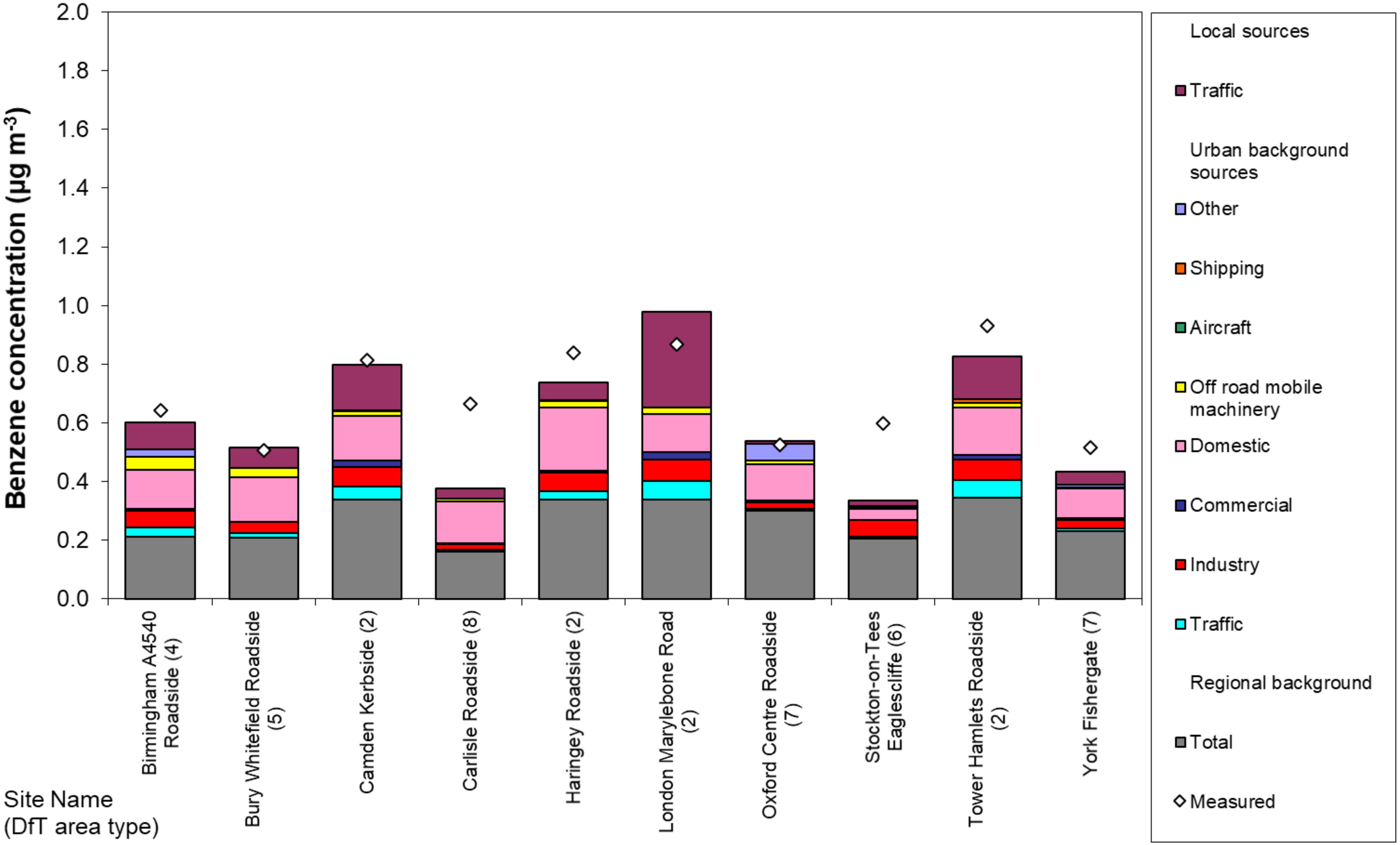

8 CO

8.1 Introduction

8.1.1 Limit values

A single limit value for ambient CO concentrations is set out in the AQD. This limit value has been specified for the protection of human health and came into force from 01/01/2005. The limit value is a maximum daily 8-hour mean concentration of 10 mg m^{-3}.

8.1.2 Objective Estimation

The maximum measured daily 8 hour running mean for 2018 are presented in Table 8.1, for all sites. Data capture was greater than 85% at all sites, during 2018. All values are below the lower assessment threshold of 5 mg m^{-3}.

Table 8.1 - Maximum daily 8-hour running mean (mg m^{-3}) in 2018[4]

EOI code	Site Name	Maximum daily 8-hour running mean (mg m^{-3})	Data capture (%)
GB0567A	Belfast Centre	0.89	97
GB0580A	Cardiff Centre	0.61	99
GB0839A	Edinburgh St Leonards	0.42	90
GB0584A	Leeds Centre	0.99	98
GB0682A	London Marylebone Road	1.3	98
GB0620A	London N. Kensington	0.86	98
GB0906A	Port Talbot Margam	2.0	98

The AQD states that objective estimation may be used to assess ambient air quality at levels below the lower assessment threshold (Article 6(4)). Objective estimation has been used to conclude that concentrations were likely to have been well below the limit value for CO in all zones during 2018. This assessment has been made on the basis of the low measured concentrations and the lack of any expected large increase in future CO emissions illustrated in the following section.

8.1.3 CO emissions

Estimates of the emissions from the UK National Atmospheric Emission Inventory 2017 (NAEI 2017) have been used in this assessment (Richmond et al., 2019). Emissions projections have been provided by the NAEI (Passant, 2019) based on BEIS EEP 2018 energy and emissions projections (BEIS, 2018). Figure 8-1 shows the UK total CO emissions for 2017 and emissions projections for 2020, 2025 and 2030 split by SNAP code, with the coding described in Table 3.2. Values for intermediate years have been interpolated in this figure.

Road transport exhaust emissions continue to decrease to 2020, with relatively small increases in emissions beyond 2020. Emissions from domestic combustion are expected to decline throughout the period. Emissions from off-road mobile machinery are expected to show a small increase. Overall, the changes in emissions shown in Figure 8-1 are relatively small when viewed in the context of the significant decreases in CO emissions from road transport, domestic combustion and combustion point sources (SNAP codes 1-3) from 1990 to 2017 present in the NAEI 2017 (Richmond et al., 2019), which led to a reduction in total UK emissions of CO over this period of 79%.

---

[4] Values have been presented to 2 significant figures to illustrate the dynamic range of the data.

Figure 8-1 - Total UK CO emissions for 2017 and emissions projections up to 2030 by SNAP code from NAEI 2017

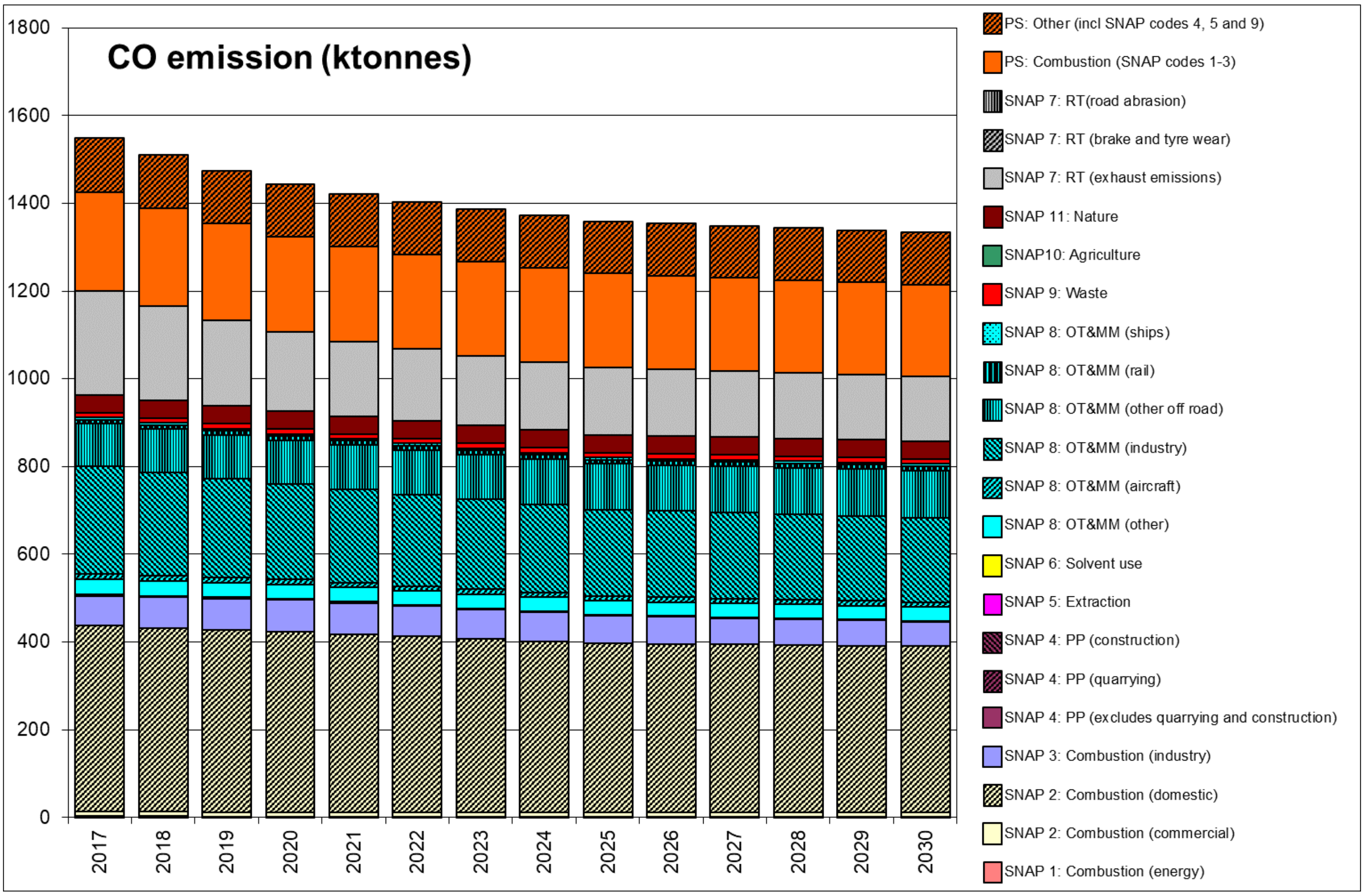

9 Ozone

9.1 Introduction

9.1.1 Target values and long-term objectives

Two target values (TV) for ambient ozone concentrations are set out in the AQD, these are:

- A maximum daily 8-hour mean concentration of 120 µg m^{-3}, not to be exceeded on more than 25 days per calendar year averaged over three years
- AOT40[5] (calculated from 1-hour values) of 18000 µg m^{-3}.h May to July averaged over five years

The TVs have been specified for the protection of human health and the protection of vegetation respectively, both came into force from 01/01/2010.

Two long term objectives (LTO) for ambient ozone concentrations are also set out in the AQD, these are:

- A maximum daily 8-hour mean concentration of 120 µg m^{-3} within a calendar year
- AOT40 (calculated from 1-hour values) of 6000 µg m^{-3}.h May to July

The LTOs have been specified for the protection of human health and the protection of vegetation respectively. The date for compliance with the LTOs has not been defined.

Results of the assessment in terms of comparisons of the modelled concentrations with the TVs and LTOs by zone have been reported in e-Reporting Data flow G (CDR, 2019).

9.1.2 Ozone modelling

An empirical mapping approach has been used for predicting ozone concentrations in 2018; this follows recommendations originally made by Bush and Targa (2005) in a study comparing the relative performance of the available techniques for modelling ozone within the UK.

The empirical approach draws upon measurements from the monitoring stations in the AURN during 2018 to produce functions describing ground-level ozone based on interpolated rural measurements of the ozone metrics corrected for local emissions of NO_X. These functions predict ozone levels at a resolution of 1 km x 1 km and the methods are briefly described in the following sections. Full details can be sourced from the cited references.

The methods used here are based upon those presented by Coyle et al. (2002), NEGTAP (2001), PORG (1998) and Murrells et al. (2011). Murrells et al. (2011) suggested that the observed dependence of the AOT40 metric on altitude, previously attributed to differences in surface deposition and reactions with local NO with altitude, was largely explained by the proximity of monitoring stations to urban areas. The 2018 assessment of the TV and LTO for AOT40, takes on the recommendations of Murrells et al. (2011) and does not include an altitude correction and thus avoids double counting the NO_X urban decrement.

9.1.3 Overview of the PCM model for ozone

Figure 9-1 shows a simplified flow diagram of the PCM model for ozone. A summary of the PCM model method, input and assumptions for ozone is presented in Table 9.1.

9.1.4 Chapter structure

This chapter describes modelling work carried out for 2018 to assess compliance with the ozone TVs and LTOs described above. Section 9.2 describes the modelling methods and results in relation to the number of days exceeding 120 µg m^{-3} metrics. Section 9.3 describes the modelling methods and results in relation to the AOT40 metrics.

---

[5] The definition of ATO40 has been given in Annex VII of the AQD

Figure 9-1 - Flow diagram for PCM ozone model

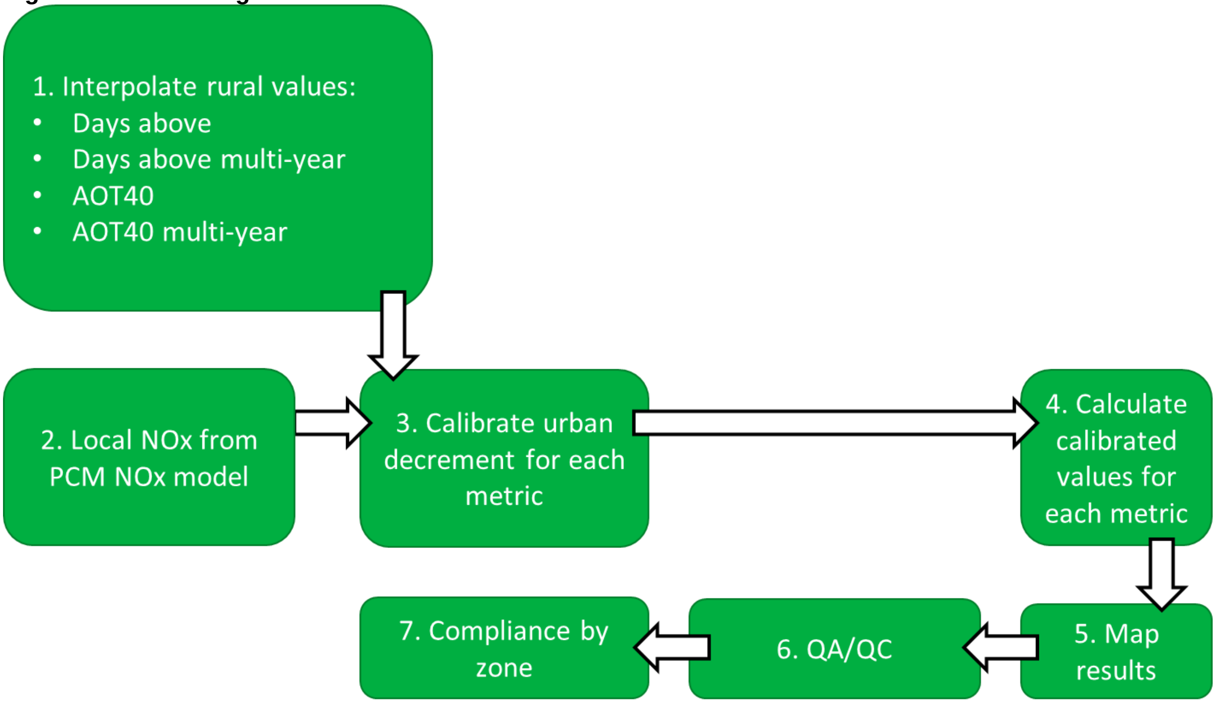

Table 9.1 – PCM model method, input and assumptions summary for ozone

Heading	Component	Details
General	Pollutant	O_3
	Year	2018, 2014-2018 mean and 2016-2018 mean
	Locations modelled	Background
	Metric	AOT40 (2018 and 2014-2018 mean), number of days with maximum 8-hour mean above 120 μg m^{-3} (2018 and 2016-2018 mean)
Input data	Emission inventory	NAEI 2017 (For NO_x)
	Energy projections	Energy Projections 2017 (For NO_x)
	Road traffic counts	2017 (For NO_x)
	Road transport activity projections	DfT (2018) traffic (re-based to 2017 NAEI), DfT (2019) car sales projections, TfL traffic (2019) and fleet (2018) projections for London
	Road transport emission factors	COPERT 5 (For NO_x)
	Measurement data	2018
	Meteorological data	Hourly data from Waddington 2018 (For NO_x)
Model components	Regional	Interpolated from rural ozone measurements
	Urban decrement	See details under “pollutant specific” heading
Calibration	Model calibrated?	Yes
	Number of background stations in calibration	66 (AOT40 2018), 67 (AOT40 2014-2018), 69 (days above 2018), 69 (days above 2016-2018)
	Number of traffic stations in calibration	n/a

Pollutant specific	Urban decrement	Empirical relationship between urban decrement and local NO_X contribution from PCM model results

9.2 Modelling the number of days exceeding 120 µg m^{-3} metric

9.2.1 Days greater than 120 µg m^{-3} methodology

Maps of the modelled number of days with maximum daily 8-hour mean ozone concentrations greater than 120 µg m^{-3}, for comparison with the LTO (2018) and TV (averaged 2016 to 2018) are presented in Figure 9-2 and Figure 9-3 respectively.

At rural locations in the UK exceedances of 120 µg m^{-3} as a maximum daily 8-hour mean are broadly consistent over wide spatial scales. As a result, measured exceedances from rural monitoring stations have been interpolated by Inverse Distance Weighting (IDW) throughout the whole of the UK to represent the likely exceedances of this metric in the absence of any influence from local emissions of NO_X from combustion sources.

The resultant interpolated maps, however, will overestimate exceedances in urban areas, where nitric oxide emissions from combustion sources deplete ozone concentrations. This effect has been accounted for by adding an empirically derived urban ozone decrement, expressed as a percentage. The percentage decrement is defined as follows:

% decrement = 100((measured concentrations - rural interpolated concentration)/rural interpolated concentration)*

The derivation of a coefficient relating the percentage decrement to the modelled local NO_X concentration is shown in Figure 9-4 and Figure 9-5. The local NO_X component is calculated as the sum of contributions from local point and area sources of NO_X emissions, calculated as described in Section 3.3.

Figure 9-4 shows the decrement plot for days greater than 120 µg m^{-3} in 2018 (the LTO for human health metric) and Figure 9-5 shows the decrement plot for days greater than 120 µg m^{-3} between 2016 and 2018 (the TV for human health metric). For some monitoring sites the decrement is positive, indicating that the measured number of days exceeding 120 µg m^{-3} is higher than the corresponding estimated rural value i.e. that the urban influence for these sites is not properly represented in the model. The cluster of low values close to the origin of these plots largely consists of the rural sites, at which there will be little difference between the rural estimated number of days exceeding 120 µg m^{-3} and the measured value. This helps to anchor the relationship to the origin. Percentage urban increments of -100% indicate that there were no measured exceedances of 120 µg m^{-3} at that monitoring site.

The calculated decrement is then used to correct the number of days where ozone concentrations are greater than 120 µg m^{-3} at rural sites, used for the interpolated maps:

Corrected days above 120 µg m^{-3} map = interpolated rural map + decrement

The decrement is a negative value and so reduces the concentration presented in the interpolated rural map to account for the reduction in ozone concentrations due to reaction with NO. Where the results of the expression predict a number of days less than 0.5, the predicted value is rounded to zero.

Figure 9-2 - Estimated number of days with an 8-hour mean ozone concentration above 120 µg m^{-3}, 2018

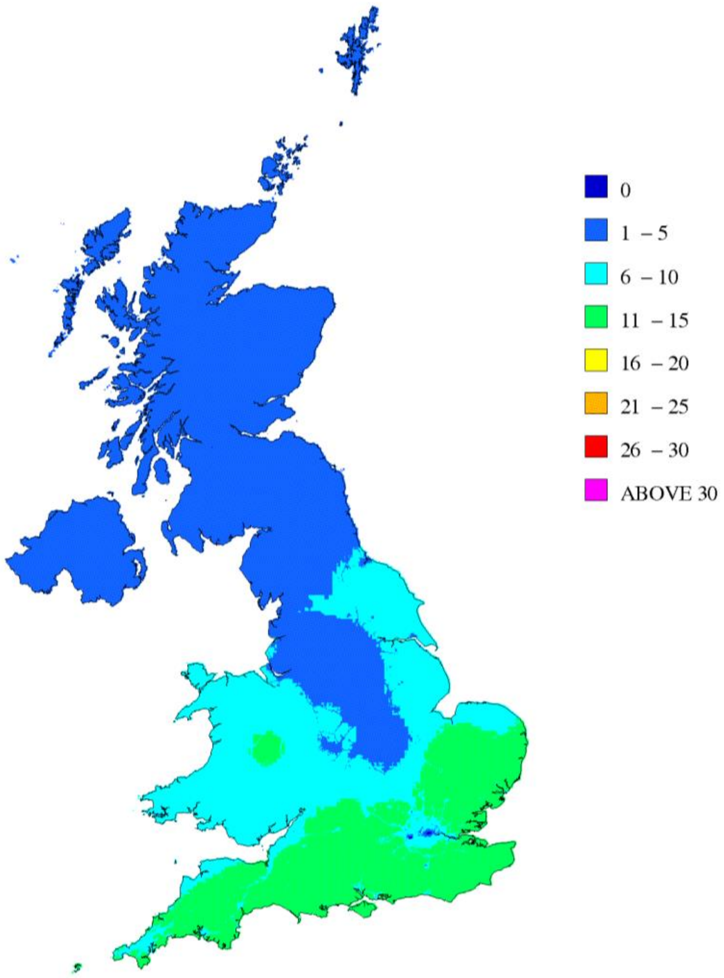

Figure 9-3 - Estimated average number of days with an 8-hour mean ozone concentration above 120 µg m^{-3}, 2016 to 2018

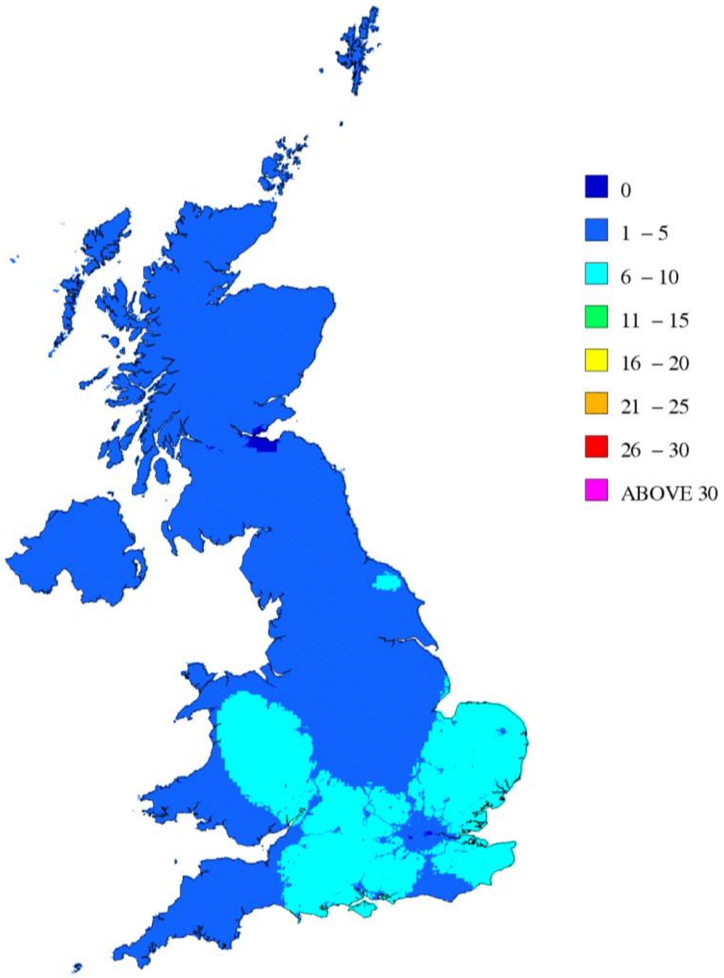

Figure 9-4 - Days greater than 120 µg m^{-3} percentage decrement in ozone concentrations, 2018

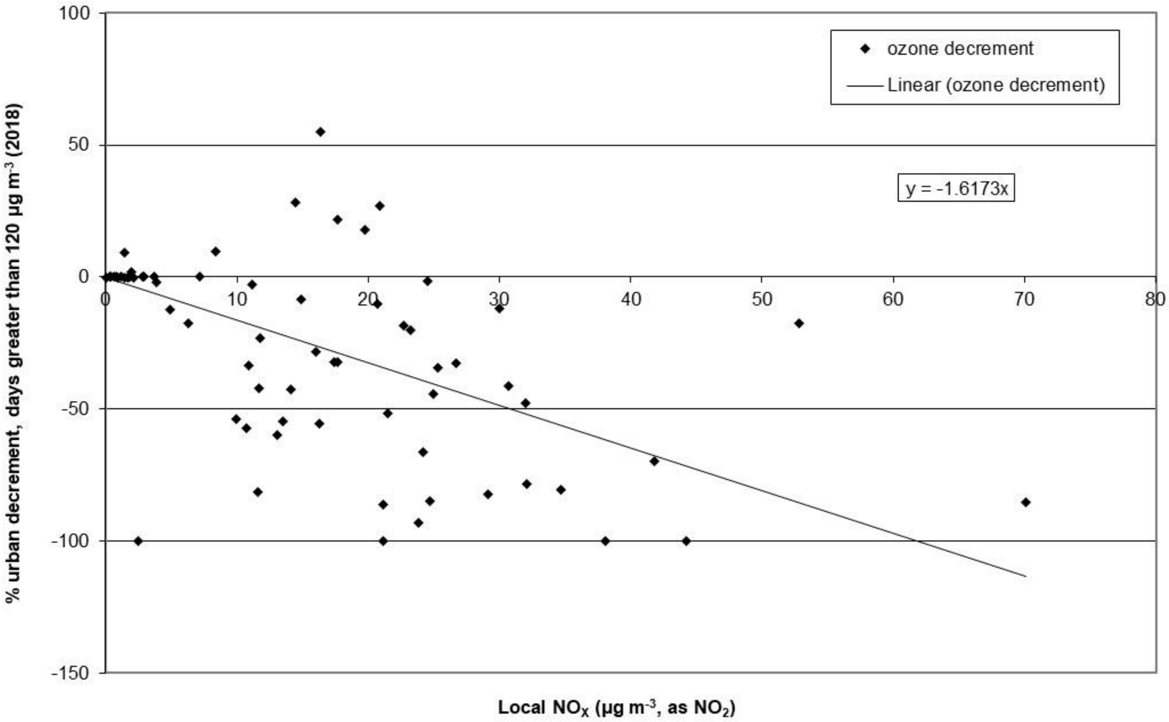

Figure 9-5 - Days greater than 120 µg m^{-3} percentage decrement in ozone concentrations, 2016-2018

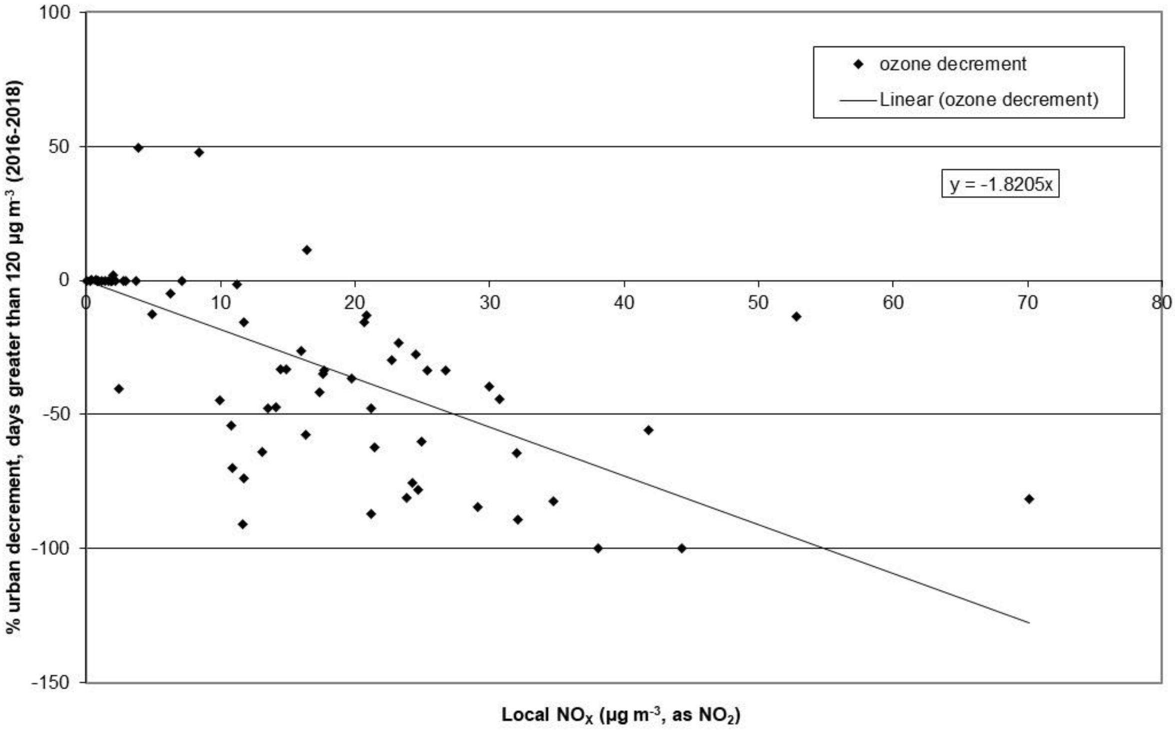

9.2.2 Verification of the number of mapped days > 120 µg m^{-3} values

Figure 9-6 and Figure 9-7 compare the number of modelled and measured days with maximum daily 8-hour mean ozone concentrations greater than 120 µg m^{-3} in 2018 and averaged 2016-2018 at background locations, respectively. Both the national network sites used to calibrate the models and the verification sites are shown. Lines representing y = x + 50 % and y = x - 50% are also shown, as this is the AQD data quality objective for modelled ozone concentrations – see Section 1.5.

Figure 9-6 - Verification of background number of days > 120 µg m^{-3} model 2018

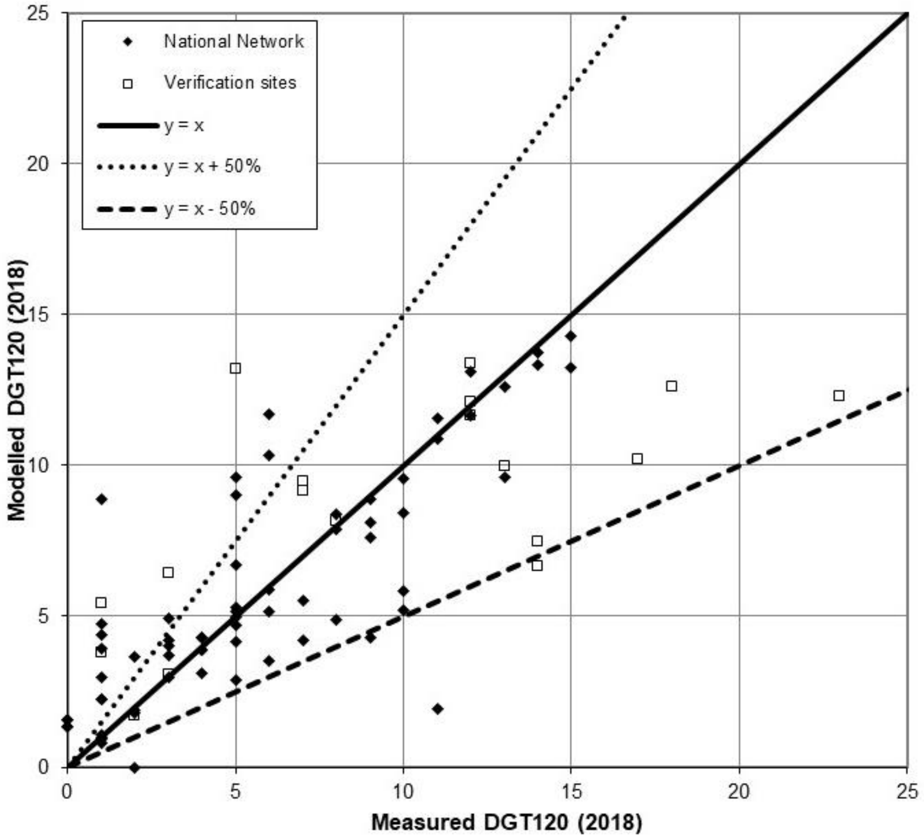

Figure 9-7 - Verification of background number of days > 120 µg m^{-3} model 2016-2018

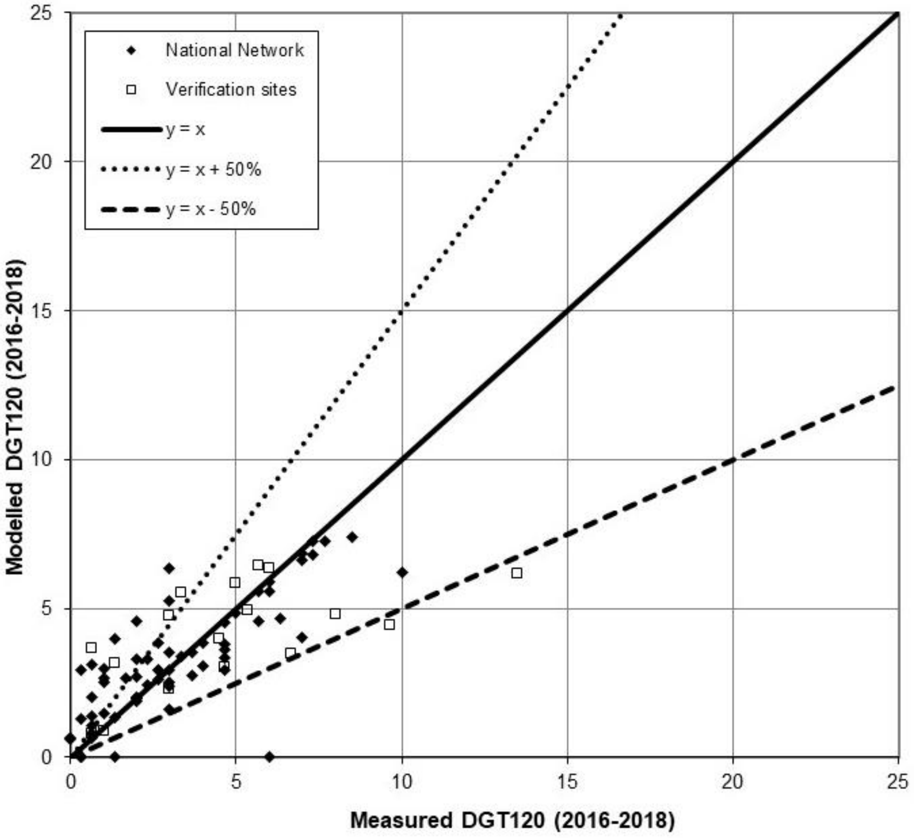

Figure 9-6 and Table 9.2 show that, on average, the model underestimates the number of days greater than 120 µg m^{-3} for the LTO compared with measurements at verification sites. Figure 9-7 and

Table 9.2 show that the model also underestimates the number of days greater than 120 µg m^{-3} for the TV compared with measurements at verification sites. For both metrics, the agreement between model estimates and measurement is good for National network sites, which reflects that these measurements are part of the calibration process. The R^2 value for the verification sites, shown in Table 9.2 is lower for both metrics. There are few independent ozone monitoring sites available for model verification.

Table 9.2 - Summary statistics for comparison between modelled and measured number of days exceeding 120 µg m^{-3} as a maximum daily 8-hour mean

		Mean of measurements (days)	Mean of model estimates (days)	R^2	% outside DQO	No. sites
National network	2018	5.7	6.0	0.66	32%	69
Verification sites	2018	9.6	8.7	0.44	28%	18
National network	2016-2018	3.2	3.3	0.63	36%	69
Verification sites	2016-2018	4.8	4.1	0.36	35%	17

9.3 Modelling the AOT40 vegetation metric

9.3.1 AOT40 methodology

Maps of modelled AOT40 for comparison with the LTO (2018) and TV (averaged 2014 to 2018) are presented in Figure 9-8 and Figure 9-9 respectively.

The AOT40 vegetation metrics for 2018 and the averaged metric for 2014-2018 were calculated from measured data at rural monitoring stations in the AURN. These data were interpolated by Inverse Distance Weighting (IDW) to produce a rural map.

An urban decrement term was subsequently defined for those monitoring stations in the AURN and the rural map to correct for the depletion of ozone in areas close to sources of NO. As for the days above 120 µg m^{-3} metric, the decrement is closely related to the annual mean NO_X concentration, and has been defined in a similar fashion, using a percentage decrement in ozone concentrations associated with local NO_X concentrations.

Using the same methodology discussed in Section 9.2.1 for the days greater than 120 µg m^{-3} maps, the decrement was then used to correct the final AOT40 maps:

Corrected AOT40 map = interpolated rural map + decrement

The relationships between the decrement and modelled NO_X concentrations for 2018 and 2014-2018 averaged metrics are presented in Figure 9-10 and Figure 9-11 respectively.

Figure 9-8 - Estimated AOT40 vegetation metric, 2018 (µg m^{-3} hours)

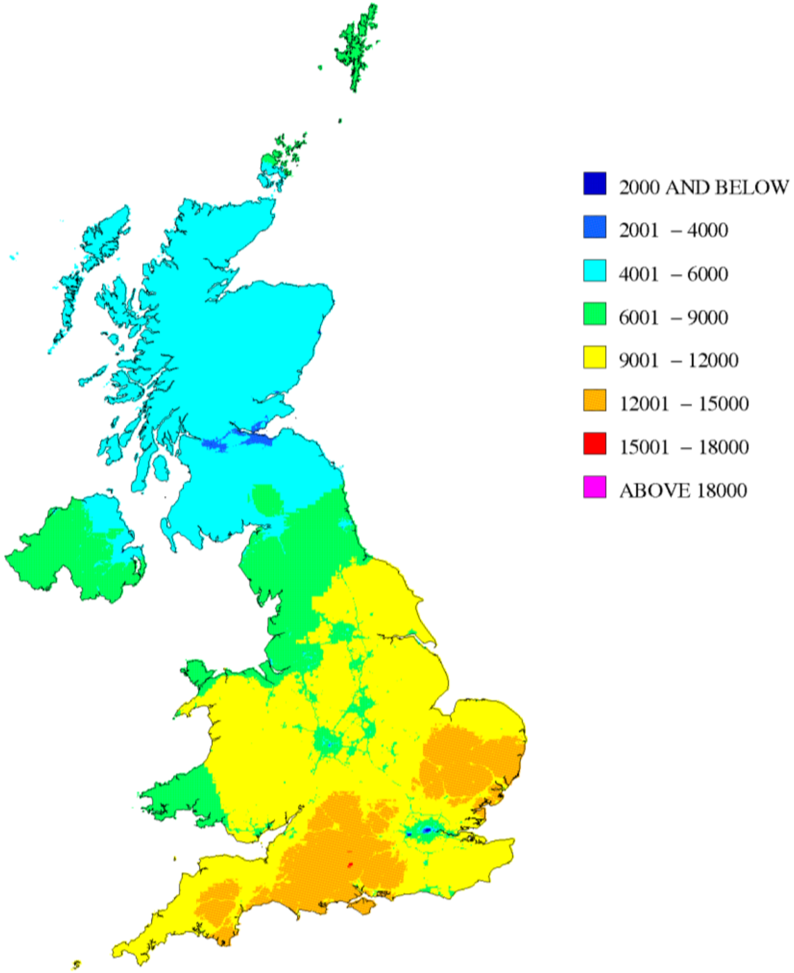

Figure 9-9 - Estimated AOT40 vegetation metric, averaged 2014-2018 (µg m^{-3} hours)

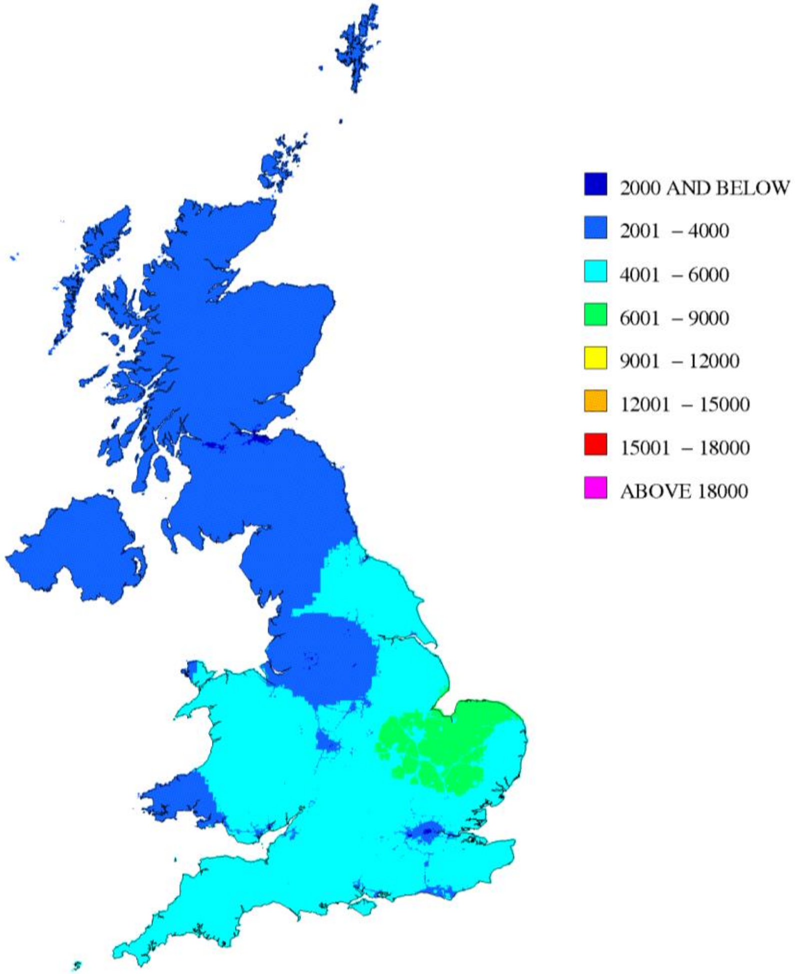

Figure 9-10 - AOT40 percentage decrement in ozone concentrations, 2018

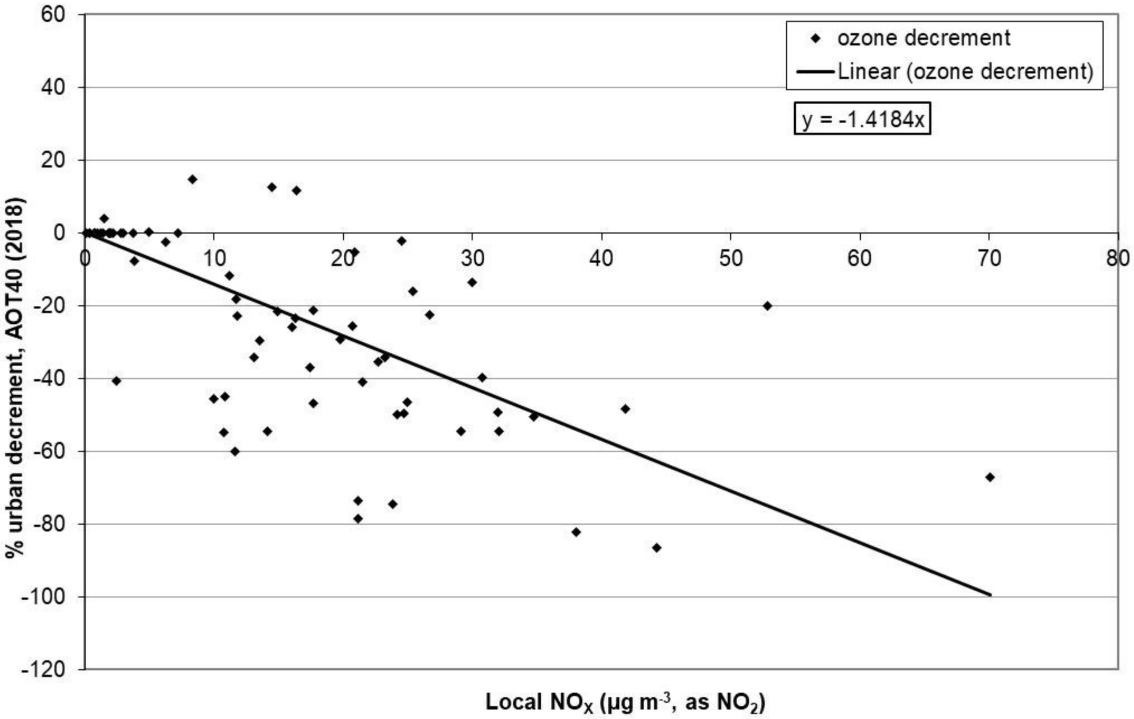

Figure 9-11 - AOT40 percentage decrement in ozone concentrations, 2014-2018

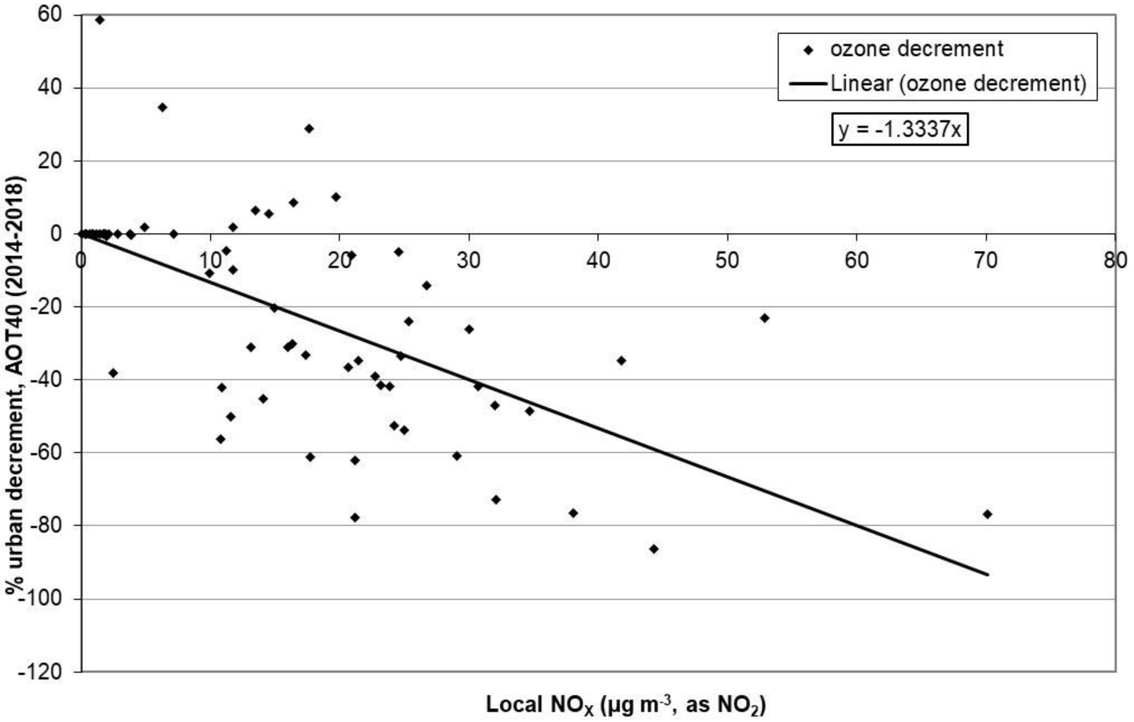

9.3.2 Verification of mapped AOT40 values

Figure 9-12 and Figure 9-13 show a comparison of modelled and measured AOT40 metrics in 2018 and averaged 2014-2018 at background locations. Both the national network sites used to calibrate the models and the verification sites are shown. Lines representing y = x + 50 % and y = x - 50% are also shown, as this is the AQD data quality objective for modelled ozone concentrations – see Section 1.5.

Figure 9-12 - Verification of background AOT40 vegetation model, 2018

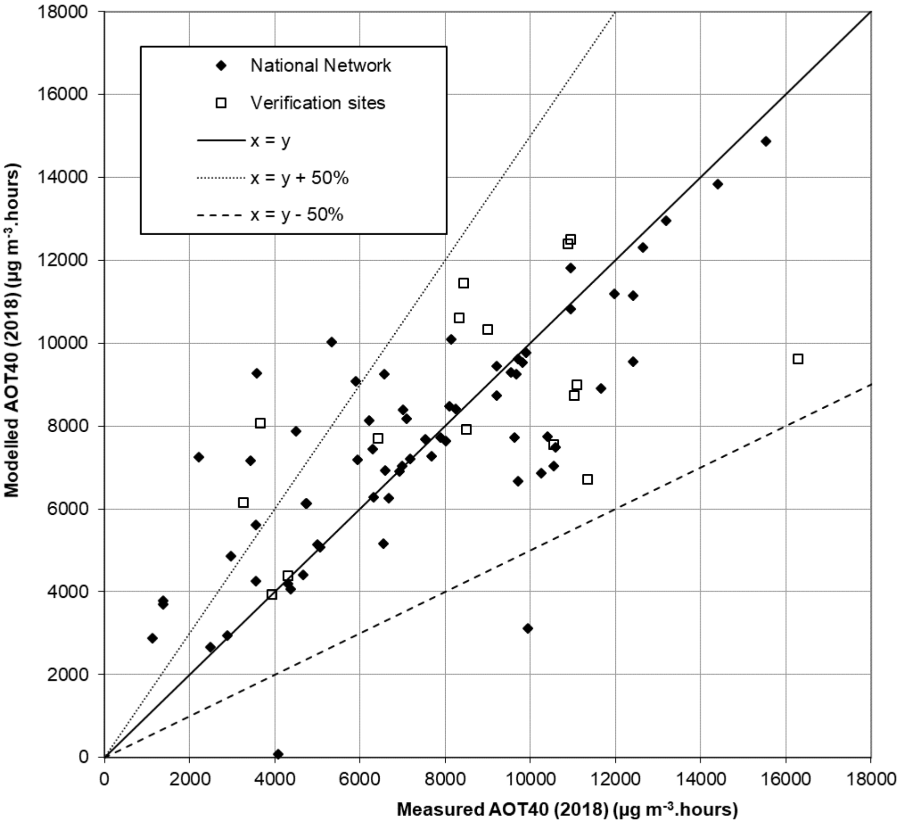

Figure 9-13 - Verification of background AOT40 vegetation model, 2014-2018

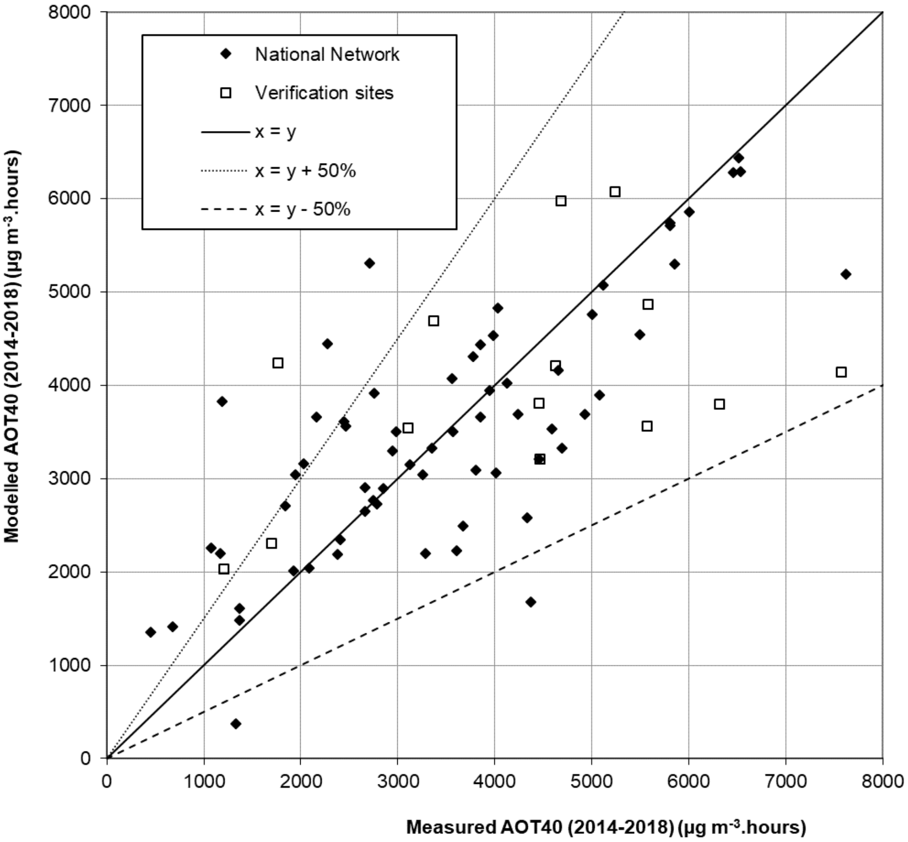

Model performance for both the LTO and TV for the AOT40 metrics is similar to that for the days greater than 120 µg m^{-3}. The R^2 values are relatively poor for the verification sites for both metrics. However, there are fewer sites outside the DQO than for the days greater than 120 µg m^{-3}.

Table 9.3 - Summary statistics for comparison between modelled and measured AOT40 vegetation metric

		Mean of measurements (µg m^{-3} hours)	Mean of model estimates (µg m^{-3} hours)	R^2	% outside DQO	No. sites
National network	2018	7389	7720	0.59	20%	66
Verification sites	2018	8626	8694	0.32	13%	16
National network	2014-2018	3509	3622	0.59	21%	67
Verification sites	2014-2018	4263	4064	0.22	14%	14

10 Arsenic, Cadmium, Nickel and Lead

10.1 Introduction

10.1.1 Target and Limit values

A single limit value for ambient lead (Pb) concentrations is set out in the AQD. This limit value has been specified for the protection of human health and came into force from 01/01/2005. The limit value is an annual mean concentration of 0.5 µg m^{-3}.

The target values (TV) for As, Cd and Ni included in the 4th Daughter Directive (AQDD4) are listed in Table 10.1. The Directive states that Member States should take all necessary measures not entailing disproportionate costs to ensure that the target values are not exceeded after the compliance date.

Table 10.1 - Target values for As, Cd, and Ni

Pollutant	Averaging period	TV (ng m^3)	Date after which the TV is not to be exceeded
As	Calendar year	6	31 December 2012
Cd	Calendar year	5	31 December 2012
Ni	Calendar year	20	31 December 2012

10.1.2 Annual mean models

Maps of annual mean As, Cd, Ni and Pb concentrations in 2018 at background locations are shown in Figure 10-2, Figure 10-3, Figure 10-4 and Figure 10-5 respectively. These maps are presented in ng m^{-3}, where 1000 ng m^{-3} = 1 µg m^{-3}.

10.1.3 Overview of the PCM models for As, Cd, Ni and Pb

Figure 10-1 shows a simplified flow diagram of the PCM models for As, Cd, Ni and Pb. A summary of the PCM model method, input and assumptions for these pollutant models is presented in Table 10.2.

Figure 10-1 – Flow diagram for PCM As, Cd, Ni and Pb models

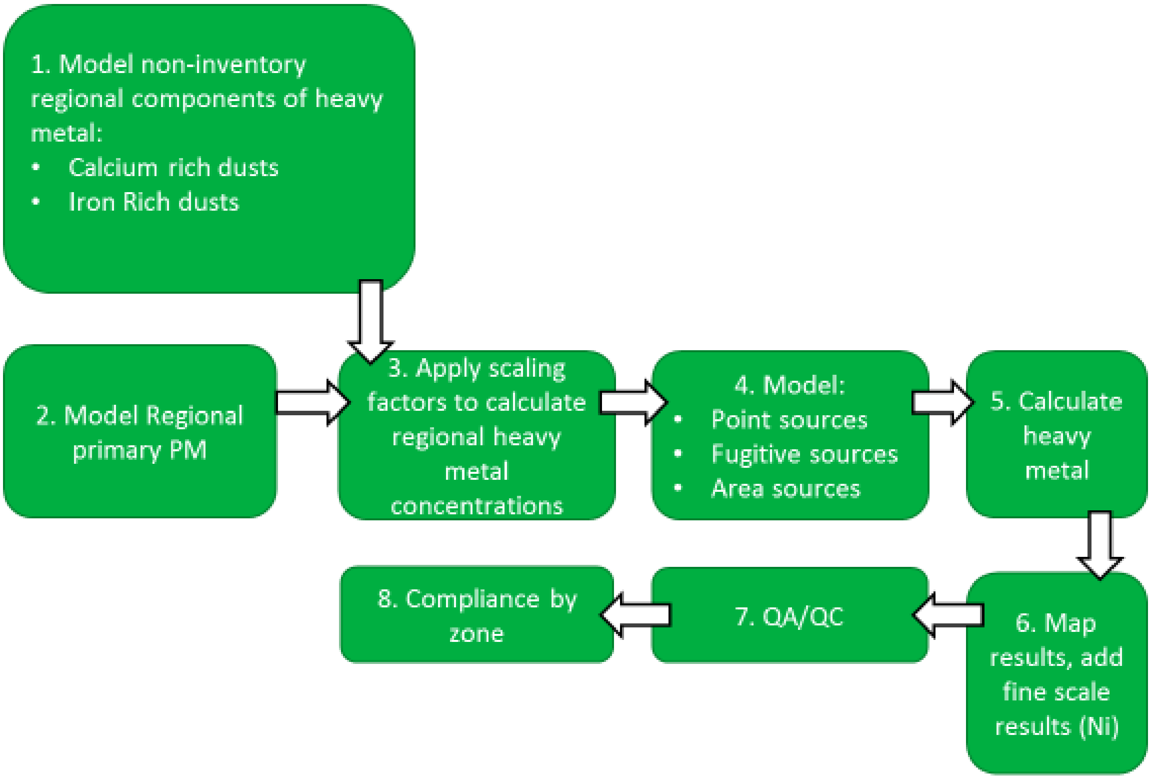

Table 10.2 – PCM model method, input and assumptions summary for As, Cd, Ni and Pb

Heading	Component	Details
General	Pollutant	As, Cd, Ni, Pb
	Year	2018
	Locations modelled	Background
	Metric	Annual mean
Input data	Emission inventory	NAEI 2017
	Energy projections	Energy Projections 2017
	Road traffic counts	2017
	Road transport activity projections	DfT (2018) traffic (re-based to 2017 NAEI), DfT (2019) car sales projections, TfL traffic (2019) and fleet (2018) projections for London
	Road transport emission factors	COPERT 5
	Measurement data	2018
	Meteorological data	Hourly data from Waddington 2018
Model components	Regional	See details under “pollutant specific” heading
	Large point sources	233 (As), 238 (Cd), 240 (Ni) and 218 (Pb) sources modelled using ADMS 5.2.
	Small point sources	PCM dispersion kernels generated using ADMS 5.2.
	Fugitive point sources	PCM dispersion kernels generated using ADMS 5.2. Fugitive emissions estimated as a proportion of reported emissions.
	ETS point sources	PCM dispersion kernels generated using ADMS 5.2.
	Large ETS point sources	106 (As), 106 (Cd), 107 (Ni) and 114 (Pb) sources modelled using ADMS 5.2.
	Area sources	PCM dispersion kernels generated using ADMS 5.2. Time varying emissions for road transport and domestic sources.
	Roadside increment	n/a
Calibration	Model calibrated?	No
	Number of background stations in calibration	n/a
	Number of traffic stations in calibration	n/a
Pollutant specific	Regional primary particles	Calculated using the TRACK receptor oriented, Lagrangian statistical model, scaled by applying heavy metal to PM_{10} emission ratio. Additional factor applied for As, Cd and Pb.
	Regional dusts from re-suspension of soils	Modelled using information on land cover (bare soil, root and cereal crops) and dispersion kernel incorporating emissions and dispersion processes. Multiplied by heavy metal concentration in soil and empirical enhancement factor.
	Dusts from re-suspension due to vehicle activity	Modelled using information on vehicle movements on major roads (HDV) and dispersion kernel incorporating emissions and dispersion processes. Multiplied by

		heavy metal concentration in soil and empirical enhancement factor.
	Fine scale modelling (Ni only)	• Contribution of emissions from an industrial source at Pontardawe modelled at 20 m spatial resolution using local meteorological measurements. Model includes building effects and terrain. • Contribution of emissions from industrial sources in Sheffield modelled at 50 m spatial resolution using local meteorological measurements and incorporating local terrain effects.

10.1.4 Outline of the annual mean models for As, Cd, Ni and Pb

The maps of background concentrations of As, Cd, Ni and Pb have been calculated by summing contributions from different sources:

- Large point source emissions
- Small point source emissions
- Fugitive point source emissions
- Point sources with emissions estimates for air quality pollutants based on reported carbon emissions (ETS points)
- Area sources related to domestic combustion
- Area sources related to road traffic
- Other area sources
- Regional primary particles
- Re-suspension from bare soils
- Re-suspension as a result of vehicle movement

These components are aggregated to a single 1 km x 1 km background grid value for each pollutant.

10.1.5 Chapter structure

This chapter describes modelling work carried out for 2018 to assess compliance with the Pb limit value and As, Cd, and Ni target values described above. Emission estimates are described in Section 10.2, Section 10.3 describes the modelling methods, and the modelling results are presented in Section 10.4 to Section 10.7. The source apportionment of ambient concentrations is discussed in each pollutant results section and is often very different from the split for total national emissions. Ambient concentrations are influenced by the location and release characteristics of the emissions and are also influenced by sources not included in the inventory, such as re-suspension.

Figure 10-2 - Annual mean background As concentration, 2018 (ng m^{-3})

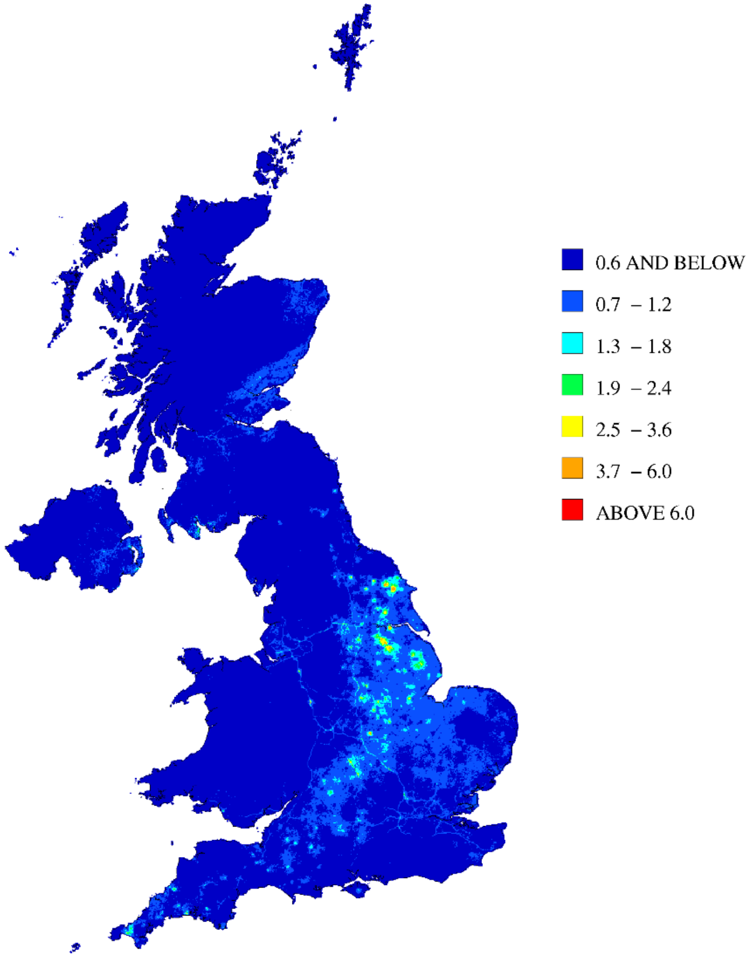

Figure 10-3 - Annual mean background Cd concentration, 2018 (ng m^{-3})

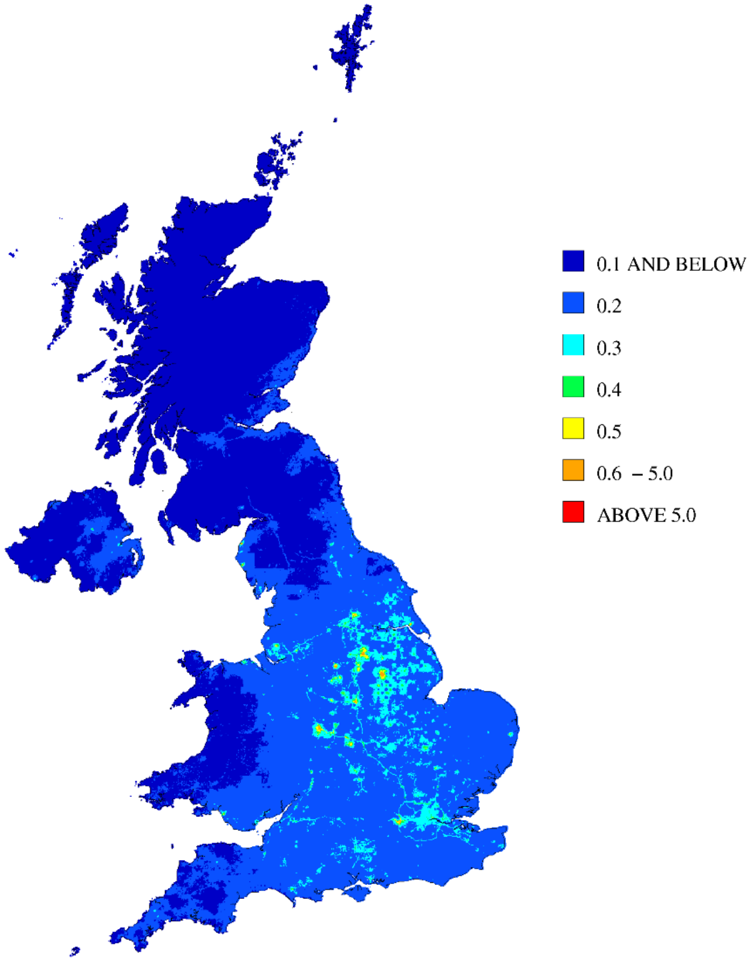

Figure 10-4 - Annual mean background Ni concentration, 2018 (ng m^{-3})

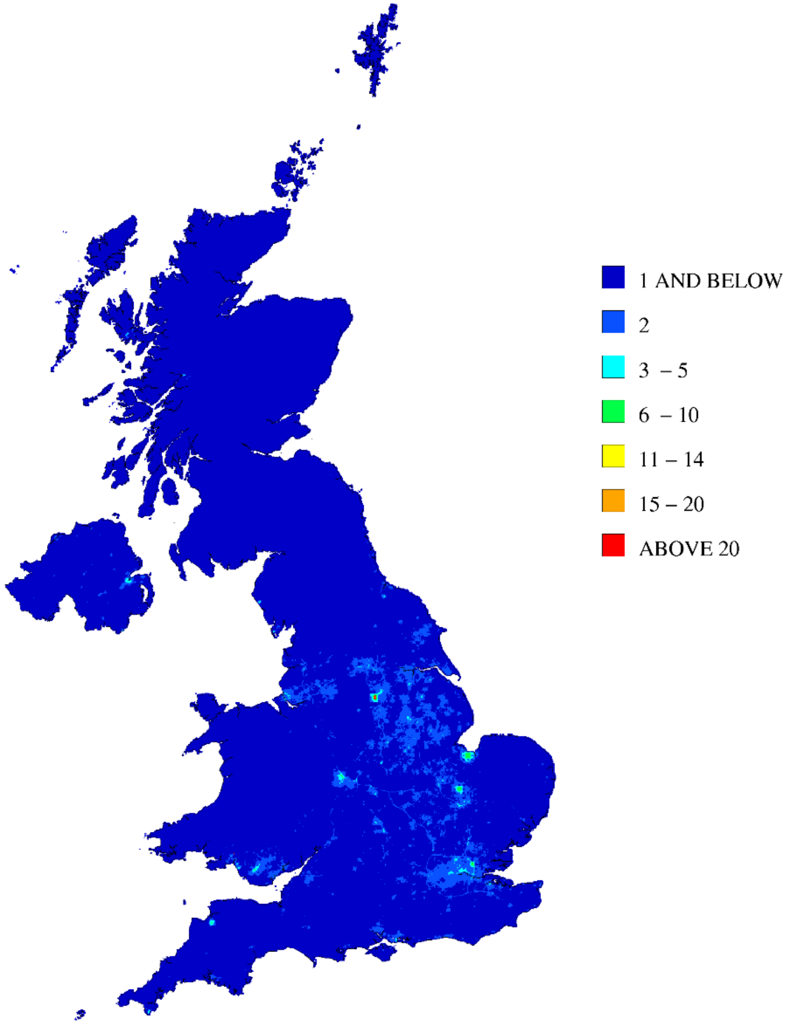

Figure 10-5 - Annual mean background Pb concentration, 2018 (µg m^{-3})

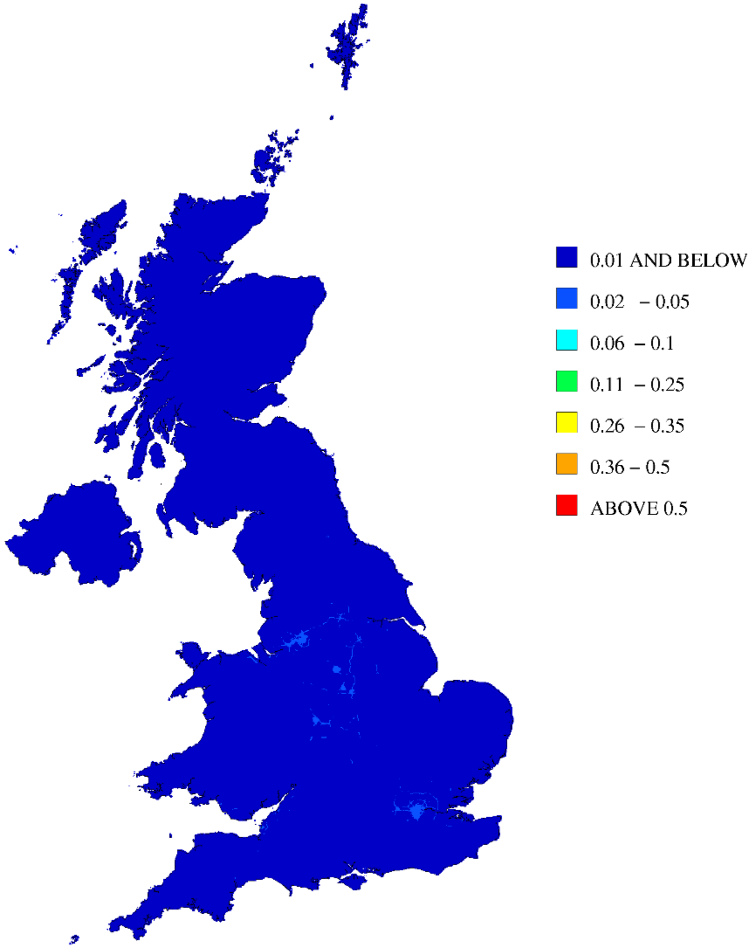

10.2 Emissions

Estimates of the emissions of Heavy Metals from the UK National Atmospheric Emissions Inventory 2017 (NAEI 2017) have been used in this study (Richmond et al., 2019). Emissions projections have been provided by the NAEI (Passant, 2019) based on BEIS EEP 2018 energy and emissions projections (BEIS, 2018). UK total emissions for 2017 and emissions projections for 2020, 2025 and 2030 split by SNAP code for As, Cd, Ni and Pb are shown in Figure 10-6, Figure 10-7, Figure 10-8 and Figure 10-9 respectively, with the coding described in Table 3.2. Values for intermediate years have been interpolated in these figures.

Figure 10-6 shows that arsenic emissions are forecast to increase between 2017 and 2020 and then remain roughly constant for the period 2020-2030. In all years, combustion in industry accounts for over 50% of the total emissions. Emissions of arsenic are primarily from the combustion of solid fuel. The majority of emissions are estimated to be from the burning of treated wood. There are no reliable estimates of the extent of this activity, and since the emission factor for this source is also very uncertain, the total emission estimate for this source is highly uncertain. The increase between 2017 and 2020 is most likely to be due to a difference between activity estimate for 2017 and the projected activity estimates for this source, which were derived from estimates for 2015. This issue should be resolved for future assessments as a result of implementation of the NAEI improvement plan for projections. Point sources are also a significant source of arsenic emissions in the UK.

Point sources and domestic combustion are the dominant source of cadmium across the time series, with road transport exhaust emissions and combustion in industry also shown as significant sources. Figure 10-7 shows total emissions of cadmium are expected to decline between 2017 and 2022 before remaining roughly constant to 2030.

Figure 10-8 shows a decline in nickel emissions from 2017 to 2030. This is driven primarily by a decrease in domestic combustion from 2017 to 2030. The figure indicates that shipping, domestic combustion and point sources are the dominant emissions sources of nickel in the UK. Nickel emissions to the atmosphere arise primarily from the combustion of liquid fuels and solid fuels derived from petroleum (petroleum coke and solid smokeless fuels).

Figure 10-9 shows that overall lead emissions are dominated by emissions from point sources, road transport brake and tyre wear, combustion in industry and solvent use (specifically Fireworks process emissions). Lead emissions remain roughly constant from 2017 to 2030.

Figure 10-6 - Total UK As emissions for 2017 and emissions projections up to 2030 by SNAP code from NAEI 2017

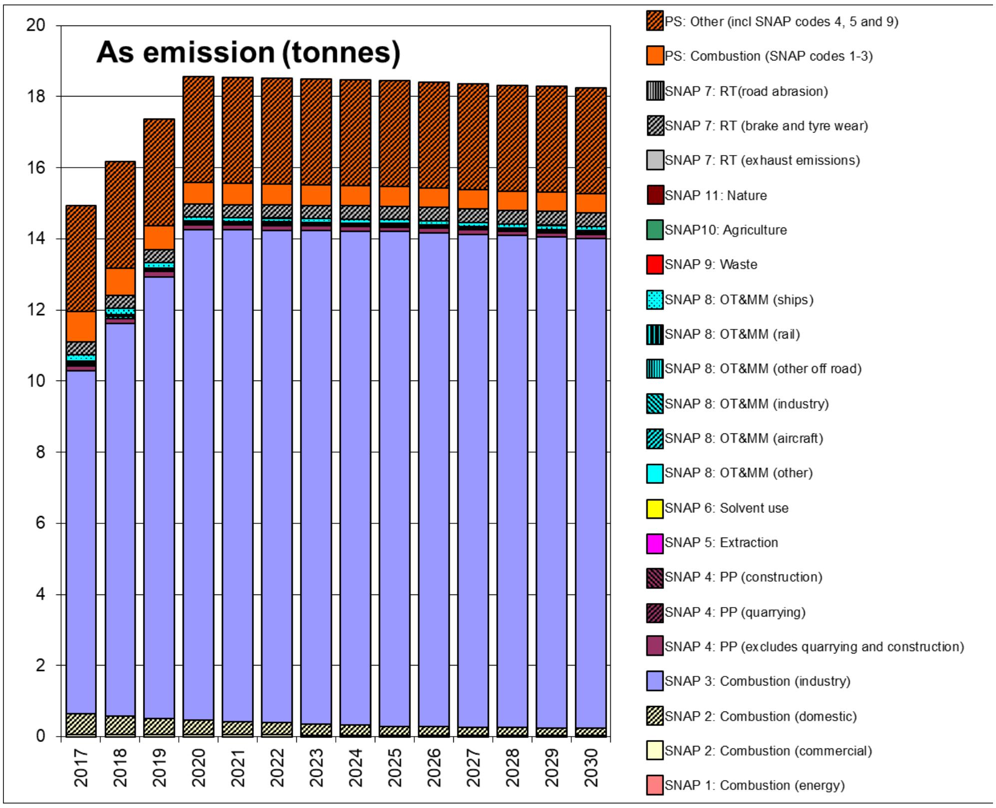

Figure 10-7 - Total UK Cd emissions for 2017 and emissions projections up to 2030 by SNAP code from NAEI 2017

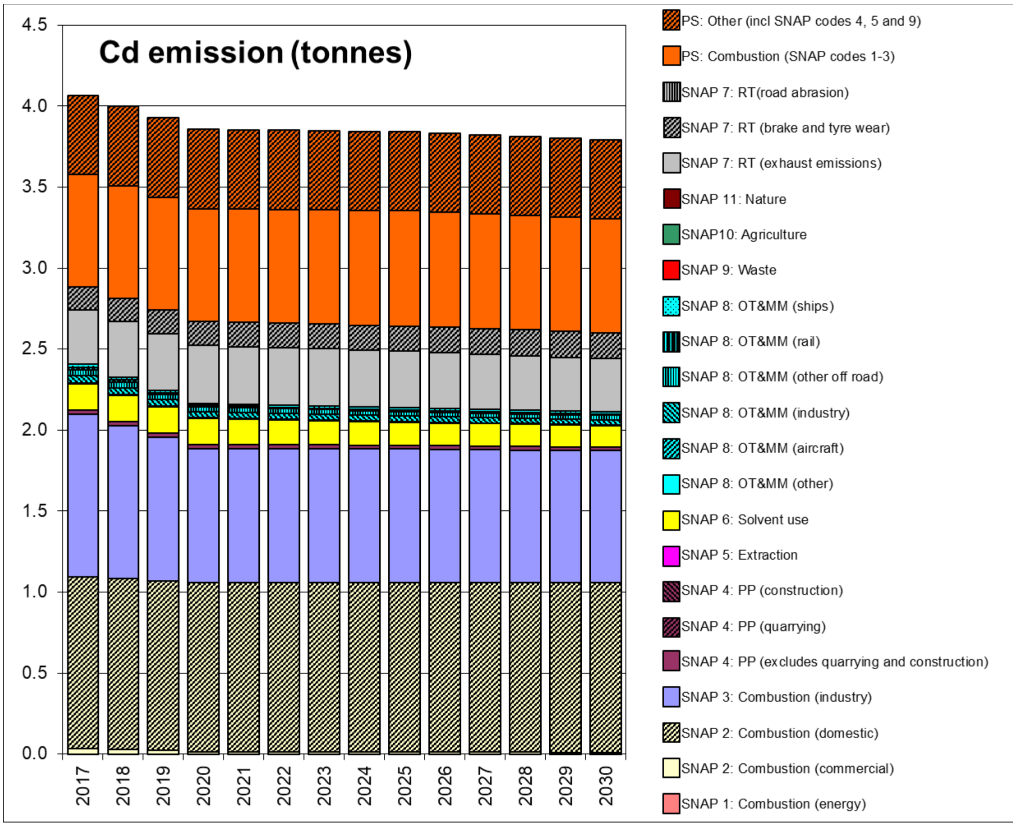

Figure 10-8 - Total UK Ni emissions for 2017 and emissions projections up to 2030 by SNAP code from NAEI 2017

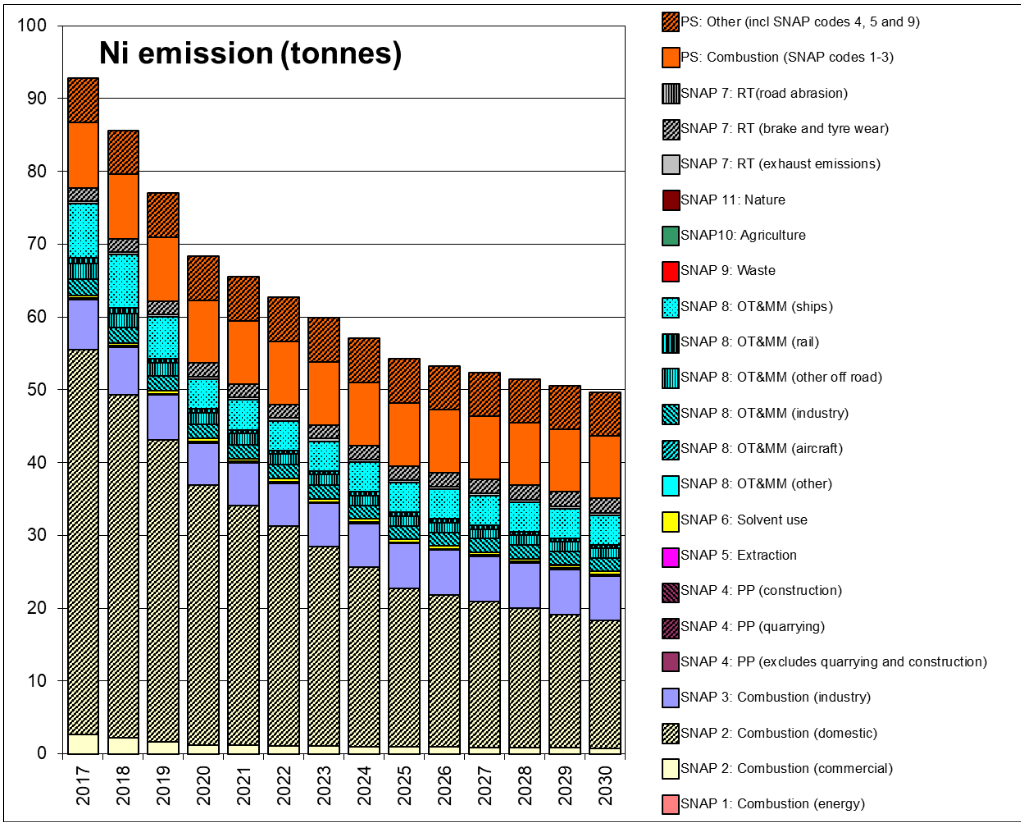

Figure 10-9 - Total UK Pb emissions for 2017 and emissions projections up to 2030 by SNAP code from NAEI 2017

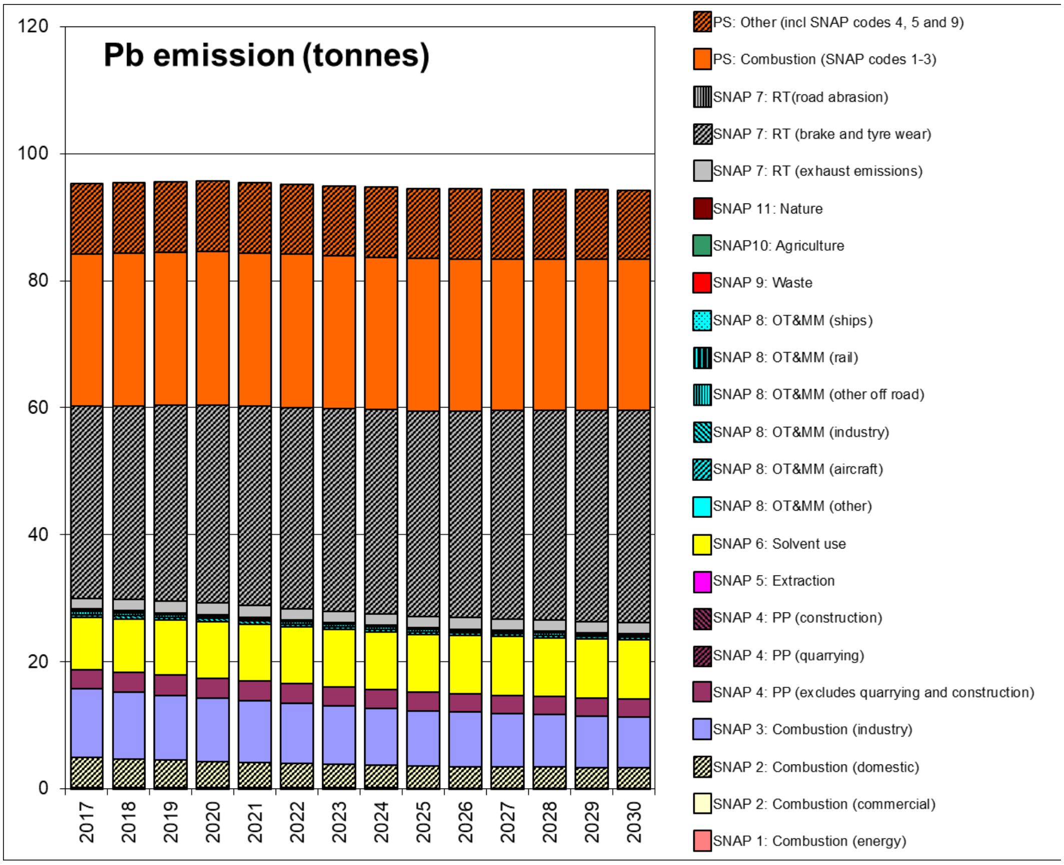

10.3 The model

10.3.1 Contribution from large point sources

Contributions to ground level annual mean heavy metal concentrations from point sources (those with annual emissions of greater than the thresholds listed by pollutant in Table 10.3, or for which emission release characteristics are known) in the NAEI 2017 were estimated by modelling each source explicitly using the atmospheric dispersion model ADMS 5.2 and sequential meteorological data for 2018 from Waddington. Surface roughness was assumed to be 0.1 m at the dispersion site and 0.1 m at the meteorological site. Concentrations were calculated for a 99 km x 99 km square composed of a regularly spaced 1 km x 1 km resolution receptor grid. Each receptor grid was centred on the point source. The total number of point sources modelled explicitly is given in Table 10.3. For each large point source information was retrieved from the PCM stack parameters database (as described in Section 3.3.1). The NAEI emissions for point sources for 2017 were scaled in order to provide values for 2018 as described in Section 3.3.1.

The Vale Clydach refinery in South Wales is located within the Pontardawe Valley a few miles from the Pontardawe Tawe Terrace monitoring station. To provide the best estimate of Ni concentrations in this area, reported 2018 emissions and updated stack parameters for this site were provided by the site operator and incorporated into the large points modelling for Ni.

A factor of 0.3 has been applied to the modelled contribution of large point sources to As concentrations, consistent with the 2013, 2014, 2015, 2016 and 2017 modelling. Factors of unity have been applied to the modelled contribution from large point sources to concentrations of Ni, Pb and Cd. Factors were chosen to provide the best agreement of total model predictions with measured heavy metal concentrations. Activity levels for combustion of coal in industry were about 50% higher in the 2012 NAEI than in the 2011 NAEI and have remained at this higher level in subsequent inventories. There has been no clear trend or change in ambient As concentrations measured in the UK over this period. A factor of less than unity was therefore required for industrial emissions of As.

The NAEI 2017 includes point source emissions estimates derived from carbon emissions data reported under the EU-Emissions Trading Scheme (ETS), most recently described in Tsagatakis et al. (2019). These point sources are referred to as ETS points in this report. These derived air quality pollutant emissions are particularly uncertain and therefore in previous assessments (e.g. Brookes et al., 2017) emissions were capped at reporting thresholds and treated as small point sources. For the 2016 and 2017 assessments (Brookes et al., 2019a, 2019b) the NAEI recommended treating the ETS points that have emissions greater than the large points modelling threshold as large points and not to apply a cap (Passant pers. comm. 2017). The 2018 assessment continues this approach. Thus, those ETS point sources of As, Cd, Ni and Pb meeting the criteria for the treatment of large point sources described above, were modelled as an additional set of large point sources (using the approach described above). The total number of ETS point sources modelled explicitly is given in Table 10.3. ETS points that were not classified as large point sources were modelled using the small and fugitive points approach described next.

10.3.2 Contributions from small point and fugitive sources

The contributions to ambient concentrations from fugitive and small point sources (those without stack parameters datasets and annual emissions less than or equal to values displayed in Table 10.3) in the NAEI 2017 were modelled using a small points model. The NAEI 2017 emissions for fugitive and small point sources have been scaled to 2018 using the same source sector specific projection factors applied to the large point sources.

The models consist of separate ‘in-square’ and ‘out-of-square’ components, in which concentrations are estimated using a point source dispersion kernel. The dispersion kernel for small points has been calculated by using the dispersion model ADMS 5.2 to model the dispersion of unit emissions from a central source to a grid of receptors at a spatial resolution of 1 km x 1 km squares with the stack characteristics as presented in Table 10.4. Hourly sequential meteorological data from Waddington in 2018 has been used to construct the dispersion kernels. The greatest concentration would be expected close to the point of emission. The receptor for the central grid square within the dispersion kernel is, however, at exactly the same location as the point of release. The concentration at this location is therefore zero. The value for the central grid square within the dispersion kernel has therefore been assigned to be equal to the highest of the values for the adjacent grid squares.

A factor of 0.3 has been applied to the modelled contribution of small point sources to As concentrations, consistent with the 2013, 2014, 2015, 2016 and 2017 modelling and the treatment of large point sources. Factors of unity have been applied to the modelled contribution from small point sources to concentrations of Ni, Pb and Cd. Factors were chosen to provide the best agreement of total model predictions with measured heavy metal concentrations.

Table 10.3 - Thresholds to determine modelling method, and number of large point sources for 2018.

Pollutant	Tonnes per year	Number of large point sources	Number of large ETS point sources
As	0.025	233	108
Cd	0.025	238	106
Ni	0.05	240	107
Pb	1.2	218	114

Table 10.4 - Stack release parameters used to characterise emissions from point sources with no available stack parameters

Variable	Parameters
Stack height	15 m
Diameter	1m
Temperature	15˚C
Emission rate as PM_{10}	1g/s
Surface roughness at dispersion site	0.5 m
Surface roughness at met site	0.02 m

Characterising the amount of fugitive heavy metal emission from industrial plant is notoriously difficult. For the modelling of Cd, Ni and Pb concentrations, assuming a fugitive emission of 0.05 times the reported emission was found to provide the best agreement with the available measurements. For the modelling of As, a fugitive emission 0.015 times the reported emission was assumed.

The emission release parameters for fugitive sources are provided in Table 10.5. Once again, the value for the central grid square within the dispersion kernel has been set to the maximum of the values in the surrounding grid squares.

Table 10.5 - Stack release parameters used to characterise fugitive emission release

Variable	Parameters
Stack height	10m
Diameter	1m
Temperature	15˚C
Emission rate as PM_{10}	1g/s
Surface roughness at dispersion site	0.5 m
Surface roughness at met site	0.02 m

10.3.3 Contributions from local area sources

The 2018 area source emissions maps for heavy metals have been calculated from the NAEI 2017 emissions maps following the method described in Section 3.3.5. ADMS derived dispersion kernels have been used to calculate the contribution to ambient concentrations on a 1 km x 1 km receptor grid, from the area source emissions within a 33 km x 33 km square surrounding each receptor. Hourly sequential meteorological data from Waddington in 2018 has been used to construct the dispersion kernels, as described in Appendix 4. Revised methods introduced in the 2011 assessment (Brookes et al., 2012) for modelling the contributions to As, Cd, Ni and Pb from SNAP 2 (domestic and non-domestic combustion) and SNAP 3 (combustion in industry) area sources were used and have been described in Section 3.3.5.

A factor of 0.3 has been applied to the modelled contribution of industrial area sources to As concentrations. A factor of 0.7 has been applied to the modelled contribution of domestic area sources to Ni concentrations. Factors of unity have been applied to the modelled contribution from area sources to concentrations of Pb and Cd, and to other area source types for As and Ni modelling. Factors were chosen to provide the best agreement of total model predictions with measured heavy metal concentrations.

For certain sectors (noted within each pollutant results section below) caps have been applied to emissions based on expert judgement of the model results to address known artefacts in the area source emissions grids and to reconcile the model results with the measured data at each monitoring site.

10.3.4 Contribution from long range transport of primary particulate matter

The contribution to ambient concentrations from long range transport of heavy metals was derived from estimates of regional primary particulate matter used in the 2018 PCM model for PM_{10} mass (Section 5.3.4). The contribution of long-range transport sources to ambient heavy metal concentrations was derived by calculating a fraction of the PM mass for each heavy metal. This fraction was estimated as the ratio of the UK total emissions for each metal for each SNAP sector to the total PM_{10} emission for that sector. The following scaling factors for long range transport of primary particulate matter were then applied: 2.0 for As, 2.0 for Cd, 0.7 for Ni and 5.0 for Pb. These factors chosen to provide the best agreement of total model predictions with measured heavy metal concentrations.

10.3.5 Heavy metal contribution from re-suspension

The 2018 model for heavy metal concentrations includes a contribution to ambient concentrations from re-suspension calculated in the same way as in the 2011 models (Brookes et al., 2012). The contributions from two processes have been included:

- Regional PM dusts from re-suspension of soils and
- PM dusts from re-suspension due to vehicle activity.

The heavy metal contribution from re-suspension has been calculated by using the methods suggested by Abbott (2008). The methods used to estimate the total PM mass from these processes are detailed in Section 5.3.5.

Abbott (2008) also suggested a method for estimating the contributions to the ambient concentrations of heavy metals from soil and vehicle related re-suspension processes. The maps of PM mass from re-suspension of soils and re-suspension associated with vehicle movements can be used to estimate the contributions to the ambient concentration of heavy metals using a combination of information on the heavy metal content of soils and enhancement factors.

The National Soil Inventory (http://www.landis.org.uk/data/natmap.cfm) provides a data set of As, Cd, Ni and Pb concentrations in topsoil at 5 km resolution throughout England and Wales. Measurement data on heavy metals concentration in topsoil for other areas of the UK is available from the Geochemical Atlas of Europe developed under the auspices of the Forum of European Geological Surveys (FOREGS) (http://weppi.gtk.fi/publ/foregsatlas/). These data were interpolated onto a 1 km x 1 km grid. The predicted annual PM emission rates and the contribution to atmospheric concentrations were multiplied by the topsoil concentrations to estimate the annual metal re-suspension rates and the contributions to atmospheric concentrations of the heavy metals.

There is some evidence that metal concentrations in the surface soils are higher than in the underlying topsoil. EMEP have suggested that there may be some enhancement of the metal content of the re-suspended dust because the metals may form complexes with humic matter (Abbott, 2008). Abbott (2008) carried out regression analyses of measured heavy metal concentrations against the combined model predictions for sites in the UK Rural Heavy Metal Network. This analysis suggested that there may be other mechanisms by which heavy metals are concentrated in the small particle fraction of soils. For example, much of the metal content may be present as the result of historical deposition of small particles or the application of sewage sludge and farmyard slurries. These materials may only be loosely bonded to the surface of the soil particles. The fine particles released by re-suspension mechanisms would therefore be likely to contain a much higher concentration of metals than the underlying topsoil. The enhancement factors listed in Table 10.6 have been chosen to provide the best agreement of total model predictions with measured heavy metal concentrations. The factors are broadly consistent with the regression coefficients determined by Abbott (2008).

Caps have been applied for the contribution generated from re-suspension of soil for some of the heavy metals. The values have been chosen as an estimate of the maximum likely concentration generated from this source and are also listed in Table 10.6.

Table 10.6 - Heavy metal enhancement factors used in the assessment

Pollutant	Enhancement factor	Maximum concentration (ng m^{-3})
As	25	3.5
Cd	25	3.5
Ni	5	7
Pb	25	5

10.4 Arsenic Results

10.4.1 Introduction

The map of modelled annual mean As concentrations is shown in Figure 10-2. There were no modelled or measured exceedances of the target value of 6 ng m^{-3} in 2018.

10.4.2 Verification of mapped concentrations

A comparison between modelled and measured annual mean As concentrations in 2018 at monitoring site locations is shown in Figure 10-10. This figure includes lines to represent the AQDD4 data quality objective for modelled annual mean As concentrations: y=x-60% and y=x+60% (see Section 1.5).

Summary statistics for modelled and measured As concentrations are listed in Table 10.7, including the percentage of sites at which modelled concentrations are outside of the data quality objectives (DQOs), and the total number of sites included in the analysis.

The means of measured and modelled concentrations are in reasonable agreement for all site types, with most sites falling within the DQOs. However, the agreement between measured and modelled concentrations on a site-by-site basis (quantified using R^2) is poor for industrial and urban background monitoring sites but is reasonably good at rural monitoring locations.

It should be noted that non-emission inventory sources (such as fugitive, re-suspension and long-range transport of primary PM) result in additional uncertainty when compared with a pollutant such as NO_X, for which the source apportionment is better known.

Figure 10-10. Verification of annual mean As across all sites.

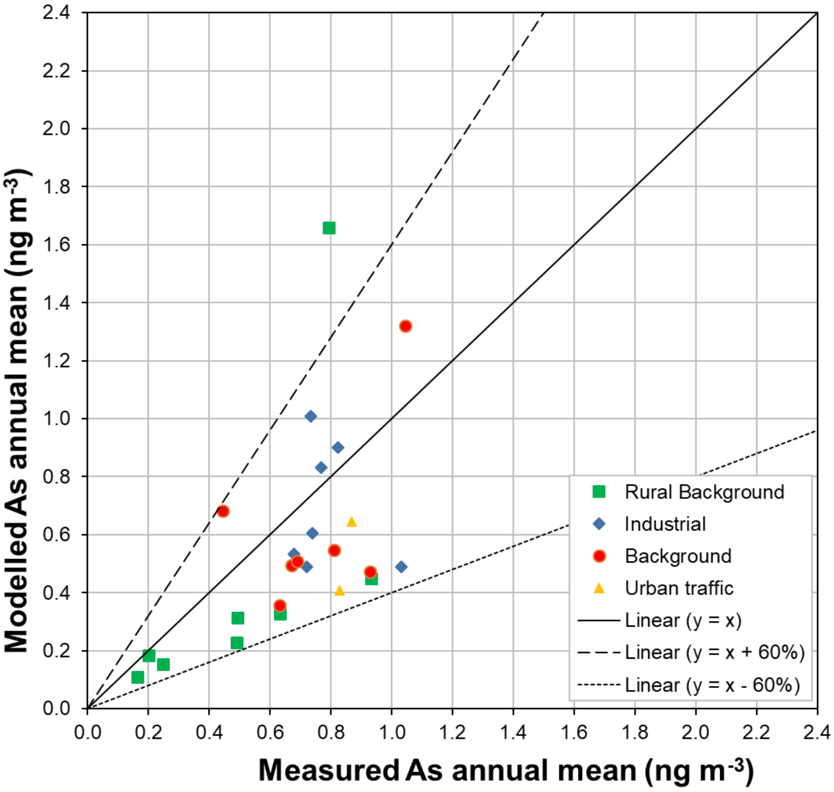

Table 10.7 - Summary statistics for comparison between modelled and measured annual mean As concentrations at different monitoring sites, 2018.

	Mean of measurements (ng/m^3)	Mean of model estimates (ng/m^3)	R^2	% of sites outside DQO of ±60%	Number of sites in assessment
Industrial sites	0.79	0.69	0.03	0%	7
Urban background sites	0.75	0.63	0.28	0%	7
Roadside sites	0.85	0.53	1.00	0%	2
Rural sites	0.50	0.43	0.37	13%	8
All	0.68	0.57	0.31	4%	**24**

10.4.3 Source apportionment

Figure 10-11 shows the modelled As contribution from different sources at monitoring site locations. Measured concentrations at the sites are also presented, giving an indication of the level of agreement between modelled and measured concentrations. This analysis suggests that the main sources of arsenic are long range transport primary, resuspension and industry.

Figure 10-11 - Annual mean As source apportionment at monitoring sites in 2018.

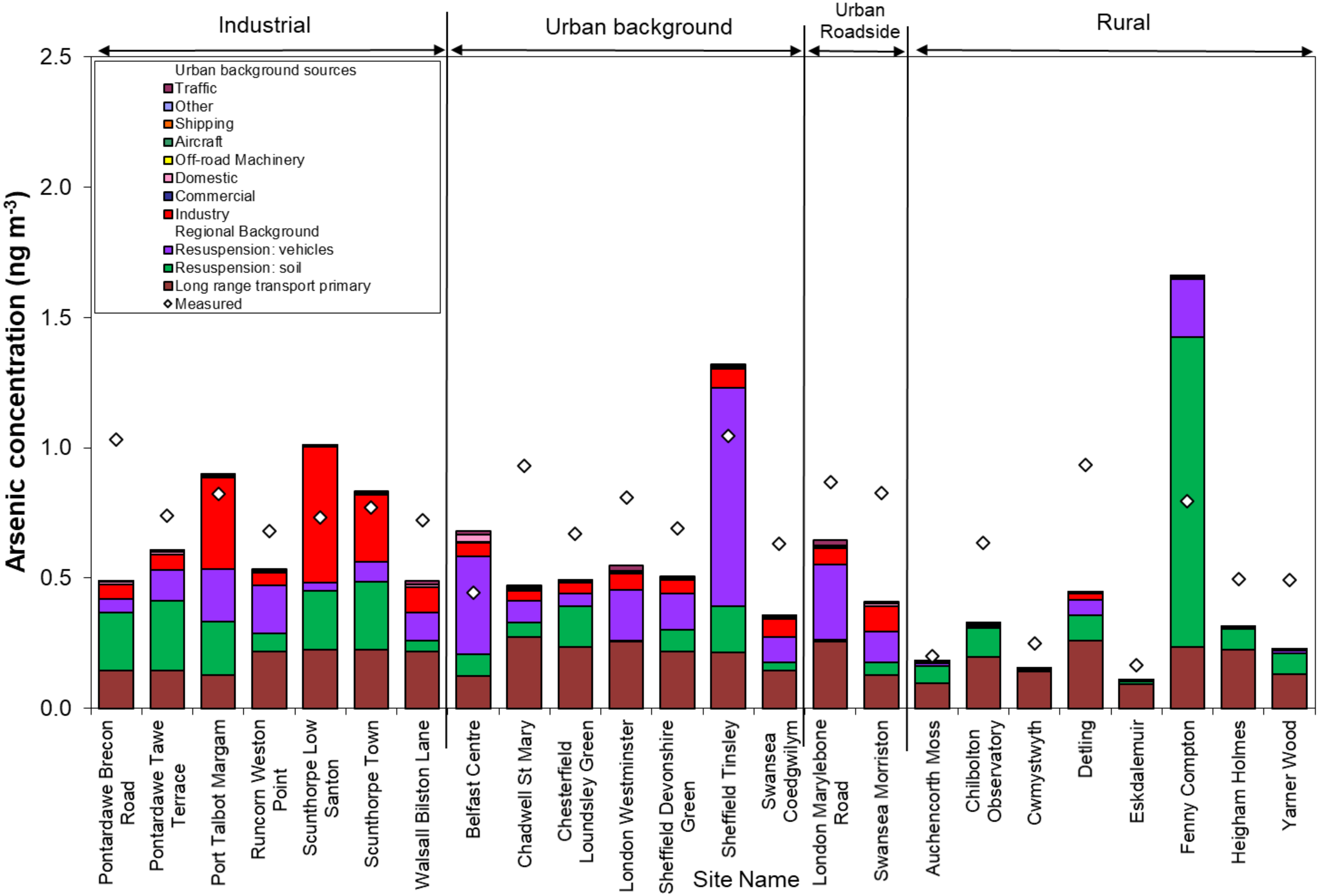

10.5 Cadmium Results

10.5.1 Introduction

The map of modelled annual mean Cd concentrations is shown in Figure 10-3. There were no modelled or measured exceedances of the target value of 5 ng m^{-3} in 2018.

10.5.2 Verification of mapped concentrations

A comparison between modelled and measured annual mean Cd concentrations in 2018 at monitoring site locations is shown in Figure 10-12. This figure includes lines to represent the AQDD4 data quality objective for modelled annual mean Cd concentrations: y=x-60% and y=x+60% (see Section 1.5).

Summary statistics for modelled and measured Cd concentrations are listed in Table 10.8, including the percentage of sites at which modelled concentrations are outside of the DQOs and the total number of sites included in the analysis.

The agreement between measured and modelled concentrations on a site-by-site basis (quantified using R^2) is good for rural monitoring locations, but poor for industrial and urban background monitoring locations.

It should be noted that non-emission inventory sources (such as fugitive, re-suspension and long-range transport of primary PM) result in additional uncertainty when compared with a pollutant such as NO_X, for which the source apportionment is better known.

Figure 10-12. Verification of annual mean Cd across all sites.

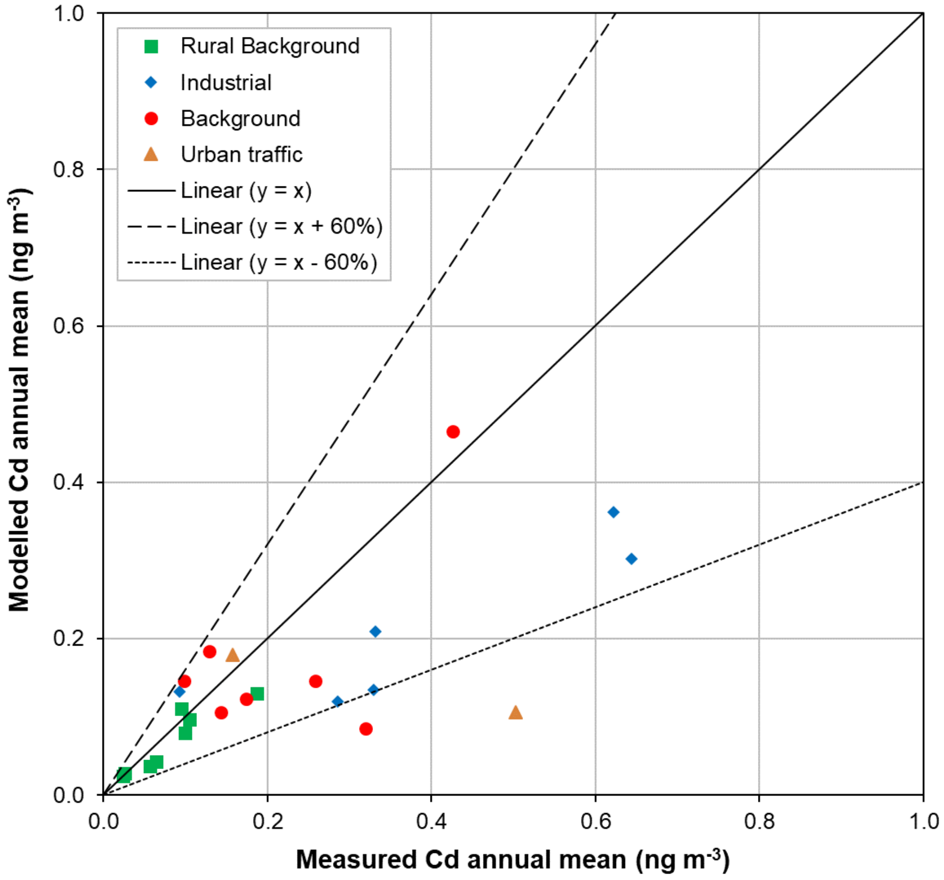

Table 10.8 - Summary statistics for comparison between modelled and measured annual mean Cd concentrations at different monitoring sites, 2018.

	Mean of measurements (ng/m^3)	Mean of model estimates (ng/m^3)	R^2	% of sites outside DQO of ±60%	Number of sites in assessment
Industrial sites	0.50	0.21	0.22	14%	7
Urban background sites	0.22	0.18	0.42	14%	7
Roadside sites	0.33	0.14	1.00	50%	2
Rural sites	0.08	0.07	0.85	0%	8
All	**0.26**	**0.15**	**0.32**	**13%**	**24**

10.5.3 Source apportionment

Figure 10-13 shows the modelled Cd contribution from different sources at monitoring site locations. Measured concentrations at the sites are also presented, giving an indication of the level of agreement between modelled and measured concentrations. This analysis suggests that at those sites where the highest concentrations are measured, the main sources of cadmium are industry, resuspension, and long-range transport primary. Industrial sites have large quantities of emissions assigned to industry.

Figure 10-13 - Annual mean Cd source apportionment at monitoring sites in 2018.

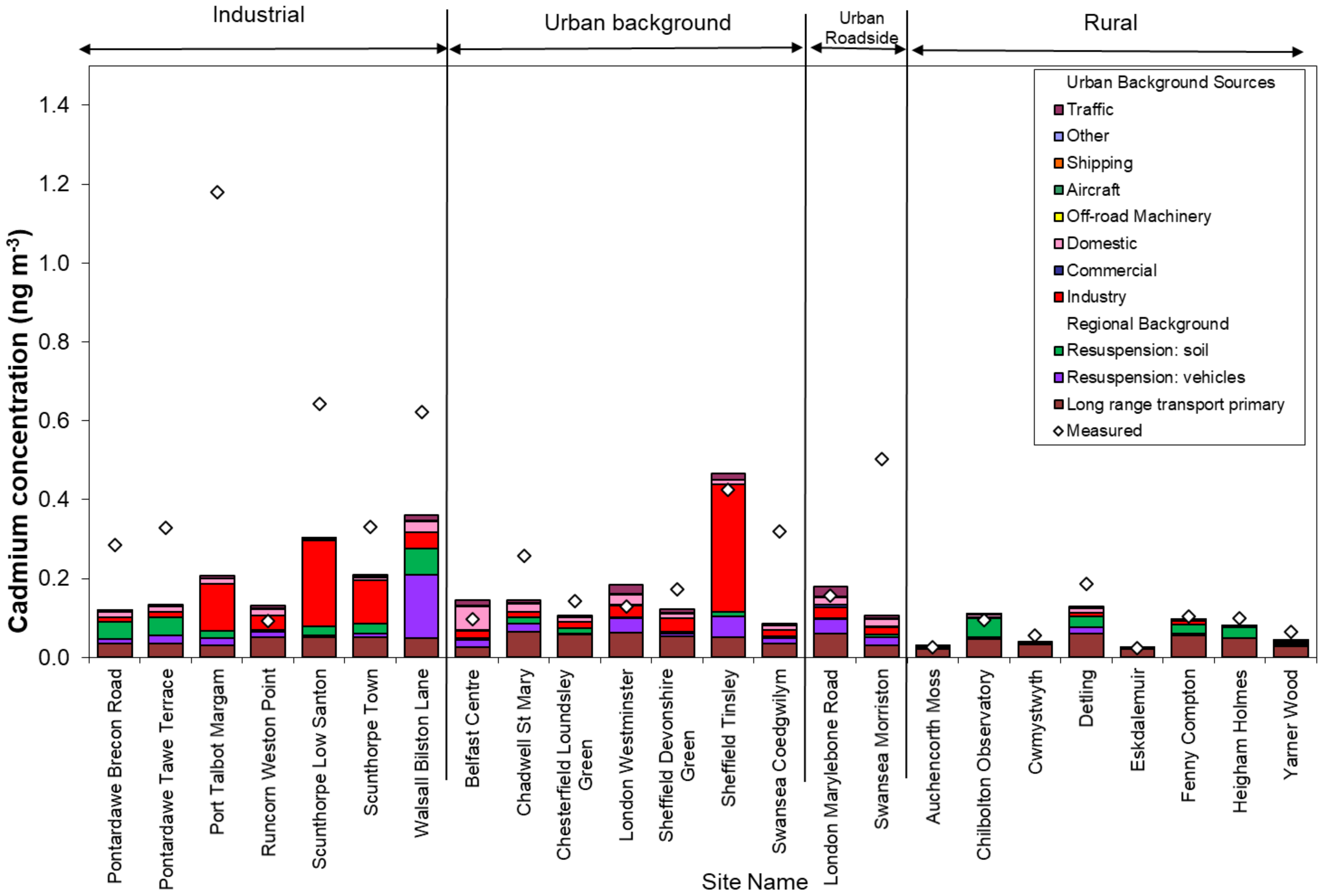

10.6 Nickel Results

10.6.1 Introduction

The method used to estimate ambient Ni concentrations across the UK is described in Section 10.3 above.

A cap of 10 t/a/km^2 also applied to shipping emissions.

The map of modelled annual mean Ni concentrations is shown in Figure 10-4. Historically there have been issues with compliance for nickel and this was the case in 2018. Detailed local modelling carried out to characterise the impact of emissions on ambient concentrations at locations associated with exceedances is discussed in Section 10.6.4.

10.6.2 Verification of mapped concentrations

A comparison between modelled and measured annual mean Ni concentrations in 2018 at monitoring site locations is shown in Figure 10-14 ((a) at full scale showing all sites, and (b) on an expanded scale to better show performance at lower concentrations). This figure includes lines to represent the AQDD4 data quality objective for modelled annual mean Ni concentrations: y=x-60% and y=x+60% (see Section 1.5).

The results for several monitoring site locations included in Figure 10-14 (Pontardawe Tawe Terrace, Sheffield Tinsley and Sheffield Devonshire Green) are covered by more detailed local modelling assessments (see Section 10.6.4). A modelled Ni concentration of 57 ng m^{-3} has been reported for the 2018 compliance assessment for the 1 km grid square containing the Pontardawe Tawe Terrace monitoring site, equal to the measured value for this monitoring site. For model verification the modelled value including the local detailed modelling was also 57 ng m^{-3} hence the modelled and measured values in Figure 10-14 for Pontardawe Tawe Terrace are equal. Modelled Ni concentrations of 23 ng m^{-3} and 2.2 ng m^{-3} have been reported for the 2018 compliance assessment for the 1 km grid squares containing the Sheffield Tinsley and Sheffield Devonshire Green monitoring sites respectively taking into account the average (median) of the detailed modelling results per 1 km grid square. For model verification the measured Ni concentrations at Sheffield Tinsley and Sheffield Devonshire Green are 20.1 ng m^{-3} and 2.2 ng m^{-3} respectively, while the modelled values for the 50 m grid squares containing the Sheffield monitoring sites from the local detailed modelling are 20.1 ng m^{-3} and 2 ng m^{-3} respectively. Hence the modelled and measured values in Figure 10-14 for Sheffield Tinsley are equal, while there is a small difference for Sheffield Devonshire Green.

Summary statistics for modelled and measured Ni concentrations are listed in Table 10.9, including the percentage of sites for which the modelled values are outside of the DQOs as well as the total number of sites included in the analysis.

The agreement between measured and modelled concentrations on a site-by-site basis are good for all monitoring sites as quantified using R^2, and poorer in terms of comparison of the measured and modelled mean concentrations where there is a tendency for the model to overestimate at lower measured concentrations. The results for the Pontardawe Tawe Terrace, Sheffield Tinsley and Sheffield Devonshire Green sites are discussed in Section 10.6.4.

It should be noted that non-emission inventory sources (such as fugitive, re-suspension and long-range transport of primary PM) result in additional uncertainty when compared with a pollutant such as NO_X, whose source apportionment is better known.

Figure 10-14. Verification of annual mean Ni across all sites.

(a) Full scale showing all sites

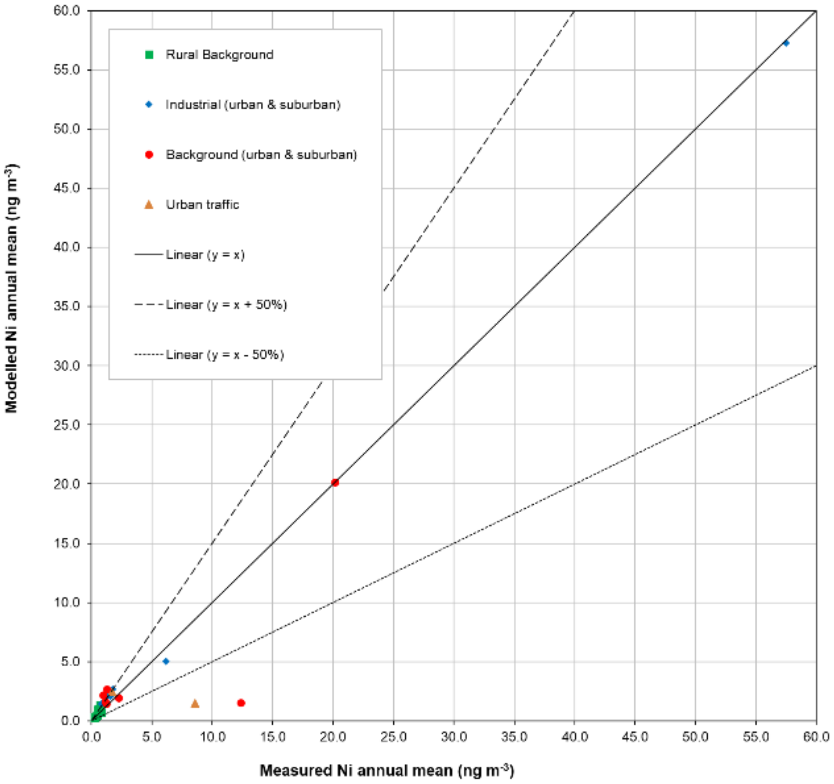

(b) Expanded scale, Tawe Terrace and Sheffield Tinsley results off scale

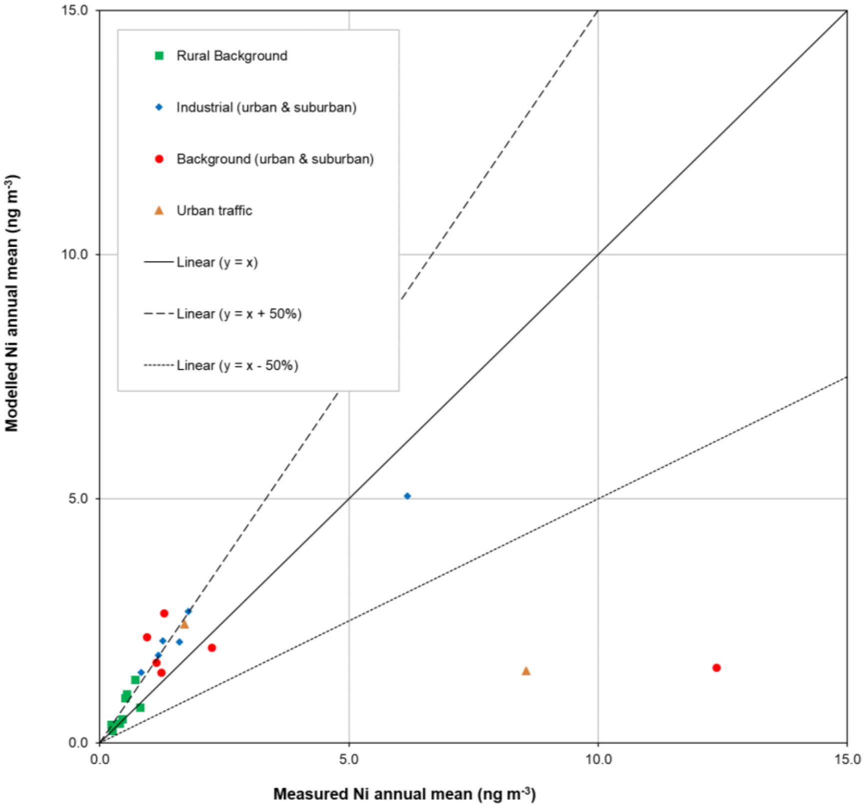

Table 10.9 - Summary statistics for comparison between modelled and measured annual mean Ni concentrations at different monitoring sites, 2018.

	Mean of measurements (ng/m^3)	Mean of model estimates (ng/m^3)	R^2	% of sites outside DQO of ±60%	Number of sites in assessment
Industrial sites	10.05	10.34	1.00	29%	7
Urban background sites	5.62	4.51	0.68	57%	7
Roadside sites	5.13	1.96	1.00	50%	2
Rural sites	0.49	0.68	0.57	50%	8
All	4.88	0.51	0.54	46%	24

10.6.3 Source apportionment

Figure 10-15 shows the modelled Ni contribution from different sources at monitoring site locations. Measured concentrations at the sites are also presented, giving an indication of the level of agreement between modelled and measured concentrations. This analysis suggests that the main sources of nickel are resuspension, long range transport primary, industry and domestic. Emissions from local industrial point sources are important for Pontardawe Brecon Road, Pontardawe Tawe Terrace and Sheffield Tinsley, and this is discussed in detail in Section 10.6.4.

Figure 10-15 - Annual mean Ni source apportionment at monitoring sites in 2018

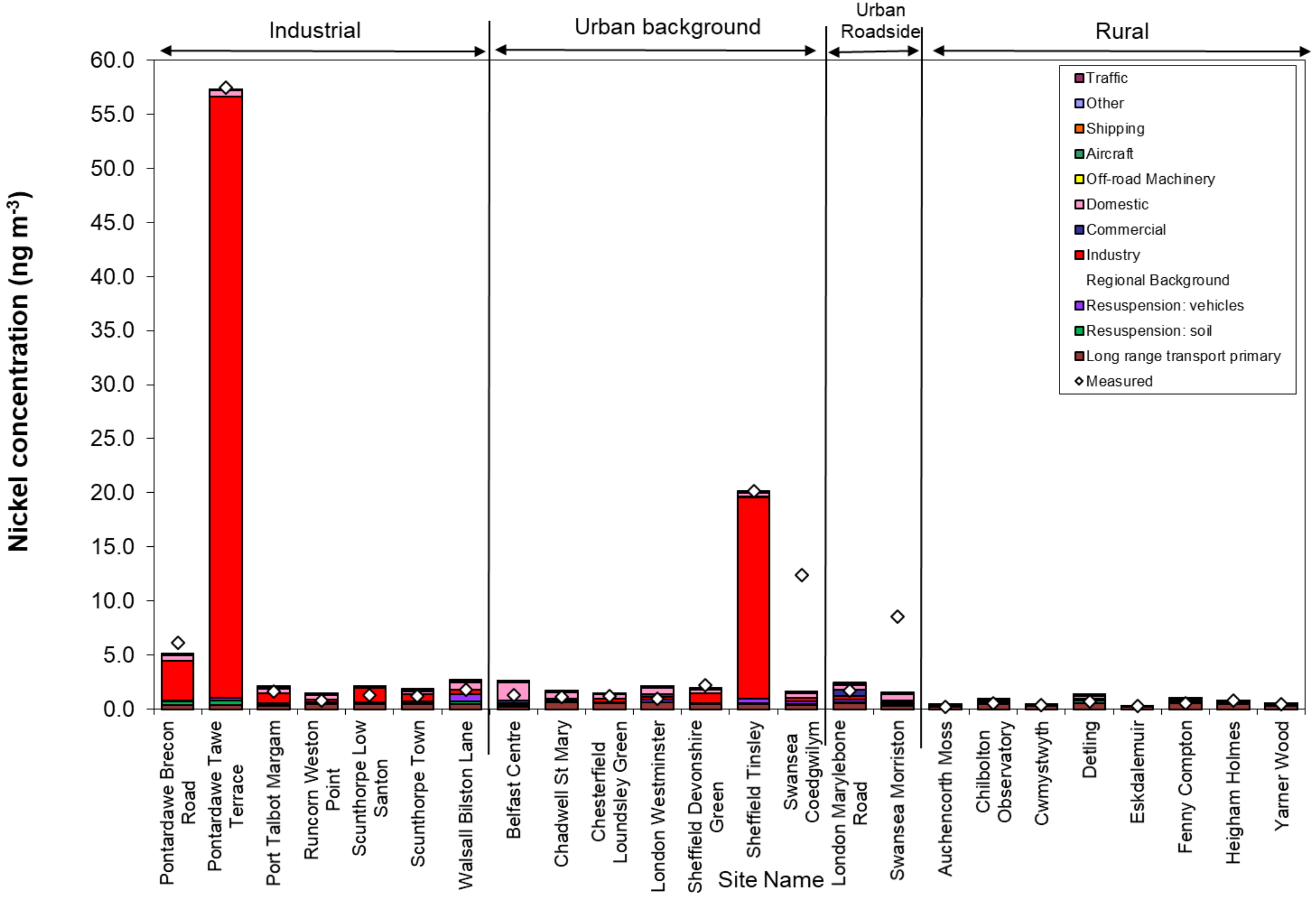

10.6.4 Detailed comparison of modelled results with the target value

10.6.4.1 Introduction

There were exceedances in four zones in 2018, one measured (Swansea Urban Area) and three modelled (Sheffield Urban Area, South Wales and Yorkshire and Humberside). Results of the assessment in terms of comparisons of the modelled concentrations with the TV have been reported in e-Reporting Data flow G (CDR, 2019). Exceedance of the Ni TV in Swansea Urban Area, South Wales and Sheffield Urban Area zones have been reported in previous years. This is the first year that Yorkshire and Humberside has been reported as an exceedance. Local monitoring and detailed modelling in the vicinity exceedances are carried out annually and inform the maximum concentration and, where applicable, area of exceedance reported in e-reporting for each zone.

Maximum concentrations of Ni for the Swansea Urban Area and South Wales zones were reported based upon the annual mean Ni concentration of 57 ng m^{-3} measured at Pontardawe Tawe Terrace. This monitoring site is within the Swansea Urban Area zone but is very near to the boundary of the South Wales zone. Detailed modelling of the principal source of local nickel emissions for the exceedance in these two zones is described below in Section 10.6.4.2.

Maximum concentrations of Ni for the Sheffield Urban Area and Yorkshire and Humberside zones were reported based upon consideration of the maximum of measured concentrations within these zones, concentrations from the national modelling and detailed local modelling of the contributions of significant industrial sources within Sheffield. A maximum concentration of 52 ng m^{-3} was reported for the Sheffield zone based on the maximum of the average (median) of exceeding 50 m grid squares from the detailed local modelling for Sheffield per 1 km grid square in the zone. Similarly, a maximum concentration of 27 ng m^{-3} was reported for the Yorkshire and Humberside zone also based on the detailed local modelling for Sheffield. Detailed modelling of the principal sources of nickel emissions for the exceedances in these zones is described below in Section 10.6.4.3.

10.6.4.2 Swansea Urban Area and South Wales Zones

Detailed dispersion modelling has been undertaken using ADMS 5.2 for the area in South Wales where exceedances of the annual mean TV of 20 ng m^{-3} have been measured in 2018. This fine-scale modelling has been used to assess the likely magnitude and spatial extent of exceedance.

Information on the Ni emissions from the principal Ni point source were provided by the site operator. Four measurements of the annual Ni emissions rate were reported by the site operator at different times of the year account for different situations at the site. These were 102.73, 53.71, 216.11 and 39.51 kg $year^{-1}$. The modelling was performed for each of these situations assuming that each was the emission for a full year to calculate the Ni contributing at the monitoring sites. A time-weighted mean was calculated using the results from the model runs based on operational information provided by the site operator and to provide the best fit to the monitoring data at Pontardawe Tawe Terrace.

Emissions were released from thirteen emission points distributed across the site. Building effects were included in the model, and a 6 km x 6 km area was extracted from the OS Terrain 50 dataset to allow the effect of the topographical features of the valley to be included in the model. The height of the terrain was specified at the centre of each 50 m x 50 m grid square.

Table 10.10 compares measured annual mean Ni concentrations with modelled concentrations. The modelled concentrations include a component resulting from the local industrial point source in Pontardawe and a background component from the annual modelling Ni concentrations across the UK. The model reproduces the measured concentration at Pontardawe Leisure Centre and Pontardawe Brecon Road well. Agreement is also good at Pontardawe Tawe Terrace, for which the measured concentration was used to inform the time weighting of emissions estimates and thus good agreement is to be expected.

Figure 10-16 shows the modelled annual mean Ni concentration on a 20 m x 20 m grid resulting from the local industrial point source in Pontardawe and including a background component from the annual modelling of Ni concentrations across the UK. The Ni concentrations in Pontardawe were strongly influenced by the terrain in the area, as can be seen in Figure 10-16. The Swansea Valley runs south-west to north-east through the village of Pontardawe, where the point source is located. The distribution of the Ni concentrations in the vicinity of Pontardawe shows the channelling of the local wind flow by the Swansea Valley.

The conclusions from this dispersion modelling study are that Ni concentrations in both the South Wales and Swansea Urban Area zones in 2018 exceeded the Ni TV.

The source apportionment plot (Figure 10-15) and scatter plot (Figure 10-14) presented earlier in this section include the modelled contribution to ambient concentrations at the Pontardawe Tawe Terrace and Pontardawe Brecon Road sites from the local industrial point source.

Figure 10-16 - Modelled annual mean Ni concentration resulting from the local industrial point source in Pontardawe in 2018.

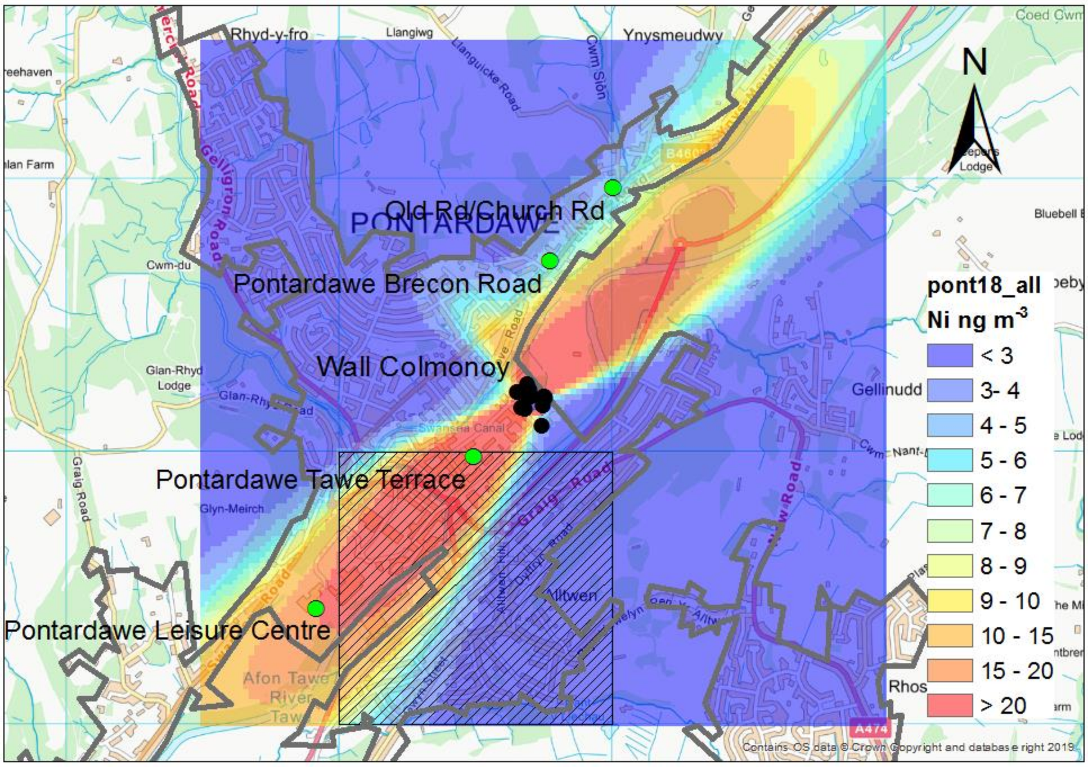

Contains Ordnance Survey data © Crown copyright and database right [2020]

Table 10.10 – Comparison of annual mean measured and modelled Ni concentrations at Pontardawe Tawe Terrace, Pontardawe Leisure Centre and Pontardawe Brecon Road in 2018.

	Measured Ni (ng m^{-3})	Modelled Ni (ng m^{-3})
Pontardawe Tawe Terrace	57	57
Pontardawe Leisure Centre	20	20
Pontardawe Brecon Road	6.2	5.1

10.6.4.3 Sheffield Urban Area and Yorkshire and Humberside Zones

The Sheffield Tinsley monitoring station is located in the valley of the river Don to the North East of Sheffield City Centre in the Sheffield Urban Area agglomeration zone. Exceedances of the annual mean TV of 20 ng m^{-3} have been reported in previous years (2014 and 2016) on the basis of measurements at the Sheffield Tinsley monitoring station. The EU Directive (2004/107/EC) requires that actions and measures are put in place to help meet the TV following an exceedance. Reports on Measures have been published[6] providing detail on the assessment of the exceedances reported in previous years and the actions and measures that have already been taken or are planned that will help the UK meet the Ni TV. Detailed dispersion modelling has been undertaken for the 2018 compliance assessment using ADMS 5.2 for an area in Sheffield covering the locations of the Sheffield Tinsley and Sheffield Devonshire Green monitoring stations and the principal industrial Ni sources. This fine scale modelling has been used to assess the likely magnitude and spatial extent of

---

[6] https://uk-air.defra.gov.uk/library/bap-nickel-measures

exceedance and takes into account work carried out for the report on measures for 2016 for the Sheffield Urban Area agglomeration zone (Defra, 2018) in terms of related modelling work and high time resolution monitoring campaigns. For other sites with Ni measurements in the Yorkshire and Humberside zone (Scunthorpe Low Santon and Scunthorpe Town) there are no reported exceedances for 2018, hence the focus of the detailed modelling has been on Sheffield.

To support this detailed modelling information on Ni emissions and release characteristics for the principal industrial Ni emission sources were provided by the Environment Agency (including data collated on sites regulated by Sheffield City Council and Rotherham Metropolitan Borough Council) and complemented by emissions data from the NAEI 2017. Emissions were released from 61 emissions sources including point, line and volume sources. Terrain effects were included in the modelling based on OS Terrain 50.

Figure 10-17 shows the modelled annual mean Ni concentration on a 50 m x 50 m grid resulting from the principal local industrial Ni sources in the Sheffield area and including a background component from the annual modelling of Ni concentrations across the UK. In order to achieve the best representation of concentrations at the Sheffield Tinsley monitoring station, the modelled contribution from the principal local sources is made up of an unscaled component derived from reported emissions and a scaled component derived by scaling the modelled contributions from sources with uncertain emissions to the North East of the Sheffield Tinsley site to fit the residual between what was measured and the sum of background and uncalibrated local contributions. This approach ensures the modelled concentrations match the measurements at Sheffield Tinsley exactly (which are not independent). It is notable that the modelled concentrations are also close to the measurements at Sheffield Devonshire Green (which are independent and not used to scale the modelling), and furthermore that the modelled proportions of the contributions from South East, North East and West directions are close to those derived for 2016 (Defra, 2018) from detailed high temporal resolution monitoring.

The conclusions from this dispersion modelling study are that Ni concentrations in both Sheffield Urban Area and Yorkshire & Humberside zones in 2018 exceeded the Ni TV.

The source apportionment plot (Figure 10-15) and scatter plot (Figure 10-14) presented earlier in this section include the modelled contribution to ambient concentrations at the Sheffield Tinsley and Sheffield Devonshire Green sites from the local industrial Ni sources in Sheffield.

Figure 10-17 - Modelled annual mean Ni concentration resulting from the local industrial sources in Sheffield Tinsley in 2018.

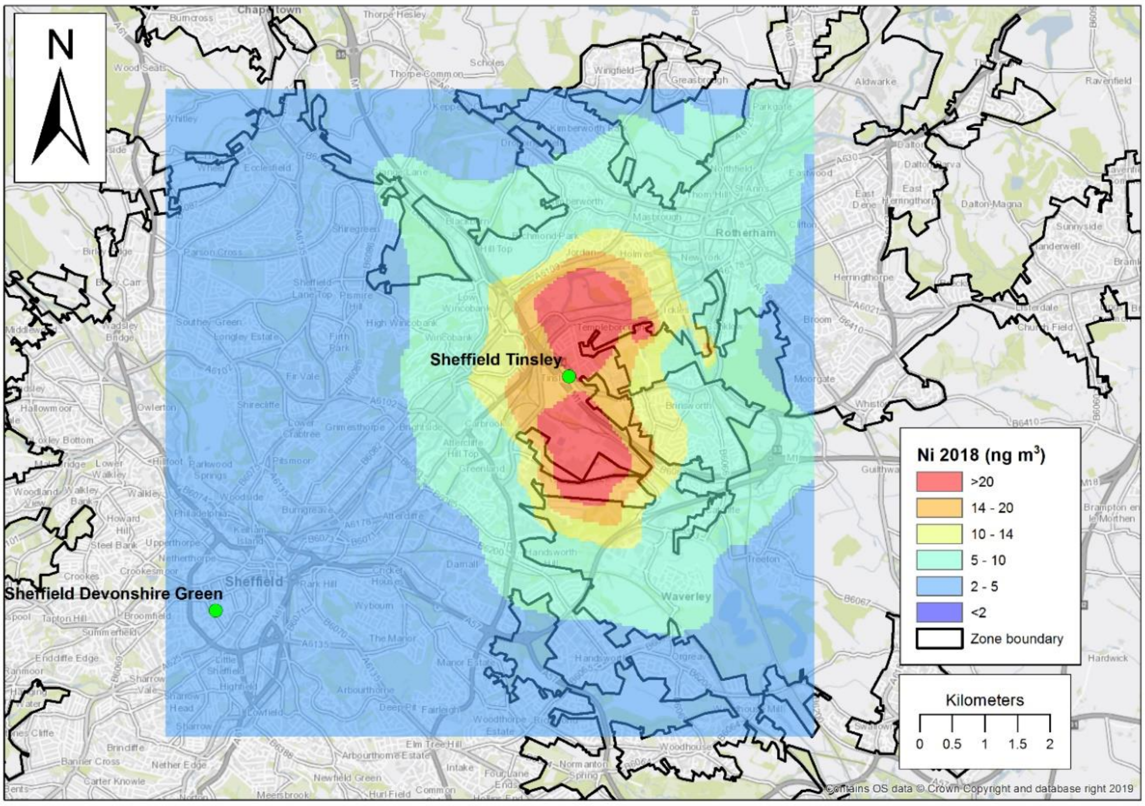

Contains Ordnance Survey data © Crown copyright and database right [2020]

10.7 Lead Results

10.7.1 Introduction

The method used to estimate the Pb ambient concentration across the UK is described in Section 10.3 above.

The map of modelled annual mean Pb concentrations is shown in Figure 10-5. There were no modelled or measured exceedances of the limit value of 0.5 µg/m^3 in 2018.

10.7.2 Verification of mapped concentrations

A comparison between modelled and measured annual mean annual mean Pb concentrations in 2018 at different monitoring site locations is shown in Figure 10-18 . These figures include lines to represent the AQD data quality objective for modelled annual mean Pb concentrations: y=x-50% and y=x+50% (see Section 1.5).

Summary statistics for modelled and measured Pb concentrations are listed in Table 10.11, including the percentage of sites at which modelled concentrations are outside of the data quality objectives (DQOs), and the total number of sites included in the analysis.

The mean and distribution (quantified using R^2) of measured and modelled concentrations agree very well for the rural monitoring sites.

It should be noted that non-emission inventory sources (such as fugitive, re-suspension and long-range transport of primary PM) result in additional uncertainty when compared with a pollutant such as NO$_X$, for which the source apportionment is better known.

Figure 10-18. Verification of annual mean Pb across all sites.

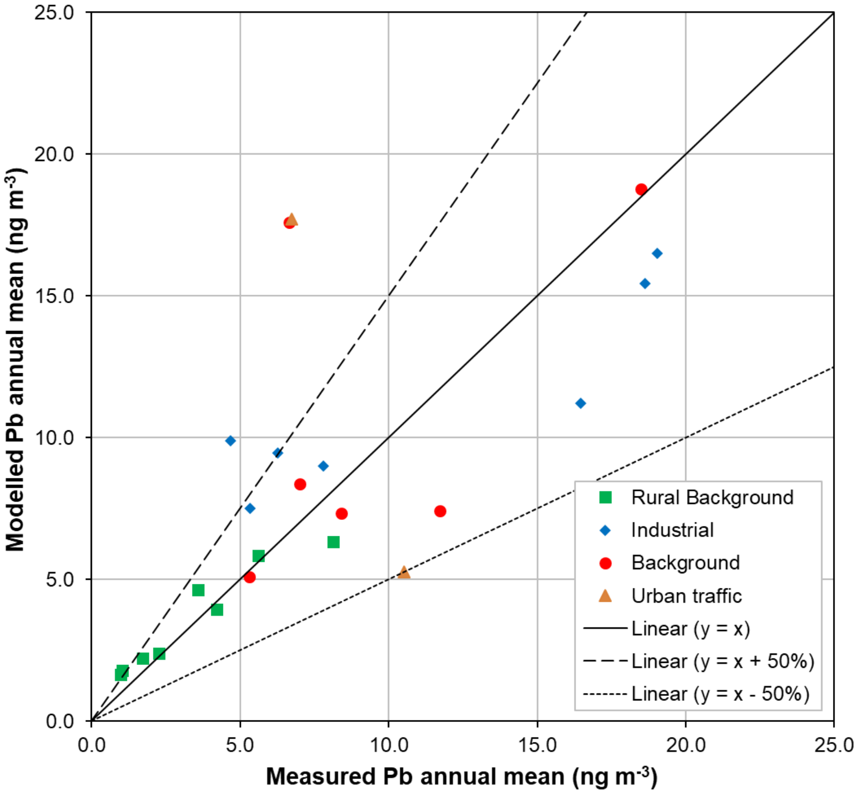

Table 10.11 - Summary statistics for comparison between modelled and measured annual mean Pb concentrations at different monitoring sites, 2018.

	Mean of measurements (ng/m^3)	Mean of model estimates (ng/m^3)	R^2	% of sites outside DQO of ±50%	Number of sites in assessment
Industrial sites	11.18	11.29	0.80	29%	7
Urban background sites	11.06	10.06	0.03	29%	7
Roadside sites	8.62	11.49	1.00	50%	2
Rural sites	3.44	3.60	0.92	25%	8
All	8.35	8.38	0.37	29%	24

10.7.3 Source apportionment

Figure 10-19 shows the modelled Pb contribution from different sources at monitoring locations. Measured concentrations at the sites are also presented, giving an indication of the level of agreement between modelled and measured concentrations. This analysis suggests that the main sources of lead are emissions from industrial emissions and re-suspension processes, and contributions from long range transport primary.

Figure 10-19 - Annual mean Pb source apportionment at monitoring sites in 2018.

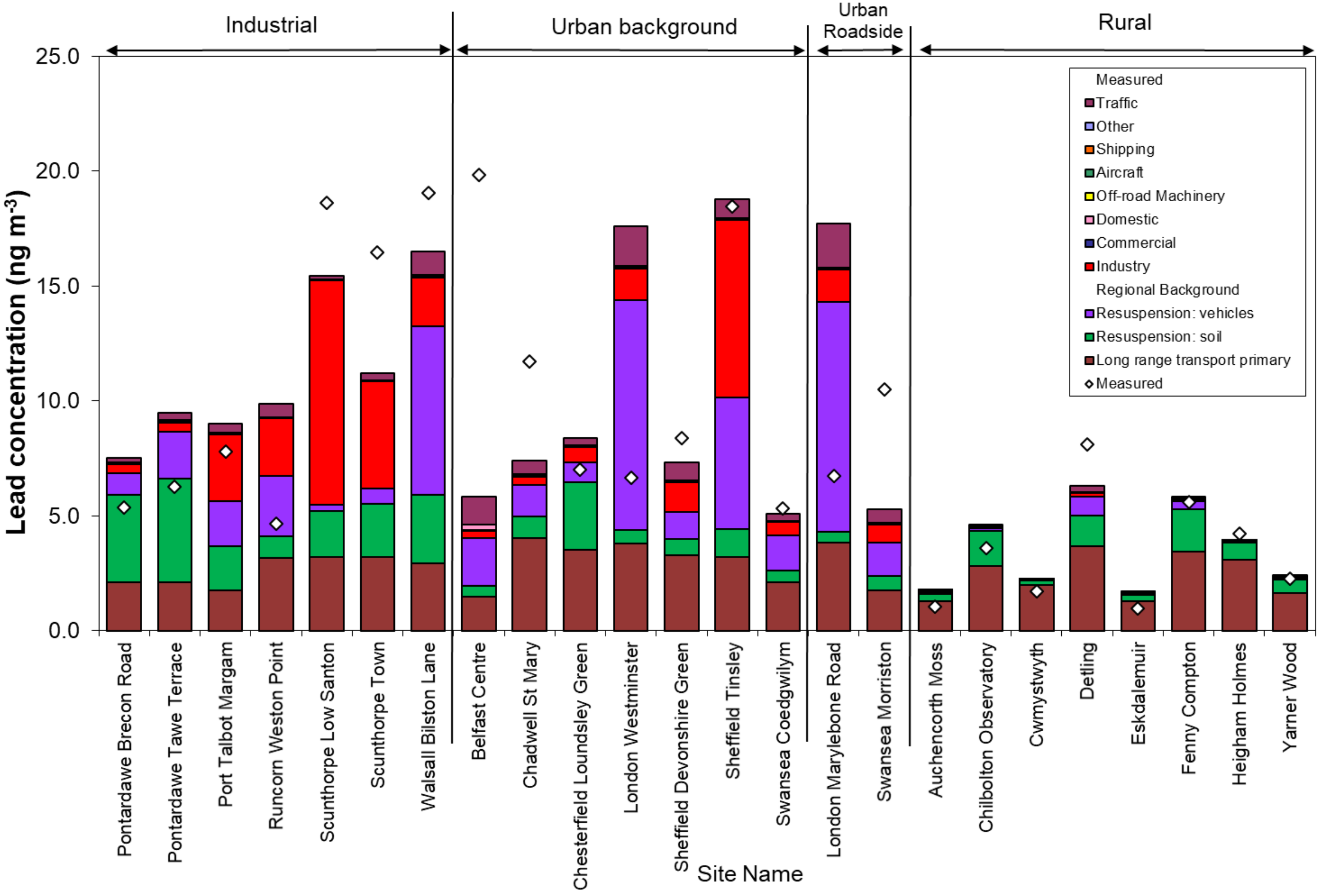

11 Benzo(a)pyrene

11.1 Introduction

11.1.1 Target values

A single target value (TV) for ambient concentrations of benzo(a)pyrene (B(a)P) is set out in AQDD4. The Directive states that Member States should take all necessary measures not entailing disproportionate costs to ensure that the target value is not exceeded after 31 December 2012. The target value is an annual mean concentration of 1 ng m^{-3}.

11.1.2 Annual mean modelling

A map of annual mean B(a)P in 2018 at background locations is shown in Figure 11-2. B(a)P concentrations were modelled for 2005 by Vincent et al. (2007) to inform the UK Preliminary Assessment for AQDD4 (Bush, 2007). 2018 is the eleventh year for which a full air quality assessment is required and national modelling of B(a)P was undertaken to assess compliance with the target value set out in the Directive.

The B(a)P annual mean model is calibrated based on monitoring data from the national network. Consideration has been given to the appropriate application of calibration factors in the model, and for this reason separate calibration factors have been used for the contributions from area sources in Great Britain and Northern Ireland and for coke ovens at steelworks in England and Wales. The 2018 assessment follows a similar approach to that adopted since the 2015 assessment (Brookes et al., 2017), including detailed local scale modelling to improve the representation of contributions from the most dominant industrial sources for B(a)P at exceedance locations (coke ovens at steelworks in England and Wales). The calibration process is described further in Sections 11.3.2, 11.4.2 and 11.4.3.

11.1.3 Overview of the PCM model for B(a)P

Figure 11-1 shows a simplified flow diagram of the PCM model for B(a)P. A summary of the PCM model method, input and assumptions for B(a)P is presented in Table 11.1.

Figure 11-1 – Flow diagram for PCM B(a)P model

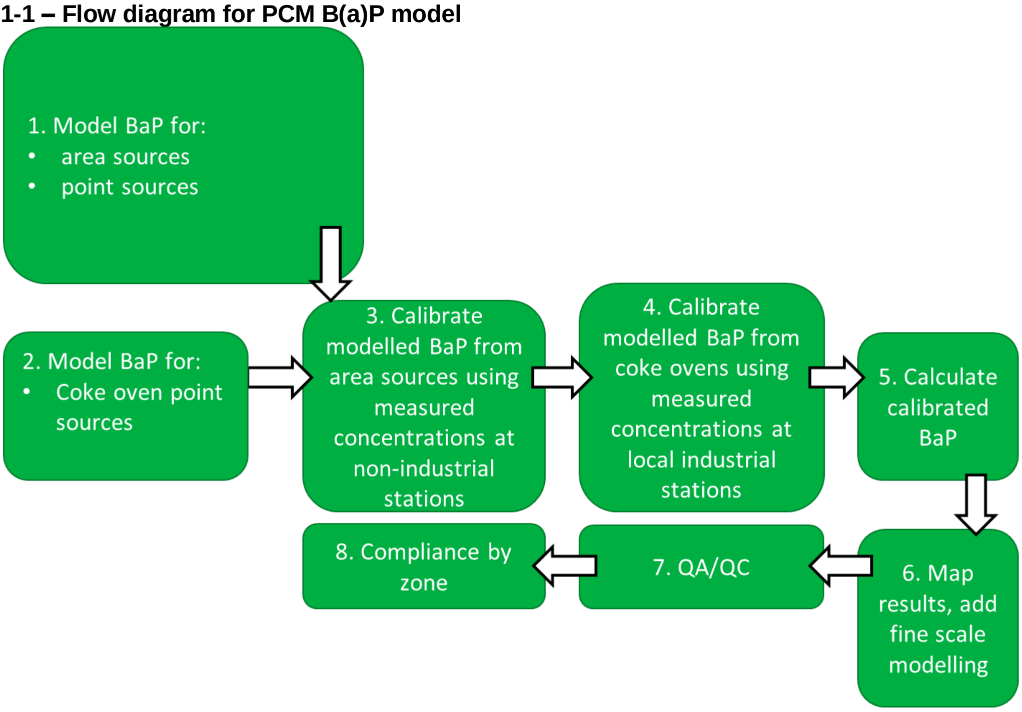

Table 11.1 – PCM model method, input and assumptions summary for B(a)P

Heading	Component	Details
General	Pollutant	BaP
	Year	2018
	Locations modelled	Background
	Metric	Annual mean
Input data	Emission inventory	NAEI 2017 plus operator data for 2018 for integrated steel works where available
	Energy projections	Energy Projections 2017
	Road traffic counts	2017
	Road transport activity projections	DfT (2018) traffic (re-based to 2017 NAEI), DfT (2019) car sales projections, TfL traffic (2019) and fleet (2018) projections for London
	Road transport emission factors	COPERT 5
	Measurement data	2018
	Meteorological data	Hourly data from Waddington 2018
Model components	Regional	n/a
	Large point sources	121 sources modelled using ADMS 5.2
	Small point sources	PCM dispersion kernels generated using ADMS 5.2.
	ETS point sources	PCM dispersion kernels generated using ADMS 5.2.
	Large ETS point sources	147 sources modelled using ADMS 5.2
	Area sources	PCM dispersion kernels generated using ADMS 5.2. Time varying emissions for road transport and domestic sources.
	Coke ovens	2 sources modelled using ADMS 5.2
	Roadside increment	n/a
Calibration	Model calibrated?	Yes (see Pollutant specific information)
	Number of background stations in calibration	23 background + 2 industrial
	Number of traffic stations in calibration	n/a
Pollutant specific	Fine scale modelling	Impact of emissions from coke ovens at Scunthorpe and Port Talbot modelled at 100 m spatial resolution using local meteorological data and incorporating terrain effects for Port Talbot. For the areas covered by the fine scale modelling, 1 km grid cells have been classified as exceeding the TV if at least nine 100 m grid squares exceed the TV or at least one square exceeds and there is population in the 1 km grid cell containing the exceeding 100m grid squares. A concentration value was defined for each 1 km grid square from the fine scale modelling from the mean of the 100 m grid squares exceeding the TV within that 1 km grid square or the mean of all 100 m grid squares for non-exceeding grid squares within the fine scale modelling domain.

Heading	Component	Details
	Calibration	Separate calibration for area sources in Great Britain (21 background stations across Great Britain) and Northern Ireland (24 background stations across the UK). Separate calibration for contributions from coke ovens (local calibration using data from 2 stations and concentrations modelled at 100 m resolution)

11.1.4 Outline of the annual mean model for B(a)P

The 1 km x 1 km annual mean background B(a)P concentration map was calculated by summing the contributions from:

- Large point sources
- Small point sources
- Point sources with emissions estimates for air quality pollutants based on reported carbon emissions (ETS points)
- Coke oven sources modelled at 100m spatial resolution.
- Local area sources

Figure 11-2 – Annual mean background B(a)P concentration, 2018 (ng m^{-3})

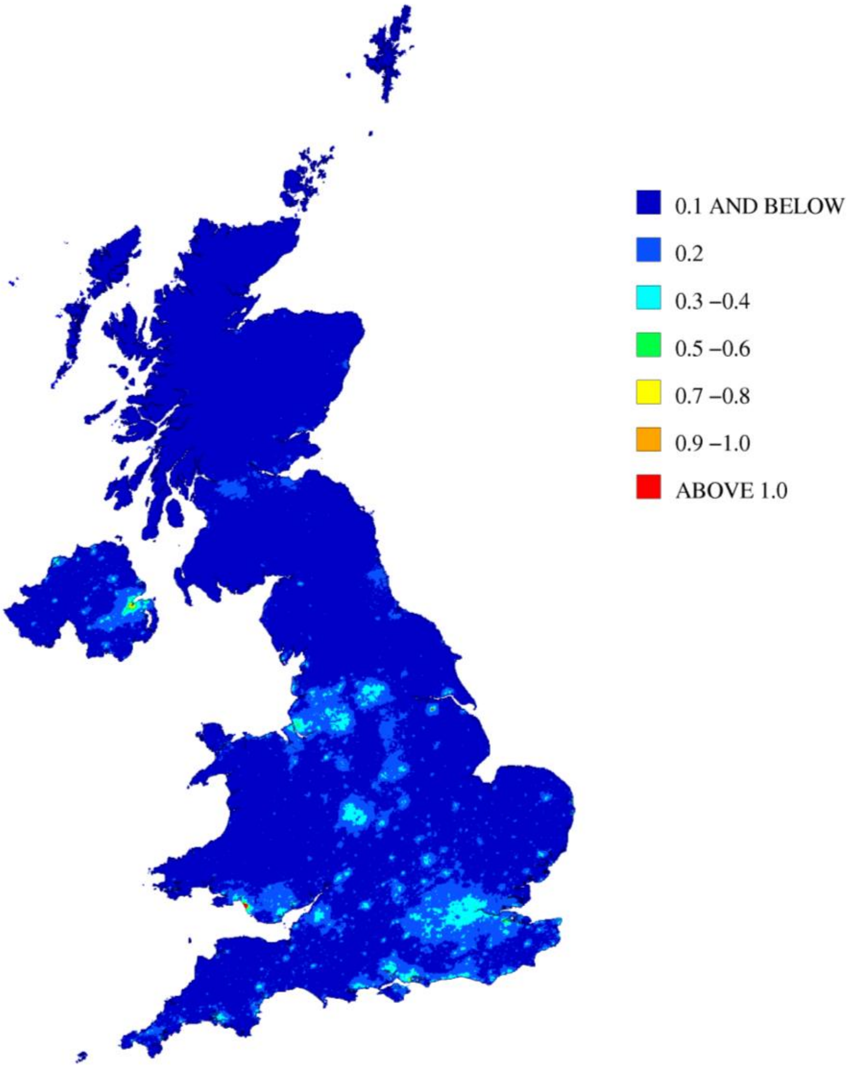

11.1.5 Chapter structure

This chapter describes modelling work carried out for 2018 to assess compliance with the B(a)P target value described above. Emissions estimates for B(a)P are described in Section 11.2. Sections 11.3 and 11.4 describes the B(a)P modelling methods for the annual mean. The modelling results are presented in Section 11.5. Detailed local scale modelling of exceedances relating to B(a)P emissions from coke ovens at steelworks in England and Wales is described in Section 11.5.3.

11.2 Emissions

B(a)P emission estimates from the UK National Atmospheric Emissions Inventory 2017 (NAEI 2017) have been used in this study (Richmond et al., 2019). Emissions projections have been provided by the NAEI based on BEIS EEP 2018 energy and emissions projections (BEIS, 2018). Figure 11-3 shows UK total B(a)P emissions for 2017 and emissions projections for 2020, 2025 and 2030 split by SNAP code, with the coding described in Table 3.2. Values for intermediate years have been interpolated in this figure.

Figure 11-3 shows that emissions from B(a)P are projected to decrease marginally from 2017 to 2030. Sectors with the largest contribution to the total in 2017 include domestic combustion and nature with domestic driving the trend.

The emissions inventory provides maps of emissions on a 1 km x 1 km grid, which is likely to be too coarse to incorporate very local variations in emissions from sources such as domestic heating, where there may be considerable in-square variation due to differences in fuel use (Vincent and Tsagatakis, 2014). SNAP 11: ‘Nature’, refers to B(a)P emissions from combustion in the natural environment such as forest fires. Despite the relatively high emissions contribution from this source sector, the method for distribution of these emissions used in the NAEI ensures that natural combustion is spread evenly across the UK and does not unduly affect the modelled ambient concentrations in any particular area. The emissions from this source are projected to remain constant through to 2030 and hence do not contribute the projected trend.

Figure 11-3 – Total UK B(a)P emissions for 2017 and emissions projections up to 2030 by SNAP code from the NAEI 2017

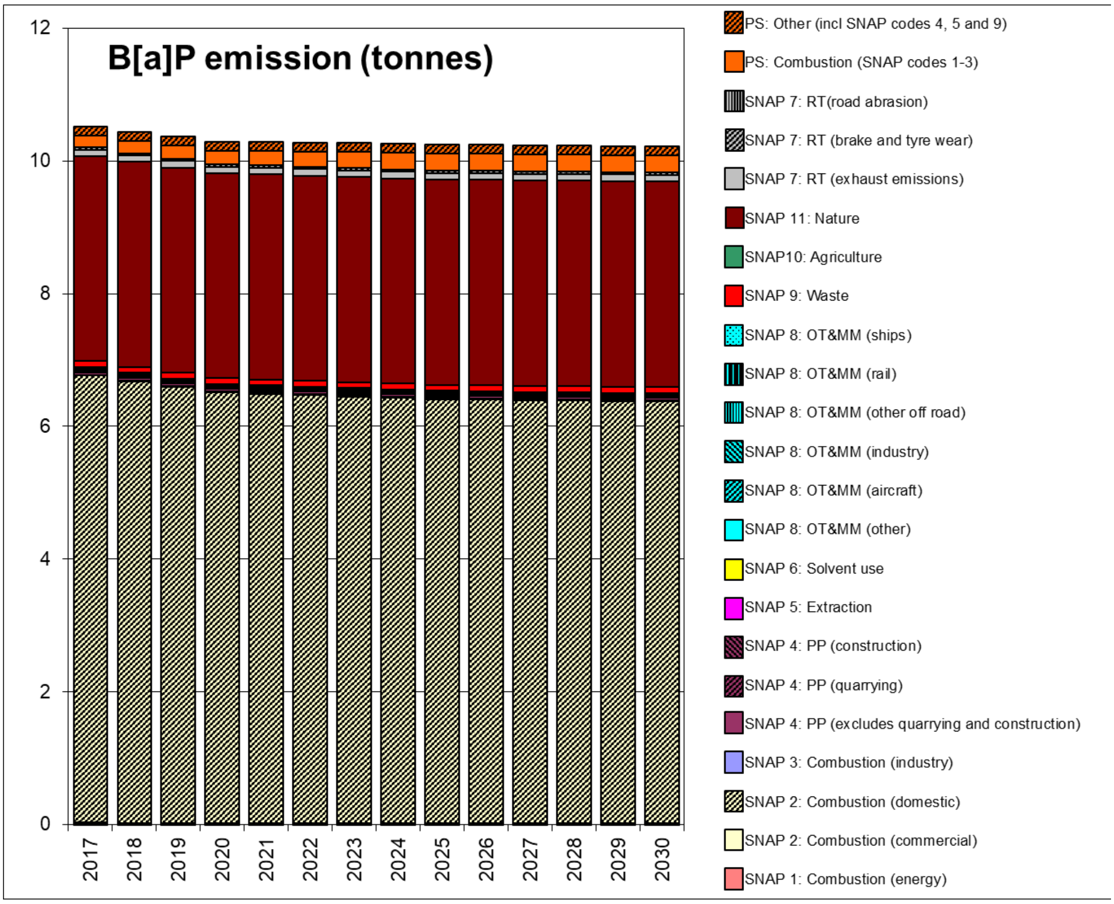

11.3 B(a)P modelling: Contributions from local area sources

11.3.1 Introduction

The 2018 area source B(a)P emissions maps have been calculated from the NAEI 2017 emissions maps following the method described in Section 3.3.5. ADMS derived dispersion kernels have been used to calculate the contribution to ambient B(a)P concentrations on a 1 km x 1 km receptor grid, from the area source emissions within a 33 km x 33 km square surrounding each receptor. Hourly sequential meteorological data from Waddington in 2018 was used to construct the dispersion kernels, as described in Appendix 4.

11.3.2 Area source model calibration

Figure 11-4 shows the separate calibration of the modelled annual mean area source B(a)P contribution for locations in Great Britain and Northern Ireland applied in the 2018 assessment. The calibration coefficient for locations in Great Britain has been derived by comparing the uncalibrated modelled area source component with measured concentrations at monitoring stations in Great Britain. The calibration coefficient for locations in Northern Ireland has been derived by comparing the uncalibrated modelled area source component with measured concentrations at monitoring stations across the UK. The measured concentrations have been adjusted to represent background (non-industrial) concentrations by subtracting the uncalibrated modelled point source contribution at these locations. Those stations where the uncalibrated point source contribution was ≥ 5% were excluded from the calibration hence the adjustment to the measured concentrations is minimal. To calculate the calibrated area source contribution for each grid square in the country the modelled area source contribution was multiplied by the relevant calibration fit coefficient.

As noted, for the 2018 assessment, a separate area source calibration has been carried out for locations in Great Britain and Northern Ireland. This approach was followed on the basis that:

- There are no measured exceedances for 2018 in Northern Ireland.
- Measured and modelled concentrations do not scale consistently between monitoring stations in Northern Ireland, while the scaling between measured and modelled concentrations is near 1:1 for background locations in Great Britain.
- Applying a separate calibration to domestic only for Northern Ireland based on Northern Ireland monitoring as per previous assessments (Walker et al. (2011), Brookes et al. (2012)) would lead to over prediction.
- The Derry Brandywell and Ballymena Ballykeel monitoring stations remain influential in the 2018 area source calibration for Northern Ireland. Including all UK sites in the calibration for Northern Ireland moderates the influence of these stations on the calibration while providing model estimates close to the observed concentrations at Kilmakee Leisure Centre.

In common with previous assessments, the indication that a greater calibration coefficient is required on area source contributions (primarily domestic) in Northern Ireland compared to area sources overall for the UK suggests further improvements are needed for quantifying and mapping domestic combustion emissions in Northern Ireland.

Figure 11-4 indicates similar scatter in the area source calibration for 2018 as for 2017 and 2016 and reduced scatter compared with 2015. The calibration coefficient for Great Britain for 2018 (0.9282) has further reduced over UK wide calibration coefficients for previous assessments (6.434 for 2014, 1.459 for 2015, 1.176 for 2016, 1.0138 for 2017), while the calibration coefficient applied to Northern Ireland (1.2192) is also close to that for recent assessments. The reduction in the fit coefficients and the improved scatter in the fit suggests improved understanding of the scale and distribution of domestic wood combustion emissions from the NAEI 2013 to the NAEI 2015, while the NAEI 2017 methodology incorporates improvements introduced in the NAEI 2015.

As part of the calibration process, emission caps have been applied to certain sectors; this is because the use of surrogate statistics for mapping area source emissions sometimes results in unrealistically large concentrations in some grid squares for a given sector. The emission caps applied are given in Table 11.2.

Table 11.2 - Emission caps applied to B(a)P sector grids

SNAP code	Description	Cap applied (kg/a/km^2)
SNAP 4 (production processes, excludes quarrying and construction)	Chemical industry – general, Non-fuel bitumen use	0.66
SNAP 4 (production processes, excludes quarrying and construction)	Electric arc furnaces, Steel production (electric arc)	0.66

Figure 11-4 - Calibration of area source model for B(a)P

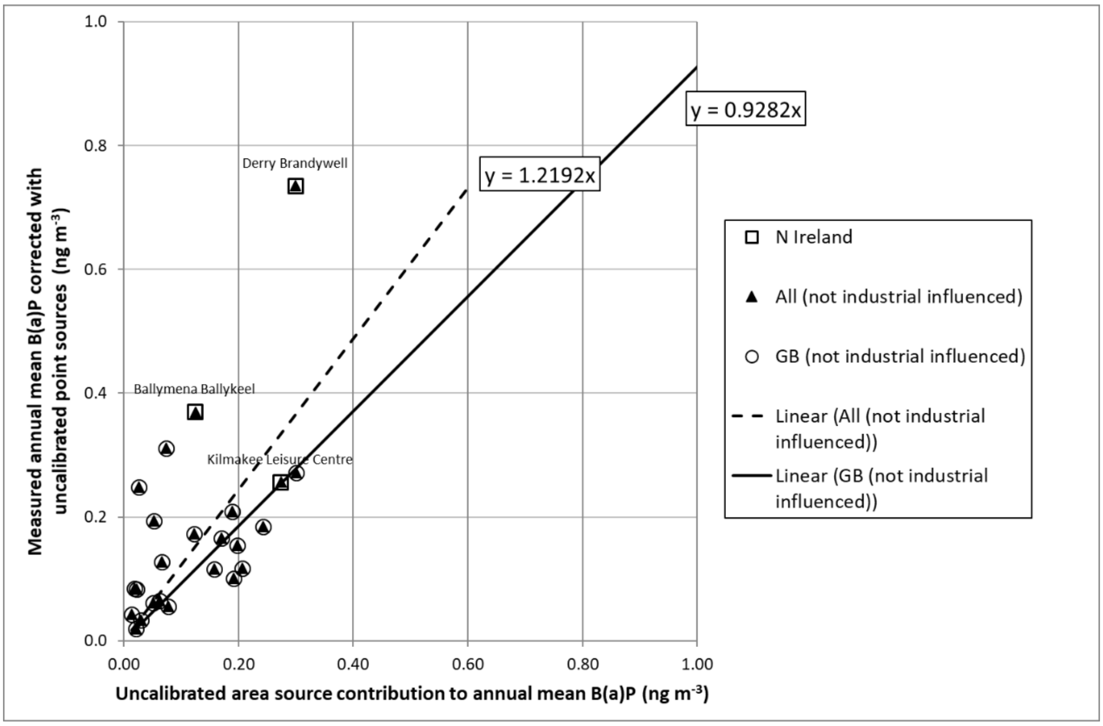

11.4 B(a)P Modelling: Contributions from large and small point sources

11.4.1 Introduction

Contributions to ground level annual mean B(a)P concentrations from large point sources (those with annual emissions greater than 0.001 tonnes, or for which emission release characteristics are known) in the NAEI 2017 have been estimated by modelling each source explicitly using the atmospheric dispersion model ADMS 5.2 and sequential meteorological data for 2018 from Waddington. Surface roughness was assumed to be 0.1 m at the dispersion site and 0.1 m at the meteorological site. Concentrations were calculated for a 99 km x 99 km square composed of a regularly spaced 1 km x 1 km resolution receptor grid. Each receptor grid was centred on the point source.

Industrial point sources of B(a)P are either fugitive (as from coking plants) or from clearly defined stacks for other sources. The emission amount is derived either from direct measurement or by emission factors. 121 point sources from the NAEI 2017 were classified as large points sources and modelled using emissions release information retrieved from the PCM stack parameters database (described in more detail in Section 3.3.1).

The NAEI 2017 also includes point source emissions estimates derived from carbon emissions data reported under the EU-Emissions Trading Scheme (ETS) (Tsagatakis et al., 2019), referred to as ETS points in this report. These derived air quality pollutant emissions are particularly uncertain and therefore in previous assessments (e.g. Brookes et al., 2017) emissions were capped at reporting thresholds and treated as small point sources. For the 2016 and 2017 assessments (Brookes et al., 2019a, 2019b) the NAEI recommended treating the ETS points that have emissions greater than the large points modelling threshold as large points and not to apply a cap (Passant pers. comm. 2017).

The 2018 assessment continues this approach. Thus, based on the criteria for the treatment of large point sources described above, 147 ETS point sources were modelled as an additional set of large point sources (using the approach described above). ETS points that were not classified as large point sources were modelled using the B(a)P small points approach.

The impact of 2 further large point sources, the coke works at Port Talbot and Scunthorpe (which are the dominant industrial sources for B(a)P), have been modelled as line sources and at finer spatial resolution on a regularly spaced 100 m x 100 m resolution receptor grid. The detailed local scale modelling of the 2 coke ovens is described in Section 11.4.2.

For the majority of large point sources NAEI 2017 emissions were applied with scaling using projection factors to provide emission values for 2018, as described in Section 3.3.1. For each sinter plant stack and coke oven bank at the integrated steelworks in England and Wales reported B(a)P emissions for the year 2018 have been acquired and applied in order to provide the best representation of contributions from the most dominant industrial sources for B(a)P at exceedance locations. The NAEI provided operator reported emissions for 2018 for the integrated steelworks at Port Talbot and Scunthorpe (Passant pers. comm. 2018b) The split between sinter plant stack emissions and coke oven emissions at Scunthorpe was not available at the time of modelling and the ratio reported for 2017 was applied to the total for 2018. Subsequent analysis showed that this estimate was very similar to the reported split.

Contributions from B(a)P point sources with less than 0.001 tonnes per year emissions and without emissions release characteristics were modelled using an area source approach. NAEI 2017 emissions for small point sources were scaled to 2018 emissions using the same source sector specific projection factors applied to the large point sources. These emissions were aggregated onto a 1 km x 1 km grid before applying an ADMS 5.2 derived dispersion kernel (for non-domestic, non-road transport) to calculate the contribution to ambient concentrations at a central receptor location from small point source emissions within a 33 km x 33 km square surrounding each receptor. The method used to generate area source dispersion kernels is described in Appendix 4.

11.4.2 Coke oven sources

Detailed dispersion modelling was undertaken to derive contributions from the coke ovens in England and Wales. Each source was modelled explicitly using the atmospheric dispersion model ADMS 5.2. Hourly sequential meteorological data for 2018 from Waddington was used in modelling the impact of the Appleby coke ovens at Scunthorpe. Hourly sequential meteorological data for 2018 incorporating observations from the Neath Port Talbot County Council monitoring station at Little Warren and the Swansea City Council monitoring station at Cwm Level Park were used in modelling the impact of the coke ovens at Port Talbot. Surface roughness was assumed to be 0.5 m at the dispersion site for both Scunthorpe and Port Talbot. Surface roughness was assumed to be 0.1 m and 0.5 m at the meteorological sites for Scunthorpe and Port Talbot respectively. Calm conditions were treated in the dispersion modelling using the ADMS calm module at the ADMS default settings. Concentrations were calculated for a 15 km x 15 km area for Scunthorpe and a 23 km x 19 km area for Port Talbot both composed of regularly spaced 100 m x 100 m resolution receptor grids, centred on the coke ovens. To account for the complex terrain surrounding Port Talbot the effect of the local topography has been included in the 2018 modelling, with terrain heights based upon the OS Terrain 50 dataset.

11.4.3 Point source model calibration

In previous assessments the modelled point source contribution (excluding coke ovens) has been calculated using a single calibration based upon monitoring data from the national network to obtain results consistent with measured concentrations. Since the 2016 assessment, the modelling and monitoring data at other industrial sites no longer supports application of a general point source calibration. With recent closures of dominant industrial sources of B(a)P there are only 2 industrial monitoring stations (Scunthorpe Low Santon and Port Talbot Margam) where the uncalibrated point source contribution is ≥ 50% of the uncalibrated modelled concentration. Thus for 2016, 2017 and 2018, only the coke ovens contribution has been calibrated, using local monitoring data and the detailed local scale modelling of these sources (described in Section 11.4.2).

There is an element of circularity involved in the calibration of both area and point sources because the calibration process for each requires the subtraction of the other to isolate the component being calibrated. An approach to minimise interdependence of the calibrations was introduced in the 2012 assessment (Brookes et al., 2013) and this was carried forward into the 2018 assessment, as follows:

- The area source component is calibrated first and as discussed in Section 11.3.2 only monitoring stations where the uncalibrated point source contribution is < 5%, are included in the area source calibration. This minimises the influence of point sources on the area source calibration, since the contribution from point sources at non-industrial monitoring stations is typically very small and is guaranteed to be < 5% by this approach.
- In addition, monitoring stations where the uncalibrated point source contribution is ≥ 5%, but still relatively low (< 50%) are excluded from the model calibration completely. Data for these stations are still included in the model verification.
- Given the two conditions above, only monitoring stations where the uncalibrated point source contribution is ≥ 50% of the uncalibrated modelled concentration (area sources plus point sources) are included in the calibration of the point sources.

Since the 2016 assessment a general point source calibration is no longer applied, hence there is no potential for interdependence of the calibrations except for the locations impacted by the coke ovens. The approach remains valuable elsewhere as it ensures the monitoring stations applied in calibrations are most representative of the source sectors being calibrated.

To calibrate the coke ovens contribution, local scaling factors have been applied (5.21994 (compared to 4.4247 for 2017) at Scunthorpe and 3.68144 (compared to 1.2394 for 2017) at Port Talbot), since a general calibration fit would otherwise lead to over or under prediction at each location. Measured concentrations at the industrial monitoring stations were adjusted by subtracting the calibrated modelled area source contribution and the uncalibrated contribution from other point sources (the sum of other large, small and ETS point source contributions, excluding the coke ovens) so that the measured value represented the coke ovens component only. The local scaling approach guarantees the modelled total B(a)P concentration provides a reasonable representation of the observed concentrations at these monitoring stations. The local scaling for Scunthorpe derives from the Scunthorpe Low Santon station only, since the uncalibrated point source contribution at the Scunthorpe Town station is < 50% of the uncalibrated modelled concentration. Furthermore, a local scaling based upon the Scunthorpe Town station would be greater than that for Scunthorpe Low Santon. Thus, applying the local scaling on the modelled coke ovens contribution based on the observation at Scunthorpe Low Santon ensures the modelling provides a reasonable representation of the peak concentration observed in the Yorkshire & Humberside zone and does not exaggerate the spatial extent of the modelled exceedance.

11.5 Results

11.5.1 Verification of mapped values

Figure 11-5 presents a comparison of modelled and measured annual mean B(a)P concentrations in 2018 at monitoring station locations differentiated by station classification. This figure includes lines to represent the AQDD4 data quality objective for modelled annual mean B(a)P concentrations: y=x-60% and y=x+60% (see Section 1.5). The results for industrial and background monitoring stations influenced by contributions from coke ovens are compared to modelled concentrations derived from the detailed local scale modelling of these sources, described in Section 11.4.2. The results for other industrial and background monitoring stations are compared to modelled concentrations derived from the national scale modelling, and therefore the model results for these stations are further differentiated in Figure 11-5.

Figure 11-5 - Verification of annual mean B(a)P across all stations

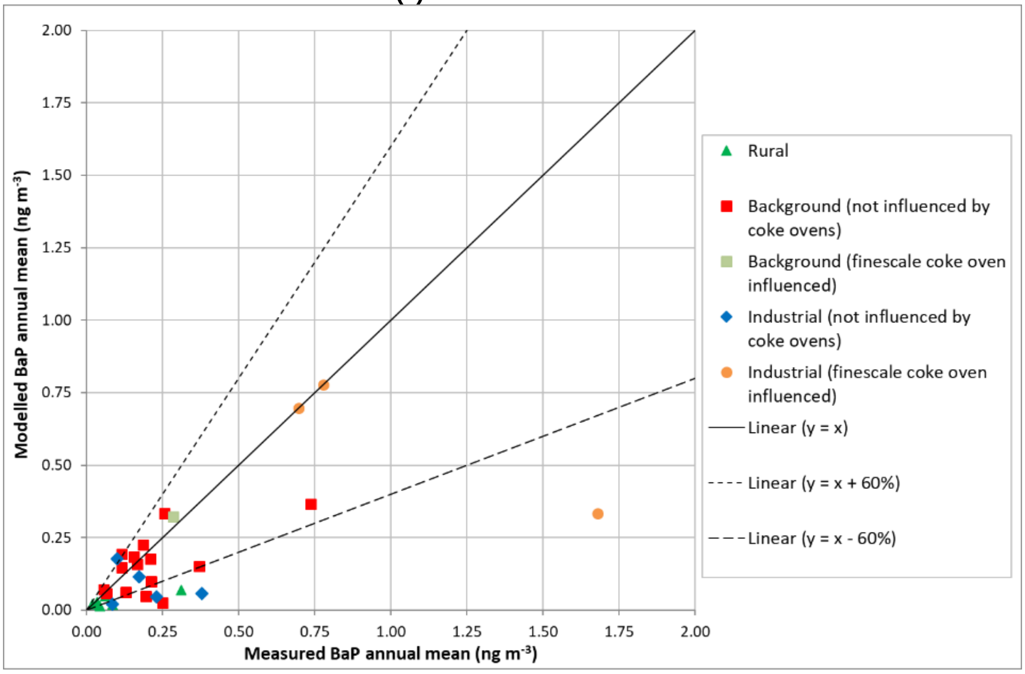

Summary statistics for modelled and measured B(a)P concentrations are listed in

Table 11.3, including the percentage of stations at which modelled concentrations are outside of the data quality objectives (DQOs), and the total number of stations included in the analysis. Summary statistics for industrial and background monitoring stations influenced by contributions from coke ovens derived from the detailed local scale modelling of the coke ovens have been indicated. Summary statistics from the national modelling have been calculated for industrial and urban background stations not influenced by coke ovens, and rural stations.

The mean measured and modelled concentrations are in reasonable agreement for all monitoring stations, except those industrial stations not influenced by contributions from coke ovens for which the dominant local industrial sources are no longer operating. The agreement between measured and modelled concentrations at industrial stations influenced by contributions from coke ovens is naturally better since for two of these three stations the model has been scaled to reproduce the observed concentrations. The R^2 value across all stations is generally better than that for individual station classes reflecting that overall the model is capturing the variation in observed concentrations. R^2 is less meaningful for the individual station classes, in particular where the number of stations is low, however it does indicate that for background stations that are primarily expected to be influenced by domestic emissions, the model captures a reasonable proportion of the observed variation in concentrations. The low concentrations at rural stations are captured by the modelling.

Table 11.3 – Summary statistics for comparison between modelled and measured annual mean B(a)P concentrations at different monitoring stations, 2018

	Mean of measurements (ng/m^3)	Mean of model estimates (ng/m^3)	R^2	% of stations outside DQO of ±60%	Number of stations in assessment
Industrial stations (not influenced by coke ovens)	0.19	0.08	0.08	80%	5
Industrial stations (coke oven influenced)	1.05	0.60	0.94	33%	3
Background stations (not influenced by coke ovens)	0.21	0.15	0.38	20%	15
Background stations (coke oven influenced)	0.28	0.32	-	0	1
Rural stations	0.09	0.03	0.67	50%	6
All	**0.27**	**0.17**	**0.38**	**37%**	**30**

11.5.2 Source apportionment

A source apportionment graph is plotted in Figure 11-6 to present the B(a)P contribution from different sources at monitoring station locations. It should be noted that for industrial and background stations in the areas covered by the fine scale modelling of the coke ovens (Scunthorpe Town, Scunthorpe Low Santon, Port Talbot Margam, Swansea Cwm Level Park), described in Section 11.4.2, the modelled source apportionment includes the local modelling. The source apportionment for stations outside these areas is from the national scale modelling. Measured concentrations at the stations are also presented, giving an indication of the level of agreement between modelled and measured concentrations. Domestic combustion, at many stations, and industry, at industrial stations, are the most important sources. The contributions from other sources are much smaller.

Figure 11-6 – Annual mean B(a)P source apportionment at background national network monitoring stations in 2018 (the area type of each station is shown in parenthesis after its name)

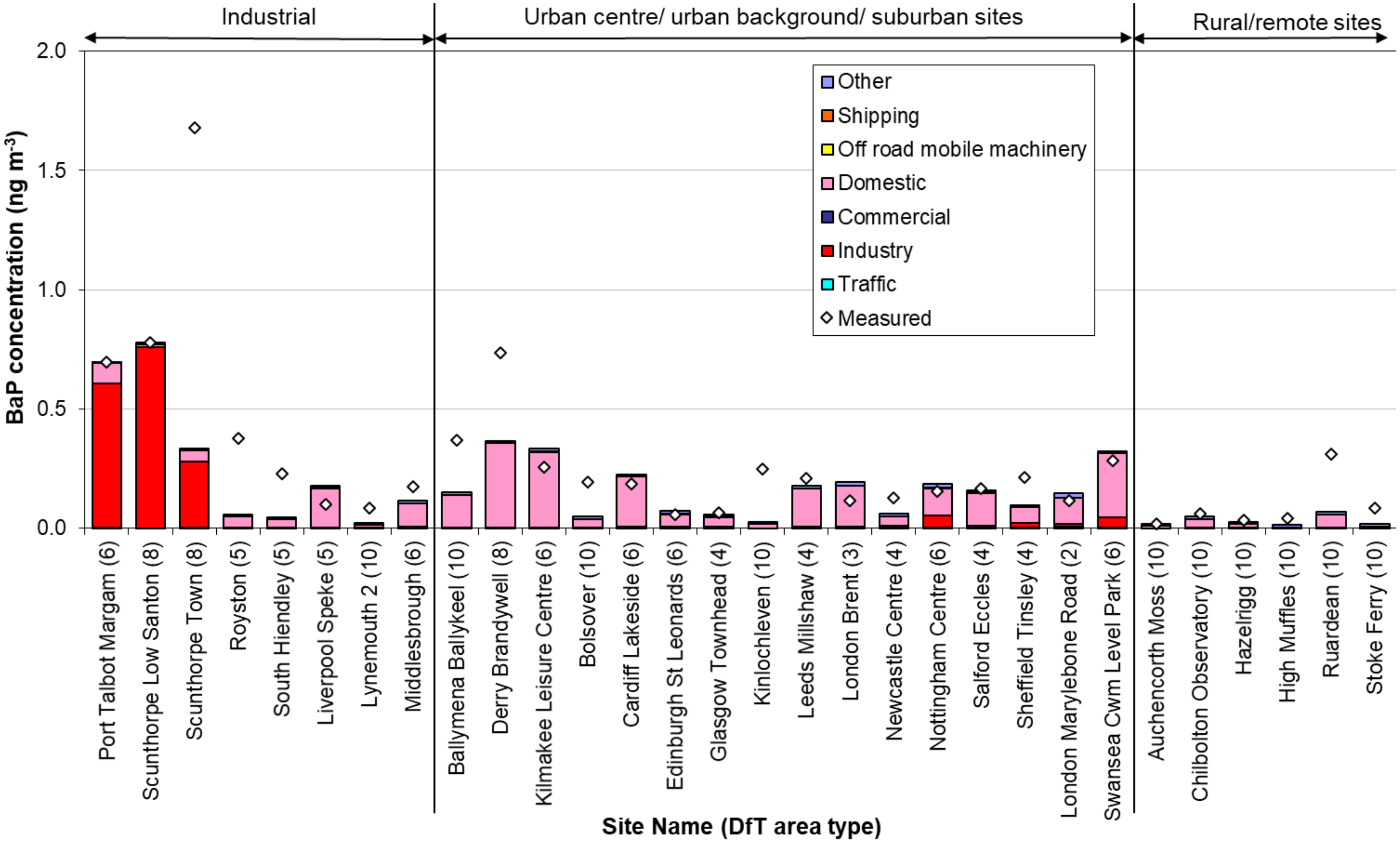

11.5.3 Detailed comparison of modelling results with the target value

Results of the assessment in terms of comparisons of the modelled concentrations with the TV have been reported in e-Reporting Data flow G (CDR, 2019). For the areas covered by the fine scale modelling, 1 km grid cells have been classified as exceeding the TV if at least nine 100 m grid squares exceed the TV or at least one 100 m square exceeds and there is population in the exceeding 1 km grid square. A concentration value was defined for each 1 km grid square from the fine scale modelling from the mean of the 100 m grid squares exceeding the TV within that 1 km grid square or the mean of all 100 m grid squares for non-exceeding grid squares within the fine scale modelling domain.

Exceedances of the 1 ng m^{-3} TV have been modelled for two zones (South Wales and Swansea Urban Area), there is one measured exceedances for 2018 (Yorkshire & Humberside). The following information is based on a source apportionment assessment including the fine scale modelling.

Exceedances in 5 km^2 of the Yorkshire & Humberside zone have been modelled, associated with the Appleby coke ovens of the Scunthorpe steelworks.

Exceedances in 14 km^2 of the South Wales zone and 4 km^2 of the Swansea Urban Area have been modelled, associated with industrial emissions from the coke oven at the steel plant at Port Talbot.

Figure 11-7 and Figure 11-8 show the modelled annual mean B(a)P concentration at a 100 m x 100 m spatial resolution in the vicinity of the coke ovens at Scunthorpe and Port Talbot respectively. Figure 11-9 shows the complex terrain surrounding Port Talbot which has been incorporated into the 2018 modelling and influences the dispersion of emissions from the coke ovens in this location.

Figure 11-7 - Modelled total annual mean B(a)P concentration in the vicinity of the Appleby coke ovens at the Scunthorpe steelworks in 2018.

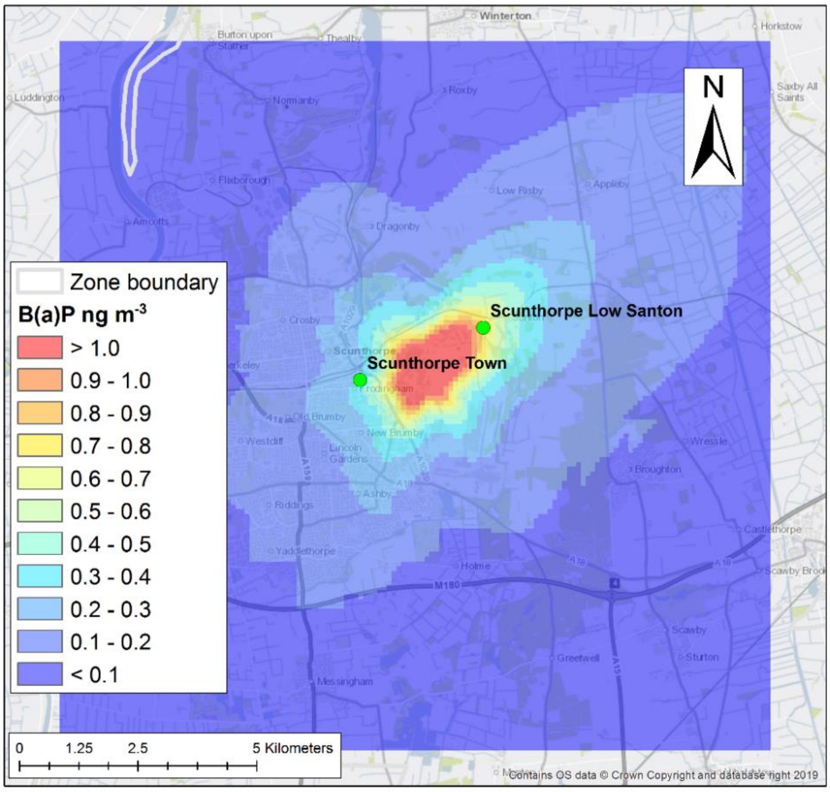

Contains Ordnance Survey data © Crown copyright and database right [2020]

Figure 11-8 – Modelled total annual mean B(a)P concentration in the vicinity of the coke ovens at the Port Talbot steelworks in 2018.

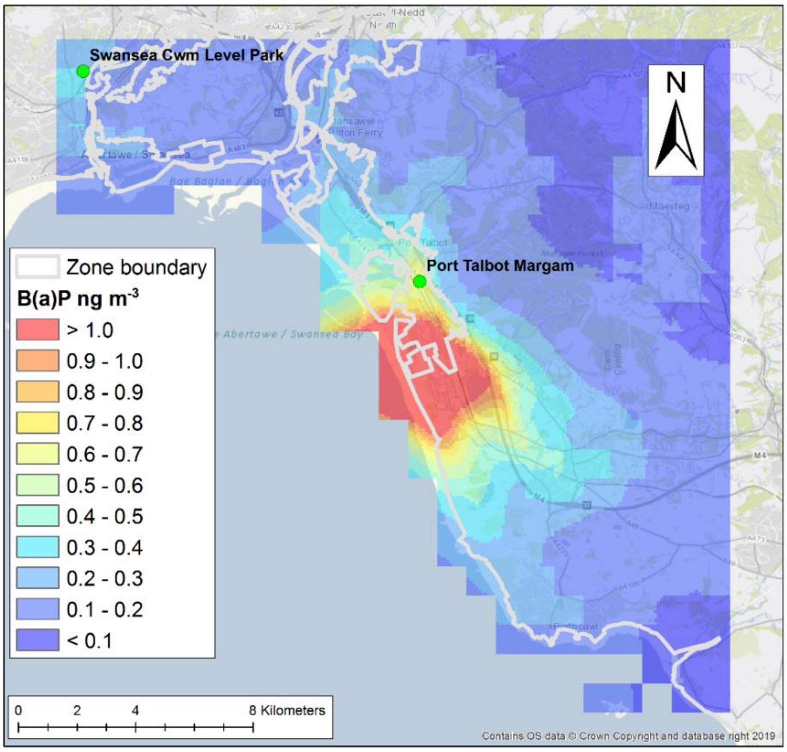

Contains Ordnance Survey data © Crown copyright and database right [2020]

Figure 11-9 – Terrain heights in the vicinity of Port Talbot

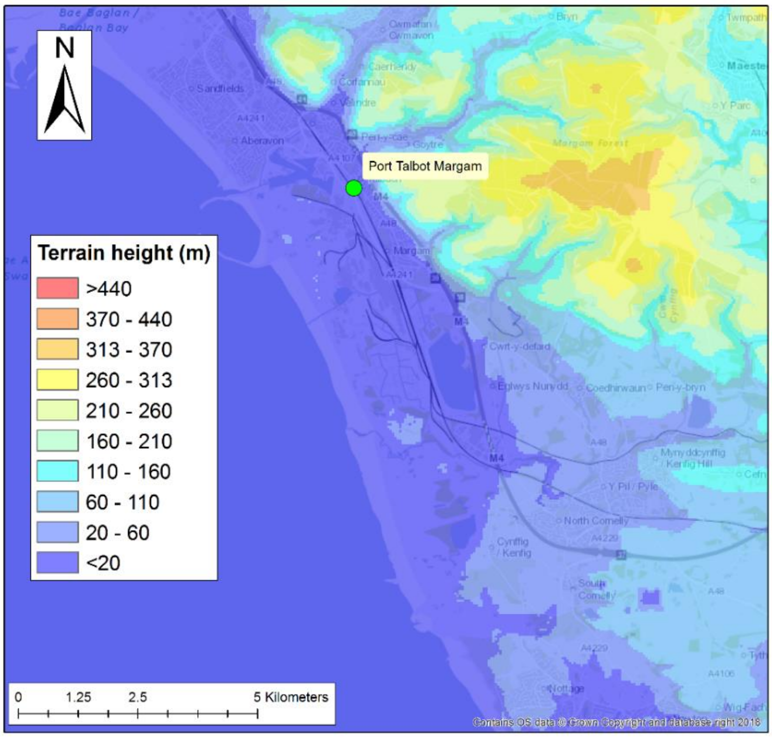

Contains Ordnance Survey data © Crown copyright and database right [2020]

12 Acknowledgements

This work was funded by the UK Department for Environment, Food and Rural Affairs, The Welsh Government, The Scottish Government and The Department of the Environment for Northern Ireland.

The authors would also like to thank: Hanson Building Products Limited for providing SO_2 measurements and INEOS for providing benzene measurements.

Detailed information and measurements for the Pontardawe Leisure Centre monitoring site was kindly provided by Neath Port Talbot County Borough Council. This monitoring site was included in the analysis for verification of the local scale modelling of Ni concentrations in Pontardawe. The authors would also like to thank the Natural Resources Wales, local authorities and plant operators for helping with the nickel emission data and release characteristics for specific plants.

The authors would like the thank providers of model input data that supported local scale modelling of B(a)P concentrations in the vicinity of the steelworks at Port Talbot and Scunthorpe. Detailed B(a)P emission data for Port Talbot and Scunthorpe were provided by the NAEI and plant operators.

13 References

Abbott, J. (2008). Modelling re-suspended heavy metal emissions. AEA report. AEAT/ENV/R/2926 Issue 2.

Abbott, J., Stedman, J. and Bower, J. (2005). Review of background air-quality data and methods to combine these with process contributions: technical modelling aspects. A report produced on behalf of the Environment Agency by AEA Energy and Environment. Science Report: SC030174/SR2. Report available from: https://www.gov.uk/government/publications/review-of-background-air-quality-data-and-methods-to-combine-these-with-process-contributions

Abbott, J. and Vincent, K. (1999). Annual average sulphur dioxide concentration maps derived by dispersion modelling. AEA Technology, National Environmental Technology Centre. Report AEAT – 4629. https://uk-air.defra.gov.uk/assets/documents/reports/empire/kvann1/so2ann.html

Abbott, J. and Vincent, K.J. (2006). Annual audits of the contribution to pollutant concentrations from processes regulated by the Environment Agency: Application of method for current case. Environment Agency (Science Report: SC030172/SR3)

Abdalmogith, S. S., Harrison, R. M. and Derwent, R. G. (2006). Particulate sulphate and nitrate in Southern England and Northern Ireland during 2002/3 and its formation in a photochemical trajectory model. Science of the Total Environment, 368, 769-780. https://doi.org/10.1016/j.scitotenv.2006.02.047

Airborne Particles Expert Group (APEG). Source Apportionment of Airborne Particulate Matter in the United Kingdom. ISBN 0-7058-1771-7, January 1999. https://uk-air.defra.gov.uk/library/reports?report_id=32

Air Pollution in the UK 2018 (September 2019). Report for The Department for Environment, Food and Rural Affairs, Welsh Government, the Scottish Government and the Department of the Environment for Northern Ireland. https://uk-air.defra.gov.uk/library/annualreport/index

Air Quality Expert Group (AQEG, 2004). Nitrogen Dioxide in the United Kingdom. https://uk-air.defra.gov.uk/library/aqeg/publications

Air Quality Expert Group (AQEG, 2005). Particulate Matter in the United Kingdom. https://uk-air.defra.gov.uk/library/aqeg/publications

Air Quality Expert Group (AQEG, 2007). Trends in Primary NO_2 in the United Kingdom. https://uk-air.defra.gov.uk/assets/documents/reports/aqeg/primary-no-trends.pdf

Department for Business, Energy & Industrial Strategy (BEIS) (2018). Updated energy and emissions projections: 2017. https://www.gov.uk/government/publications/updated-energy-and-emissions-projections-2017

BEIS Domestic Wood Use Survey (BEIS, 2016). https://www.gov.uk/government/publications/summary-results-of-the-domestic-wood-use-survey and https://www.gov.uk/government/publications/energy-trends-march-2016-special-feature-article-summary-results-of-the-domestic-wood-use-survey

Brookes, D. M., Stedman, J. R., Grice, S. E., Kent, A. J., Walker, H. L., Cooke, S. L., Vincent, K. J., Lingard, J. J. N., Bush, T. J. and Abbott, J. (2011). UK air quality modelling under the Air Quality Directive (2008/50/EC) for 2010 covering the following air quality pollutants: SO_2, NOx, NO_2, PM_{10}, $PM_{2.5}$, lead, benzene, CO, and ozone. Report for The Department for Environment, Food and Rural Affairs, Welsh Government, the Scottish Government and the Department of the Environment for Northern Ireland. AEA report. AEAT/ENV/R/3215 Issue 1. https://uk-air.defra.gov.uk/library/reports?report_id=697

Brookes, D. M., Stedman, J. R., Kent, A. J., King, R. J., Venfield, H. L., Cooke, S. L., Lingard, J. J. N., Vincent, K. J., Bush, T. J. and Abbott, J. (2012). Technical report on UK supplementary assessment under the Air Quality Directive (2008/50/EC), the Air Quality Framework Directive (96/62/EC) and Fourth Daughter Directive (2004/107/EC) for 2011. Report for The Department for Environment, Food and Rural Affairs, Welsh Government, the Scottish Government and the Department of the

Environment for Northern Ireland. Ricardo-AEA. Report AEAT/ENV/R/3316. https://uk-air.defra.gov.uk/library/reports?report_id=768

Brookes, D. M., Stedman, J. R., Kent, A. J., Morris, R. J., Cooke, S. L., Lingard, J. J. N., Rose, R., Vincent, K. J., Bush, T. J. and Abbott, J. (2013). Technical report on UK supplementary assessment under the Air Quality Directive (2008/50/EC), the Air Quality Framework Directive (96/62/EC) and Fourth Daughter Directive (2004/107/EC) for 2012. Report for The Department for Environment, Food and Rural Affairs, Welsh Government, the Scottish Government and the Department of the Environment for Northern Ireland. Ricardo-AEA. Report Ricardo-AEA/R/3380 Issue 1. https://uk-air.defra.gov.uk/library/reports?report_id=780

Brookes, D. M., Stedman, J. R., Kent, A. J., Morris, R. J., Cooke, S. L., Lingard, J. J. N., Rose, R., Vincent, K. J., Bush, T. J. and Abbott, J. (2015). Technical report on UK supplementary assessment under the Air Quality Directive (2008/50/EC), the Air Quality Framework Directive (96/62/EC) and Fourth Daughter Directive (2004/107/EC) for 2013. Report for The Department for Environment, Food and Rural Affairs, Welsh Government, the Scottish Government and the Department of the Environment for Northern Ireland. Ricardo-AEA. Report Ricardo-AEA/R/3421 Issue 1. https://uk-air.defra.gov.uk/library/reports?report_id=797

Brookes, D. M., Stedman, J. R., Kent, A. J., Morris, R. J., Cooke, S. L., Lingard, J. J. N., Rose, R., Vincent, K. J., Bush, T. J. and Abbott, J. (2016). Technical report on UK supplementary assessment under the Air Quality Directive (2008/50/EC), the Air Quality Framework Directive (96/62/EC) and Fourth Daughter Directive (2004/107/EC) for 2014. Report for The Department for Environment, Food and Rural Affairs, Welsh Government, the Scottish Government and the Department of the Environment for Northern Ireland. Ricardo Energy & Environment. Report Ricardo Energy & Environment/R/3459. https://uk-air.defra.gov.uk/library/reports?report_id=813

Brookes, D. M., Stedman, J. R., Williams, C. J., Whiting, S. L., Kent, A. J., Morris, R. J., Rose, R. (2017). Technical report on UK supplementary assessment under the Air Quality Directive (2008/50/EC), the Air Quality Framework Directive (96/62/EC) and Fourth Daughter Directive (2004/107/EC) for 2015. Report for The Department for Environment, Food and Rural Affairs, Welsh Government, the Scottish Government and the Department of the Environment for Northern Ireland. Ricardo Energy & Environment. Report Ricardo Energy & Environment/R/3465. https://uk-air.defra.gov.uk/library/reports?report_id=910

Brookes, D. M., Stedman, J. R., Kent, A. J., Whiting, S. L., Rose, R., Williams, C. J. (2019a). Technical report on UK supplementary assessment under the Air Quality Directive (2008/50/EC), the Air Quality Framework Directive (96/62/EC) and Fourth Daughter Directive (2004/107/EC) for 2016. Report for The Department for Environment, Food and Rural Affairs, the Welsh Government, the Scottish Government and the Department of the Environment for Northern Ireland. Ricardo Energy & Environment. Report Ricardo Energy & Environment/R/3467. https://uk-air.defra.gov.uk/library/reports?report_id=933

Brookes, D. M., Stedman, J. R., Kent, A. J., Whiting, S. L., Rose, R., Williams, C. J. (2019b). Technical report on UK supplementary assessment under the Air Quality Directive (2008/50/EC), the Air Quality Framework Directive (96/62/EC) and Fourth Daughter Directive (2004/107/EC) for 2017. Report for The Department for Environment, Food and Rural Affairs, the Welsh Government, the Scottish Government and the Department of the Environment for Northern Ireland. Ricardo Energy & Environment. Report Ricardo Energy & Environment/R/3469. https://uk-air.defra.gov.uk/library/reports?report_id=965

Bush, T. (2000). Article 5 Assessment of Nitrogen Dioxide, PM10, sulphur dioxide and lead in the UK. Report to the Department for Environment, Food and Rural Affairs, the Scottish Executive, Welsh Assembly Government and the Department of the Environment in Northern Ireland. AEA Technology, National Environmental Technology Centre. Report AEAT/R/ENV/0165. https://uk-air.defra.gov.uk/library/reports?report_id=303

Bush, T. (2007). Preliminary Assessment of PAH and heavy metal levels in the UK. Report to the Department for Environment, Food and Rural Affairs, the Scottish Executive, Welsh Assembly Government and the Department of the Environment in Northern Ireland. AEA Technology, National Environmental Technology Centre. Report AEAT/R/ENV/2243. https://uk-air.defra.gov.uk/library/reports?report_id=496

Bush. T., Targa, J., (2005). Ozone Mapping Techniques for the 3rd Daughter Directive; OSRM vs Empirical modelling Comparison Report. A report to The Department for Environment, Food and Rural Affairs, Welsh Assembly Government, The Scottish Executive and the Department of the Environment for Northern Ireland. AEA Technology plc, Netcen, Harwell. Report AEAT/ENV/R/2053.

Bush, T., Targa, J., and Stedman, J. (2006). UK Air Quality modelling for annual reporting 2004 on ambient air quality assessment under Council Directives 96/62/EC and 2002/3/EC relating to ozone in ambient air. A report to the Department for Environment Food and Rural Affairs, Welsh Assembly Government, The Scottish Executive and the Department of the Environment for Northern Ireland. AEAT/ENV/R/2053. https://uk-air.defra.gov.uk/library/reports?report_id=379

Bush, T., Xu, Y., Stedman, J., and Brophy, N. (2007). UK and Gibraltar air quality modelling for annual reporting 2005 on ambient air quality assessment under Council Directives 96/62/EC and 2002/3/EC relating to ozone in ambient air. Report to Department for Environment, Food and Rural Affairs, the Scottish Executive, Welsh Assembly Government, the Department of the Environment in Northern Ireland and the Government of Gibraltar. AEA/ENV/R/2403. https://uk-air.defra.gov.uk/library/reports?report_id=456

Carslaw, D. C., Beevers, S. D., Westmoreland, E., Williams, M. L., Tate, J. E., Murrells, T., Stedman, J., Li, Y., Grice, S., Kent, A., and Tsagatakis, I. (2011). Trends in NO_x and NO_2 emissions and ambient measurements in the UK. Version: July 2011. https://uk-air.defra.gov.uk/library/reports?report_id=673

Carslaw DC, Ropkins K (2012). “openair — An R package for air quality data analysis.” Environmental Modelling & Software, 27–28(0), 52–61. ISSN 1364-8152, doi: https://doi.org/10.1016/j.envsoft.2011.09.008

CDR (2019) Reporting under air quality directives 2004/107/EC and 2008/50/EC. http://cdr.eionet.europa.eu/gb/eu/aqd/

Coleman, P., Bush, T., Conolly, C., Irons, S., Murrells, T., Vincent, K. J., and Watterson, J. (2001). Assessment of Benzo[a]pyrene Atmospheric concentrations in the UK to Support the Establishment of a National PAH Objective. Report produced for the Department for Environment, Food and Rural Affairs, the National Assembly for Wales, the Scottish Executive and the Department of the Environment for Northern Ireland. AEAT/ENV/R/0620. https://uk-air.defra.gov.uk/library/reports?report_id=24

COPERT 5 (May 2017). http://emisia.com/products/copert/copert-5

Council Directive of 7 March 1985 on air quality standards for nitrogen dioxide (85/203/EEC). From the Official Journal of the European Communities, 07/03/1985.

Council Directive 96/62/EC, of 27 September 1996. On ambient air quality assessment and management (The Framework Directive). From the Official Journal of the European Communities, 21.11.1996, En Series, L296/55.

Council Directive 1999/30/EC, of 22 April 1999 relating to limit values for sulphur dioxide, nitrogen dioxide and oxides of nitrogen, particulate matter and lead in ambient air (The First Daughter Directive). From the Official Journal of the European Communities, 29.6.1999, En Series, L163/41.

Council Directive 2000/69/EC, of 16 November 2000 relating to limit values for benzene and carbon monoxide in ambient air (The Second Daughter Directive). From the Official Journal of the European Communities, 13.12.2000, En Series, L313/12.

Council Directive 2002/3/EC, of 12 February 2002 relating to ozone in ambient air (The Third Daughter Directive). From the Official Journal of the European Communities, 9.3.2002, En Series, L67/14.

Council Directive 2004/107/EC, of 15 December 2004 relating to arsenic, cadmium, mercury, nickel and polycyclic aromatic hydrocarbons in ambient air (The Fourth Daughter Directive, AQDD4). From the Official Journal of the European Communities, 26.1.2005, En Series, L23/3.

Council Directive 2008/50/EC, of 21 May 2008. On ambient air quality and cleaner air for Europe (the ‘Air Quality Directive’ or AQD). From the Official Journal of the European Union, 11.6.2008, En series, L152/1.

Council Directive 2010/75/EU, of 24 November 2010. On industrial emissions (integrated pollution prevention and control). From the Official Journal of the European Union, 17.12.2010, En series, L334/17. Which is known as the ‘Industrial Emissions Directive’ (IED).

Coyle M., Smith R., Stedman J., Weston K. and Fowler D., (2002). Quantifying the spatial distribution of surface ozone concentration in the UK. Atmospheric Environment, 36, 1013-1024. https://doi.org/10.1016/S1352-2310(01)00303-X

Day, T., (2006). Degree-days: Theory and application. CIBSE. TM41. https://www.cibse.org/Knowledge/knowledge-items/detail?id=a0q20000008I73TAAS

Decision 2004/461/EC: Commission Decision of 29 April 2004 laying down a questionnaire to be used for annual reporting on ambient air quality assessment under Council Directives 96/62/EC and 1999/30/EC and under Directives 2000/69/EC and 2002/3/EC of the European Parliament and of the Council

Decision 2011/850/EU: Commission Implementing Decision of 12 December 2011 laying down rules for Directives 2004/107/EC and 2008/50/EC of the European Parliament and of the Council as regards the reciprocal exchange of information and reporting on ambient air quality

Department for Environment, Food and Rural Affairs (Defra) (2009). UK Notification to the European Commission to secure additional time to meet the limit values for particulate matter for certain zones/agglomerations in accordance with the Council Directive 2008/50/EC on Ambient Air Quality and Cleaner Air for Europe. https://webarchive.nationalarchives.gov.uk/20091118105042/http://www.defra.gov.uk/environment/quality/air/airquality/eu-int/eu-directives/airqual-directives/notification.htm

Department for the Environment Food and Rural Affairs (Defra), Ricardo Energy & Environment, (2018). Report on measures for 2016 exceedance of the Target Value for Nickel in Sheffield Urban Area agglomeration zone (UK0007). https://uk-air.defra.gov.uk/assets/documents/reports/bap-nickel-measures/ni_sheffield_UK0007_reportonmeasures_2016.pdf

Department for Transport (DfT) (2016). Road traffic statistics. https://www.gov.uk/government/collections/road-traffic-statistics

Design Manual for Roads and Bridges (DMRB, 2005). Volume 6, Section 1, Part 2, TD 27/05, “Cross-Sections and Headrooms”, https://www.gov.uk/guidance/standards-for-highways-online-resources

Entec. (2010). UK Ship Emissions Inventory. Retrieved from https://uk-air.defra.gov.uk/reports/cat15/1012131459_21897_Final_Report_291110.pdf

Grice, S. E., Cooke, S. L., Stedman, J. R., Bush, T. J., Vincent, K. J., Hann, M., Abbott, J. and Kent, A. J. (2009). UK air quality modelling for annual reporting 2007 on ambient air quality assessment under Council Directives 96/62/EC, 1999/30/EC and 2000/69/EC. Report to the Department for Environment, Food and Rural Affairs, the Scottish Executive, Welsh Assembly Government and the Department of the Environment in Northern Ireland. AEA report. AEAT/ENV/R/2656 Issue 1. https://uk-air.defra.gov.uk/library/reports?report_id=554

Grice, S. E., Cooke, S. L., Stedman, J. R., Bush, T. J., Vincent, K. J., Hann, M., Abbott, J. and Kent, A. J. (2010a). UK air quality modelling for annual reporting 2008 on ambient air quality assessment under Council Directives 96/62/EC, 1999/30/EC and 2000/69/EC. Report to The Department for Environment, Food and Rural Affairs, Welsh Assembly Government, the Scottish Government and the Department of the Environment for Northern Ireland. AEA report. AEAT/ENV/R/2859 Issue 1. https://uk-air.defra.gov.uk/library/reports?report_id=594

Grice, S. E., Brookes, D. M., Stedman, J. R., Kent, A. J., Walker, H. L., Cooke, S. L., Vincent, K. J., Lingard, J. J. N., Bush, T. J., Abbott, J. and Yap, F. W. (2010b). UK air quality modelling under the Air Quality Directive (2008/50/EC) for 2009 covering the following air quality pollutants: SO_2, NO_x, NO_2, PM_{10}, $PM_{2.5}$, lead, benzene, CO, and ozone. Report for The Department for Environment, Food and Rural Affairs, Welsh Assembly Government, the Scottish Government and the Department of the Environment for Northern Ireland. AEA report. AEAT/ENV/R/3069 Issue 1. https://uk-air.defra.gov.uk/library/reports?report_id=695

Harrison, R.M., Yin., J., Tilling, R.M., Cai, X., Seakins, P.W., Hopkins, J.R., Lansley, D.L., Lewis, A.C., Hunter, M.C., Heard, D.E., Carpenter, L.J., Creasey, D.J., Lee, J.D., Pilling, M.J., Carslaw, N., Emmerson, K.M., Redington, A., Derwent, R.G., Ryall, D., Mills, G. and Penkett, S.A. (2006).

Measurement and modelling of air pollution and atmospheric chemistry in the U.K. West Midlands conurbation: Overview of the PUMA consortium project. Science of the Total Environment, 360, 5-25. https://doi.org/10.1016/j.scitotenv.2005.08.053

Harrison, R. M. and Yin, J. (2006). Characterisation of particulate matter in the United Kingdom. Final Project Report. University of Birmingham. CPEA 6.

IPR 2013. Guidance on the Commission Implementing Decision laying down rules for Directives 2004/107/EC and 2008/50/EC of the European Parliament and of the Council as regards the reciprocal exchange of information and reporting on ambient air (Decision 2011/850/EU). http://ec.europa.eu/environment/air/quality/legislation/pdf/IPR_guidance1.pdf

Jenkin, M.E. (2004). Analysis of sources and partitioning of oxidant in the UK-Part 1: the NOx-dependence of annual mean concentrations of nitrogen dioxide and ozone. Atmospheric Environment, 38, 5117–5129. http://dx.doi.org/10.1016/j.atmosenv.2004.05.056

Jenkin, M.E. (2012). Investigation of the NOx-dependence of oxidant partitioning at UK sites using annual mean data 1991-2011. Report 05-12. Atmospheric Chemistry Services, Okehampton, Devon, UK. Available upon request.

Kent, A.J., Grice, S.E., Stedman, J.R., Bush, T.J., Vincent, K.J., Abbott, J., Hobson, M. and Derwent, R.G. (2007a). UK air quality modelling for annual reporting 2005 on ambient air quality assessment under Council Directives 96/62/EC, 1999/30/EC and 2000/69/EC. Report to the Department for Environment, Food and Rural Affairs, the Scottish Executive, Welsh Assembly Government and the Department of the Environment in Northern Ireland. AEA report. AEAT/ENV/R/2278 Issue 1. https://uk-air.defra.gov.uk/library/reports?report_id=453

Kent, A.J., Grice, S.E., Stedman, J.R., Cooke, S., Bush, T.J., Vincent, K.J. and Abbott, J. (2007b). UK air quality modelling for annual reporting 2006 on ambient air quality assessment under Council Directives 96/62/EC, 1999/30/EC and 2000/69/EC. Report to the Department for Environment, Food and Rural Affairs, the Scottish Executive, Welsh Assembly Government and the Department of the Environment in Northern Ireland. AEA report. AEAT/ENV/R/2502 Issue 1. https://uk-air.defra.gov.uk/library/reports?report_id=514

Kent, A.J. and Stedman, J.R. (2007). UK and Gibraltar air quality modelling for annual reporting 2006 on ambient air quality assessment under Council Directives 96/62/EC and 2002/3/EC relating to ozone in ambient air. Report to Department for Environment, Food and Rural Affairs, the Scottish Executive, Welsh Assembly Government, the Department of the Environment in Northern Ireland and the Government of Gibraltar. AEA/ENV/R/2499. https://uk-air.defra.gov.uk/library/reports?report_id=526

Kent, A.J. and Stedman, J.R. (2008). UK and Gibraltar air quality modelling for annual reporting 2007 on ambient air quality assessment under Council Directives 96/62/EC and 2002/3/EC relating to ozone in ambient air. Report to Department for Environment, Food and Rural Affairs, the Scottish Executive, Welsh Assembly Government, the Department of the Environment in Northern Ireland and the Government of Gibraltar. AEA/ENV/R/2681. https://uk-air.defra.gov.uk/library/reports?report_id=552

Kent, A.J., Stedman, J.R., Yap, F. W. (2010). UK and Gibraltar air quality modelling for annual reporting 2008 on ambient air quality assessment under Council Directives 96/62/EC and 2002/3/EC relating to ozone in ambient air. Report to Department for Environment, Food and Rural Affairs, the Scottish Executive, Welsh Assembly Government, the Department of the Environment in Northern Ireland and the Government of Gibraltar. AEA Technology Energy & Environment. AEA/ENV/R/3097. https://uk-air.defra.gov.uk/library/reports?report_id=595

Land Cover Map 2000 (2009). https://www.ceh.ac.uk/services/land-cover-map-2000

Lee, D.S., Kingdon, R.D., Jenkin, M.E. and Garland, J.A. (2000). Modelling the atmospheric oxidised and reduced nitrogen budgets for the UK with a Lagrangian multi-layer long-range transport model. Environmental Modelling and Assessment, 5, 83-104. https://doi.org/10.1023/A:1019049325337

Murrells, T., Cooke, S., Kent, A., Grice, S., Derwent, R., Jenkin, M., Pilling, M., Rickard, A. and Redington, A., (2008). Modelling of Tropospheric Ozone: First Annual Report. AEA Report AEAT/ENV/R/2567. https://uk-air.defra.gov.uk/library/reports?report_id=510

Murrells, T., Cooke, S., Abbott, J., Fraser, A., Derwent, R., Jenkin, M., Rickard, A., Young, J. (2011). Modelling of Tropospheric Ozone Annual Report 2010. AEA report. AEAT/ENV/R/3134 Issue 1. https://uk-air.defra.gov.uk/library/reports?report_id=856

NETS 2011 SYS. The National Grid Seven Year Statement 2011, http://www2.nationalgrid.com/UK/Industry-information/Future-of-Energy/Electricity-ten-year-statement/SYS-Archive/.

NEGTAP 2001, Transboundary Air Pollution: Acidification, Eutrophication and Ground-level ozone in the UK. Prepared by the National Expert Group on Transboundary Air Pollution (NEGTAP) on behalf of the Department for Environment, Food and Rural Affairs, the Scottish Executive, Welsh Assembly Government and the Department of the Environment in Northern Ireland. ISBN 1 870393 61 9. https://uk-air.defra.gov.uk/library/reports?report_id=109

Personal communication from Neil Passant, Ricardo Energy & Environment (2017). Ricardo Energy & Environment, Harwell, UK.

Personal communication from Neil Passant, Ricardo Energy & Environment (2018a). Ricardo Energy & Environment, Harwell, UK.

Personal communication from Neil Passant, Ricardo Energy & Environment (2018b). Ricardo Energy & Environment, Harwell, UK.

Personal communication from Neil Passant, Ricardo Energy & Environment (2019). Ricardo Energy & Environment, Harwell, UK.

PORG (UK Photochemical Oxidants Review Group), 1998. Ozone in the UK. 4th report of the UK Photochemical Oxidants Review Group, 1st Edition. The Department of the Environment Transport and the Regions. https://uk-air.defra.gov.uk/library/reports?report_id=108

Redington, A.L., Derwent, R.G., Witham, C.S., Manning, A.J., 2009. Sensitivity of modelled sulphate and nitrate aerosol to cloud, pH and ammonia emissions. Atmospheric Environment 43, 3227-3234. https://doi.org/10.1016/j.atmosenv.2009.03.041

Redington, A.L., Derwent, R.G. Modelling Secondary Organic Aerosol in the United Kingdom, 2013. Atmospheric Environment 64, 349-357. https://doi.org/10.1016/j.atmosenv.2012.09.074

Richmond B, Misra A, Broomfield M, Brown P, Karagianni E, Murrells T, Pang Y, Passant N, Pearson B, Stewart R, Thistlethwaite G, Wakeling D, Walker C, Wiltshire J, Hobson M, Gibbs M, Misselbrook T, Dragosits U, Tomlinson S (2019). UK Informative Inventory Report (1990 to 2017). National Atmospheric Emissions Inventory, Ricardo Energy & Environment. https://naei.beis.gov.uk/reports/reports?report_id=978

Stedman, J. R. and Bush, T. (2000). Mapping of nitrogen dioxide and PM_{10} in the UK for Article 5 Assessment. AEA Technology, National Environmental Technology Centre. Report AEAT/ENV/R/0707. https://uk-air.defra.gov.uk/library/reports?report_id=96

Stedman, J.R., Bush, T.J., Murrells, T.P. and King, K. (2001a). Baseline PM_{10} and NO_x projections for PM_{10} objective analysis. AEA Technology, National Environmental Technology Centre. Report AEAT/ENV/R/0726. https://uk-air.defra.gov.uk/library/reports?report_id=17

Stedman, J.R., Goodwin, J.W.L., King, K., Murrells, T.P. and Bush, T.J. (2001b). An Empirical Model For Predicting Urban Roadside Nitrogen Dioxide Concentrations in the UK. Atmospheric Environment. 35 1451-1463. http://dx.doi.org/10.1016/S1352-2310(00)00363-0

Stedman, J.R., Bush, T.J. and Vincent, K.J. (2002). UK air quality modelling for annual reporting 2001 on ambient air quality assessment under Council Directives 96/62/EC and 1999/30/EC. AEA Technology, National Environmental Technology Centre. Report AEAT/ENV/R/1221. https://uk-air.defra.gov.uk/library/reports?report_id=158

Stedman, J.R., Bush, T.J., Vincent, K.J. and Baggott S. (2003). UK air quality modelling for annual reporting 2002 on ambient air quality assessment under Council Directives 96/62/EC and 1999/30/EC. AEA Technology, National Environmental Technology Centre. Report AEAT/ENV/R/1564. https://uk-air.defra.gov.uk/library/reports?report_id=232

Stedman, J. R., Bush, T. J., Grice, S. E., Kent, A. J., Vincent, K. J. and Abbott, J. (2005). UK air quality modelling for annual reporting 2003 on ambient air quality assessment under Council Directives 96/62/EC, 1999/30/EC and 2000/69/EC. AEA Technology, National Environmental Technology Centre. Report AEAT/ENV/R/1790. https://uk-air.defra.gov.uk/library/reports?report_id=284

Stedman, J. R., Bush, T. J., Grice, S. E., Kent, A. J., Vincent, K. J., Abbott, J. and Derwent, R. G. (2006). UK air quality modelling for annual reporting 2004 on ambient air quality assessment under Council Directives 96/62/EC, 1999/30/EC and 2000/69/EC. AEA Technology, National Environmental Technology Centre. Report AEAT/ENV/R/2052. https://uk-air.defra.gov.uk/library/reports?report_id=416

Stedman, J. R., Kent, A. J., Grice, S., Bush, T. J. and Derwent, R. G. (2007). A consistent method for modelling PM_{10} and $PM_{2.5}$ concentrations across the United Kingdom in 2004 for air quality assessment. Atmospheric Environment, 41, 161-172. https://doi.org/10.1016/j.atmosenv.2006.07.048

Tang, Y.S., Braban, C. F., Twigg, M. M., Jones, M. R., Poskitt, J., Nemitz, E., Sutton, M.A., Simmons, I., van Dijk, N., Cape, J.N. (2015). Development of a new model DELTA sampler and assessment of potential sampling artefacts in the UKEAP AGANet DELTA system. Report for the UK Department for Environment, Food and Rural Affairs (DEFRA) and NERC. Centre for Ecology and Hydrology (CEH). https://uk-air.defra.gov.uk/library/reports?report_id=861

Tsagatakis, I., Ruddy, M., Richardson, J., Otto, A., Pearson, B., Passant, N. (2019). UK Emission Mapping Methodology. A report of the National Atmospheric Emissions Inventory 2017, Ricardo Energy & Environment. https://naei.beis.gov.uk/reports/reports?report_id=997Personal communication from Brian Underwood, AEA (2009). AEA Technology, Harwell, UK.

Sotiris Vardoulakis, Bernard E.A Fisher, Koulis Pericleous, Norbert Gonzalez-Flesca, Modelling air quality in street canyons: a review, Atmospheric Environment, Volume 37, Issue 2, January 2003, Pages 155-182, ISSN 1352-2310, https://doi.org/10.1016/S1352-2310(02)00857-9

Vincent, K., Bush, T. and Coleman, P. (2007) Assessment of Benzo[a]Pyrene Concentrations in the UK in 2005, 2010, 2015 and 2020. Report to The Department for Environment, Food and Rural Affairs, Welsh Assembly Government, the Scottish Executive and the Department of the Environment for Northern Ireland. AEA report. AEA/ENV/R/2373 Issue 1. https://uk-air.defra.gov.uk/library/reports?report_id=467

Vincent, K. J., Bush, T. and Telling, S. (2010). Preliminary Assessment for the Ambient Air Quality Directive (2008/50/EC) for the United Kingdom. Report to The Department for Environment, Food and Rural Affairs, Welsh Assembly Government, the Scottish Government and the Department of the Environment for Northern Ireland. AEA report. AEAT/ENV/R/2961 Issue 1. https://uk-air.defra.gov.uk/library/reports?report_id=638

Vincent, K. and Tsagatakis, I. (2014). Local scale modelling of Benzo[a]Pyrene concentrations in Northern Ireland. Report for The Department for Environment, Food and Rural Affairs, Welsh Government, the Scottish Government and the Department of the Environment for Northern Ireland. Ricardo-AEA. Report Ricardo-AEA/R/3404.

Walker, H. L., Kent, A. J., Stedman, J. R., Grice, S. E., Vincent, K. J., Yap, F. W., Brookes, D. M. (2010). UK modelling under the Air Quality Framework Directive (96/62/EC) and Fourth Daughter Directive (2004/30/EC) for 2009 covering As, Cd, Ni and B(a)P. Report for The Department for Environment, Food and Rural Affairs, Welsh Assembly Government, the Scottish Government and the Department of the Environment for Northern Ireland. AEA report. AEAT/ENV/R/3070 Issue 1. https://uk-air.defra.gov.uk/library/reports?report_id=694

Walker, H. L., Kent, A. J., Stedman, J. R., Brookes, D. M., Vincent, K. J. (2011). UK modelling under the Air Quality Framework Directive (96/62/EC) and Fourth Daughter Directive (2004/30/EC) for 2010 covering As, Cd, Ni and B(a)P. Report for The Department for Environment, Food and Rural Affairs, Welsh Government, the Scottish Government and the Department of the Environment for Northern Ireland. AEA report. AEAT/ENV/R/3216 Issue 1. https://uk-air.defra.gov.uk/assets/documents/reports/cat09/1204301510_dd42010mapsrep_v0.pdf

Yap, F.W., Kent, A.J., Stedman, J.R., Grice, S.E. and Vincent, K.J. (2009). UK air quality modelling for annual reporting 2008 on ambient air quality assessment under Council Directives 96/62/EC, 1999/30/EC and 2004/107/EC. Report to The Department for Environment, Food and Rural Affairs, Welsh Assembly Government, the Scottish Government and the Department of the Environment for Northern Ireland. AEA Report. AEAT/ENV/R/2860 Issue 1. https://uk-air.defra.gov.uk/library/reports?report_id=596

Appendices

Appendix 1 - Monitoring sites used to verify the mapped estimates

Table A1.1 lists the air quality monitoring network names for the sites used to verify the 2018 model output of the pollutants, which are given in Table A1.2. Table A1.2 also lists additional monitoring sites, operated by Hanson Building Products Ltd., which are used to verify the SO_2 models, and INEOS, which are used to verify the benzene modelling.

Table A1.1 Air quality monitoring network and URL

Air quality monitoring network/data provider	Abbreviation	URL
Air Quality England	AQE	http://www.airqualityengland.co.uk/
Welsh Air Quality Network	WAQN	https://airquality.gov.wales/
Heathrow Airwatch		http://www.heathrowairwatch.org.uk/
London Air Quality Network*	LAQN	http://www.londonair.org.uk/LondonAir/Default.aspx
Northern Ireland Automatic Urban Network	NIAUN	http://www.airqualityni.co.uk/
Scottish Automatic Rural Network	SARN	http://www.scottishairquality.co.uk/
Scottish Automatic Urban Network	SAUN	http://www.scottishairquality.co.uk/
ERG*		

***** Data extracted using the OpenAir (Carslaw and Ropkins, 2012) import KCL function from a database of air quality monitoring data made available by King's College London Environmental Research group (ERG). Data was extracted on 18/06/2019.

Table A1.2 Monitoring sites available for verification of the mapped estimates (PM_{10} measurements by Osiris instruments were not included in the verification)

Site name	Site type	Network	NO_X, NO_2	PM_{10}	$PM_{2.5}$	SO_2	O_3	C_6H_6
Barking and Dagenham - Rush Green	Suburban	London Air Quality Network	Y			Y		
Barking and Dagenham - Scrattons Farm	Suburban	London Air Quality Network	Y	Y				
Bexley - Belvedere	Suburban	London Air Quality Network	Y	Y				
Bexley - Belvedere West	Urban Background	London Air Quality Network	Y	Y			Y	
Brent - ARK Franklin Primary Academy	Roadside	London Air Quality Network	Y	Y				
Brent - Ikea	Roadside	London Air Quality Network	Y	Y			Y	

Site name	Site type	Network	NO_X, NO_2	PM_{10}	$PM_{2.5}$	SO_2	O_3	C_6H_6
Brent - John Keble Primary School	Roadside	London Air Quality Network	Y	Y				
Brent - Neasden Lane	Industrial	London Air Quality Network	Y					
Castle Point - Hadleigh	Roadside	London Air Quality Network	Y					
Chichester - A27 Chichester Bypass	Roadside	London Air Quality Network	Y					
Chichester - Lodsworth	Rural	London Air Quality Network					Y	
Chichester - Orchard Street	Roadside	London Air Quality Network	Y					
City of London - Beech Street	Roadside	London Air Quality Network	Y	Y				
City of London - Farringdon Street	Kerbside	London Air Quality Network			Y			
City of London - Sir John Cass School	Urban Background	London Air Quality Network	Y		Y			
City of London - Walbrook Wharf	Roadside	London Air Quality Network	Y					
Crawley - Gatwick Airport	Urban Background	London Air Quality Network	Y					
Croydon - Norbury	Kerbside	London Air Quality Network	Y					
Croydon - Norbury Manor	Urban Background	London Air Quality Network			Y			
Croydon - Park Lane	Roadside	London Air Quality Network	Y	Y				
Croydon - Purley Way A23	Roadside	London Air Quality Network	Y					

Site name	Site type	Network	NO_X, NO_2	PM_{10}	$PM_{2.5}$	SO_2	O_3	C_6H_6
Ealing - Acton Vale	Urban Background	London Air Quality Network	Y	Y				
Ealing - Hanger Lane Gyratory	Roadside	London Air Quality Network	Y	Y				
Ealing - Western Avenue	Roadside	London Air Quality Network	Y	Y				
Eastbourne - Devonshire Park	Urban Background	London Air Quality Network	Y				Y	
Eastleigh - Southampton Road	Roadside	London Air Quality Network	Y	Y				
Eastleigh - Steele Close	Urban Background	London Air Quality Network	Y					
Enfield - Bowes Primary School	Roadside	London Air Quality Network	Y					
Enfield - Bush Hill Park	Suburban	London Air Quality Network	Y					
Enfield - Derby Road	Roadside	London Air Quality Network	Y			Y		
Enfield - Prince of Wales School	Urban Background	London Air Quality Network	Y					
Greenwich - A206 Burrage Grove	Roadside	London Air Quality Network	Y		Y			
Greenwich - Blackheath	Roadside	London Air Quality Network	Y	Y				
Greenwich - Falconwood	Roadside	London Air Quality Network	Y	Y			Y	
Greenwich - Falconwood FDMS	Roadside	London Air Quality Network			Y			
Greenwich - Fiveways Sidcup Rd A20	Roadside	London Air Quality Network	Y	Y				

Site name	Site type	Network	NO_X, NO_2	PM_{10}	$PM_{2.5}$	SO_2	O_3	C_6H_6
Greenwich - Plumstead High Street	Roadside	London Air Quality Network	Y		Y		Y	
Greenwich - Trafalgar Road (Hoskins St)	Roadside	London Air Quality Network	Y	Y				
Greenwich - Westhorne Avenue	Roadside	London Air Quality Network	Y	Y	Y		Y	
Greenwich - Woolwich Flyover	Roadside	London Air Quality Network	Y	Y			Y	
Hackney - Old Street	Roadside	London Air Quality Network	Y	Y			Y	
Harrow - Pinner Road	Roadside	London Air Quality Network	Y	Y				
Hastings - Bulverhythe	Roadside	London Air Quality Network	Y	Y				
Havering - Rainham	Roadside	London Air Quality Network	Y	Y	Y			
Havering - Romford	Roadside	London Air Quality Network	Y	Y				
Horsham - Cowfold	Roadside	London Air Quality Network	Y					
Horsham - Park Way	Roadside	London Air Quality Network	Y	Y				
Islington - Arsenal	Urban Background	London Air Quality Network	Y					
Islington - Holloway Road	Roadside	London Air Quality Network	Y	Y				
Kensington and Chelsea - North Ken FIDAS	Urban Background	London Air Quality Network		Y	Y			
Kingston Upon Thames - Tolworth Broadway	Roadside	London Air Quality Network	Y	Y				

Site name	Site type	Network	NO_X, NO_2	PM_{10}	$PM_{2.5}$	SO_2	O_3	C_6H_6
Lambeth - Bondway Interchange	Industrial	London Air Quality Network	Y			Y		
Lambeth - Brixton Road	Kerbside	London Air Quality Network	Y	Y				
Lambeth - Streatham Green	Urban Background	London Air Quality Network	Y	Y				
Leicester - Abbey Lane	Roadside	London Air Quality Network	Y	Y				
Leicester - Glenhills Way	Roadside	London Air Quality Network	Y	Y				
Leicester - Melton Road	Roadside	London Air Quality Network	Y					
Leicester - St Matthews Way	Roadside	London Air Quality Network	Y					
Leicester - Vaughan Way	Roadside	London Air Quality Network	Y	Y				
Lewes - West Street	Roadside	London Air Quality Network	Y	Y				
Lewisham - Catford	Urban Background	London Air Quality Network	Y					
Lewisham - Loampit Vale	Roadside	London Air Quality Network	Y					
Lewisham - New Cross	Roadside	London Air Quality Network	Y	Y	Y			
London Teddington Bushy Park	Suburban	London Air Quality Network			Y			
Merton - Morden Civic Centre 2	Roadside	London Air Quality Network	Y					
Redbridge - Gardner Close	Roadside	London Air Quality Network	Y	Y				

Site name	Site type	Network	NO_X, NO_2	PM_{10}	$PM_{2.5}$	SO_2	O_3	C_6H_6
Redbridge - Ley Street	Urban Background	London Air Quality Network	Y	Y	Y		Y	
Reigate and Banstead - Horley South East	Suburban	London Air Quality Network	Y					
Reigate and Banstead - Poles Lane	Rural	London Air Quality Network	Y				Y	
Richmond Upon Thames - Barnes Wetlands	Suburban	London Air Quality Network	Y				Y	
Richmond Upon Thames - Castelnau	Roadside	London Air Quality Network	Y	Y				
Richmond Upon Thames - Chertsey Road	Roadside	London Air Quality Network	Y					
Rother - De La Warr Road	Roadside	London Air Quality Network	Y					
Rother - Rye Harbour	Rural	London Air Quality Network					Y	
Sevenoaks - Bat and Ball	Roadside	London Air Quality Network	Y	Y				
Sevenoaks - Greatness Park	Urban Background	London Air Quality Network	Y				Y	
Southampton - Onslow Road	Roadside	London Air Quality Network	Y					
Southampton - Victoria Road	Roadside	London Air Quality Network	Y					
Southwark - Elephant and Castle	Urban Background	London Air Quality Network	Y	Y			Y	
Sutton - Beddington Lane	Industrial	London Air Quality Network	Y	Y				
Sutton - Beddington Lane north	Industrial	London Air Quality Network	Y	Y	Y			

Site name	Site type	Network	NO_X, NO_2	PM_{10}	$PM_{2.5}$	SO_2	O_3	C_6H_6
Sutton - Wallington	Kerbside	London Air Quality Network	Y	Y				
Sutton - Worcester Park	Kerbside	London Air Quality Network	Y					
Thurrock - Calcutta Road Tilbury	Roadside	London Air Quality Network	Y					
Thurrock - London Road (Purfleet)	Roadside	London Air Quality Network	Y	Y				
Tower Hamlets - Blackwall	Roadside	London Air Quality Network	Y		Y		Y	
Wandsworth - Lavender Hill (Clapham Jct)	Roadside	London Air Quality Network	Y	Y				
Wandsworth - Putney	Urban Background	London Air Quality Network	Y	Y				
Wandsworth - Putney High Street	Kerbside	London Air Quality Network	Y					
Wandsworth - Putney High Street Facade	Roadside	London Air Quality Network	Y					
Wandsworth - Tooting High Street	Roadside	London Air Quality Network	Y	Y				
Wandsworth - Wandsworth Town Hall	Urban Background	London Air Quality Network	Y				Y	
Wealden - Isfield	Rural	London Air Quality Network					Y	
Westminster - Covent Garden	Urban Background	London Air Quality Network	Y					
Westminster - Oxford Street	Kerbside	London Air Quality Network	Y	Y				
Windsor and Maidenhead - Aldebury Road	Urban Background	London Air Quality Network	Y					

Site name	Site type	Network	NO_X, NO_2	PM_{10}	$PM_{2.5}$	SO_2	O_3	C_6H_6
Windsor and Maidenhead - Clarence Road	Roadside	London Air Quality Network	Y					
Windsor and Maidenhead - Frascati Way	Roadside	London Air Quality Network	Y	Y				
Barnsley A628 Pogmoor Roadside	Roadside	Air Quality England	Y					
Barnsley A635 Kendray Roadside	Roadside	Air Quality England		Y				
Bedford Lurke Street	Traffic	Air Quality England	Y					
Bedford Prebend Street	Traffic	Air Quality England	Y					
Birmingham Airport 2	Airport	Air Quality England	Y	Y		Y	Y	
Bradford-on-Avon Masons Lane	Roadside	Air Quality England	Y	Y				
Breckland East Wretham	Rural	Air Quality England	Y	Y			Y	
Breckland Swaffham	Roadside	Air Quality England	Y					
Bury Prestwich	Roadside	Air Quality England	Y	Y				
Bury Radcliffe	Roadside	Air Quality England	Y	Y				
Cam Road	Traffic	Air Quality England	Y	Y				
Cambridge Gonville Place	Roadside	Air Quality England	Y	Y	Y			
Cambridge Montague Road	Roadside	Air Quality England	Y	Y				
Cambridge Newmarket Road	Roadside	Air Quality England	Y		Y			
Cambridge Parker Street	Roadside	Air Quality England	Y	Y				
Dacorum Northchurch High Street	Traffic	Air Quality England	Y	Y	Y			
Devizes Sidmouth Street	Roadside	Air Quality England	Y	Y				
Earls Court Road	Roadside	Air Quality England	Y	Y				
East Herts Hertford Gascoyne Way	Traffic	Air Quality England	Y		Y			

Site name	Site type	Network	NO_X, NO_2	PM_{10}	$PM_{2.5}$	SO_2	O_3	C_6H_6
Fareham Portland Street	Traffic	Air Quality England	Y					
Farnham The Woolmead	Roadside	Air Quality England	Y	Y				
Gateshead A1 Dunston	Roadside	Air Quality England	Y		Y			
Gateshead Lychgate Court	Roadside	Air Quality England	Y		Y			
Girton Road	Traffic	Air Quality England	Y	Y	Y			
Gosport Road	Traffic	Air Quality England	Y					
Great Yarmouth South Denes	Urban Background	Air Quality England	Y	Y	Y			
Heathrow Green Gates	Airport	Air Quality England	Y	Y	Y			
Heathrow LHR2	Airport	Air Quality England	Y	Y	Y			
Heathrow Oaks Road	Airport	Air Quality England	Y	Y	Y			
Helsby	Urban Background	Air Quality England		Y	Y			
Henley	Roadside	Air Quality England	Y					
Hertsmere Borehamwood Bowling Club	Urban Background	Air Quality England		Y	Y			
Hertsmere Borehamwood Roadside	Roadside	Air Quality England	Y	Y	Y			
Hillingdon 1 - South Ruislip	Roadside	Air Quality England	Y	Y				
Hitchin Stevenage Road	Traffic	Air Quality England	Y					
Hitchin Stevenage Road Particulates	Roadside	Air Quality England		Y	Y			
Hounslow Brentford	Roadside	Air Quality England	Y	Y	Y			
Hounslow Chiswick	Roadside	Air Quality England	Y	Y	Y			
Hounslow Feltham	Traffic	Air Quality England	Y	Y				
Hounslow Gunnersbury	Traffic	Air Quality England	Y	Y				

Site name	Site type	Network	NO_X, NO_2	PM_{10}	$PM_{2.5}$	SO_2	O_3	C_6H_6
Hounslow Hatton Cross	Roadside	Air Quality England	Y	Y				
Hounslow Heston	Roadside	Air Quality England	Y	Y				
Huntingdon Pathfinder House	Roadside	Air Quality England	Y	Y	Y			
Ipswich Chevallier Street	Roadside	Air Quality England	Y					
London Barnet Chalgrove School	Urban Background	Air Quality England	Y	Y				
London Hillingdon Harmondsworth	Urban Background	Air Quality England	Y	Y				
London Hillingdon Harmondsworth Os	Urban Background	Air Quality England		Y	Y			
London Hillingdon Hayes	Roadside	Air Quality England	Y	Y				
London Hillingdon Oxford Avenue	Urban Centre	Air Quality England	Y	Y				
London Luton Airport	Urban	Air Quality England		Y				
Luton Dunstable Road East	Traffic	Air Quality England	Y	Y	Y			
Manchester Oxford Road	Kerbside	Air Quality England	Y	Y				
New Forest - Fawley	Urban Industrial	Air Quality England		Y		Y		
Oxford St Ebbes (Cal Club)	Urban Background	Air Quality England					Y	
Plymouth Mutley Plain	Roadside	Air Quality England	Y					
Reading Caversham Road	Roadside	Air Quality England	Y	Y				
Reading Oxford Road	Roadside	Air Quality England	Y	Y				
Redcar Dormanstown	Industrial	Air Quality England	Y	Y		Y	Y	
S Cambs Impington	Roadside	Air Quality England	Y	Y				
S Cambs Orchard Park School	Urban Background	Air Quality England	Y	Y				
Salford M60	Roadside	Air Quality England	Y	Y	Y		Y	
Salisbury Exeter Street	Roadside	Air Quality England	Y	Y				

Site name	Site type	Network	NO_X, NO_2	PM_{10}	$PM_{2.5}$	SO_2	O_3	C_6H_6
Sipson	Urban Background	Air Quality England	Y					
Slough Brands Hill London Road	Roadside	Air Quality England	Y	Y				
Slough Chalvey	Roadside	Air Quality England	Y					
Slough Colnbrook	Urban Background	Air Quality England	Y	Y				
Slough Colnbrook Osiris	Urban Background	Air Quality England		Y	Y			
Slough Lakeside 1 Osiris	Urban Background	Air Quality England		Y	Y			
Slough Lakeside 2	Urban Background	Air Quality England	Y	Y				
Slough Lakeside 2 Osiris	Urban Background	Air Quality England		Y	Y			
Slough Town Centre A4	Urban Background	Air Quality England	Y	Y				
Slough Town Centre Wellington Street	Roadside	Air Quality England	Y					
Slough Windmill Bath Road	Roadside	Air Quality England	Y	Y				
South Holland Westmere School	Rural	Air Quality England	Y	Y			Y	
Spalding Monkhouse School	Urban Background	Air Quality England	Y	Y				
Spelthorne Sunbury Cross	Urban Background	Air Quality England	Y	Y	Y			
Stevenage Lytton Way	Roadside	Air Quality England	Y		Y			
Stockport Cheadle A34	Roadside	Air Quality England	Y	Y				
Stockport Hazel Grove	Roadside	Air Quality England	Y	Y				
Suffolk Coastal Woodbridge 2	Roadside	Air Quality England	Y					
Tally Ho	Kerbside	Air Quality England	Y	Y				
Tameside Mottram Moor	Traffic	Air Quality England	Y	Y				
Tichborne Way	Roadside	Air Quality England	Y	Y				
Tower Hamlets - Millwall Park	Background	Air Quality England	Y	Y			Y	

Site name	Site type	Network	NO_X, NO_2	PM_{10}	$PM_{2.5}$	SO_2	O_3	C_6H_6
Tower Hamlets - Victoria Park	Background	Air Quality England	Y	Y		Y		
Trafford	Urban Background	Air Quality England	Y	Y				
Trafford A56	Roadside	Air Quality England	Y	Y				
Trafford Wellacre Academy	Urban Background	Air Quality England	Y					
Wallingford	Roadside	Air Quality England	Y					
Waltham Crooked Billet	Kerbside	Air Quality England	Y	Y				
Waltham Forest Dawlish Rd	Urban Background	Air Quality England	Y	Y				
Waltham Forest Leyton	Urban Background	Air Quality England	Y	Y				
Watford Town Hall	Traffic	Air Quality England	Y	Y	Y			
Watlington	Traffic	Air Quality England	Y					
Welwyn Hatfield	Roadside	Air Quality England			Y			
Widnes Marzahn Way	Kerbside	Air Quality England	Y	Y				
Wootton Bassett High Street	Roadside	Air Quality England	Y					
Wren Close	Traffic	Air Quality England	Y	Y				
Wycombe Stokenchurch	Roadside	Air Quality England	Y					
York Fulford Road	Roadside	Air Quality England	Y					
York Gillygate	Roadside	Air Quality England	Y		Y			
York Heworth Green	Roadside	Air Quality England	Y					
York Holgate	Roadside	Air Quality England	Y	Y				
York Lawrence Street	Roadside	Air Quality England	Y					
York Nunnery Lane	Roadside	Air Quality England	Y					
York Plantation Drive	Roadside	Air Quality England		Y				

Site name	Site type	Network	NO_X, NO_2	PM_{10}	$PM_{2.5}$	SO_2	O_3	C_6H_6
Bradley Fen	Brick-Works	Hanson Building Products Limited				Y		
Whittlesey	Brick-Works	Hanson Building Products Limited				Y		
7 Melrose Drive Grangemouth	Refinery	Ineos						Y
Abbotsinch173 Boness Road Grangemouth	Refinery	Ineos						Y
Beechwood Low Causeway Culross Fife	Refinery	Ineos						Y
KG Gate	Refinery	Ineos						Y
Kinneil Kerse near boundary fence of Kinneil Gas Plant	Refinery	Ineos						Y
Kinneil Kerse on road near Waste Tip	Refinery	Ineos						Y
Mercer Street Kincardine Fife	Refinery	Ineos						Y
Road Station Gate 1	Refinery	Ineos						Y
Stores/Poly Gate 14	Refinery	Ineos						Y
Technical Building Gate 4	Refinery	Ineos						Y
Belfast Newtownards Road	Roadside	Northern Ireland Automatic Urban Network	Y					
Belfast Ormeau Road	Roadside	Northern Ireland Automatic Urban Network	Y					
Belfast Westlink Roden Street	Roadside	Northern Ireland Automatic Urban Network	Y					
Castlereagh Dundonald	Roadside	Northern Ireland Automatic	Y					

Site name	Site type	Network	NO_X, NO_2	PM_{10}	$PM_{2.5}$	SO_2	O_3	C_6H_6
		Urban Network						
Derry Dales Corner	Roadside	Northern Ireland Automatic Urban Network	Y					
Downpatrick Roadside	Roadside	Northern Ireland Automatic Urban Network	Y					
Lisburn Dunmurry Seymour Hill	Urban Background	Northern Ireland Automatic Urban Network		Y		Y		
Newry Canal Street	Roadside	Northern Ireland Automatic Urban Network	Y	Y				
Newtownabbey Antrim Road	Roadside	Northern Ireland Automatic Urban Network	Y					
North Down Holywood A2	Roadside	Northern Ireland Automatic Urban Network	Y	Y				
Strabane Springhill Park	Urban Background	Northern Ireland Automatic Urban Network		Y		Y		
Glasgow Waulkmillglen Reservoir	Rural	Scottish Automatic Rural Network	Y	Y	Y		Y	
Aberdeen Anderson Dr	Roadside	Scottish Automatic Urban Network	Y	Y				

Site name	Site type	Network	NO_X, NO_2	PM_{10}	$PM_{2.5}$	SO_2	O_3	C_6H_6
Aberdeen King Street	Roadside	Scottish Automatic Urban Network	Y	Y	Y			
Aberdeen Market Street 2	Roadside	Scottish Automatic Urban Network	Y	Y	Y			
Alloa A907	Roadside	Scottish Automatic Urban Network	Y	Y	Y			
Angus Forfar Glamis Rd	Roadside	Scottish Automatic Urban Network		Y				
Dundee Broughty Ferry Road	Urban Industrial	Scottish Automatic Urban Network	Y	Y				
Dundee Lochee Road	Kerbside	Scottish Automatic Urban Network	Y	Y	Y			
Dundee Meadowside	Roadside	Scottish Automatic Urban Network	Y	Y				
Dundee Seagate	Kerbside	Scottish Automatic Urban Network	Y	Y				
Dundee Whitehall Street	Roadside	Scottish Automatic Urban Network	Y	Y				
E Ayrshire Kilmarnock St Marnock St	Roadside	Scottish Automatic Urban Network	Y	Y	Y			
East Dunbartonshire Bearsden	Roadside	Scottish Automatic Urban Network	Y	Y				
East Dunbartonshire Bishopbriggs	Roadside	Scottish Automatic	Y	Y				

Site name	Site type	Network	NO_X, NO_2	PM_{10}	$PM_{2.5}$	SO_2	O_3	C_6H_6
		Urban Network						
East Dunbartonshire Kirkintilloch	Roadside	Scottish Automatic Urban Network	Y	Y	Y			
East Dunbartonshire Milngavie	Roadside	Scottish Automatic Urban Network	Y	Y				
East Lothian Musselburgh N High St	Roadside	Scottish Automatic Urban Network	Y	Y				
Edinburgh Currie	Suburban	Scottish Automatic Urban Network	Y	Y				
Edinburgh Glasgow Road	Roadside	Scottish Automatic Urban Network	Y	Y				
Edinburgh Gorgie Road	Roadside	Scottish Automatic Urban Network	Y					
Edinburgh Queensferry Road	Roadside	Scottish Automatic Urban Network	Y	Y				
Edinburgh Salamander St	Roadside	Scottish Automatic Urban Network	Y	Y				
Edinburgh St Johns Road	Kerbside	Scottish Automatic Urban Network	Y	Y	Y			
Falkirk Banknock	Roadside	Scottish Automatic Urban Network		Y	Y			
Falkirk Boness	Urban Industrial	Scottish Automatic Urban Network				Y		

Site name	Site type	Network	NO_X, NO_2	PM_{10}	$PM_{2.5}$	SO_2	O_3	C_6H_6
Falkirk Grangemouth MC	Urban Background	Scottish Automatic Urban Network	Y	Y		Y		
Falkirk Grangemouth Zetland Park	Urban Industrial	Scottish Automatic Urban Network				Y		
Falkirk Haggs	Roadside	Scottish Automatic Urban Network	Y	Y				
Falkirk Hope St	Roadside	Scottish Automatic Urban Network	Y	Y		Y		
Falkirk Main St Bainsford	Roadside	Scottish Automatic Urban Network	Y	Y				
Falkirk West Bridge Street	Roadside	Scottish Automatic Urban Network	Y	Y	Y			
Fife Cupar	Roadside	Scottish Automatic Urban Network	Y	Y	Y			
Fife Dunfermline	Roadside	Scottish Automatic Urban Network	Y	Y	Y			
Fife Kirkcaldy	Roadside	Scottish Automatic Urban Network	Y	Y	Y			
Fife Rosyth	Roadside	Scottish Automatic Urban Network	Y	Y	Y			
Glasgow Anderston	Urban Background	Scottish Automatic Urban Network	Y	Y	Y			
Glasgow Burgher St.	Roadside	Scottish Automatic	Y	Y				

Site name	Site type	Network	NO_x, NO_2	PM_{10}	$PM_{2.5}$	SO_2	O_3	C_6H_6
		Urban Network						
Glasgow Byres Road	Roadside	Scottish Automatic Urban Network	Y	Y	Y			
Glasgow Dumbarton Road	Roadside	Scottish Automatic Urban Network	Y	Y	Y			
Glasgow Nithsdale Road	Roadside	Scottish Automatic Urban Network	Y	Y	Y			
Inverness Academy Street	Roadside	Scottish Automatic Urban Network	Y					
N Lanarkshire Chapelhall	Roadside	Scottish Automatic Urban Network	Y	Y	Y			
North Ayrshire Irvine High St	Kerbside	Scottish Automatic Urban Network	Y	Y	Y			
Paisley Gordon Street	Roadside	Scottish Automatic Urban Network	Y	Y				
Perth Atholl Street	Roadside	Scottish Automatic Urban Network	Y	Y	Y			
Perth Crieff	Roadside	Scottish Automatic Urban Network	Y	Y	Y			
Perth High Street	Roadside	Scottish Automatic Urban Network	Y		Y			
Perth Muirton	Urban Background	Scottish Automatic Urban Network		Y				

Site name	Site type	Network	NO_X, NO_2	PM_{10}	$PM_{2.5}$	SO_2	O_3	C_6H_6
Renfrew Cockels Loan	Roadside	Scottish Automatic Urban Network	Y	Y				
Renfrewshire Johnstone	Roadside	Scottish Automatic Urban Network		Y	Y			
South Ayrshire Ayr Harbour	Roadside	Scottish Automatic Urban Network	Y		Y			
South Lanarkshire Cambuslang	Kerbside	Scottish Automatic Urban Network	Y	Y	Y			
South Lanarkshire East Kilbride	Roadside	Scottish Automatic Urban Network	Y	Y	Y			
South Lanarkshire Hamilton	Roadside	Scottish Automatic Urban Network	Y	Y	Y			
South Lanarkshire Lanark	Kerbside	Scottish Automatic Urban Network	Y	Y	Y			
South Lanarkshire Raith Interchange 2	Roadside	Scottish Automatic Urban Network	Y	Y	Y			
South Lanarkshire Rutherglen	Roadside	Scottish Automatic Urban Network	Y	Y	Y			
South Lanarkshire Uddingston	Roadside	Scottish Automatic Urban Network	Y	Y	Y			
Stirling Craigs Roundabout	Roadside	Scottish Automatic Urban Network	Y	Y				
West Dunbartonshire Clydebank	Roadside	Scottish Automatic	Y	Y	Y			

Site name	Site type	Network	NO_X, NO_2	PM_{10}	$PM_{2.5}$	SO_2	O_3	C_6H_6
		Urban Network						
West Lothian Broxburn	Roadside	Scottish Automatic Urban Network	Y	Y	Y			
West Lothian Linlithgow High Street 2	Roadside	Scottish Automatic Urban Network	Y	Y	Y			
West Lothian Newton	Roadside	Scottish Automatic Urban Network	Y	Y				
Anglesey Felin Cafnan	Rural	Welsh Air Quality Network		Y	Y			
Anglesey Llynfaes	Other	Welsh Air Quality Network		Y	Y			
Anglesey Penhesgyn 3	Rural	Welsh Air Quality Network		Y	Y			
Caerphilly Blackwood High Street	Roadside	Welsh Air Quality Network	Y	Y				
Caerphilly Fochriw	Roadside	Welsh Air Quality Network		Y	Y			
Caerphilly Islwyn Road Wattsville	Roadside	Welsh Air Quality Network	Y					
Caerphilly White Street	Roadside	Welsh Air Quality Network	Y	Y				
Cimla Road / Victoria Gardens	Roadside	Welsh Air Quality Network	Y					
Nantgarw Road	Roadside	Welsh Air Quality Network	Y					
Newport M4 Junction 25	Roadside	Welsh Air Quality Network	Y				Y	

Site name	Site type	Network	NO_X, NO_2	PM_{10}	$PM_{2.5}$	SO_2	O_3	C_6H_6
Port Talbot Little Warren	Urban Industrial	Welsh Air Quality Network		Y				
Port Talbot Prince Street 2	Urban Industrial	Welsh Air Quality Network		Y	Y			
Port Talbot Twll-yn-y-Wal Park	Roadside	Welsh Air Quality Network		Y				
Rhondda Mountain Ash	Roadside	Welsh Air Quality Network	Y					
Rhondda Pontypridd Gelliwastad Rd	Roadside	Welsh Air Quality Network	Y					
Rhondda-Cynon-Taf Broadway	Roadside	Welsh Air Quality Network	Y					
Swansea Cwm Level Park	Urban Background	Welsh Air Quality Network	Y				Y	
Swansea Hafod DOAS	Roadside	Welsh Air Quality Network	Y				Y	Y
Swansea Morfa Road NOX	Roadside	Welsh Air Quality Network	Y					
Swansea Morriston Roadside	Roadside	Welsh Air Quality Network	Y		Y		Y	
Swansea St Thomas DOAS	Roadside	Welsh Air Quality Network	Y			Y	Y	Y
Swansea Station Court High Street	Roadside	Welsh Air Quality Network	Y					
Twynyrodyn	Urban Industrial	Welsh Air Quality Network		Y	Y			
V Glamorgan Windsor Road Penarth	Roadside	Welsh Air Quality Network	Y	Y			Y	

Appendix 2 - Monitoring sites for As, Cd, Ni, Pb and B(a)P

The monitoring stations operating during 2018 for the purpose of AQD and AQDD4 reporting have been listed within e-Reporting Data flow C (Assessment Regimes), which can be found on the CDR (CDR, 2019). A summary of the annual mean As, Cd, Ni, Pb and B(a)P measurements used for calibrating and verifying the modelling used in the assessment are provided here.

Heavy Metal Monitoring sites

2018 annual mean concentrations of As, Cd, Ni and Pb are presented in Table A2.1 for heavy metal monitoring sites where data capture was at least 75%. The mass concentrations presented are rounded to two significant figures.

Table A2.1 – Summary of urban and rural heavy metal mass concentrations, 2018

EoI code	Site name	Site type*	Annual mean (ng m^{-3})				%dc
			As	Cd	Ni	Pb	
GB0048R	Auchencorth Moss	RB	0.2	0.026	0.23	1	100
GB0567A	Belfast Centre	UB	0.45	0.098	1.3	20	96
GB0985A	Chadwell St Mary	UB	0.93	0.26	1.1	12	100
GB1046A	Chesterfield Loundsley	UB	0.67	0.14	1.2	7	96
GB1055R	Chilbolton Observatory	RB	0.63	0.095	0.51	3.6	99
GB0854A	Cwmystwyth	RB	0.25	0.057	0.39	1.7	100
GB0886A	Detling	RB	0.93	0.19	0.71	8.1	97
GB0002R	Eskdalemuir	RB	0.17	0.024	0.26	0.98	93
GB1048A	Fenny Compton	RB	0.8	0.1	0.55	5.6	100
GB0017R	Heigham Holmes	RB	0.5	0.1	0.81	4.2	97
GB0682A	London Marylebone Road	UT	0.87	0.16	1.7	6.7	100
GB0743A	London Westminster	UB	0.81	0.13	0.94	6.7	100
GB1015A	Pontardawe Brecon Road	SI	1	0.29	6.2	5.3	98
GB1016A	Pontardawe Tawe Terrace	UI	0.74	0.33	57	6.3	100
GB0906A	Port Talbot Margam	UI	0.82	1.2	1.6	7.8	100
GB0877A	Runcorn Weston Point	UI	0.68	0.093	0.83	4.7	98
GB1004A	Scunthorpe Low Santon	UI	0.73	0.64	1.3	19	98
GB0841A	Scunthorpe Town	UI	0.77	0.33	1.2	16	95
GB1027A	Sheffield Devonshire Green	UB	0.69	0.17	2.2	8.4	100
GB0538A	Sheffield Tinsley	UB	1	0.43	20	18	100
GB0981A	Swansea Coedgwilym	UB	0.63	0.32	12	5.3	100
GB0979A	Swansea Morriston	UT	0.83	0.5	8.6	11	100
GB0983A	Walsall Bilston Lane	UI	0.72	0.62	1.8	19	52
GB0013R	Yarner Wood	RB	0.49	0.065	0.45	2.3	99

*RB = Rural Background, UB = Urban Background, UT = Urban Traffic, UI = Urban Industrial, SI = Suburban Industrial, SB = Suburban Background.

B(a)P Monitoring sites

2018 annual B(a)P mean concentrations are presented in Table A2.2 for those sites where data capture was at least 75%. The mass concentrations presented are rounded to two significant figures. All measurements were obtained using Digitel DHA-80 samplers.

Table A2.2 – Summary of B(a)P mass concentrations, 2018

EoI code	Site name	Site type*	Annual mean B(a)P, ng/m^3	%dc
GB0048R	Auchencorth Moss	RB	0.019	99
GB0934A	Ballymena Ballykeel	UB	0.37	99
GB0700A	Bolsover	UB	0.19	97
GB0869A	Cardiff Lakeside	UB	0.18	99
GB1055R	Chilbolton Observatory	RB	0.061	100
GB0944A	Derry Brandywell	UB	0.74	99
GB0839A	Edinburgh St Leonards	UB	0.056	100
GB1028A	Glasgow Townhead	UB	0.065	99
GB0702A	Hazelrigg	RB	0.033	100
GB0014R	High Muffles	RB	0.042	99
GB1023A	Kilmakee Leisure Centre	UB	0.26	100
GB0705A	Kinlochleven	UB	0.25	99
GB0867A	Leeds Millshaw	UB	0.21	98
GB0777A	Liverpool Speke	UI	0.1	99
GB0849A	London Brent	UB	0.12	99
GB0682A	London Marylebone Road	UT	0.12	99
GB1010A	Lynemouth 2	SI	0.084	98
GB0583A	Middlesbrough	UI	0.17	100
GB0568A	Newcastle Centre	UB	0.13	98
GB0646A	Nottingham Centre	UB	0.15	98
GB0906A	Port Talbot Margam	UI	0.7	98
GB0940A	Royston	UI	0.38	99
GB1088R	Ruardean	RB	0.31	97
GB0660A	Salford Eccles	UB	0.17	99
GB1004A	Scunthorpe Low Santon	UI	0.78	100
GB0841A	Scunthorpe Town	UI	1.7	100
GB0538A	Sheffield Tinsley	UB	0.21	98
GB0942A	South Hiendley	UI	0.23	100
GB0004R	Stoke Ferry	RB	0.085	100
GB0943A	Swansea Cwm Level Park	UB	0.28	99

*RB = Rural Background, UB = Urban Background, UT = Urban Traffic, UI = Urban Industrial, SI = Suburban Industrial.

Appendix 3 – Small point source model

Introduction

Small industrial sources were generally represented in early maps (Stedman et al., 2002) as 1 km square volume sources. However, this approach in some cases lead to unreasonably high concentrations close to the source. The overestimation arose because the release height, buoyancy and momentum of discharges from industrial chimneys are not taken into account. A revised small point source model was developed that uses dispersion kernels that take these factors into account.

The dispersion model ADMS 3.0 was used to prepare the dispersion kernels.

Discharge Conditions

The National Atmospheric Emission Inventory contains limited information concerning the discharge characteristics of individual emission sources. In many cases the information is limited to data on the total annual emission of individual pollutants. It is therefore necessary to make some general assumptions concerning the discharge height, the discharge temperature, the volumetric flow rate of the discharge and the discharge velocity. The approach adopted has been to make reasonable, but generally conservative assumptions corresponding to industrial practice.

Sulphur dioxide

For sulphur dioxide, it was assumed that the plant operates continuously throughout the year. The stack height was estimated using the following equations taken from the 3rd edition of the Chimney Heights Memorandum:

If the sulphur dioxide emission rate, R_A kg/h, is less than 10 kg/h, the chimney height, U m, is given by:

$$U = 6R_A^{0.5},$$

If R_A is in the range 10-100 kg/h:

$$U = 12R_A^{0.2},$$

Emission rates in excess of 100 kg/h were not considered in this study.

No account was taken of the effects of buildings: it was assumed that the increase in chimney height to take account of building effects provided by the Memorandum would compensate for the building effects.

It was then assumed that the sulphur dioxide concentration in the discharge would be at the limit for indigenous coal and liquid fuel for new and existing plant provided by Secretary of States Guidance-Boilers and Furnaces, 20-50 MW net rated thermal input PG1/3(95). The limit is 3000 mg m^{-3} at reference conditions of 273 K, 101.3 kPa, 6% oxygen for solid fuel firing and 3% oxygen for liquid firing and dry gas. It was assumed that the oxygen content in the discharge corresponds with the reference condition. The moisture content of the discharge was ignored. It was assumed that the temperature of discharge was 373 K: higher temperatures would lead to improved buoyancy and hence lower ground level concentrations while lower temperatures usually result in unacceptable water condensation. A discharge velocity of 10 m/s was selected to be representative of most combustion source discharges. The discharge diameter d m was calculated from:

$$d = \sqrt{\frac{4qT}{273\pi cv}},$$

where: q is the sulphur dioxide emission rate, g s^{-1}
T is the discharge temperature, 373 K
c is the emission concentration at reference conditions, 3 g m^{-3}
v is the discharge velocity, 10 m s^{-1}

Table A3.1 shows the modelled stack heights and diameters.

Table A3.1. Modelled stack heights and diameters for sulphur dioxide

Emission rate			Stack height, m	Stack diameter, m
$g\ s^{-1}$	$kg\ h^{-1}$	$t\ a^{-1}$		
0.1	0.36	3.2	3.60	0.08
0.2	0.72	6.3	5.09	0.11
0.5	1.8	15.8	8.05	0.17
1	3.6	31.5	11.38	0.24
2	7.2	63.1	16.10	0.34
5	18	157.7	21.39	0.54
10	36	315.4	24.57	0.76
20	72	630.7	28.23	1.08

Oxides of nitrogen

For nitrogen dioxide, it was assumed that the plant operates continuously throughout the year. The stack height was estimated using the following equation taken from the 3rd edition of the Chimney Heights Memorandum for very low sulphur fuels:

$$U = 1.36Q^{0.6}(1 - 4.7\times10^{-5}Q^{1.69}),$$

where: Q is the gross heat input in MW.

This relationship applies for heat inputs up to 150 MW. For larger heat inputs a fixed height of 30 m was used corresponding to an approximate lower limit derived from available data on stack heights for large sources.

The gross heat input used in the above equation was calculated from the oxides of nitrogen emission rate using an emission factor of 10600 kg/MTh (0.100 g/MJ) for oxides of nitrogen emitted from natural gas combustion in non-domestic non-power station sources taken from the NAEI.

For fuels containing significant sulphur, the actual stack height will be greater to allow for the dispersion of sulphur dioxide so that the approach taken is expected to lead to an overestimate of ground level concentrations.

The emission limits for oxides of nitrogen provided by Secretary of States Guidance-Boilers and Furnaces, 20-50 MW net rated thermal input PG1/3(95) depend on the type of fuel and are in the range 140-650 mg m^{-3} at reference conditions. A value of 300 mg m^{-3} was used in the calculation of the stack discharge diameter. Other assumptions concerning discharge conditions followed those made for sulphur dioxide above. Table A3.2 shows the modelled stack heights and diameters.

Table A3.2. Modelled stack heights and diameters for oxides of nitrogen

Emission rate		Stack height, m	Stack diameter, m
$g\ s^{-1}$	$t\ a^{-1}$		
0.1	3.2	1.36	0.24
0.2	6.3	2.06	0.34
0.5	15.8	3.57	0.54
1	31.5	5.40	0.76
2	63.1	8.15	1.08
5	157.7	13.72	1.70
10	315.4	19.12	2.41
20	630.7	21.34	3.41
50	1576.8	30.00	5.38
100	3153.6	30.00	7.61

Particulate matter, PM_{10}

The stack heights and diameters used for oxides of nitrogen were also used to provide the kernels for particulate matter PM_{10}. This will provide a conservative assessment of PM_{10} concentrations for the following reasons. The emission limits for total particulate matter provided by Secretary of States Guidance-Boilers and Furnaces, 20-50 MW net rated thermal input PG1/3(95) depend on the type of fuel and are in the range 5-300 mg m^{-3} at reference conditions. The emission limit for total particulate matter includes but is not limited to the contribution from PM_{10}.

Dispersion Modelling

The dispersion model ADMS 3.0 was used to predict ground level concentrations on two receptor grids:

- an “in-square” grid covering an area 1 km x 1 km with the source at the centre and with receptors at 33.3 m intervals;
- an “outer-grid” covering an area 30 km x 30 km with the source at the centre and with receptors at 1 km intervals.

A surface roughness value of 0.5 m was used, corresponding to areas of open suburbia. Meteorological data for Heathrow for the years 1993-2002 was used in the assessment, with most model runs using the 2000 data.

Results

Sulphur dioxide

Table A3.3 shows the predicted “in-square average” concentration for the 1 km square centred on the emission source for 2000 meteorological data.

Table A3.3. Predicted in-square concentration, for sulphur dioxide

Emission rate, g s^{-1}	Average in square concentration, μg m^{-3}
0.1	0.599
0.2	0.934
0.5	1.555
1	2.19
2	2.92
5	4.57
10	6.56
20	8.86

The results shown in Table A3.3 may be approximated by the relationship

$$C = Aq^{0.5},$$

where: C is the in-square concentration, μg m^{-3} and q is the emission rate, g s^{-1}. A is a proportionality factor (2.07 in 2000).

Table A3.4 shows the predicted in-square concentration for an emission rate of 10 g s^{-1} for meteorological years 1993-2002. Table A3.4 also shows the inter-annual variation in the factor A.

Table A3.4. In-square concentrations for 10 g/s emissions

Year	In-square concentration, µg m^{-3}	Factor *A*
1993	6.21	1.96
1994	6.01	1.90
1995	6.12	1.94
1996	6.23	1.97
1997	6.10	1.93
1998	6.18	1.95
1999	6.49	2.05
2000	6.56	2.07
2001	6.32	2.00
2002	6.51	2.06

Figure A3.1 shows the predicted “outer-grid” concentration along the east-west axis through the source for 2000 meteorological data for a range of rates of emission (in g/s). Figure A3.1 does not include results for the 1 km source square.

Figure A3.1. Sulphur dioxide concentration on east-west axis, 2000 meteorological data

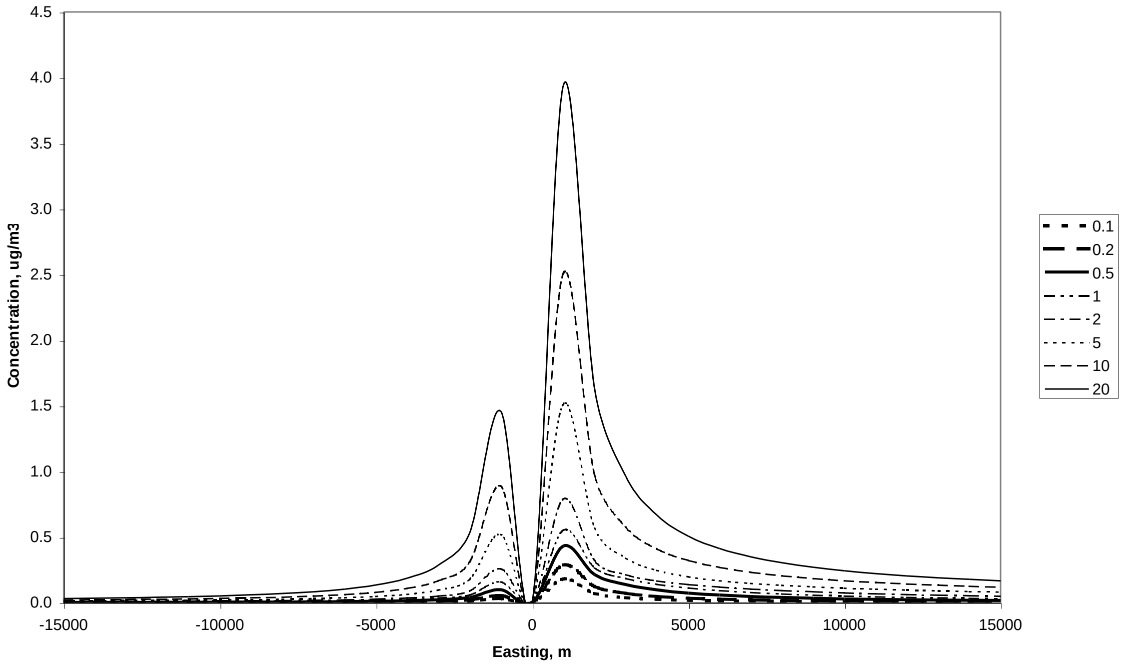

Figure A3.2 shows the same model results plotted as C/q$^{2/3}$. The spread of the model results is greatly reduced so that as a reasonable approximation all the model results may be reduced to a single line.

Figure A3.2. Reduced sulphur dioxide concentrations on the east-west axis, 2000 meteorological data

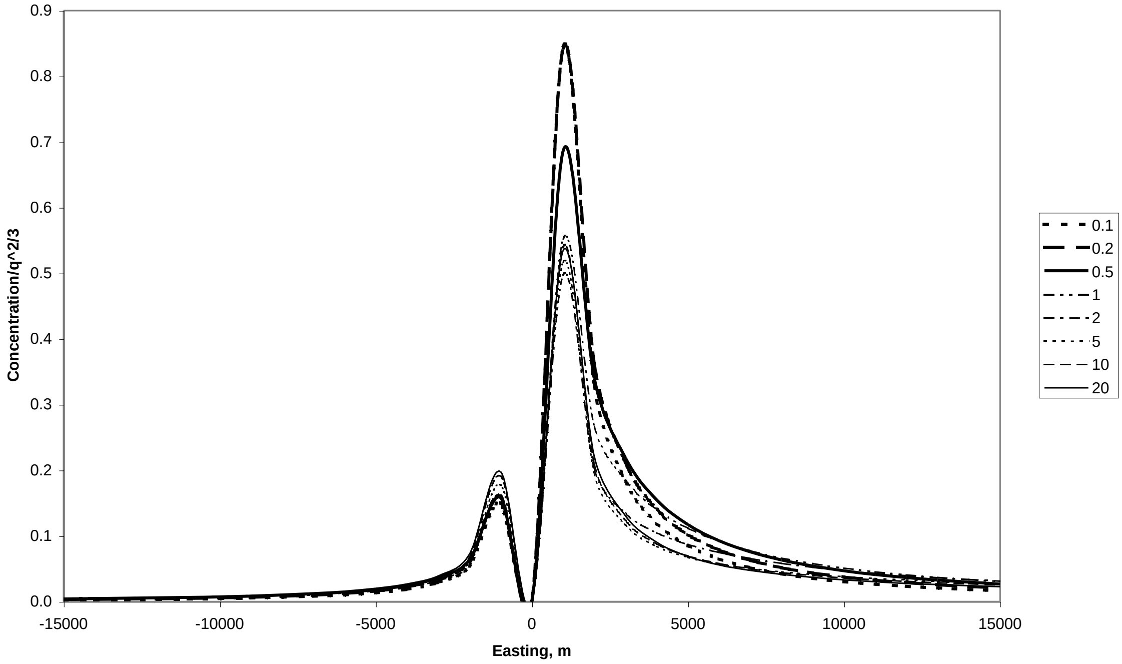

Thus, it is proposed to use the results for an emission rate of 10 g/s for all emission rates in the range 0.1-20 g/s in the preparation of dispersion kernels for industrial sulphur dioxide emissions. The dispersion kernel will be multiplied by $10.(q/10)^{2/3}$ to provide estimates of the impact of emission q (g s^{-1}) at each receptor location. Separate kernels have been created from each meteorological data year 1993-2002.

Oxides of nitrogen

Table A3.5 shows the predicted “in-square average” concentration for the 1 km square centred on the emission source for 2000 meteorological data.

Table A3.5. In-square oxides of nitrogen concentrations, 2000

Emission rate, g s^{-1}	In square concentration, μg m^{-3}
0.1	0.464
0.2	0.764
0.5	1.37
1	1.97
2	2.6
5	3.31
10	3.58
20	4.34
50	3.745
100	4.3

The results shown in Table A3.5 may be approximated in the range 0.1-20 g s^{-1} by the relationship

$$C = B \log_{10}(10q)+0.464,$$

where: C is the in-square concentration, μg m^{-3} and q is the emission rate, g s^{-1}. and B is a numerical constant, 1.68 in 2000.

For emission rates in the range 20-100 g s^{-1}, the in-square concentration is approximately 4 μg m^{-3}.

Table A3.6 shows the predicted in-square concentration for an emission rate of 20 g s^{-1} for meteorological years 1993-2002. Table A3.6 also shows the inter-annual variation in the factor B.

Table A3.6. Inter annual variation in in-square oxides of nitrogen concentration

Year	In-square concentration, μg m^{-3}	Factor B
1993	3.62	1.37
1994	3.88	1.48
1995	3.74	1.42
1996	4.3	1.67
1997	3.66	1.39
1998	3.64	1.38
1999	4.14	1.60
2000	4.34	1.68
2001	4.02	1.55
2002	4.68	1.83

Figure A3.3 shows the predicted “outer-grid” oxides of nitrogen concentration along the east-west axis through the source for a range of rates of emission (in g s^{-1}).

Figure A3.3. Oxides of nitrogen concentration on east-west axis, 2000 meteorological data

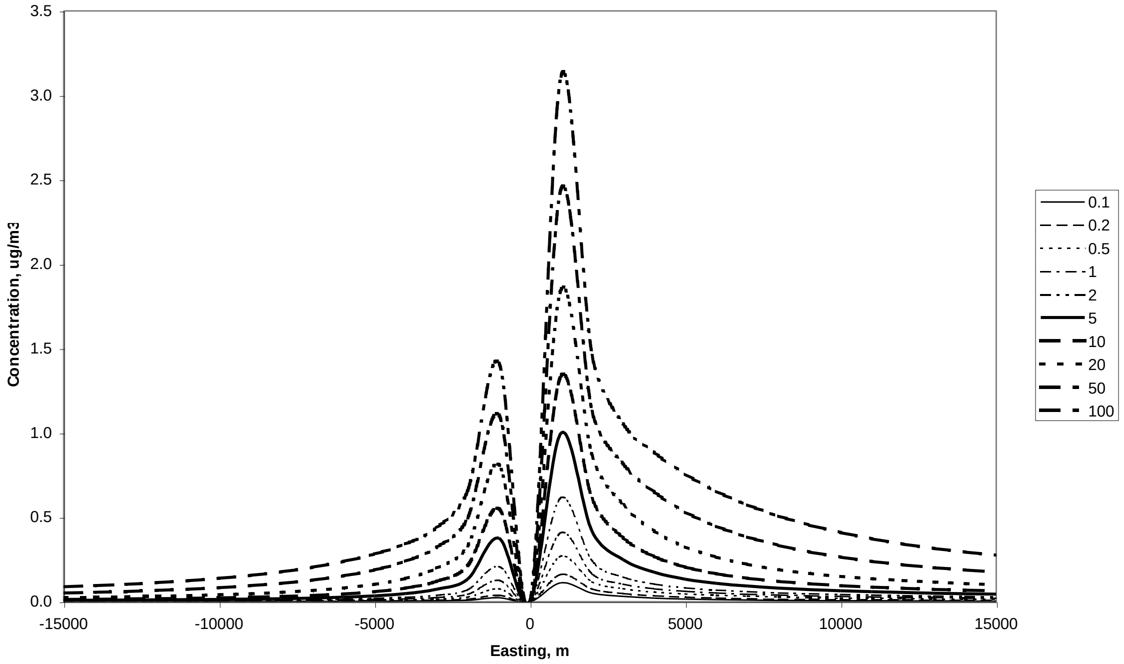

Figure A3.4 shows the same model results plotted as $C/q^{0.6}$. The spread of the model results is greatly reduced so that as a reasonable approximation all the model results may be reduced to a single line.

Figure A3.4. Reduced oxides of nitrogen concentrations on the east-west axis, 2000 meteorological data

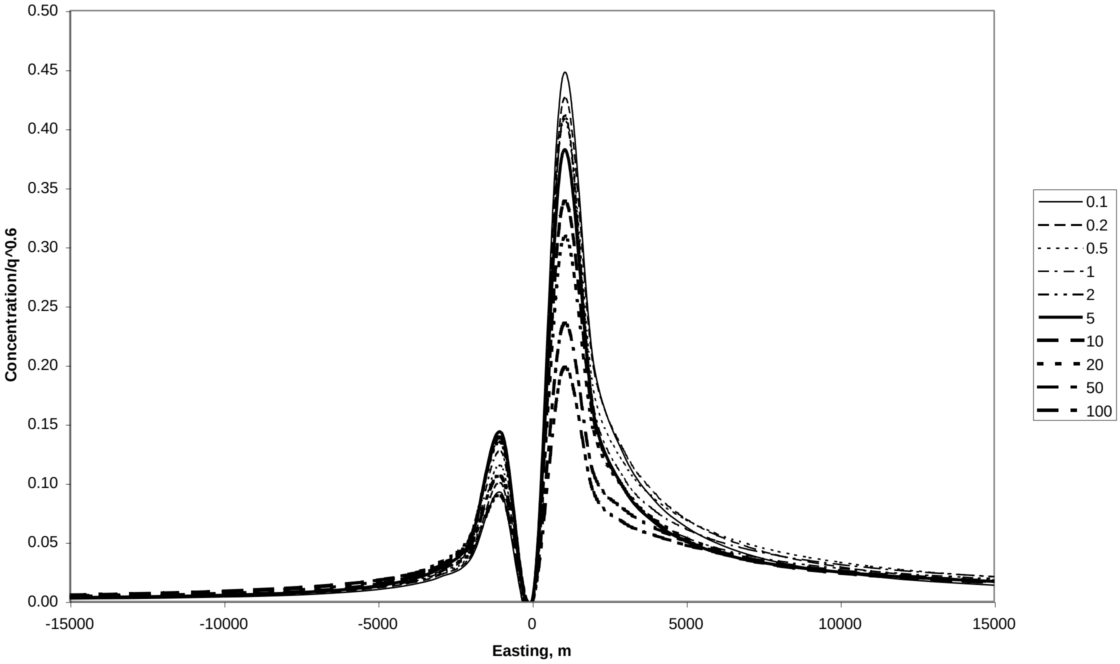

Thus, it is proposed to use the results for an emission rate of 20 g s^{-1} for all emission rates in the range 0.1-100 g s^{-1} in the preparation of dispersion kernels for oxides of nitrogen emissions. The dispersion kernel will be multiplied by $20.(q/20)^{0.6}$ to provide estimates of the impact of emission q g s^{-1} at each receptor location. Separate kernels have been created for each meteorological data year 1993-2002.

Method

Sulphur dioxide

Point sources with emissions greater than or equal to 500 tonnes per year (15.85 g s^{-1}) have been modelled explicitly using ADMS. Point sources with emissions less than 500 tonnes per year have been modelled using the small points model. This model has two components.

The in-square concentration for each source has been calculated using the following function:

$$C = 1.98.q^{0.5}$$

where C is the in-square concentration, µg m^{-3} and q is the emission rate, g s^{-1} and 1.98 is a numerical constant, calculated as the average value over the years 1993-2002 for met data at Heathrow.

The outer-grid concentration has been calculated by adjusting the emissions for each source using the function:

$$Q = 10.(q/10)^{0.667},$$

where: q is the emission rate, g s^{-1} and Q is the adjusted emissions. The sum of the adjusted emission was then calculated for each grid square and the outer-grid concentration calculated using a small points dispersion kernel (which was calculated as the average over the years 1993-2002 for met data at Heathrow).

The in-square and outer-grid concentrations were then summed to calculate the total contribution to ambient annual mean concentrations from these small point sources.

Oxides of nitrogen

Point sources with emissions greater than or equal to 500 tonnes per year (15.85 g s^{-1}) have been modelled explicitly using ADMS. Point sources with emissions less than 500 tonnes per year have been modelled using the small points model. This model has two components.

The in-square concentration for each source has been calculated using the following function:

$$C = 1.54.\ \log_{10}(10q)+0.464,$$

where: C is the in-square concentration, $\mu g\ m^{-3}$ and q is the emission rate, $g\ s^{-1}$ and 1.54 is a numerical constant, calculated as the average value over the years 1993-2002 for met data at Heathrow.

The outer-grid concentration has been calculated by adjusting the emissions for each source using the function:

$$Q = 20.\ (q/20)^{0.6},$$

where: q is the emission rate, $g\ s^{-1}$ and Q is the adjusted emissions. The sum of the adjusted emission was then calculated for each grid square and the outer-grid concentration calculated using a small points dispersion kernel (which was calculated as the average over the years 1993-2002 for met data at Heathrow).

The in-square and outer-grid concentrations were then summed to calculate the total contribution to ambient annual mean concentrations from these small point sources.

PM_{10} and $PM_{2.5}$

The method for PM_{10} and $PM_{2.5}$ was the same as for NO_x, except that point sources with emissions greater than or equal to 200 tonnes per year (6.34 $g\ s^{-1}$) have been modelled explicitly using ADMS. Point sources with emissions less than 200 tonnes per year have been modelled using the small points model.

Benzene

The method for benzene was the different. Point sources with combustions emissions greater than or equal to 5 tonnes per year (0.16 $g\ s^{-1}$) have been modelled explicitly using ADMS. Fugitive and process point sources have been modelled using a different small points model, as described in Section 7.3.2.

Appendix 4 – Dispersion kernels for the area source model

Dispersion kernels for calculating the annual mean contribution of emissions from area sources to ambient annual mean concentrations were calculated using ADMS 5.2. Separate kernels were calculated for traffic, domestic and other area sources (which were assumed to have a constant temporal profile of emissions). Kernels were generated for the assessment year using sequential meteorological data from Waddington. The dispersion parameters used to calculate the kernels are listed in Table A4.1. The emission profiles used to represent traffic emissions for the traffic kernels are shown in Figures A4.1a and A4.1b. These profiles result from developments for the 2015 assessment modelling to update the temporal profiles for road traffic. The profiles by month of the year, hour of the day and day of the week were obtained from DfT traffic flow data for all traffic in Great Britain averaged over the period 2010-2014 (DfT, 2016).

Figure A4.1a. Normalised hourly and daily temporal profiles of traffic emissions

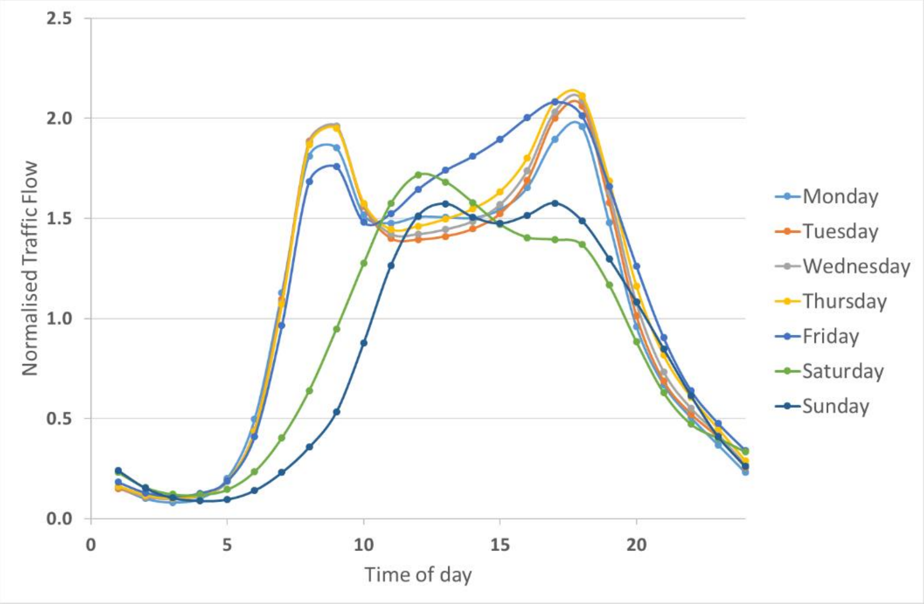

Figure A4.1a. Normalised monthly profile of traffic emissions

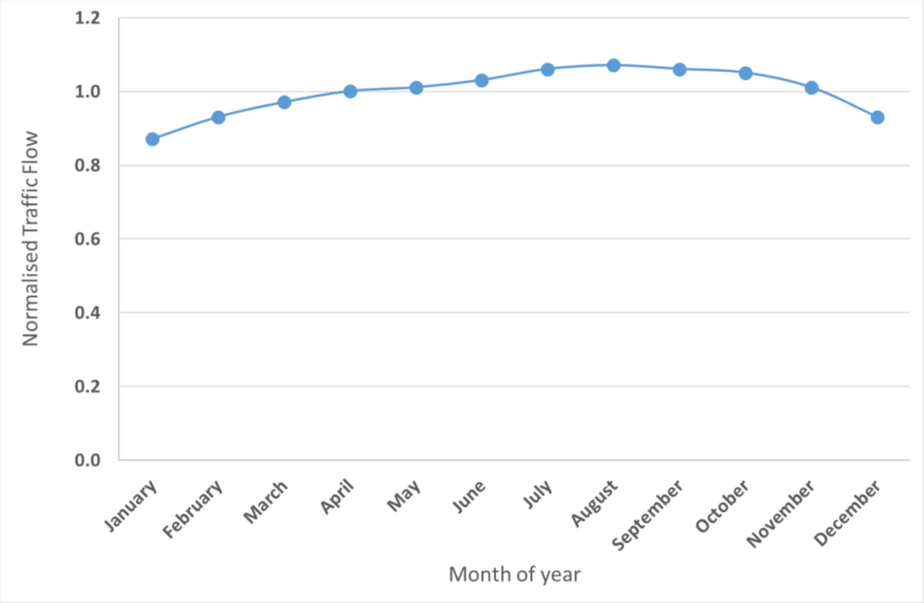

A time varying emissions profile was applied for domestic sources the first time in the 2011 assessment to better represent emissions related to domestic combustion. Both seasonal and diurnal profiles have been used to weight domestic emissions. These weightings have been developed and applied following a similar method to Coleman et al. (2001). In this work a normalised diurnal profile has been superimposed onto a seasonal profile based on degree days calculated from temperature data for the Waddington meteorological station and the assessment year. The diurnal profile applied has been estimated from Coleman et al. (2001), see Figure A4.2. Degree days provide a simple but effective tool to relate energy use and emissions from buildings to the weather (Day et al, 2006). A degree day is unit used to determine the heating requirements of buildings, representing a fall of one degree below a specified average outdoor temperature (15.5 C, in this case). Degree days for Waddington have been calculated from the equation:

$$D_d = \frac{\sum_{i=1}^{N} \theta_b - \theta_{o,i}{}_{(\theta_b - \theta_{o,i} \geq 0)}}{N}$$

Where D_d is the daily degree days for one day, θ_b is the base temperature, $\theta_{o,i}$ is the ambient (or outdoor) air temperature and N is the number of hours of available data in a given day. Figure A4.3 shows the seasonal profile of degree days calculated for the year 2018. The seasonal profile of degree days has been verified versus National Grid, National Transmission System gas demand data.

Figure A4.2. Diurnal profile of domestic emissions estimated from Coleman et al. (2001)

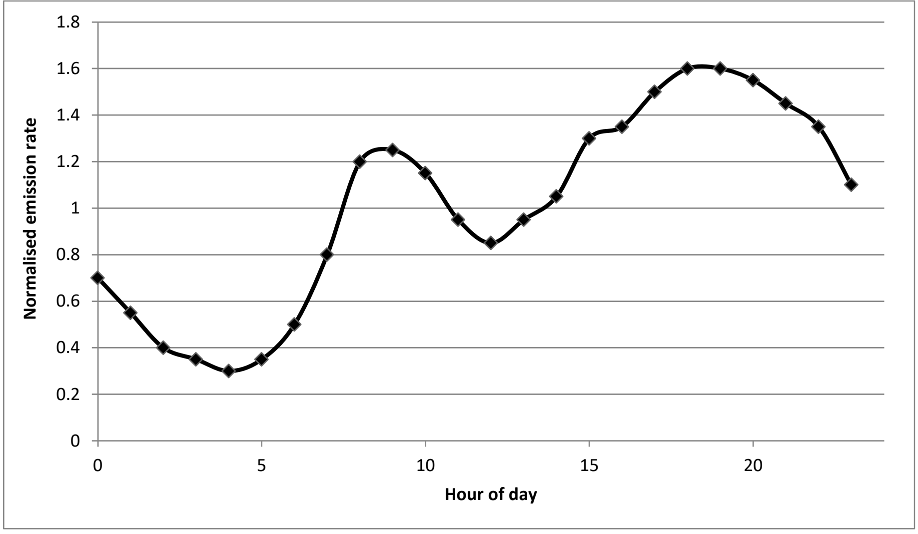

Figure A4.3. Seasonal profile of degree days calculated for the Waddington meteorological station in 2018 (base temperature of 15.5°C)

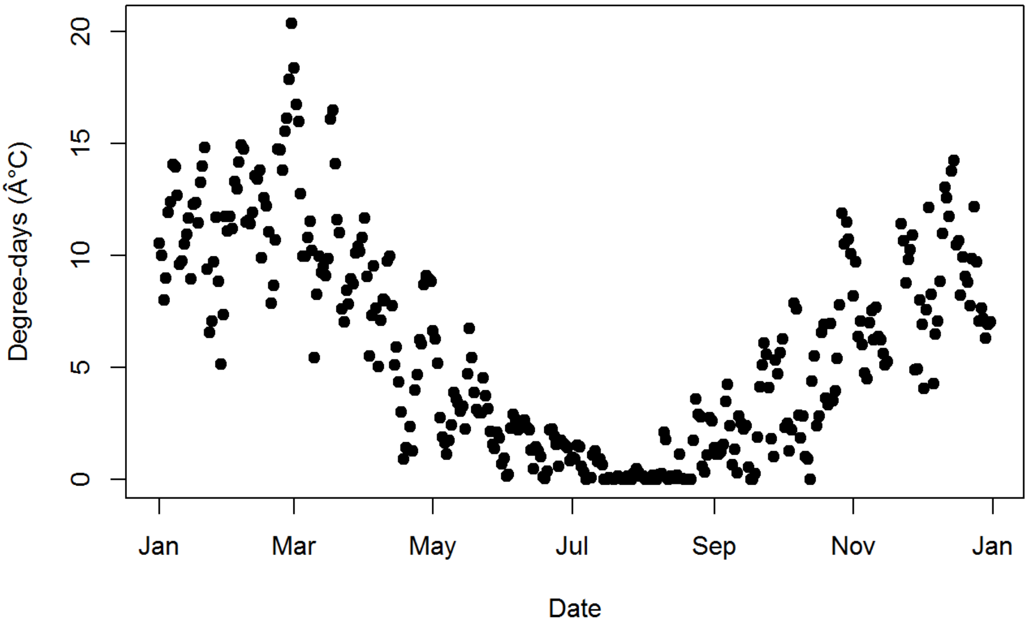

For SO_2, NO_x, NO_2, PM_{10}, $PM_{2.5}$, C_6H_6, heavy metals (Pb, As, Cd, Ni) and B(a)P the area source dispersion kernels are on a 1 km x 1 km resolution matrix and are made using ADMS 5.2. The centre squares have been scaled to remove the impact of sources within 50 m of the receptor location in that square on the basis that background sites are not located very close to specific sources such as major roads. Different kernels have been made for different area types, to take into account different dispersion conditions in urban areas of different sizes. The kernels have been made specific to different types of location by varying minimum Monin Obukhov Length (LMO) and surface roughness due to different land use. The location of the different area types are shown in Figure A4.4.

Table A4.1. Summary of inverted dispersion kernel parameters

Kernel name	Area types	Type of location	LMO (m)	Surface roughness		Height (m) of volume source	Variable emission profile?	Emission rate (g m^{-3} s^{-1})
				Disp. site	Met. site			
Non-road transport	1,2,4	Conurbation	25	0.5	0.1	30	N	3.33E-08
Non-road transport	3,4,5,6,7,8	Smaller urban	20	0.5	0.1	30	N	3.33E-08
Non-road transport	9,10	Rural	10	0.5	0.1	30	N	3.33E-08
Domestic	1,2,4	Conurbation	25	0.5	0.1	20	Y	5.0E-08
Domestic	3,4,5,6,7,8	Smaller urban	20	0.5	0.1	20	Y	5.0E-08
Domestic	9,10	Rural	10	0.5	0.1	20	Y	5.0E-08
Road transport	1,2,4	Conurbation	25	0.5	0.1	10	Y	1.0E-7
Road transport	3,4,5,6,7,8	Smaller urban	20	0.5	0.1	10	Y	1.0E-7
Road transport	9,10	Rural	10	0.5	0.1	10	Y	1.0E-7

ADMS 4.2 recommended using a minimum Monin Obukhov Length (LMO) of 30 m for an urban area. However, sensitivity testing showed 20 m worked better in ADMS 4.2. The same settings have been applied in ADMS 5.2 after sensitivity tests indicated only marginal differences between the outputs for the area source kernels, between the different versions of ADMS.

The dispersion kernels used for fugitive and process point sources of benzene are the same as the non-road transport kernels but with the values for the central receptor location calculated as described in Section 7.3.2.

Figure A4.4. Map of UK area types

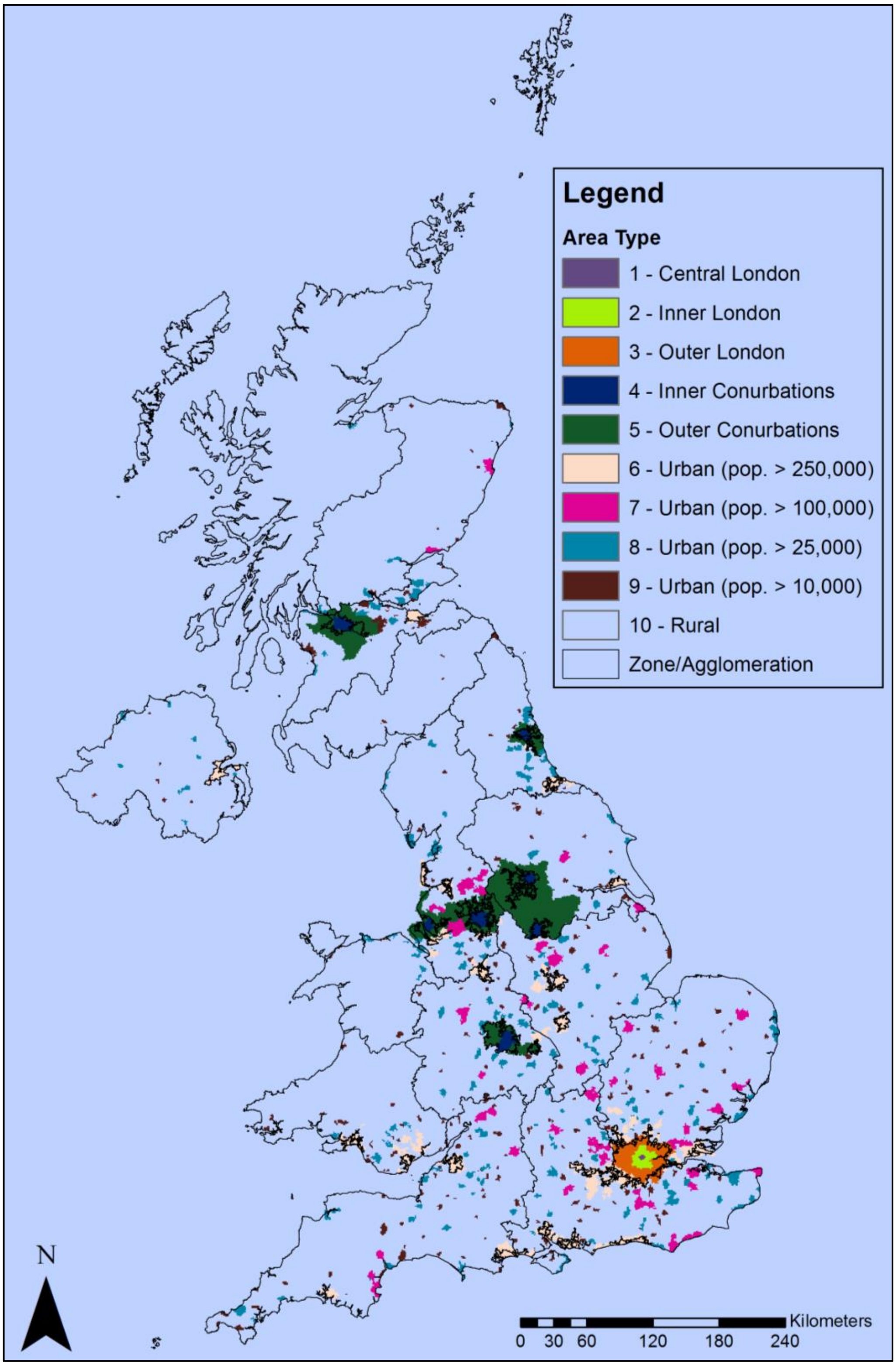

Appendix 5 – Method for calculating and mapping emissions from aircraft and shipping

Aircraft

Aircraft emissions were calculated using data obtained from the NAEI (Richmond et al., 2019)for emissions from planes in various phases of flying (e.g. take off, landing, taxiing). The NAEI provides estimates of total emissions for aircraft, which include emissions up to a height of 1000 m. Ground level emissions for use in PCM modelling were calculated on the basis of:

Ground level emissions = *Taxi out + Hold + Taxi in + APU arrival + APU departure +*
(0.5 x Take off) + (0.5 x Landing) + (0.5 x Reverse thrust).

The factor of 0.5 has been chosen on the basis of findings from detailed studies (Underwood, 2009). Initial climb, climb-out and approach are included in the emission inventory but excluded from ground level emissions used for the PCM model.

Figures A5.1 and A5.2 show good agreement between the measured and modelled annual mean ground-level NO_X concentrations at monitoring sites in the vicinity of Heathrow and Gatwick airports for 2008, respectively, based on this approach.

Figure A5.1. Comparison of the measured and modelled annual mean NO_X at Heathrow Airport for 2008

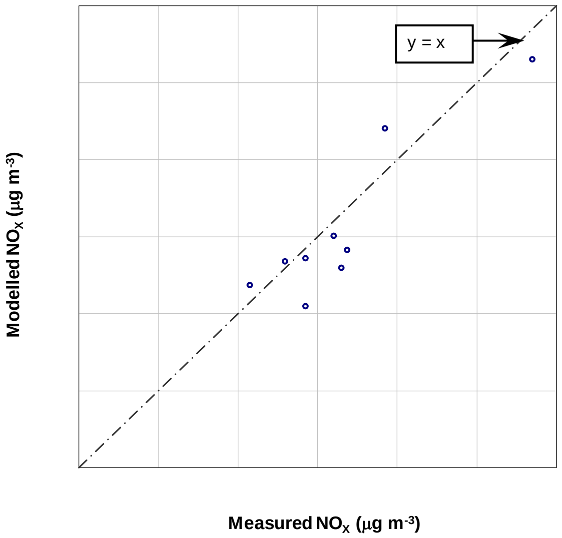

Figure A5.2. Comparison of the measured and modelled annual mean NO_X at Gatwick Airport for 2008

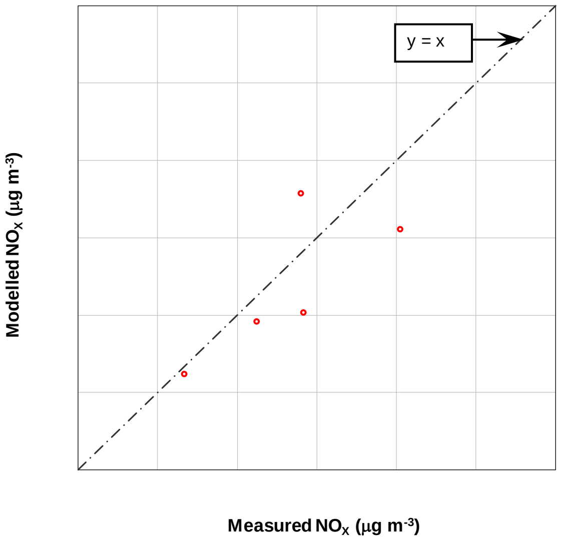

Shipping

A revised, more sophisticated, method has been used to map UK shipping emissions for the NAEI 2016 and NAEI 2017. Previously, shipping emissions were estimated by modelling fuel consumption from a database of shipping activities around UK waters for different vessel, fuel and journey types (Entec, 2010). This approach provided the best available solution at that time but had some recognised issues such as the age of the dataset (dating from 2007), estimated location of vessels rather than actual locations, low spatial resolution compared with other NAEI outputs[7] and insufficient representation of shipping types other than internationally trading vessels. Improvements made to the shipping emissions modelling for the NAEI National Inventory reporting, which were first reported in Scarbrough et al. (2017), provides higher resolution and greater accuracy to shipping emissions estimates (through improved coverage of various vessel types), as well as enabling a deeper understanding of the spatial pattern of emissions compared with the previous approach.

The revised method has been developed using Automatic Identification System (AIS) data supplied by the Maritime and Coastguard Agency. AIS is an on-board ship system that transmits a message containing a vessel's position - and other information such as speed - every few seconds, to be received by other vessels, onshore or by satellites[8]. A complete set of one year’s worth of AIS data received by terrestrial UK receivers was obtained and processed to give a dataset that records shipping activity at five-minute intervals for the whole of the year 2014. This was then used to calculate fuel consumption and emissions for each vessel for the year 2014 in conjunction with a second dataset of technical characteristics of individual vessels. The estimates for year 2014 were then forecast to the current NAEI year accounting for activity changes over time, the 2015 sulphur emission control area change in sulphur content limit, fleet-wide efficiency gains and additional NO_X emission factor changes to account for fleet turnover. A detailed discussion of the methodology used to develop a shipping emissions inventory from AIS data can be found in Scarborough, *et al* (2017).

The process of inventory mapping seeks to spatially disaggregate NAEI inventory totals in a way that represents how those emissions are geographically distributed in the real world. AIS data are inherently spatial as they record a vessel’s position, and so emissions from each ship can be easily attributed to the NAEI 1 km grid using the longitude and latitude accompanying each AIS message. A small number of messages are erroneously located upon terrestrial grid squares (Scarborough et al., 2017, p. 10) or are legitimately in non-UK water bodies within the NAEI mapping area (e.g. vessel movements within major rivers in north-eastern France). These emissions should not exist within the UK shipping map and have been removed.

Emissions caps applied for the shipping sector for 2018 were consistent with those applied in previous years. The NAEI shipping inventory improvements have resulted in a significantly lower impact of these caps, resulting in an emissions loss of around 1% compared with 5% before the inventory improvement as a result of being more realistically distributed.

---

[7] NAEI maps are drawn on 1x1km resolution grid, but pre-2016 shipping emissions were based on 5x5km gridded emissions and the NAEI inherited this lower resolution limit.

[8] http://www.imo.org/en/OurWork/Safety/Navigation/Pages/AIS.aspx

Appendix 6 – Monitoring stations used in $PM_{2.5}$ AEI calculation

Table A6.1. List of urban and suburban background monitoring stations used in AEI calculation

EoI code	Station name	Station classification	Instrument type
GB0729A	Aberdeen	Urban Background	(TEOM FDMS)
GB0567A	Belfast Centre	Urban Background	(TEOM FDMS)
GB1013A	Birmingham Acocks Green	Urban Background	(TEOM FDMS)
GB1097A	Birmingham Ladywood	Urban Background	(TEOM FDMS)
GB0851A	Birmingham Tyburn*	Urban Background	(TEOM FDMS)
GB0882A	Blackpool Marton	Urban Background	(TEOM FDMS)
GB0884A	Bristol St Paul's	Urban Background	(TEOM FDMS)
GB0580A	Cardiff Centre	Urban Background	(TEOM FDMS)
GB0929A	Chesterfield*	Urban Background	(TEOM FDMS)
GB1046A	Chesterfield Loundsley Green	Urban Background	(TEOM FDMS)
GB1034A	Coventry Allesley	Urban Background	(TEOM FDMS)
GB0739A	Coventry Memorial Park*	Urban Background	(TEOM FDMS)
GB1005A	Eastbourne	Urban Background	(TEOM FDMS)
GB0839A	Edinburgh St Leonards	Urban Background	(TEOM FDMS)
GB0641A	Glasgow Centre*	Urban Background	(TEOM FDMS)
GB1028A	Glasgow Townhead	Urban Background	mixed
GB0776A	Hull Freetown	Urban Background	(TEOM FDMS)
GB0643A	Leamington Spa	Urban Background	(TEOM FDMS)
GB0584A	Leeds Centre	Urban Background	(TEOM FDMS)
GB1026A	Leicester University	Urban Background	(TEOM FDMS)
GB0608A	London Bexley	Suburban Background	(TEOM FDMS)
GB0566A	London Bloomsbury	Urban Background	(TEOM FDMS)
GB0586A	London Eltham	Suburban Background	(TEOM FDMS)
GB0959A	London Harrow Stanmore*	Urban Background	(TEOM FDMS)
GB0620A	London N. Kensington	Urban Background	(Ref.eq)
GB0644A	London Teddington*	Urban Background	(TEOM FDMS)
GB1025A	London Teddington Bushy Park	Urban Background	(TEOM FDMS)
GB0613A	Manchester Piccadilly	Urban Background	(TEOM FDMS)
GB0568A	Newcastle Centre	Urban Background	(TEOM FDMS)
GB0962A	Newport	Urban Background	(Ref.eq)
GB0995A	Norwich Lakenfields	Urban Background	(TEOM FDMS)
GB0646A	Nottingham Centre	Urban Background	(TEOM FDMS)
GB0920A	Oxford St Ebbes	Urban Background	(TEOM FDMS)
GB0687A	Plymouth Centre	Urban Background	(TEOM FDMS)

EoI code	Station name	Station classification	Instrument type
GB0733A	Portsmouth	Urban Background	(TEOM FDMS)
GB0731A	Preston	Urban Background	(TEOM FDMS)
GB0840A	Reading New Town	Urban Background	(TEOM FDMS)
GB0615A	Sheffield Centre*	Urban Background	(TEOM FDMS)
GB1027A	Sheffield Devonshire Green	Urban Background	(TEOM FDMS)
GB0598A	Southampton Centre	Urban Background	(TEOM FDMS)
GB0728A	Southend-on-Sea	Urban Background	(TEOM FDMS)
GB0658A	Stoke-on-Trent Centre	Urban Background	(TEOM FDMS)
GB0863A	Sunderland Silksworth	Urban Background	(TEOM FDMS)
GB0864A	Wigan Centre	Urban Background	(TEOM FDMS)
GB0730A	Wirral Tranmere	Urban Background	(TEOM FDMS)
GB0918A	York Bootham	Urban Background	(TEOM FDMS)
GB0741A	Bournemouth	Urban Background	(BAM)
GB0860A	Brighton Preston Park	Urban Background	(GRAV EMFAB)
GB0620A	London N. Kensington	Urban Background	(Ref.eq)
GB0743A	London Westminster	Urban Background	(BAM)
GB0738A	Northampton*	Urban Background	(GRAV EMFAB)
GB1019A	Northampton Kingsthorpe*	Urban Background	(GRAV EMFAB)
GB1073A	Northampton Spring Park	Urban Background	(BAM)

* No longer operational. Not used in calculation of AEI for 2018.

Appendix 7 – The PCM Roads Kernel Model

Description of the model

The PCM Roads Kernel Model (PCM-RKM) has been set up to calculate roadside concentrations of NO_2, NO_x, PM_{10}, $PM_{2.5}$ and benzene on urban major roads. The model uses the ADMS-Roads dispersion model[9] (Version 4.1). Individual model runs are carried out for the approximately 9000 census points covering UK urban major roads. Each model run is parameterised using specific input data for the census point. These inputs are as follows and are described below:

- Road geometry
- Traffic speeds, emissions and traffic counts
- Meteorology
- Receptor locations

Road geometry

The PCM model uses a line coverage[10] to represent the layout of UK major roads, in combination with the census point dataset which describes the traffic flows on these roads. There is one census point per major road between junctions with other major roads. The traffic flow between major road junctions is assumed to be constant based on the assumption that the majority of traffic joins or leaves major roads at junctions with other major roads.

An assessment of variation in modelled concentrations with road orientation (not detailed here) suggests that differences in road orientation can make an approximately +/- 40% change for a receptor at 4 m from the roadside. This assessment evaluated the relative change in concentration modelled for receptors at various distances from the road for all road links. For each census point, the concentration modelled for a receptor at a particular distance from the roadside was compared to the concentration modelled for an identical road link aligned due north at the same distance from the road. The relative change is largely independent of road type, traffic flow and road width; hence the orientation of a particular road is important to the modelled concentration that results. This difference is driven by the orientation of the road relative to the prevailing wind direction.

The orientation of roads within the PCM model can be described at three levels. The coarsest level is the census point level where multiple UK major road sections are associated with each census point. This level of detail corresponds to the end nodes of the road links. The major road sections level data set, which comes from Ordnance Survey data, contains major road links but has nodes at junctions with both major roads and minor roads. Finally, there is the x, y coordinate level, where the coordinates of each arc of every link which makes up the major roads GIS dataset are available, therefore several grid references correspond to each link.

The number of road links for each census point means that the stretches of road are too long to be accurately described by one orientation calculated from the end nodes of the full length of road. To best represent the road orientation the x, y coordinate level would be most accurate. However, this would produce approximately 40 records for each census point, and it would be unfeasible to resolve variations in roadside concentrations down to this level when the underlying traffic data is represented at a much coarser level. Hence to represent the orientation of road links associated with each census point the end nodes of the major road sections have been used to calculate the bearing of the road link with respect to due north. The nearest UK major road section associated with the census point is used to define the orientation for all sections associated with that census point, given that it most closely represents the situation at the census point.

Road sources within ADMS-Roads are treated as line sources of variable width. To represent road widths as accurately as possible for all roads within the UK urban major roads coverage, the width has been estimated based on lane counts provided in the census point dataset. Road widths have been calculated assuming an average width of 4 metres per lane for urban single and dual carriageway A-roads and urban motorways. The 4-metre lane width assumption corresponds to those recommended by the Design Manual for Roads and Bridges (DMRB, 2005), where a lane width of

---

[9] http://www.cerc.co.uk/environmental-software/ADMS-Roads-model.html

[10] A set of lines within Geographical Information System

3.65 metres is more typical and the difference in lane width takes into account the hardstrip for urban A-roads.

To provide confidence in the lane counts from the census points dataset and the lane widths calculated, these were verified for a subset of road links for the following cases:

- Where lane counts were not available
- Where only a single lane was indicated
- For road links with the highest traffic flows
- For road links where predictions indicated the highest concentrations in a zone

Excluding those road links where only a single lane was indicated, for the assessed road links an average of 4 metres per lane was typical. Wider and more varied widths were observed for roads with only single lanes, but these are not characteristic of the complete dataset, typically being slip roads or small urban A-roads and carrying the least traffic (and represent less than 0.5% of the census points). All road sources are set up as line sources of length 2000 m. For road links that have not been assessed and a lane count has not been provided, the following default road widths have been assumed. The default characteristics are summarised in Table A7.1.

Table A7.1 - Default road source characteristics

Road type	Assumed number of lanes in each direction	Total width (m)	Length (m)
Single carriageway A-road	1	8	2000
Dual carriageway A-road	2	16	2000
Motorway	3	32	2000

Traffic speeds, emissions and traffic counts

ADMS-Roads uses traffic speeds and flows by vehicle category to estimate vehicle induced turbulence. The PCM-RKM uses traffic emissions for major road links in the UK provided directly by the NAEI and incorporates the vehicle induced turbulence as calculated by ADMS-Roads. Unitary emissions of 1 g/km/s are applied such that output concentrations profiles can be treated as kernels providing weightings for the pollutant specific road link emissions from the NAEI. The roadside increment concentration is calculated by multiplying concentrations modelled for unit emissions by the emissions rate for each road link. Traffic flows (annual average daily flows, AADFs) by census point have been aggregated into 2 vehicle categories i.e. light and heavy-duty vehicles for the calculation of vehicle induced turbulence.

Traffic speed assumptions by vehicle category have been applied following categories based upon UK area type and road type following a methodology similar to the NAEI and taking data from DfT congestion statistics to estimate the speeds. The categories, the data source used to develop the assumptions and the methodology applied are summarised in Table A7.2. The spatial distribution of the area types is illustrated in Figure A4.4, Appendix 4.

Emissions are assumed to be time varying, with temporal profiles varying by hour of the day, day of the week and having a seasonal monthly variation. The time varying emissions profiles for traffic are the same as those used for treating area source emissions from traffic in the PCM area source model (see Figures A4.1a and A4.1b, Appendix 4). The profiles were obtained from DfT traffic flow data for all traffic in Great Britain averaged over the period 2010-2014 (DfT, 2016).

Table A7.2 - Summary of the categories, data sources and methods applied to estimate vehicle speeds, and estimated speeds in PCM-RKM

Description	Classification (based on UK area type, and road type)	Data Source and methodology	LDV[11] Speed (km/h)	HDV[12] Speed (km/h)
Central London A roads	1_Urban_Major_Principal	DfT's "Congestion on local authority managed 'A' roads: 2010/11"[13] linked table CGN0201a. No split by vehicle type, flow weighted and based on weekday morning peak. Averaged across 2006/7 to 2010/11 and assumed City of London corresponds to central London (area type 1).	15	15
Inner London A roads	2_Urban_Major_Principal	DfT's "Congestion on local authority managed 'A' roads: 2010/11" linked table CGN0201a. No split by vehicle type, flow weighted and based on weekday morning peak. Averaged across 2006/7 to 2010/11 inner London boroughs excluding City of London (assumed area type 2).	21	21
Outer London A roads	3_Urban_Major_Principal	DfT's "Congestion on local authority managed 'A' roads: 2010/11" linked table CGN0201a. No split by vehicle type, flow weighted and based on weekday morning peak. Averaged across 2006/7 to 2010/11 Outer London boroughs (assumed area type 3).	29	29
Local authority A roads	4,5_Urban_Major_Principal	DfT's "Congestion on local authority managed 'A' roads: 2010/11" linked table CGN0201a. No split by vehicle type, flow weighted and based on weekday morning peak. Averaged across 2006/7 to 2010/11 and England (assumed area type 4,5).	40	40
Local authority A roads	6,7,8,9_Urban_Major_Principal	DfT's "Congestion on local authority managed 'A' roads: 2010/11" linked table CGN0201a. No split	40	40

---

[11] Light Duty Vehicles (cars and LGV)

[12] Heavy Duty Vehicles (HGVs and buses)

[13] http://webarchive.nationalarchives.gov.uk/20121107103953/http:/www.dft.gov.uk/statistics/releases/congestion-on-local-authority-managed-a-roads-2010-11/

Description	Classification (based on UK area type, and road type)	Data Source and methodology	LDV[11] Speed (km/h)	HDV[12] Speed (km/h)
		by vehicle type, flow weighted and based on weekday morning peak. Averaged across 2006/7 to 2010/11 and England (assumed area type 6,7,8,9).		
Inter urban trunk roads	4,5_Urban_Major_Trunk (single carriageway)	For single carriageway A-roads in urban areas the speed limit has been applied.	48	48
Inter urban trunk roads	6,7,8,9_Urban_Major_Trunk (single carriageway)	For single carriageway A-roads in urban areas the speed limit has been applied.	48	48
Rural A roads	10_Rural_Major	DfT's free flow vehicle speed statistics, GB 2010[14], Table SPE0101, flow weighted average across vehicle types, assuming single carriageway roads	76	72
Inter urban trunk roads	4,5_Urban_Major_Trunk	DfT's "Congestion on inter-urban roads, for the year ending December 2010"[15] linked table CGN0103. No split by vehicle type, not flow weighted, average of monthly average speeds for trunk A roads, Mar 2008-Nov 2010	82	82
Inter urban trunk roads	6,7,8,9_Urban_Major_Trunk	DfT's "Congestion on inter-urban roads, for the year ending December 2010" linked table CGN0103. No split by vehicle type, not flow weighted, average of monthly average speeds for trunk A roads, Mar 2008-Nov 2010	82	82
Urban motorways	3_Urban_Motorways	DfT's "Congestion on inter-urban roads, for the year ending December 2010" linked table CGN0103. No split by vehicle type, not flow weighted, average of monthly average speeds	95	95

---

[14] http://webarchive.nationalarchives.gov.uk/20121107103953/http:/www.dft.gov.uk/statistics/releases/free-flow-vehicle-speeds-in-great-britain-2010/

[15] http://webarchive.nationalarchives.gov.uk/20110314114542/http:/dft.gov.uk/pgr/statistics/datatablespublications/roads/congestion/

Description	Classification (based on UK area type, and road type)	Data Source and methodology	LDV[11] Speed (km/h)	HDV[12] Speed (km/h)
		for motorways, Mar 2008-Nov 2010		
Urban motorways	4,5_Urban_Motorways	DfT's "Congestion on inter-urban roads, for the year ending December 2010" linked table CGN0103. No split by vehicle type, not flow weighted, average of monthly average speeds for motorways, Mar 2008-Nov 2010	95	95
Urban motorways	6,7,8,9_Urban_Motorways	DfT's "Congestion on inter-urban roads, for the year ending December 2010" linked table CGN0103. No split by vehicle type, not flow weighted, average of monthly average speeds for motorways, Mar 2008-Nov 2010	95	95
Rural motorways	10_Rural_Motorways	DfT's free flow vehicle speed statistics, GB 2010, Table SPE0101, flow weighted average across vehicle types, motorway non-built up roads even though "urban" area type	111	91

Meteorology

Hourly sequential meteorological data from Waddington (Lincolnshire) in the reference year has been used in the setup of the ADMS-Roads model runs. Table A7.3 shows the other assumptions applied for details of the meteorological conditions at the roads, which are dependent on the area type and meteorological site. These are in common with the setup for the area source dispersion kernels in the PCM model (see Appendix 4).

Table A7.3 - Summary of meteorological parameters applied by area type

Area types (from Table A7.2)	Types of location	Minimum Monin–Obukhov length (m)		Surface roughness (m)	
		Dispersion site	Meteorological site	Dispersion site	Meteorological site
1,2,4	Conurbation	25	10	0.5	0.1
3,5,6,7,8	Smaller urban	20	10	0.5	0.1
9,10	Rural	10	10	0.5	0.1

Receptors locations

Model runs are set up with a road source for each major road link nearest to a census point. This road source represents the link at the road angle determined from the coordinates of its end nodes. Concentrations are modelled for 49 receptors, with one at the road centre line of the road link, and 24 each side perpendicular to the road link. Close to the road receptors are spaced at 1m intervals, after 15m from the roadside the receptor spacing progressively increases to a maximum of 200 m from the roadside. A diagram illustrating the position of receptors and road source is given in Figure A7.1.

Figure A7.1 - Schematic diagram of road source (blue) and receptors (red)

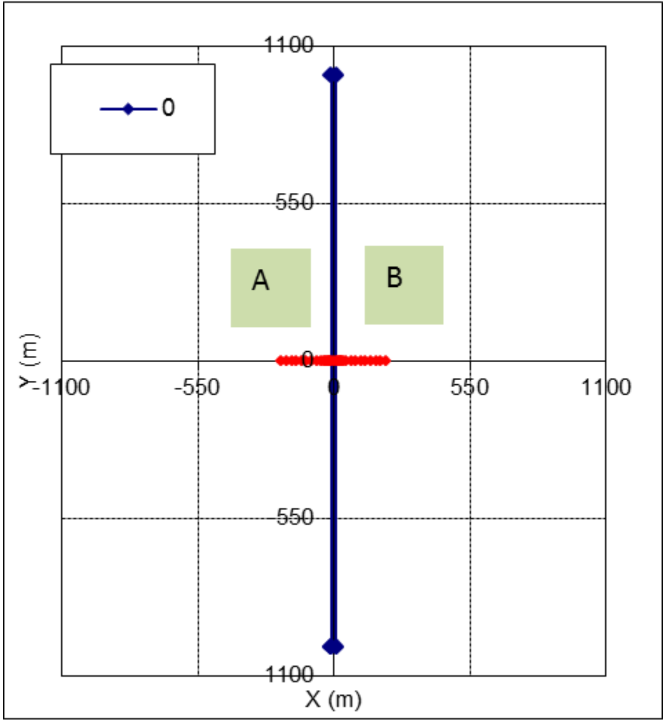

Model outputs

Modelled concentrations can be derived from the ADMS-Roads model outputs for all receptor locations specified. In the PCM-RKM modelling the average concentration across each side of the road at a distance of 4 m from the kerb for all census points has been selected for comparison with the measured concentrations at roadside (traffic) stations for model calibration. The same output has also been used for the compliance assessment for roadside (traffic) concentrations. To illustrate the variation in concentration modelled with distance from the road a normalised concentration profile is presented in Figure A7.2.

Figure A7.2 - Example normalised concentration profile

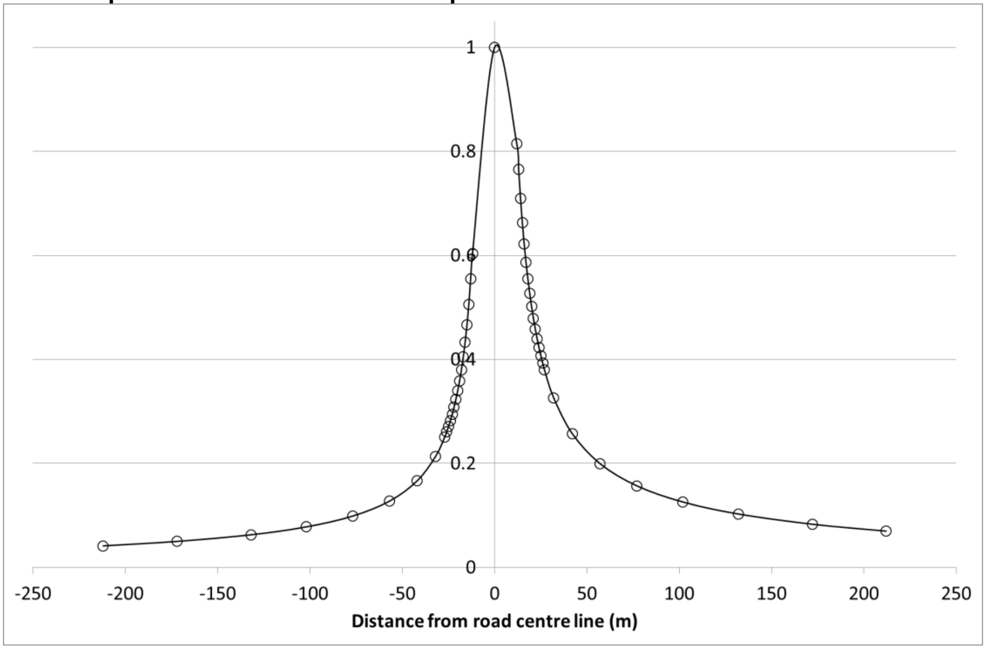

Model calibration

The PCM-RKM uses the PCM roadside increment approach for the prediction of the local contribution to total concentrations at the roadside. As such the annual mean concentration at roadside locations has been assumed to be made up of two parts: a background concentration (excluding local sources) and a roadside increment.

Roadside concentration = background concentration + roadside increment.

To calibrate the model, modelled concentrations are compared to measured roadside increment concentrations (i.e. measured roadside concentration minus modelled background concentration) at AURN roadside traffic stations. Figure 3-9 in Chapter 3 presents the calibration plot for NO_X for 2018 for the PCM-RKM.

Adjustment factors applied to road link emissions

The effect of street canyons has not been explicitly included in the PCM-RKM model. Instead the model calibration based on the comparison of measured and modelled roadside concentration increments implicitly includes some influence of street canyon effects, dependent on how much the local environment of the AURN road traffic stations used to calibrate the model can be characterised as street canyons. Street canyons are typically characterised in terms of aspect ratio, the ratio of the road width to the height of buildings lining the road. Vardoulakis et al. (2003) characterised avenue canyons as those with aspect ratios (AR) < 0.5, and deep canyons as those where AR = 2.

Motorways are expected to have a more open aspect than the urban streets where the AURN road traffic stations used to calibrate the model are situated. An adjustment factor has therefore been derived for motorways.

The AURN road traffic stations used to calibrate the model have been characterised in terms of AR from estimates of the average road widths (building façade to building façade) and average building heights determined by examining the roads within ArcMap, Google Earth and Google Streetview.

A motorway adjustment factor of 0.9 has been applied in the PCM-RKM for 2018. A fixed value of 0.9was chosen following the observation that the ratio of the NO_X calibration factor for traffic stations where AR < 0.5, to the NO_X calibration factor for all AURN traffic stations has been found to be close to this value in recent years:

$$\boldsymbol{F} = \frac{C_{AR<0.5}}{C_{All}}$$

In development of the PCM-RKM, comparison of roadside modelling results to the previous PCM model output indicated significant increases in the modelled concentrations for roads with high traffic flows predicted by using ADMS-Roads. These increases are not thought realistic and indicate under-prediction of dispersion for the widest and highest flow roads since dispersion is likely to be most efficient on these roads. To address this, in addition to the general scaling applied to road link emissions for motorways, further adjustment factors have been developed to apply to the road link emissions for motorways and A-roads where the traffic flow exceeds an annual average daily flow of 75,000.

The combined traffic flow and motorway adjustment factors as a function of traffic flow are presented in Figure A7.4.

Figure A7.4 – Combined adjustment factors applied to road link emissions for 2018

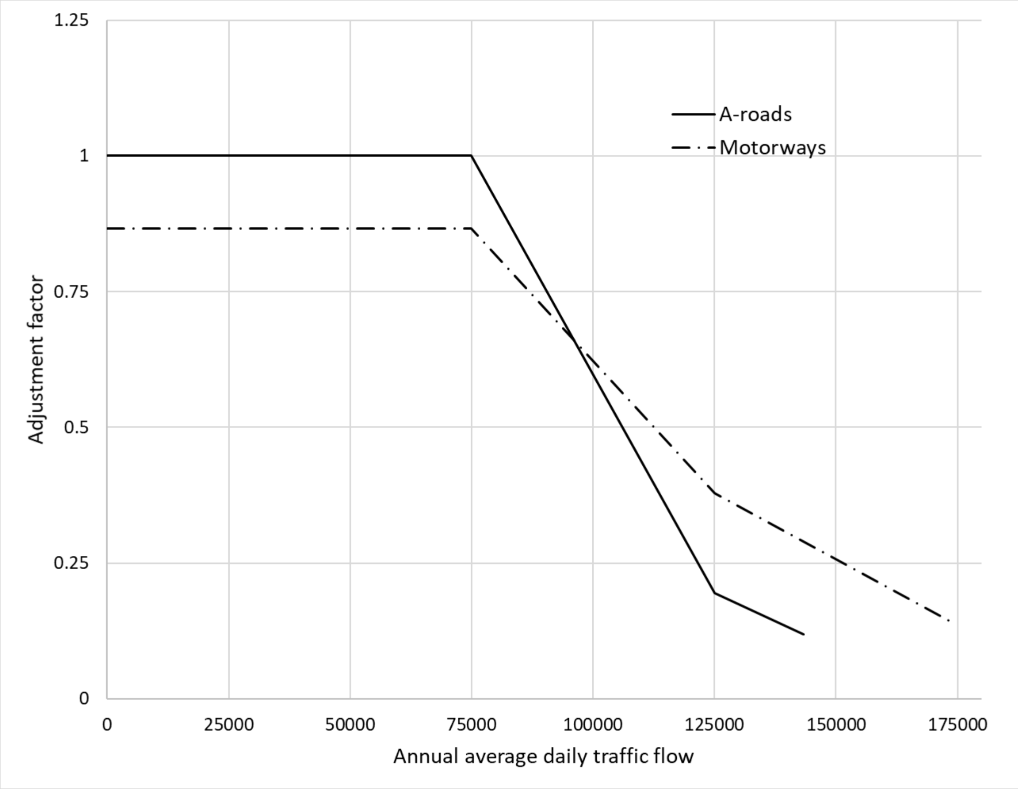

Model verification

Verification of the PCM-RKM for NO_X, NO_2, PM_{10}, $PM_{2.5}$, and benzene for the assessment year is discussed in the body of this report.

Appendix 8 – Selected acronyms

ADMS	Atmospheric Dispersion Modelling System
AEI	Average exposure indicator
AGANet	UK Acid Gases and Aerosols Monitoring Network (UK)
AOT40	Accumulated exposure index above a threshold concentration of 40 ppb
APU	Auxiliary power unit (aircraft)
AQD	Directive on ambient air quality and cleaner air for Europe (2008/50/EC), known as the ‘Air Quality Directive’
AQDD4	The fourth Daughter Directive 2004/107/EC (AQDD4) under the Air Quality Framework Directive (1996/62/EC)
As	Arsenic
AURN	Automatic urban and rural network (UK)
B(a)P	benzo(a)pyrene, a polycyclic aromatic hydrocarbon
BEIS	Department for Business, Energy & Industrial Strategy
Cd	Cadmium
CDR	Central Data Repository of the European Environment Agency
CL	Critical level
CO	Carbon monoxide
COPERT	Software tool used to calculate air pollutant emissions from road transport
CORINAIR	Core Inventory of Air Emissions
DECC	Department of Energy and Climate Change
Defra	Department for Environment, Food & Rural Affairs
DQO	Data quality objective
ECO	Exposure concentration obligation
EEP	Energy and emissions projections
EMEP	European Monitoring and Evaluation Programme under the Convention on Long-range Transboundary Air Pollution
ERG	Environmental Research Group, Kings College London
ETS	Emissions Trading Scheme
FIDAS	A fine dust measurement system for ambient air quality measurement
$f\text{-}NO_2$	The fraction of NO_x emissions emitted as primary NO_2 (by volume)
HDV	Heavy duty vehicles
IDW	Inverse Distance Weighting
IED	Industrial Emissions Directive (2010/75/EU)
IPR	Implementing Provisions on Reporting (Decision 2011/850/EU)
LAQN	London Air Quality Network
LEZ	Low Emission Zone
LMO	Monin Obukhov Length
LTO	Long term objective
LV	Limit value
MAAQ	Modelling Ambient Air Quality

NAEI	National Atmospheric Emissions Inventory (UK)
NAME	Numerical Atmospheric-dispersion Modelling Environment
NAMN	National Ammonia Monitoring Network (UK)
NERT	and national exposure reduction target
Ni	Nickel
NO	Nitrogen monoxide
NO_2	Nitrogen dioxide
NOx	Oxides of nitrogen
O_3	Ozone
OSGB	Ordnance Survey Great Britain
Pb	Lead
PCM	Pollution Climate Mapping
PCM-RKM	Pollution Climate Mapping Roads Kernel Model
PM	Particulate Matter
PM_{10}	Particulate matter 10 micrometres or less in diameter
$PM_{2.5}$	Particulate matter 2.5 micrometres or less in diameter
SIA	Secondary inorganic aerosol
SNAP	Standardized Nomenclature for Air Pollutants (emissions inventory sector splits)
SO_2	Sulphur dioxide
SOA	Secondary organic aerosol
TEOM	Tapered element oscillating microbalance
TEOM FDMS	Tapered element oscillating microbalance and Filter Dynamics Measurement System
TRACK	A receptor oriented, Lagrangian statistical air quality model
TV	Target value
UKEAP	United Kingdom Eutrophying & Acidifying Network
ULEZ	Ultra Low Emission Zone
VCM	Volatile correction model

The Gemini Building
Fermi Avenue
Harwell
Didcot
Oxfordshire
OX11 0QR
United Kingdom
t: +44 (0)1235 753000
e: enquiry@ricardo.com

ee.ricardo.com